



● La Silla
● La Serena
● Santiago

EL MENSAJERO



MAIN LIBRARY

No. 63 – March 1991

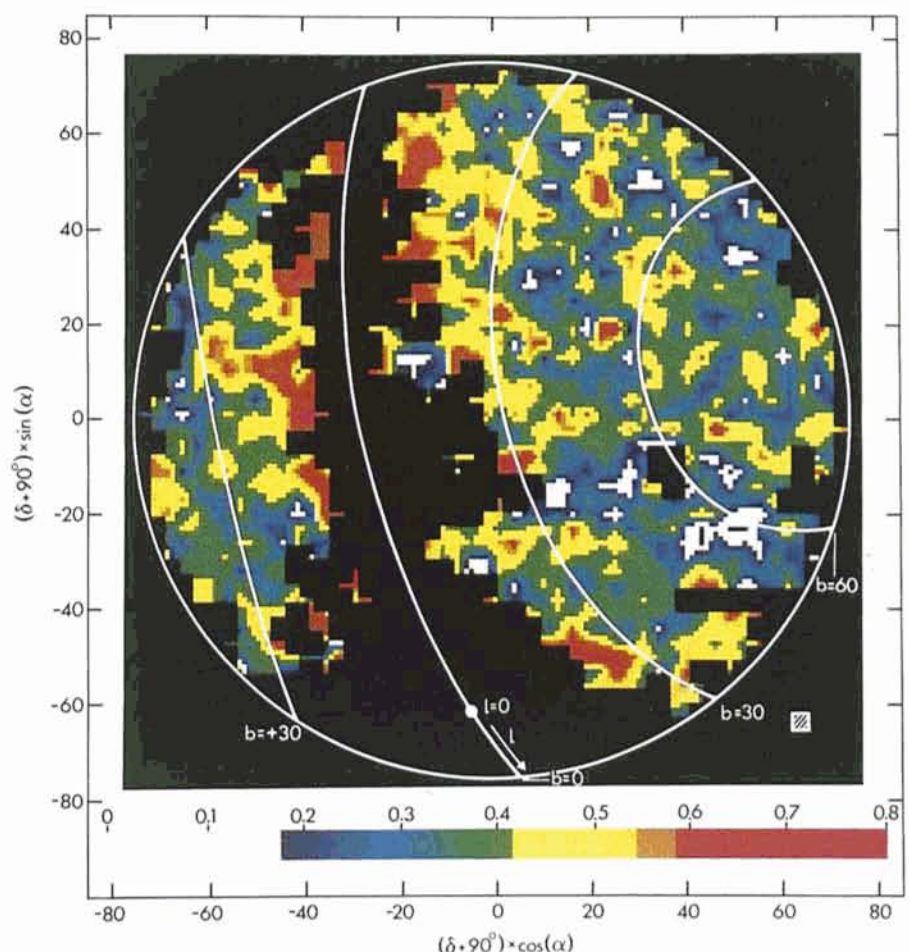
A New Southern Hemisphere Galactic Extinction Map Based on Surface Brightnesses of External Galaxies

J. CHOŁONIEWSKI, *Astronomical Observatory of the Warsaw University, Poland*
E. A. VALENTIJN, *ESO and Laboratory for Space Research, Groningen, the Netherlands*

1. Introduction

The precise surface brightness values listed for about 12,000 homogeneously selected galaxies in "The Surface Photometry Catalogue of the ESO-Uppsala Galaxies" (Lauberts and Valentijn 1989, hereafter ESO-LV; see also the *Messenger* 34, 10, and 56, 31, and this issue) have been used to derive galactic extinction values for a large part of the Southern Sky, cf. Figure 1. The new extinction measures are thought to reflect the effect of the diffuse interstellar

Figure 1: A map of the relative extinction in the B band in polar equatorial coordinates. The derived extinction values have been averaged inside $3^\circ \times 3^\circ$ pixels and are here displayed using 1.5×1.5 pixels – some interpolation has been applied to fill pixels without data (~5% of total). The credibility of apparent structures can be assessed by using the following information: the uncertainty of A_B inside one resolution element (inset box at the lower right) is 0.13^m , roughly corresponding to one colour step on the map. The zero point is somewhat arbitrary, but a lower limit could be deduced by avoiding negative extinctions in regions with a minimum extinction (not at the South Pole) and a deconvolution of the observed frequency distribution of A_B with the measurement error function.



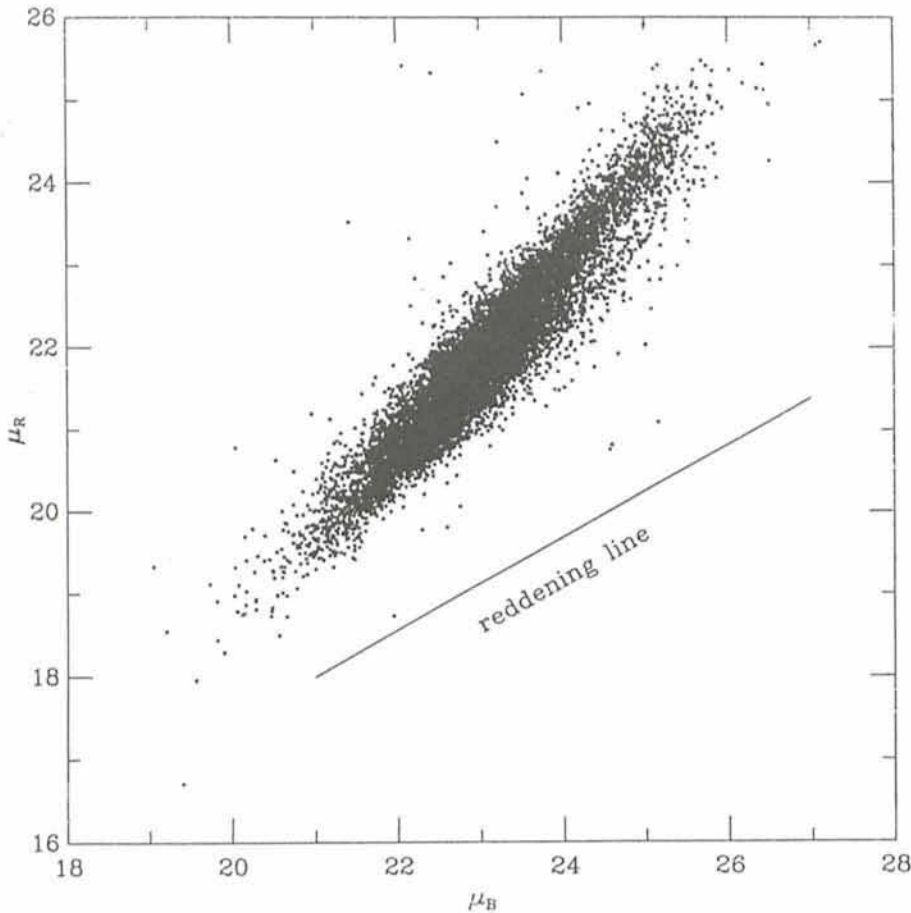


Figure 2: Surface brightness (measured at the effective isophote) of ESO-LV galaxies in B and R bands.

medium in our own Galaxy and the technique we have employed should trace the same component as has been studied before in so-called 'reddening' studies. The current analysis uses parameters of *detected* galaxies, in similarity with previous reddening studies, and is not sensitive to those regions of the sky that may be so heavily obscured that we start to miss objects located behind these regions. These heavily obscured regions can be better traced by galaxy counts, a separate project, which is still in progress. Here, we announce some first results of our extinction studies, in particular a 3-degree resolution extinction map of the Southern Sky with a $\sigma(A_B) \approx 0.13^m$ and $\sigma(E(B-V)) \approx 0.06^m$.

2. The Technique

The hitherto most frequently used model for the extinction in the Southern Galactic hemisphere (Burstein, Heiles) is exclusively based on the mapping of neutral hydrogen. Since this mapping was done with a rather poor spatial sampling, the resulting extinction map was grossly dominated by interpolations of data. Furthermore, using HI data relies on a constant HI-to-extinction ratio. The overall value of this ratio is uncertain

by at least a factor two, and is thought to deviate more locally. This motivated Burstein and Heiles to include also galaxy counts, when deriving their extinction model for the Northern Hemisphere, but this could unfortunately not be done for the South. Motivated by the recent availability of the photometric data in the ESO-LV catalogue, we have undertaken some statistical experiments to see whether the data would allow an improvement of this situation.

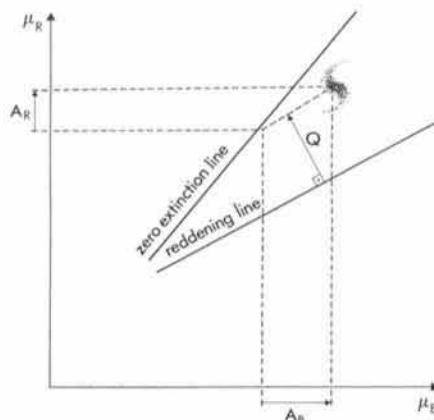


Figure 3: The idea of extinction measurements using the surface brightness of galaxies in two bands.

Although the surface brightness of an external galaxy at a particular single band should respond in a linear way to the extinction in the Galaxy, such single-band surface brightness values are not good extinction indicators, since they have a too large scatter around the mean value ($\sigma \approx 0.6$ mag). If however, we have a sample of galaxies with measured surface brightness in *two* bands (B and R for ESO-LV), then we can take into account the fact that they are strongly correlated with each other (Fig. 2); as a measure of extinction of each individual galaxy, we can use its distance from the average regression curve of unreddened surface brightnesses, measured along the direction of the reddening vector (see Fig. 3).

However, in order to obtain this distance we have to know the location of the curve describing the unreddened surface brightnesses, but to obtain this curve we must know the extinction for each galaxy – just the set of values we are looking for. The only solution to this difficulty is to obtain *both* the extinctions and the location of the curve simultaneously – in one step. This is possible with help of the "analysis of variance" statistical technique. This technique reproduces the well documented ratio $A_R/A_B = 0.565$ and in the further processing this value has been adopted. In constructing the unreddened curve we made use of the parameter Q which is independent of extinction but dependent on surface brightness. In short, the statistical analysis solves the function $f(Q)$ and $A_B(l,b)$ in one step. The introduction of the Q parameter is closely related to a similar parameter used for the analysis of the reddening of stars.

The full description of the above method and its application to ESO-LV is expected to be published soon (Chofoniewski and Valentijn, 1991, in preparation).

The uncertainty of the derived extinction in the B band is $\sigma(A_B) \approx 0.4^m$ per galaxy. This corresponds to $\sigma(E(B-V)) \approx 0.1^m$ which is comparable to the accuracy of extinction estimates deduced from the photometry of stars. When averaging over larger areas (ESO-LV has about one galaxy per square degree) a formally much more accurate value for such an area can be obtained. For instance, the average A_B over one ESO sky survey plate has been deduced with an error of 0.1^m , which corresponds to an uncertainty in $E(B-R) \approx 0.04$. Such values are useful to evaluate the large scale distribution of the extinction, but indeed, we do not know how much spatial structure is present within these averaged areas, a problem inherent in this sort of research.

3. The Map

In Figure 1 we present a map of the relative extinction in the Southern Hemisphere. The photometry of external galaxies cannot provide absolute extinction, or in other words, it cannot provide the zero point. Formally, the technique provides the relative extinction compared to an overall mean of $A_B=0$. We have not finalized the constant yet (our work on this is still in progress) but we can easily deduce a lower limit for it. We cannot allow negative extinctions to occur (the white and blue regions in Fig. 1) and more formally, we can deconvolve the observed frequency distribution of A_B with the formal σA_B error function. This way, we derive a lower limit to the zero point of 0.4^m , which has been included in the scale of Figure 1.

Our understanding of Figure 1 is that most of the structures that can be seen

are real. We checked that they do not correlate with the spatial distribution of the target galaxies, while around the Southern Galactic pole we could observe a good spatial correspondence with the IRAS cirrus maps of Boulanger et al. We can also compare the extinction in a small, but still significantly large, part of the Northern Galactic Hemisphere (92 ESO survey plates) with that in the Southern Galactic Hemisphere. In the regions of absolute galactic latitude in the range $10^\circ-30^\circ$, we find on average about 0.1^m more extinction (A_B) in the South. If our evaluation of the lower limit on the zero-point is correct, then the average extinction at low galactic latitudes ($<70^\circ$) should be $A_B > 0.25^m$.

4. Availability of the Data

Our results for the relative extinction in the B band (A_B) in our Galaxy will be

available in the following forms:

1. In our paper we anticipate a printed list of overall extinction values for each of the 404 ESO sky survey plates that were assessed in the ESO-LV project.
2. A computer programme AEJ (in MIDAS environment) which fills two columns of the digitized version of the ESO-LV catalogue (the MIDAS table PCAT): column # 102 which contains A_B 'per galaxy' and column # 105 which contains the average A_B per plate. It is distributed, on request, by the data archivist of ESO.
3. An ASCII file which contains three columns: R. A., Decl. and A_B for each of 10,930 galaxies. It is distributed, on request, by J. Choloniewski (Astronomical Observatory of the Warsaw University, Aleje Ujazdowskie 4, 00-478 Warszawa, Poland) on 5.25 or 3.5 floppy disk.

The Recent Outburst of (X-Ray) Nova Muscae 1991

M. DELLA VALLE, B.J. JARVIS and R.M. WEST, ESO

Discovery

The transient X-ray source, GRS 1121-68 (Nova Muscae 1991), was almost simultaneously detected by the WATCH all-sky X-ray camera installed

on the Soviet GRANAT satellite on January 9 and the All Sky X-ray Monitor aboard Ginga on January 8, 1991. Lund and Brandt (IAU Circ. 5161) reported that this new X-ray source was at that

time about twice as bright as the well-known X-ray emitting Crab Nebula. The search for a possible optical counterpart began on La Silla on January 11, using the GPO astrograph without success.

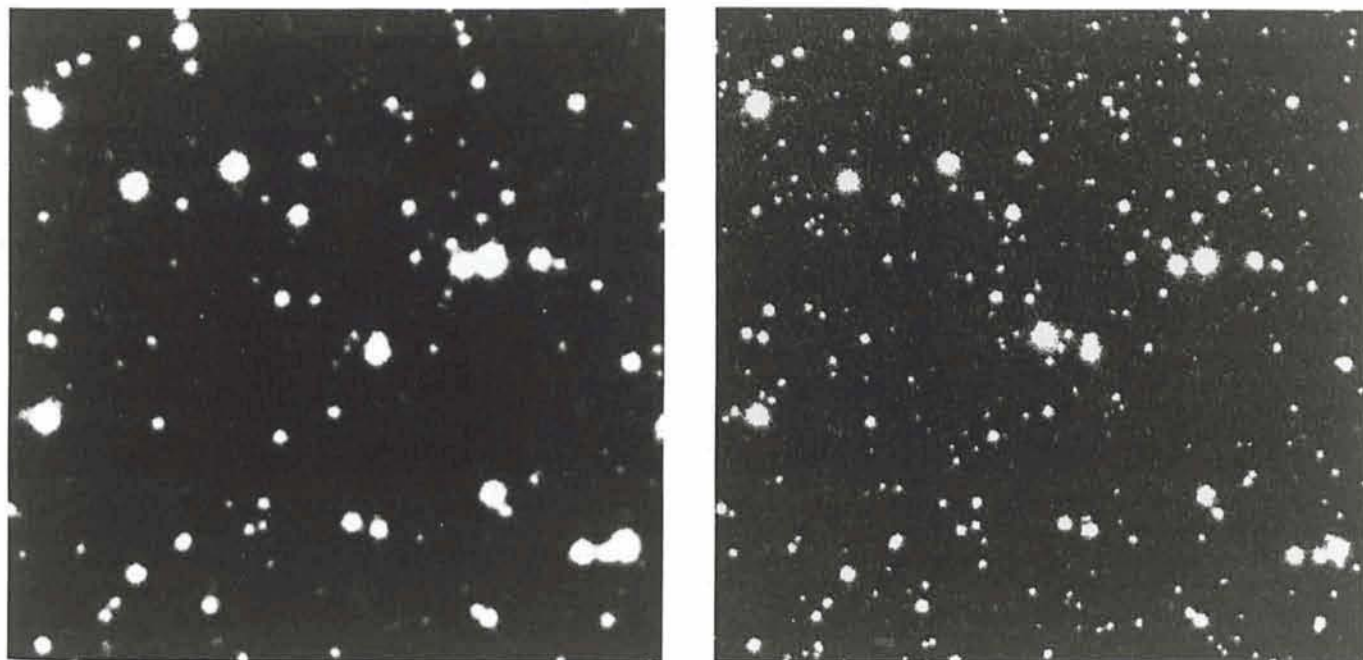


Figure 1: This photo shows Nova Muscae 1991 which flared up in early January 1991 in the southern constellation Musca (the Fly). The left frame is a reproduction of an earlier red-sensitive ESO Schmidt plate (120-min exposure on IIIa-F + RG630; 29 January 1976; observer G. Pizarro). To the right is the same sky field, observed with the ESO New Technology Telescope (EMMI + CCD, 5-sec exposure in R; 15 January 1991, 7:22 UT; seeing 0.9 arcsec; observers M. Della Valle and B. Jarvis); here the nova can be seen as the bright object at the centre. The pre-nova is faintly visible at the same position in the left frame.

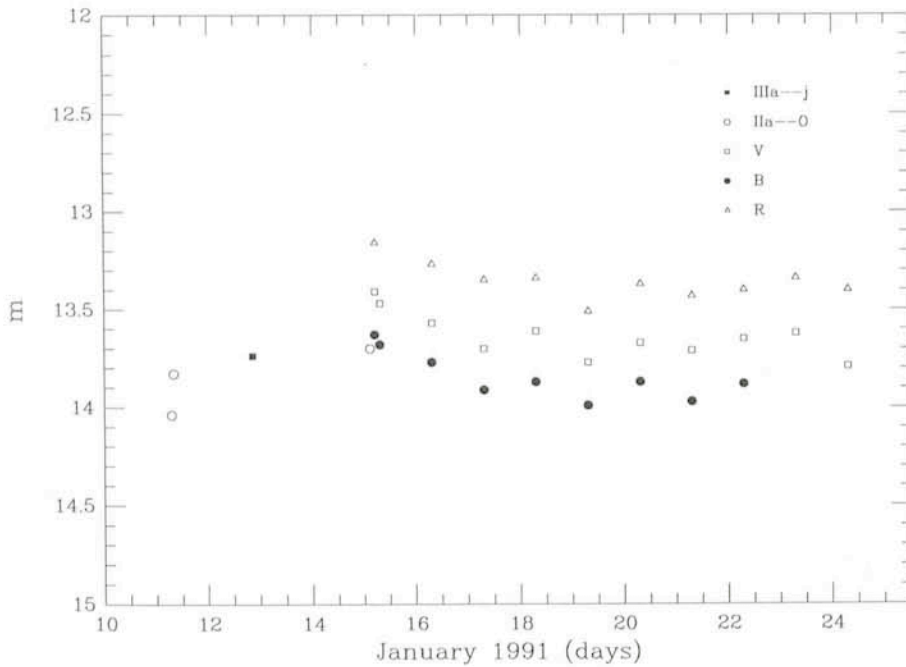


Figure 2: Preliminary light curve of Nova Muscae 1991 during the early stages after outburst.

Makino and the Ginga Team (IAU Circ. 5161) subsequently reported a new and more accurate position from which a 45-min ESO Schmidt IIIa-J plate was obtained on January 13. Nova Muscae 1991 was identified on this plate (IAU Circ. 5165) as a star of $m_v \sim 13.5$, near the edge of the error box reported by them.

The Progenitor

A faint, star-like object could be seen on the deepest, pre-1991 plates at the approximate position of the nova (Fig. 1). A total of twelve photographic plates which cover the area around Nova Muscae 1991 were available at ESO and have been measured.

In order to verify the identity with the progenitor, accurate astrometric positions of the presumed pre-nova star were measured on the deepest blue plate (SRC 2172) and a combined R (290-min) frame, and then compared with the position of the nova as measured in a 5-sec R-frame, obtained at the NTT on January 15.3, 1991. It was possible to measure the pre-nova position to an accuracy of $\sim \pm 0.2$ arcsec. The interpolated positions of the pre-nova and the nova are given in Table 1 and demonstrate that it is the same object.

Table 1: Astrometric positions

Object	R.A.(1950)	Dec.(1950)
pre-nova (B)	11 24 18.51	-68 24 01.9
pre-nova (R)	11 24 18.52	-68 24 02.2
Nova (R)	11 24 18.49	-68 24 01.7

be determined. The resulting, mean magnitudes of the pre-nova are $B = 20.9 \pm 0.2$ and $R = 19.8 \pm 0.2$.

Photometric and Spectroscopic Follow-up

Photometric and spectroscopic observations, mostly carried out with the ESO NTT and 2.2-m telescopes at La Silla Observatory, have been carried out since January 15. The star had increased in brightness by about 8–9 magnitudes from minimum (Fig. 2). Although these characteristics are typical of galactic novae, the spectrum, obtained on January 15.3 UT with the NTT (Fig. 3), shows a number of features (generally) not seen in the spectra of classical novae at early stages. The *pre-maximum* and *principal* spectrum of galactic novae are normally distinguished by FeI, NaI, OI and Balmer emission lines coupled with *P Cyg* absorptions (Payne-Gaposchkin 1957). These features are normally superimposed on a continuum similar to that of A-F supergiant stars. In contrast the spectrum of Nova Muscae exhibits a very blue continuum with H_{α} , H_{β} , H_{γ} , He-I (587.6 nm), He-II (468.6 nm), and NIII (464.0 nm) emission lines without *P-Cyg* profiles, making it similar to the spectra of dwarf novae in outburst.

Subsequent spectroscopic observations carried out on the following three days (IAU Circ. 5167) confirm this. Moreover, the strong X-ray emission preceding or accompanying the optical

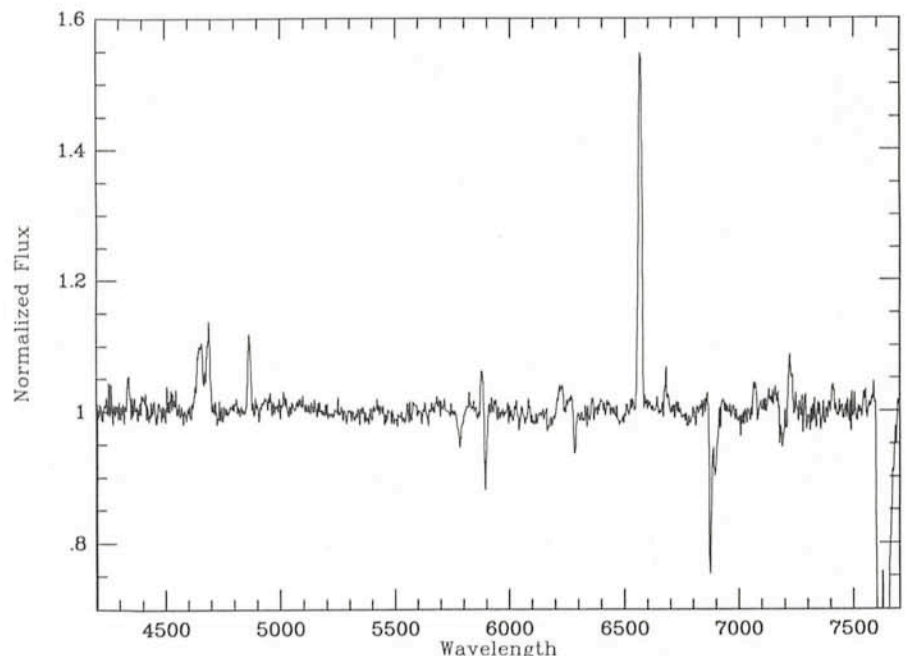


Figure 3: Continuum removed spectrum of Nova Muscae 1991 obtained on January 15.3 UT at NTT + EMMI (3-min exposure).

increase in brightness, suggests that this object almost certainly belongs to the low-mass X-ray binary (LMXB's) class of objects and in particular to the small sub-class of *X-ray Novae*. This sub-class includes such objects as: V 616 Mon 1975 (Mon X-1), V 2107 Oph 1977 (H1705-25), V822 Cen 1980 (Cen X-4) and V 404 Cyg 1989 (GS2023+338). Furthermore, the equivalent width of the HeII (468.6 nm) ($EW=2.5 \text{ \AA}$) and H_{β} ($EW=1.8 \text{ \AA}$) emission lines are consistent with the values found for other LMXB's (e.g. van Paradijs and Verbunt, 1984, see their Fig. 1).

Some Current Views of X-Ray Novae

The energy source during the paroxysm of LMXB's, and cataclysmic variables (CV's), is generally believed to be provided by two mechanisms: (a) the thermonuclear energy released by nuclear runaway of the accreted matter onto the surface of the degenerate companion, and (b), the gravitational potential energy released by the accreting material from the disk onto the compact star. At minimum, the luminosity of both CV's and LMXB's is mainly provided by the mass transfer rate. The first mechanism is commonly believed to explain the Nova explosion and the X-ray

bursts in some LMXB's while the second mechanism is believed to be responsible for the eruptions both of the dwarf novae and the X-ray novae. According to current understanding, mechanism (b) can be triggered by an accretion rate from the disk onto the white dwarf smaller than the mass transfer rate from the secondary to the disk (the so-called *disk-instability model*) and/or through sudden bursts of mass transfer rate from the secondary to the white dwarf (the so-called *mass transfer instability model*).

The main difference between the LMXB's and other CV's is the large amount of X-ray emission during the outburst. For the X-ray novae (including Nova Muscae 1991) the L_x/L_{opt} is generally ≥ 100 (at least) that of CV's. This difference is due to the dramatic difference between the physical nature of the compact companion. Whereas for the CV's the material is normally transferred from a main-sequence star to the white dwarf ($D=10^{-2} R_{\odot}$), for the X-ray novae, the material is transferred from the main-sequence star onto a neutron star ($D=10^{-5} R_{\odot}$) or possibly a black hole (McClintock and Remillard, 1986). The outburst in the UV and optical is caused by the reprocessing of the X-ray radiation (produced by the accretion onto the neutron star) which warms up the outer layers of the accretion disk.

Tentative Time-table of Council Sessions and Committee Meetings in 1991

April 3:	Finance Committee
May 6-7:	Users Committee
May 13-14:	Scientific Technical Committee
May 16-17:	Finance Committee
May 28-29:	Observing Programmes Committee
June 3-4:	Council
November 11-12:	Scientific Technical Committee
November 14-15:	Finance Committee
November 28-29:	Observing Programmes Committee
December: 2-3:	Council

References

- Della Valle, M., Jarvis, B., West, R. 1991, IAU Circ. 5165.
 Della Valle, M., Pakull, M. 1991, IAU Circ. 5167.
 Lundt, N., Brandt, S. 1991, IAU Circ. 5161.
 Makino, F., and the Ginga Team 1991, IAU Circ. 5161.
 McClintock, J., Remillard, R. 1986, *Ap.J.* **308**, 110.
 Payne-Gaposchkin, C. 1957, *The Galactic Novae*, chapter 10.
 van Paradijs J., Verbunt, F. 1984, in *High Energy Transients in Astrophysics*, ed. S.E. Woosley, p. 49.

Schott Successfully Casts an 8-m Mirror Blank

A test run for the manufacture of mirror blanks in the 8-m class, for use in the world's largest optical telescope, the ESO 16-m equivalent Very Large Telescope (VLT), has been successfully performed at Schott in Mainz, Germany. The test blank had a diameter of 8.6 metres and a surface area of more than 55 m². This is the first time that it has been possible to cast such a large glass-ceramic blank in one piece. To accomplish this impressive feat, Schott has developed a number of new technological procedures.

During the next years, Schott will produce the four mirror blanks needed for the VLT. Each of them will have a final diameter of 8.2 metres and be unusually thin, only 177 mm, in order to be so flexible that their surface form can be easily controlled and maintained in optimal shape by means of an active optics system. This technique has already been successfully installed in the ESO 3.5-m New Technology Telescope for which the mirror blank was also produced by Schott. The editor



The first 8.6-m mirror blank at Schott, shortly after the molten glass was poured into the rotating form (Photo: Schott).

For the manufacture of the very large VLT mirror blanks, Schott uses the spin-casting technique. In the 2400 m² production hall on the bank of river Rhine which was specially constructed for the VLT Project, 45 tons of molten glass is poured into a rotating mould with curved bottom; it makes about six revolutions per minute. In this way the blank is given the desired, curved shape

which is retained when the glass cools and solidifies.

This prototype blank will spend about three months in an oven while it is slowly cooled to room temperature. Then follows a mechanical correction of the shape and thereafter a renewed thermal treatment, the so-called ceramization process, by which the material achieves its zero-expansion properties, making it

insensitive to temperature changes and suited for use in astronomical telescopes.

ESO has congratulated Schott on the successful casting of the first mirror blank of this size. Smaller blanks of the same material are used in other advanced astronomical instruments like the Keck telescope, ROSAT, Galileo and AXAF.

Flexible Scheduling at the NTT, a New Approach to Astronomical Observations

J. BREYSACHER, M. TARENGHI, ESO

The Recent NTT Experience

Already at the time of first light of the NTT on March 23, 1989 (see *The Messenger* No. 56, June 1989), there was the confirmation that the La Silla sky was able to give stellar images of dimension two or three times better than the normal experience. An observation resulting in stellar images with a diameter of 0.33 arcsec contains such a large quantity of information that not all instruments are capable to benefit, unless they are designed for such conditions.

Other characteristics of the NTT have transformed or stopped old traditions of optical astronomers. For example, because the pointing of the NTT is better than 1.3 arcsec rms, in the direct imaging mode there is no need of checking the field before starting the exposure. It is obvious that it will become essential to arrive at the telescope with precise coordinates if the observer wants to make an efficient use of precious telescope time.

The extensive campaign of site test-

ing organized by M. Sarazin was not only beneficial for the exploration of the best site for the VLT observatory, but it resulted also in an undertaking that has given important and new results about the atmospheric properties and their influence on astronomical observations.

We are now confident about the frequency of excellent seeing and we start to understand its time behaviour. The next step is to forecast the expected seeing. We are considering the possibility to install a number of seeing

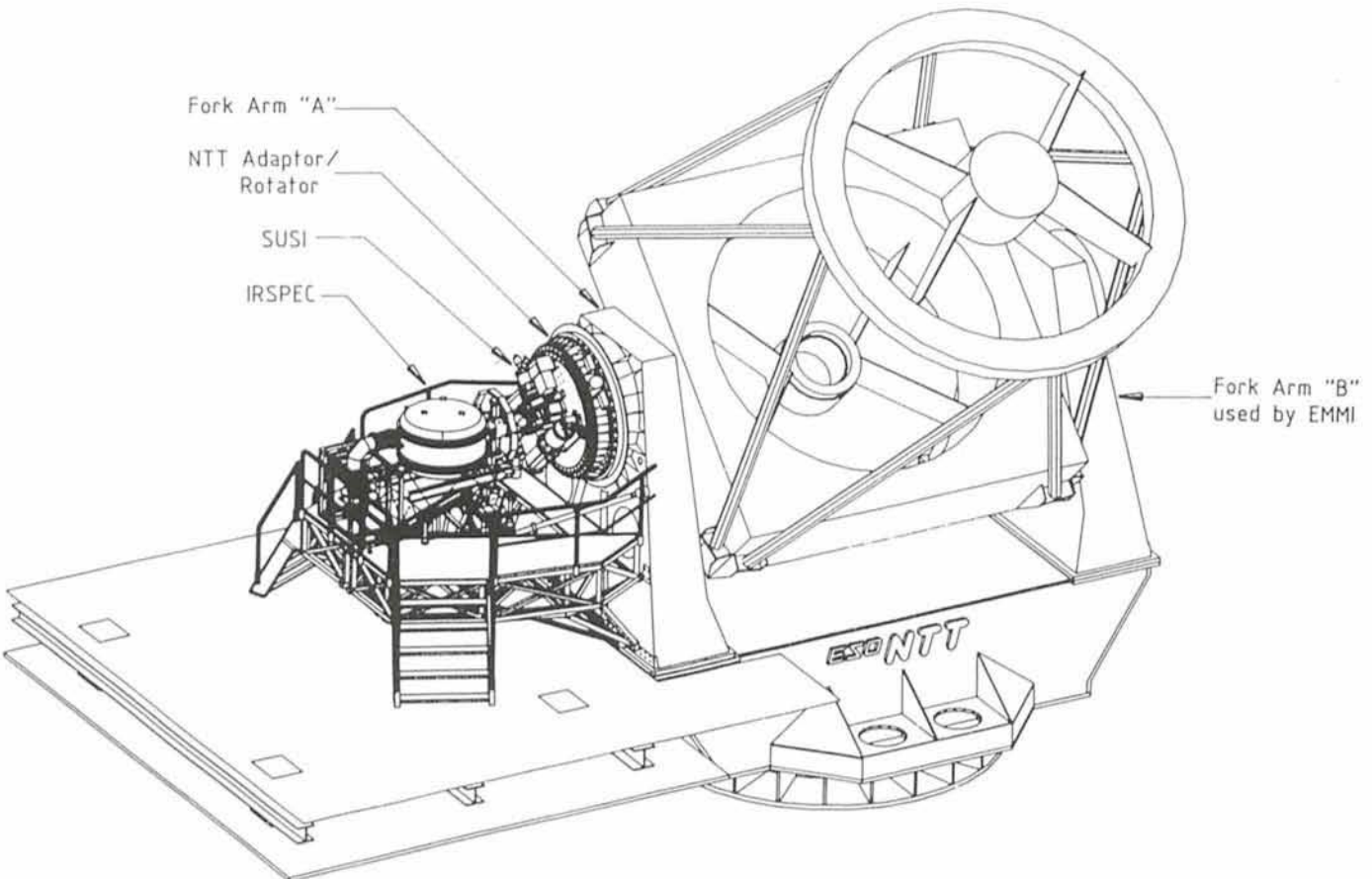


Figure 1: Schematic layout of the NTT showing the location on Fork Arm "A" of SUSI and IRSPEC.

monitors in strategic locations to flag the arrival of conditions of superb seeing. From the existing data it is expected that on La Silla the seeing will be less than 0.5 arcsec for about 200 hours per year.

The Need for New Instrumentation

The success of the NTT experience and the rediscovery of the potentiality of La Silla imply the development of a new type of instrumentation tuned to new goals. The two original instruments designed and realized for the NTT: EMMI (the ESO Multi-Mode Instrument) and IRSPEC (the Infrared Spectrometer) are among the most sophisticated and versatile astronomical apparatus ever built. Their complexity and the basic goals of their multi-mode approach imply some limitation on the performances in extreme conditions. It is important to remember that the EMMI project started in November 1985, the IRSPEC one being even older. At that time the seeing limits attainable were not established. ESO has immediately grasped the importance of the situation and started forthwith the design of new instruments such as SUSI.

SUSI

SUSI (the Superb Seeing Imager) is an instrument physically distinct from EMMI but complementing its observing capabilities. It consists of a supporting plate mounted on the adaptor of the Nasmyth A focus of the NTT, in front of the infrared spectrometer IRSPEC. Figure 1 shows the CAD image of the telescope and instrument. Figure 2 gives more details of the flange and SUSI. The change from focus A (SUSI or IRSPEC) to focus B (EMMI) and vice versa takes a few minutes only. A remotely-controlled 45-degree mirror mounted on this plate can deviate the telescope beam to a CCD camera. The image scale on the detector is that of the F/11 focus (1 arcsec = 186 microns or 5.36 arcsec/mm) and thus a standard CCD of 15-30 μm pixel size can fully exploit the optical quality of the telescope for imaging in periods of excellent seeing. Particular attention will be paid to the optimization of the detectors, these being the dominant component of this simple instrument. The characteristics of the TK1024 CCD which is likely to be used for the first run are the following: the pixel size will correspond to 0.13 arcsec, the field to 2.2×2.2 arcmin. A detailed description of SUSI will be given by S. D'Odorico and H. Kozlowski in a coming issue of the *Messenger*.

The integration of SUSI on the NTT

SUSI (SUperb Seeing Imager)

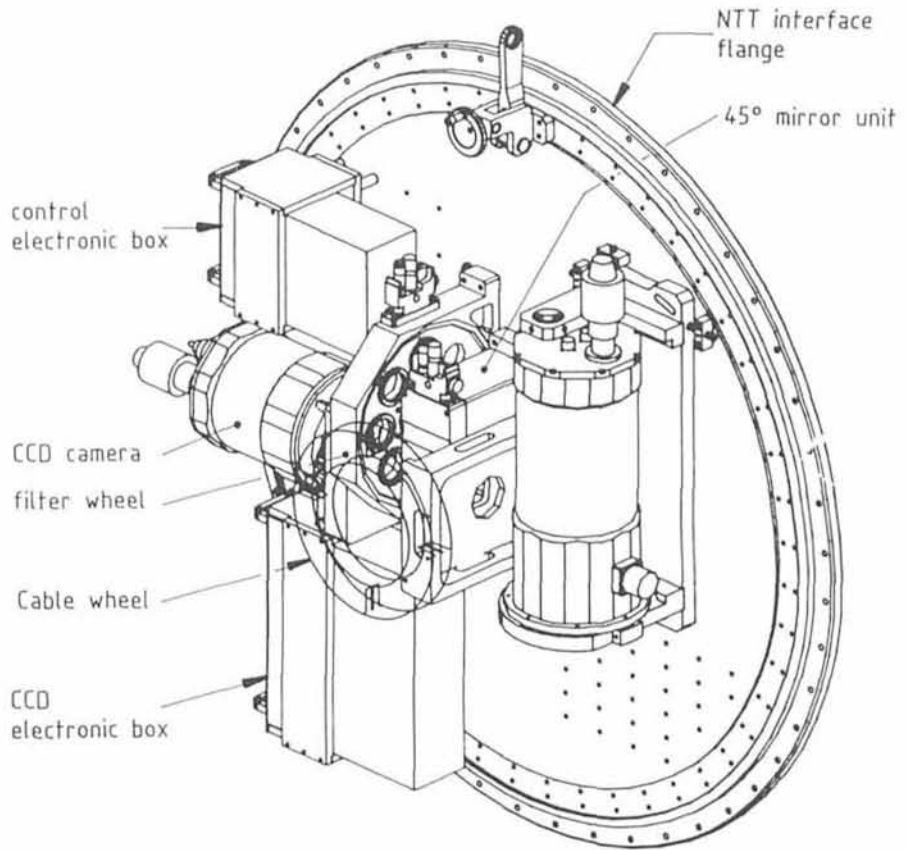


Figure 2: Technical details of SUSI components. The second dewar could be an infrared array camera or will be used as counterweight.

will start at the end of March. After its installation on the telescope, although the instrument is very simple, a number of test nights will be necessary not only to adjust the instrument but also to train the operators to a new observing style. According to the present planning, SUSI should become available to visiting astronomers in the course of Period 47.

The Need for a New Policy of Time Distribution

The distribution of telescope time at ESO, as in most of the other major ground-based "mission" observatories, is done twice a year. Only the start of each six-month period may differ from one institution to another. A detailed review of both the procedure of time allocation and the many parameters that one has to take into account when preparing the observing schedule for various telescopes has been given by Breyssacher (1988, in *Coordination of Observational Projects in Astronomy*, eds C. Jaschek and C. Sterken, Cambridge University Press). Therefore we will not repeat it in full again here and limit ourselves to remind that a particular constraint, much more severe than one

would at first assume, is the absolute need to reduce to a minimum the chance of focal-plane instruments on the telescopes. This is a strong requirement for efficient scheduling because any exchange of instruments implies delicate but also time-consuming mechanical and optical adjustments. An instrument cannot, for instance, be mounted for one short observation only, because the associated loss of telescope time to the community is then of the same order as that gained for a single user.

In short, the important and unavoidable consequence of all the constraints imposed on the scheduler is that once the "puzzle" for an observing period has finally been solved, the resulting observing schedule is so stiff that almost no change in it can then be envisaged without substantial modifications of the whole. The fact that travel arrangements for visiting astronomers to La Silla have to be made about two months in advance is a further strong limitation to modification at short notice of the observing schedule.

Such a situation is clearly not compatible with the implementation of flexible scheduling which, ideally, should allow

to refit the schedule every night, almost in real time, according to the meteorological conditions – excellent seeing or low atmospheric vapour content, for example – prevailing at the observatory. Technically, such a mode of operation evidently requires that on the telescopes having various focal-plane instruments, one is able to execute any change-over without loss of observing time.

Flexible Scheduling of the NTT in the Second Half of 1991

Ground-based telescopes of the new generation, like the NTT, have their auxiliary equipment especially designed for this mode of operation. This is why ESO will start implementing flexible scheduling – although not at the ideal level described above – on this telescope as from Period 48 (1 October 1991 – 1 April 1992). The available instruments being EMMI, IRSPEC and SUSI, in a first stage the following policy has been proposed to and discussed with the OPC by the Director General. Three categories of programmes are considered.

(A) Programmes presented for observations with EMMI which explicitly include a back-up programme to be conducted by the observer with SUSI, should the seeing conditions become superb during his/her EMMI run.

(B) Programmes requesting either EMMI or IRSPEC exclusively, not capable of using superb seeing for decisive scientific advantage and which should be considered as “programmes with risk interruption”, because if optimum seeing conditions appear, the astronomer-in-charge on La Silla is able to decide to interrupt such a programme in order to carry out a programme of type (C) with SUSI (by service mode). To compensate for the risk, such programmes should be allocated a minimum of three nights in order to ensure that these can still be carried out with some success even when interrupted.

(C) Programmes requiring direct imaging with excellent seeing conditions and hence SUSI exclusively. As these kinds of observations are unpredictable, they will be conducted in service

mode. Typically, hours rather than whole nights will be requested. However, if applications for SUSI observations cannot be conducted during the requested period they will not be carried over to the next observing Period.

A Gain of Experience for the VLT

The flexible scheduling experiment described above aims at the best possible use of La Silla's best nights at the NTT. It will also contribute to establish detailed rules required for an efficient implementation of flexible scheduling in the future.

SUSI's deep high-resolution images of the sky will provide important information, new ideas, ancillary and complementary observations to the Space Telescope, transforming our paradigms of direct imaging.

The use of EMMI, IRSPEC and SUSI in a flexible mode will certainly contribute to achieve familiarity for the future use of the VLT with regard to instrumental design, operations mode and observing schedule optimization.

PROFILE OF A KEY PROGRAMME:

The Distance of the Centaurus Group – a Test for Various Distance Indicators

G.A. TAMMANN¹, B. BINGGELI¹, M. CAPACCIOLI², M. DELLA VALLE³, E. GIRAUD³,
R. KRAAN-KORTEWEG¹, G. PIOTTO², A. SANDAGE⁴, M.-P. VÉRON⁵, P. VÉRON⁵,
S. WAGNER⁶, R.M. WEST⁷

¹Astronomisches Institut der Universität Basel, Binningen, Switzerland; ²Osservatorio Astronomico di Padova, Italy; ³ESO, La Silla; ⁴Observatories of the Carnegie Institution, Pasadena, USA; ⁵Observatoire de Haute-Provence, France; ⁶Landessternwarte Heidelberg-Königstuhl, Germany; ⁷ESO, Garching

Introduction

Extragalactic distances are not only important for the determination of the intrinsic properties of galaxies and clusters of galaxies, but also for the calibration of the (present) value of the Hubble constant H_0 , which is one of the fundamental parameters of cosmology. This calibration has posed great difficulties in the past, mainly because of poorly controlled selection effects and because of the faintness of reliable distance indicators at the required distances. The NTT opens here new possibilities.

Background

Presently many extragalactic distance indicators are used without an objective judgement on the intrinsic merits of the

specific method. For the Virgo Cluster more than eight different individual distance determinations (globular clusters¹, novae², supernovae³, D_n - σ relation⁴, Tully-Fisher method⁵, planetary nebulae⁶, $H\beta$ - σ relation of HII-regions⁷, surface brightness fluctuations,⁸ etc.) are available, but the results are at least partially uncertain and discrepant, such that the Virgo distance is still considered to be controversial (with values between 15 and 22 Mpc)⁹. An objective analysis of the different methods and their uncertainties is very difficult here because of the relatively large distance of the Virgo cluster and the heterogeneity of the data.

In the present programme, therefore, the reliability of as many distance indicators as possible will be tested in a

nearer group of galaxies, where also Cepheids – the most reliable distance indicators at present – are still accessible, and where the dependence of the distance indicators on galaxy type and galaxy luminosity can be studied.

The Key Programme intends to determine the distance of five members (2 early-type, 3 late-type galaxies, covering a wide range in luminosity) of the Centaurus group using Cepheids, novae, globular clusters, planetary nebulae, brightest stars and others as far as possible. This group is 2 to 4 times nearer than the Virgo cluster and the observational limitations are therefore much less severe. On the other hand the group is distant enough that CCD frames cover a significant fraction on individual group members.

The Centaurus group not only provides an excellent intercomparison and international-consistency test for various distance indicators, but also the mean distance of the group (containing the unique galaxy NGC 5128 = Cen A!) is particularly uncertain – with estimates ranging from 3 Mpc¹¹ to 7.9 Mpc¹² – and deserves a special effort.

Scientific Aim

The following results are expected from the Key Programme:

(1) An accurate distance to the Centaurus group from various distance indicators will establish the most distant reliable milestone in the Universe.

(2) The Cepheids in one large Sc galaxy and two small Im galaxies will directly exhibit the metallicity effect on the period-luminosity (P-L) relation, which is crucial to derive a first-class LMC distance from Galactic Cepheids.

(3) An intercomparison of the results from Cepheids and other distance indicators (novae, globular clusters, planetary nebulae, brightest stars) is obtained. This will allow to assign proper weights to the distance indicators of the Virgo cluster. With the cluster velocity with respect to the Machian frame now at hand¹⁰, this will lead to a high-accuracy determination of H_0 .

(4) The Centaurus group is prolific in supernovae and its distance will provide a fundamental calibration of the luminosity of supernovae of type Ia as standard candles (opening a direct, *independent* route to H_0)¹³ and other supernovae.

(5) There is presently no distance from primary distance indicators known for

an E or S0 galaxy (with the exception of the peculiar E galaxy M32). The two S0 galaxies of the group should be important to calibrate the $D_{\square}-\sigma$ relation⁴ and the surface brightness fluctuation method⁸.

(6) The gravitational pull of a galaxy on the Local Group is proportional to its *apparent* luminosity (if $M/L = \text{const.}$). Because Cen A is roughly as bright as the integrated Virgo Cluster, its decelerating effect of $\Delta v = H_0 r - v_{\text{obs}}$ (where r is the distance of the Centaurus group and v_{obs} the observed mean velocity of that group [$v_{\text{obs}} = 273 \text{ km s}^{-1}$, corrected for Virgocentric infall]) is expected to be of the same order as the local infall into the Virgo cluster¹⁰. A confirmation would greatly contribute to our understanding of the correlation between (visible) density fluctuations and peculiar velocities.

Strategy

For an evaluation of the feasibility of the Key Programme a relatively large distance is *assumed*, i.e. $(m-M)_{\text{AB}} \sim 29.0$ and $(m-M)^{\circ} \sim 28.8$ (5.8 Mpc). The angular separation of the galaxies, which agree closely in redshift, suggests a depth effect – sphericity assumed – of $0^{\text{m}} 4$, but the multiple distance information and the apparent association of NGC 5128/UKS 1324–41 and NGC 5236/NGC 5264 will offer a good handle to solve for any appreciable depth effect.

The Key Programme will rely primarily on the following distance indicators:

(1) Cepheids. The three late-type galaxies will have an ample number of Cepheids with $P > 10^4$ within one suit-

ably placed frame. 24 exposures in B, taken at 2-day intervals (except during bright time) are needed for the period determination. The Cepheids have mean magnitudes $\langle m_B \rangle \leq 26.1$ (requiring a *detection* limit of 27.0 at minimum) and $m_B(\text{max}) \leq 25.2$. If the group is (improbably) more distant than assumed, the P-L relation at maximum light can be used solely with little loss of accuracy¹⁴. For optimal control of inter-national absorption additional plates in V, R and I are needed, but because the amplitudes are progressively smaller at longer wavelengths 6, 6, and 4 exposures, respectively, are here sufficient to obtain reliable mean and/or maximum magnitudes¹⁵.

(2) Novae. NGC 5128 produces ~ 30 novae per year¹⁶. The search will be done on V exposures because of their large field and the high quantum efficiency. Essentially all of the novae are contained in four V frames, two on either side of the dust lane. 45 exposures of the four frames, spaced by 2 days (incl. some grey time), will yield ~ 7 novae. These novae will be searched for in real time and must be followed in B (five plates each, spaced by 2 days), because the luminosity-decline rate relation is locally calibrated only in B¹⁷. The fainter novae must be followed down to $m_B = 25.0$ with $S/N = 10$. No nova rate is available for NGC 5236. If its distance is as small as 3 Mpc, its absolute magnitude would be only ~ -19.5 and the nova rate would be correspondingly low. A search programme is therefore postponed until a more accurate distance is known, which will allow to predict the success rate.

(3) Globular clusters. NGC 5128 has a

Idyllic La Silla!



Not all visiting astronomers are so engulfed in their observational work that they have no time to enjoy the beautiful night sky at La Silla. Susanne Hüttemeister from the Max-Planck-Institut für Radioastronomie in Bonn (Germany) is one of these and during an observing trip to the SEST in late September 1990, she took the two photos shown here. On a moonlit night, the light from that orb is reflected in the SEST, and the southern latitude of La Silla is indicated by the fact that the north celestial pole is below the horizon.

total population of 900 globular clusters within 16:1¹⁸. For a good distance determination they should be followed 2 mag beyond the peak of their luminosity function^{1,19}, i.e. $M_B = -5$ or $m_B = 24.0$. Their identification will rest (a) on statistical subtraction of foreground stars and background galaxies, and (b) on (partial) resolvability. Because of the relatively large number of foreground stars, a large field must be surveyed, particularly since it is not yet known down to which magnitude the clusters will appear to be resolved with the NTT. 16 blue frames are needed, of which the inner six are expected to be available from the nova follow-up. Almost the entire field will be covered by 6 V frames that are needed for colour information. Scaling by luminosity, 350 clusters within 10"0 are expected for NGC 5102. This requires 9 blue and 4 V frames. The cluster population of NGC 5236 must be much smaller (~80?). Here the cluster identification depends entirely on resolution. Nine blue frames are requested under optimal observing conditions for later follow-up spectroscopy (this not being part of the present proposal). Eventually the globular clusters in this Sc galaxy are decisive to test whether their luminosity function depends on galaxy type.

(4) Planetary nebulae. To establish the luminosity function of planetary nebulae for different galaxy types one central frame in each of the five programme galaxies is needed. For a reliable identification four exposures in the red channel are required: [O III] $\lambda 5007\text{\AA}$ -on, $\lambda 5007\text{\AA}$ -off, H α -on, and H α -off. Judging from the luminosity functions presented for the Virgo Cluster⁶, the photometry should be carried out down to 26.5 mag. Because of the narrow filters grey time is permissible.

(5) Brightest stars. The B and V frames under (3) of the two S0 galaxies are likely to resolve the brightest stars of the red-giant tip; they will be valuable as future distance indicators for E and S0 galaxies. Additional distance information will be obtained from the brightest blue and red stars²⁰ of the three late-type galaxies. They will be identified from B, V colour magnitudes diagrams. The necessary frames are obtained under (1) and (3); only four additional V frames are needed for NGC 5236.

Conclusion

The first nine half-nights have been allotted to the Key Programme, beginning in April, 1991. They will be devoted almost entirely to the Cepheids. The decisive test is to demonstrate that they appear within the expected magnitude range. In the positive case, even a pre-

SEST Users' Meeting and Workshop on Millimetre-Wave Interferometry

The second SEST Users' Meeting will be held at ESO Garching on Wednesday 22 May 1991, and it will be followed by a one-day workshop on current developments in millimetre-wave interferometry on Thursday 23 May. Further information can be obtained from the Secretariat of the Science Division.

liminary Cepheid distance of the Centaurus Group will allow to further optimize the strategy for the other distance indicators.

Until the new generation of instruments will become available on Space Telescope, the NTT is probably the only telescope with which the present project can be carried out. If successful, the project should also outline future avenues of the VLT.

It is obvious that the present programme would have little hope of success without the institution of the Key Programme.

References

- Harris, W.E. 1988, in *The Extragalactic Distance Scale*, ASP Conference Series No. 4, eds. S. van den Bergh and C.J. Pritchet (Provo: Brigham Young Univ. Press), p. 231.
- Pritchet, C.J., and van den Bergh, S. 1987, *Ap.J.* **318**, 507. — Capaccioli, M., Cappellaro, E., Della Valle, M., D'Onofrio, M., Rosino, L., and Turatto, M. 1990, *Ap.J.* **350**, 110.
- Leibundgut, B., and Tammann, G.A. 1990, *Astron. Astrophys.* **230**, 81.
- Dressler, A. 1987, *Ap.J.* **317**, 1.
- Kraan-Korteweg, R.C., Cameron, L., and Tammann, G.A. 1988, *Ap.J.* **331**, 620. — Fouqué, P., Bottinelli, L., Gouguenheim, L., and Paturel, G. 1990, *Ap.J.* **349**, 1. — Pierce, M.J., and Tully, R.B. 1988, *Ap.J.* **330**, 579.
- Jacoby, G.H., Ciardullo, R., and Ford, H.C. 1990, *Ap.J.* **356**, 332.
- Melnick, J., Terlevich, R., and Moles, M. 1988, *M.N.R.A.S.* **235**, 297.
- Tonry, J.L., Ajhar, E.A., and Luppino, G.A. 1990, *A.J.*, in press.
- For reviews of the Virgo Cluster distance cf. e.g. Tammann, G.A. 1988, in: *The Extragalactic Distance Scale*, ASP Conference Series No. 4, eds. S. van den Bergh and C.J. Pritchet (Provo: Brigham Young Univ. Press), p. 231 — Tully, R.B. 1990, *Astrophysical Ages and Dating Methods*, 5th IAP Meeting, Paris, in press. — van den Bergh, S. 1989, *Astron. Astrophys. Rev.* **1**, 111.
- Sandage, A., and Tammann, G.A. 1990, *Ap.J.* **365**, 1.
- Tonry, J.L. and Schechter, P.L. 1991, in press.
- Sandage, A., and Tammann, G.A. 1975, *Ap.J.* **194**, 223.
- Branch, D., and Tammann, G.A. 1991, *Ann. Rev. Astron. Astrophys.*, in press.
- Sandage A. 1988, *P.A.S.P.* **100**, 935.
- Freedman, W.L. 1991, *Ap.J.*, in press.
- Ciardullo, R., Ford, H.C., Williams, R.E., Tamblin, P., and Jacoby, G. 1990, *A.J.* **99**, 1079.
- Capaccioli, M., Della Valle, M., D'Onofrio, M., and Rosino, L. 1989, *A.J.* **97**, 1622, and 1990, *Ap.J.* **360**, 63.
- Harris, H.C., Harris G.L.H. and Hesser, J.E. 1988, in: *The Harlow-Shapley Symposium on Globular Cluster Systems in Galaxies*, eds. J.E. Grindlay and A.G.D. Philip, IAU Sympos. No. 126, p. 205.
- Wagner, S., Richtler, T., and Hopp, U. 1991, *Astron. Astrophys.*, 241, 399.
- Sandage, A., and Carlson, G. 1988, *A.J.* **96**, 1599.
- Zickgraf, F.-J., Humphreys, R.M., Sitko, M.L., and Manley, T. 1990, *PASP* **102**, 920.

STAFF MOVEMENTS

Arrivals

Europe:

ALBRECHT, Miguel (D),
Astronomer/Data Archivist
BECKER, Joachim (D), VLT Project
Manager/Head VLT Division
CAROLLO, Marcella (I), Student
CLASS, Shala (D), Laboratory
Technician (Photography)
DE JONGE, Peter (NL),
Construction Site Manager
DE RUIJSSCHER, Resy (NL),
Technical Secretary
SILBER, Armin (D), Technician
(Instrument Integration)

Chile:

ALTIERI, Bruno (F), Coopérant
GREDEL, Roland (D), Fellow
JORDA, Laurent (F), Coopérant

Departures

Europe:

FERRARO, Francesco (I), Fellow
PRUGNIEL, Philippe (F), Fellow
SCHLÖTELBURG, Martin (D), Fellow

Chile:

HUTSEMÉKERS, Damien (B), Fellow

Instrumentation Beyond the Year 2000

Panel Discussion at the XII ERAM in Davos

On the occasion of the XIIth ERAM in Davos, a panel discussion organized on October 11, 1990, was devoted to "Instrumentation Beyond the Year 2000". Such a panel fitted well the general theme of the Davos meeting entitled "European astronomers look to the future", and was also a valuable follow-up to the panel of the previous day on "Cooperation in astronomy in the new

Europe" (see a report by P. Léna in the *Messenger* No. 62, p. 19–20, December 1990).

Four panel members presented their thoughts on "Radio astronomy in the year 2000, and beyond" (R. Booth), "Post VLT optics and telescopes" (R. Wilson), "The future of X- and γ -ray astronomy" (G. Bignami) and "Future far infrared and sub-mm astronomy"

(R. Genzel).

Two other panelists had been invited but were not present: A. Finkelstein and A. Labeyrie, the latter having sent some transparencies for a short presentation of an optical very large array.

In the present issue of the *Messenger* we have the pleasure of presenting these contributions.

J.P. SWINGS, Liège (Convener)

Radio Astronomy – Towards the 21st Century

R.S. BOOTH, Chalmers University of Technology, Onsala Space Observatory, Sweden

1. Introduction

Advances in radio astronomy may be related to technical developments in several major areas. Among these I would list increased sensitivity of receivers and receiving systems, extended spectral range to cover the whole of the radio band of the electromagnetic spectrum, higher resolution – spectral, temporal and spatial (angular), together with improved data analysis facilities and techniques.

Radio systems have now reached a high degree of sophistication but improvements are certain in the 2000s especially in spectral range – the extension of the radio band to cover millimetre and submillimetre wavelengths and in angular resolution through VLBI.

2. Sensitivity of Receiving Systems

The performance of a radio telescope and associated receiver is characterized in terms of the figure of merit, G/T , where G is the system gain and T the equivalent noise temperature of the system. The gain of a telescope is given in terms of its area, A , wavelength, λ by $4\pi A/\lambda^2$. This factor is further modified by an efficiency factor, h , related to the efficiency of illumination by the primary feed and the surface accuracy (an rms accuracy of $\lambda/20$ reduces the gain by a factor of ~ 1.5).

2.1 Large telescopes for the 21st century

Large antennas are required to improve G and at centimetre wavelengths the ultimate size for a fully steerable

telescope, in terms of cost, seemed to have been reached in the 100-m Effelsberg antenna. Its design is based on the homology principle where gravity deformations are constrained so that the primary reflector maintains a parabolic shape, albeit with varying focal length. The focal position changes with elevation angle and the primary feed or secondary mirror (when in Gregorian configuration) is moved to compensate. The success of the homology design is demonstrated by the fact that the 100-m telescope is still 30% efficient at a wavelength as small as 7 mm. The homology principle is adopted in most new radio telescopes.

The unexpected collapse of the 300-ft transit telescope at NRAO in W. Virginia has provided the incentive to build another large fully steerable antenna in the USA. This will be the new Green Bank Telescope which will have an unblocked aperture, 100 m in diameter. This will be achieved with an offset design involving a primary/Cassegrain secondary focus arrangement suspended on a large beam above the main reflector (see Fig. 1). I do not expect that there will be any further large telescope in the West, in the early 2000s at least, but we will see the completion of the Soviet 70-m telescope near Samarkand. This antenna, and the Green Bank telescope will be operated at wavelengths down to 3 mm.

2.2 System temperature

Receiver noise temperatures, T_r , have improved dramatically during the past 5 years through the use of high electron mobility transistors (HEMTs), cooled to physical temperatures of around 15 K, and at wavelengths down to about

1 cm, receiver noise temperatures are approaching the quantum limit, T_q . However, the total system temperature, T , has a number of other contributions.

$$T = T_q + T_{cb} + T_{at} + T_{sl} + T_r$$

where T_{cb} is the cosmic background temperature, T_{at} is the contribution from the atmosphere which is most severe at very long (m) and very short (mm) wavelengths due to the ionosphere and troposphere respectively, and T_{sl} represents the noise power picked up in the sidelobes. T_{sl} includes a contribution from man-made interference which has

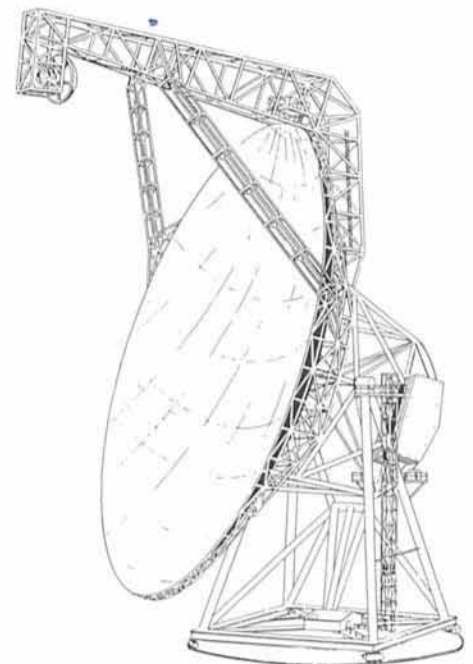


Figure 1: Diagram demonstrating the concept of the Green Bank Telescope.

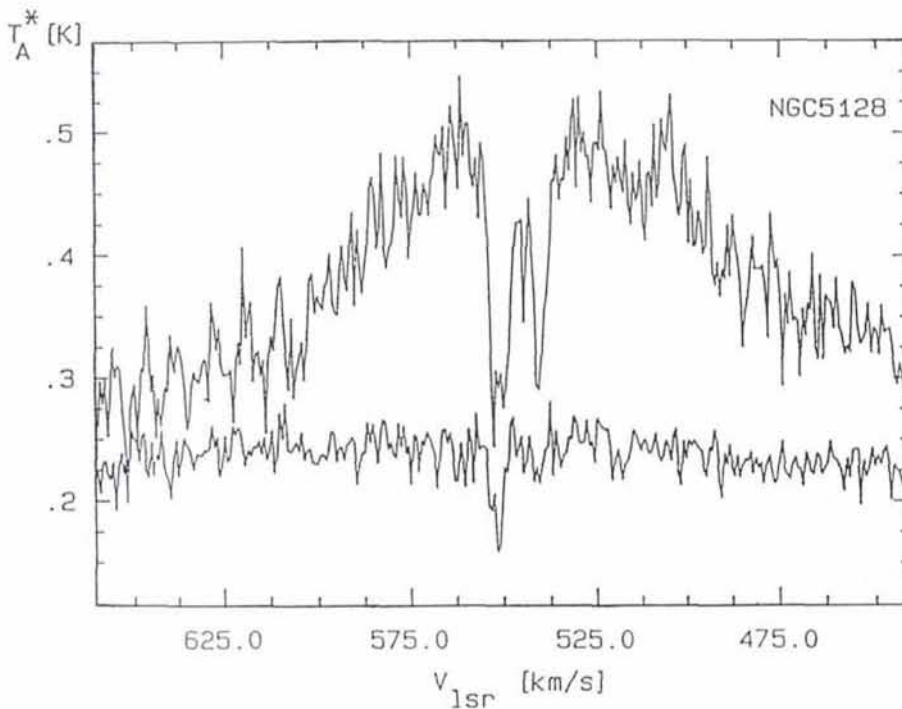


Figure 2: $^{12}\text{CO}(1-0)$ (upper) and $^{13}\text{CO}(1-0)$ spectra taken towards the central region of Centaurus A with the SEST telescope. The spectra contain broad emission lines continuing outside the spectral window. The line emission is superposed on the nuclear continuum of about 0.2 K. The relatively narrow absorption lines are seen in both ^{12}CO and ^{13}CO . It is clear that it is mainly nuclear continuum which is absorbed by the cold CO gas since the ^{13}CO absorption is deeper than the line emission.

become serious at some wavelengths and will probably become worse in the 21st century. However, minimum noise temperatures of about 20 K are currently achieved at centimetre wavelengths in an interference free environment.

At millimetre wavelengths receiver temperatures should also reach the quantum limit by the 2000s. Much effort is going into replacing the current Scottky and SIS (superconducting) mixers by HEMT amplifiers for 7 mm and 3 mm wavelengths. The extension of SIS technology to even shorter (submillimetre) wavelengths is being actively studied and expectations are high. For observation at millimetre wavelengths, high, dry sites are important to reduce the atmospheric (tropospheric) contribution to the system noise.

3. Spectral Range – Bridging the Gap Between Radio and Infrared Astronomy

The discovery of interstellar molecules and their importance in stellar evolution has been a major driver in the development of millimetre/submillimetre radio astronomy. The spectral transitions observed are, in the main, rotational transitions which have their ground state lines at these wavelengths. Molecular emission is now detected in nearby galaxies and, with improvements in sensitivity, in not so nearby galaxies

(e.g. CO has been detected in a galaxy with a redshift, $z = 0.163(1)$) thus giving us information on stellar evolution in these extragalactic systems. Figure 2 shows interesting observations in the CO line of the southern galaxy Centaurus A from Eckart et al.

However, molecular studies are not the only reason for pushing to higher frequencies. At wavelengths of about 1 mm it becomes possible to observe emission from interstellar dust. This emission is optically thin and readily interpreted – in fact, measuring the dust emission from galaxies at 1 mm may become the standard technique for measuring the masses of most galaxies(2).

Finally, the extension of the spectral range for continuum measurements on quasars and radio galaxies is also very important. In particular, the observation of radio quiet quasars is of great interest, for it is in the submillimetre or far infrared that their emission must turn off.

3.1 Telescopes for millimetre/sub-millimetre astronomy

The importance of astronomy at the shortest radio wavelengths is shown by the large number of telescopes built or planned. 14 telescopes with diameter greater than 10 m have been listed by Booth(3) and several more are being built.

The largest instruments are the Nobeyama (Japan) 45-m antenna and the 30-m telescope in Pico Veleta (Spain) of the Institute for Radio Astronomy at Millimetre wavelengths (IRAM), the French-German institute based in Grenoble. The latter telescope is operating regularly at a wavelength of 1.3 mm. As we have seen, dry mountain sites are important for the shortest wavelengths since tropospheric water vapour severely attenuates the signals and its emission degrades receiver performance. Therefore 2 telescopes for use at submillimetre wavelengths have been built on Mauna Kea in Hawaii (altitude 4000 m) (the Caltech 10.4-m and the James Clerk Maxwell Telescope (JCMT), a 15-m telescope operated jointly by the UK, the Netherlands and Canada) and a third, the Swedish-ESO Submillimetre Telescope (SEST), has been constructed on the ESO site of La Silla in Chile (altitude 2300 m). This telescope is important because of its coverage of the southern skies. In addition, the Max-Planck-Institut für Radioastronomie in collaboration with the Steward Observatory in Arizona is building a 10-m submillimetre telescope on Mount Graham in Arizona.

Most of the millimetre telescopes use the homology principle in their design. An important new step for the next decade could be the inclusion of a phase corrector plate or a deformable sub-reflector to further compensate for non-homologous gravitational (and even wind) deformations.

3.2 Millimetre wave arrays

Several arrays have been constructed for high-resolution mapping using the aperture synthesis technique. In particular we cite the Hat Creek array of three 6-m antennas and the Caltech 3×10 m array at Owens Valley. Both arrays are operating at 3 mm wavelength (where they have angular resolution ≈ 1 arcsec) and plans to extend their frequency coverage to 1.3 mm with an increased number of elements are going ahead. A Japanese array of five 10-m antennas has been built at Nobeyama and an IRAM 3×15 m element array is now operational on Plateau de Bure in the French Alps. Again both instruments will be upgraded by the addition of more elements to increase their speed during the next few years.

Further millimetre/submillimetre arrays for the 2000s are planned. NRAO will probably build a large millimetre array near the VLA site in New Mexico and the Smithsonian Astrophysical Observatory is working on a submillimetre array which will be built on Mauna Kea. Finally, now ESO has chosen Cerro Pa-

ranal as the site for the VLT, some of us are interested to investigate the possibility of building a millimetre/submillimetre array on the plateau to the south of the peak. This would be a significant complement to the Australian telescope for southern hemisphere observations.

3.3 Further technical developments

Galactic Molecular Clouds may be up to $10-15^\circ$ in angular extent but can contain components or structural variations on scales of less than one arcsecond. The same applies to the overall molecule structure of galaxies. Thus, to map them fully even with a 10-m telescope (beam width at $3\text{ mm} \approx 1.5\text{ arcmin}$) is a time consuming process. For this reason focal plane arrays (radio cameras) are being developed for single antennas which will improve the mapping speed by an order of magnitude. Such an array with eight beams is operational on the 12-m NRAO Kitt Peak telescope(4).

In addition, imaging analysis techniques such as the maximum entropy method are being developed which utilize all the information (spatial and velocity (frequency)) in the spectroscopic data and impose natural constraints such as positivity to achieve the highest available resolution(5). Further, techniques combining interferometer and single telescope data and mosaicking several fields of view are providing large-scale maps with the resolution of the interferometer ($\approx 1\text{ arcsec}$)(6). These techniques are only possible with the use of large fast computers but are already producing a wealth of detail on the molecular clouds and hence the star formation process.

3.4 Submillimetre telescopes of the future

In order to bridge the final gap between the submillimetre far infrared regions of the spectrum it becomes essential to place telescopes above the earth's atmosphere since its transmission becomes extremely low at these wavelengths. Some balloon-borne telescopes are under development and a telescope is regularly flown in a high flying aircraft – the Kuiper observatory. These are all relatively small telescopes and they are not entirely free of atmospheric attenuations. Thus to achieve a significant development in the 500 GHz to 1 THz spectral region it becomes essential to place a telescope in space.

An important project, the Far InfraRed and Submillimetre Telescope (FIRST) has been defined as a cornerstone in the

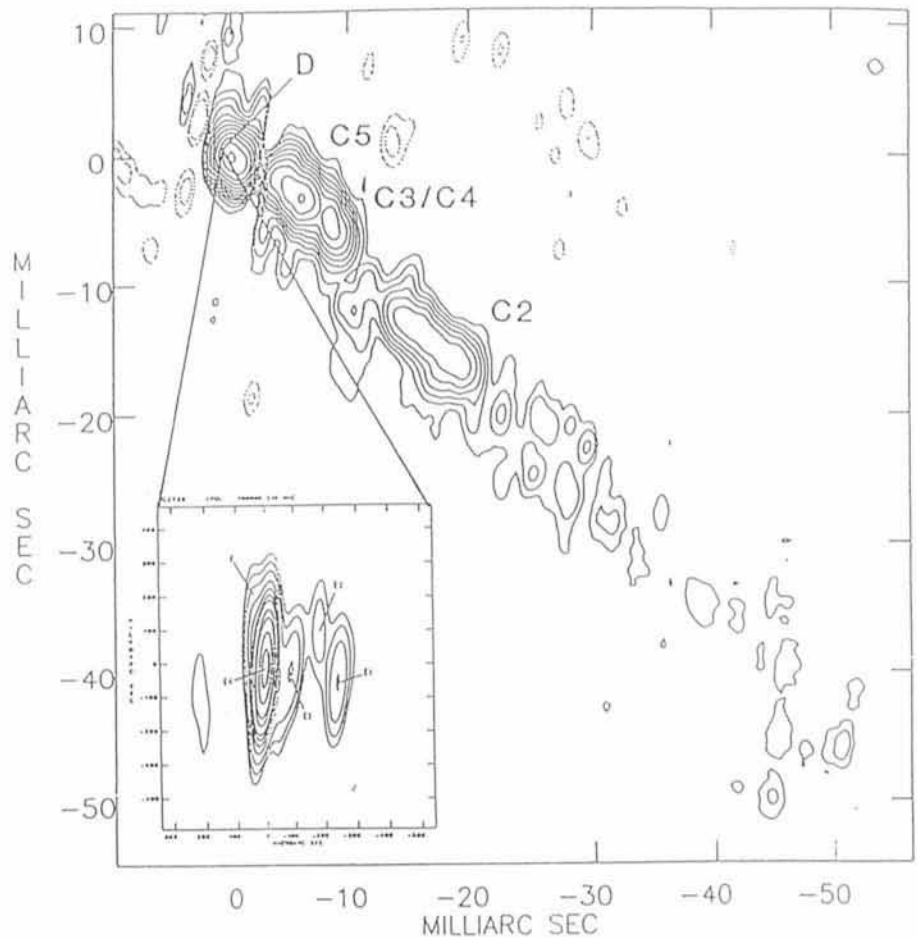


Figure 3: A VLBI map of the central region in the quasar 3C273. The resolution (FWHM) is $0:001$. The lowest contour level is 0.05 per cent of the peak. The high dynamic range in this map makes it one of the best maps ever made from VLBI data (from Zensus, Bååth, Cohen, 1988). Inserted is a map from a recent VLBI experiment at 3 mm wavelength showing the core (component D) in much finer details. The resolution of this map is $0:00005$ (from Bååth et al., 1991).

ESA programme, Horizon 2000. This 4.5-m antenna will be launched sometime after the turn of the century. In the USA a more ambitious project, the large deployable reflector, LDR, has been proposed. This telescope will be a composite reflector, of 20 m in diameter. It will be realized only well into the 2000s. At least 2 more smaller satellite-borne submillimetre telescopes for observations in the 500 GHz region are in the design phase. These are SWAS a 50-cm antenna to be launched as part of the explorer series in the USA and MOSES, a combined astronomy and aeronomy project being studied by a Swedish team of European astronomers. If they successfully pass all the study phases, both will be launched in the mid-90s.

Although in the distant future, the larger projects are of great interest since they open up regions of the spectrum where the bulk of the dust emission is to be seen. In addition, high excitation lines of molecules and fine structure lines of abundant atoms are to be found. As an example of the importance of this

region, about one per cent of the luminosity of the bright star burst galaxy M82 is emitted in the 61-micron line of oxygen(2). Observations in this line will give a totally new set of data for such objects.

4. Improvements in Angular Resolution – VLBI

4.1 Current status

Despite the inherent limitations imposed by diffraction at long wavelengths, radio astronomy provides the highest angular resolution in astronomy. This is achieved through very long baseline interferometry (VLBI) where widely spaced radio telescopes, often in different continents, simultaneously observe radio sources to create interferometers with resolution (= wavelength/baseline) as fine as 50 microarcseconds. This is more than 2 orders of magnitude finer than the space telescope. Even at this resolution there are still unresolved components in the core of a typical quasar or active galactic nucleus.

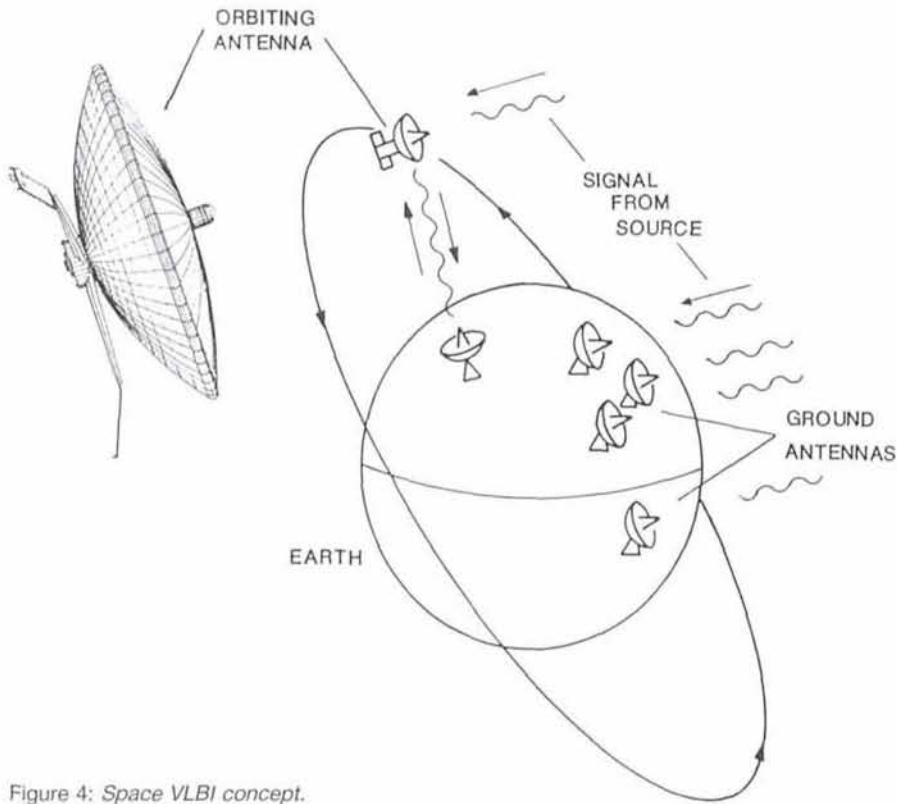


Figure 4: Space VLBI concept.

Since the cores of these nuclei are believed(7) to contain the central energy supply for the radio source, with a massive object (black hole) dominating the gravitational field in the "transrelativistic domain" (10^{15} - 10^{18} cm) inside the so-called broad line region, VLBI observations with the highest resolution and over a wide frequency range are extremely important.

In VLBI it is impossible to connect the interferometer elements directly, so at each telescope the receiver must be provided with a phase stable local oscillator, usually locked to a hydrogen maser frequency standard (short-term stability a few parts in 10^{-15}). There must also be a means of synchronizing the clocks at each of the telescopes and a device (tape recorder) for storing the received signal and precise timing information. The VLBI system is completed with a playback system for correlating the recorded data. VLBI has been described in ref. (8).

VLBI at centimetre wavelengths is now well organized. The world's radio telescopes regularly combine to form two networks, one in the USA, and one in Europe, which sometimes operate separately but often together as a "World Array" consisting of ≈ 15 telescopes. The aperture synthesis technique is employed and sophisticated image processing software enables images of radio sources to be produced with dynamic range $\approx 1000:1$.

4.2 Recent developments

Several developments are in progress: A detected array of telescopes for VLBI is being constructed in the USA. This Very Long Baseline Array (VLBA) will consist of ten 25-m diameter antennas optimally spaced across the USA from the Virgin Islands to Hawaii and a dedicated processor for playback.

In Europe where more telescopes will join the VLBI network, we must build a bigger processor centre and we have applied to the EEC for funding – so far with only limited success.

In Australia a new interferometer network, the Australian telescope (AT) was dedicated recently. It consists of an array of telescopes at Calgoora near Narrabri, Siding Spring near Coonabarabran and at Parkes. These telescopes will operate together with the NASA antenna in Tasmania and a telescope at Hobart in Tasmania to form a north-south array with baselines ranging from 100 to 1500 km. This array will extend the VLBI technique to observations of low declination radio sources only visible from the southern hemisphere.

Finally, VLBI at millimetre wavelengths has recently reached maturity with the production of the first good quality radio source maps at both 7 mm and 3 mm. Figure 3 is a map of the quasar 3C273 at a wavelength of 6 cm(9). The insert is a 3-mm map ob-

tained with a network of millimetre telescopes: Onsala (20-m), U.Mass (14-m), NRAO Kitt Peak (12-m), Hat Creek, Berkeley (6-m), Caltech (10-m), and Nobeyama, Japan (45-m). The resolution is 50 micro arcsec and corresponds to about half a light-year linear resolution at the distance of 3C273(10).

4.3 The future: space VLBI

The size of the earth and the position of the available telescopes limits the resolution in VLBI to $\approx 300 \mu$ arcsec at cm wavelengths and 50μ arcsec at 3 mm, thus to further probe the unresolved components in radio sources it is necessary to have one or more telescopes in space. Space VLBI has more advantages than simply that of increased resolution. It can enable us to achieve the same resolution at say a wavelength of 1 cm as we do on the ground at 3 mm, thus enabling us to examine the spectral properties of the non-thermal emission mechanism producing the observed compact components.

The major difference between Space VLBI and terrestrial VLBI is the use of a phase transfer radio link to convey the reference frequency from a precision frequency standard on the ground to the spacecraft (it is not envisaged currently that the frequency standard will be on-board the spacecraft) and a network of telemetry stations to track the spacecraft and receive the astronomical data by means of another radio link, see Figure 4.

Space VLBI is not simply a figment of our imagination! It has been demonstrated in 2 experiments by a US-Japanese-Australian group led by scientists at JPL who used an antenna of the Tracking and Data Relay Satellite System (TDRSS) in configuration with the NASA 64-m diameter antenna in Canberra, Australia and the 64-m diameter antenna of the Japanese Institute for Space and Astronautical Science at Usuda(11).

Three dedicated space VLBI projects have been proposed: QUASAT(12) – a collaboration between ESA and NASA to put a 15-m antenna into an orbit with apogee 30,000 km; RADIOASTRON(13), a Soviet project to fly a 10-m antenna out to 75,000 km; and VSOP(14), a Japanese project to put a 10-m antenna into an orbit with an apogee of 20,000 km. QUASAT, although highly regarded scientifically, was rejected by ESA on grounds of cost; the other two projects seem certain to be realized before the mid-1990's. We are also studying a second-generation space VLBI mission for the next decade, the International VLBI Satellite, IVS. This will be a 25-m spaceborne antenna operating at wavelengths

as short as 5 mm. It will be used primarily for VLBI down to 7 mm wavelength but will have a single-dish spectroscopic capability for observations of interstellar oxygen. The O₂ lines near 60 GHz are of course not observable from the ground because of the severe absorption by atmospheric oxygen. In its present concept, IVS will have an ESA payload launched by the Soviet Energia rocket and will involve NASA tracking stations.

Current Space VLBI observations, of course, rely on the ground networks as well as the space antennas and since the space element orbits the earth, they become truly international employing ground-based telescopes in all continents. Negotiations are currently underway between the ground organizations and the space agencies. With the experience of cooperation in VLBI already gained, we can expect very successful results in the future.

Well into the 21st century, when space VLBI is established, we may see arrays of telescopes in space providing resolutions as fine as 1 microarcsecond. Perhaps it will be possible to measure quasar proper motions!

5. Epilogue

I have already mentioned the grave problems caused in radio astronomy by man-made interference. In many ways this is not surprising because of the extremely small signals received by radio astronomers (the unit of flux density is 10⁻²⁶ watts Hz⁻¹ m⁻²) and the proliferation of communications equipment. At the World Administrative Radio Conference (WARC) where the frequency bands of the spectrum are allocated to the various services, radio astronomers have to fight hard to keep their precious observing bands. This is because commercial and military users are always demanding more and more channels – sometimes for reasons which can hardly be judged to be important. The situation is becoming so critical in some parts of the spectrum (e.g. near 18 cm wavelength), that suggestions to put radio telescopes on the far side of the moon are being taken seriously.

Radio astronomy is vital to our understanding of the universe and must not be squeezed out of existence by commercial demands. We appeal to our scientific colleagues in other disciplines to help expunge the harmful pollution of the spectrum.

References

- (1) D.B. Sanders, N.Z. Scoville and B.T. Soifer, *Astrophys. J.* **335**, (1988), L.1.
- (2) J.W. Welsh, Tutorial lecture presented at the XXII URSI General Assembly, Tel Aviv (1987).

- (3) R.S. Booth, Proc. ESO-IRAM-ONSALA Workshop on (Sub)millimetre Astronomy. ESO proc. No. 22 (1985), eds. P.A. Shaver and K. Kj ar.
- (4) J.M. Payne, Proc. IEEE, **77**, 993, 1989.
- (5) G. Rydbeck,   Hjalmarson, T. Wiklind and O.E.H. Rydbeck, in *Molecular Clouds in the Milky Way and External Galaxies* (1988), eds. R.L. Dichmann and J. Young.
- (6) L.G. Mundy, T.J. Cornwell, C.R. Masson, N.Z. Scoville, L.B. B  ath and L.E.B. Johansson, *Astrophys. J.* **325** (1988), 382.
- (7) M.J. Rees, IAU Symp. No. 119 (1986), Swarup and Kapalu (eds.), Dordrecht, Reidel.
- (8) R.S. Booth, in *High Resolution in Astronomy* by R.S. Booth, J.W. Brault and L. Labeyrie (1985), Geneva Observatory (publ.).
- (9) A. Zensus, L.B. B  ath and H. Cohen, *Nature* **334** (1988), 410.
- (10) L.B. B  ath et al., 1991, *Astron. Astrophys.* in press.
- (11) G.S. Levy et al., *Science* **234** (1986), 187.
- (12) R.T. Schilizzi, Proc. IAU Symp. No. 129 *The Impact of VLBI on Astrophysics and Geophysics*, eds. M.J. Reid and J. Moran, Dordrecht, Reidel, p. 441 (1987).
- (13) N.S. Kardashev and V.I. Slysh, *Ibid.*, p. 433 (1987).
- (14) H. Hirabayashi, *Ibid.*, p. 441 (1987).

Infrared/Sub-mm Astronomy After ISO (1 μm-0.3 mm)

ISO:	2-200 μm photometry, imaging + moderate resolution spectroscopy at excellent sensitivity
POST-ISO:	High spatial resolution: 1" at 100 μm → D = 10 m 8 m at 2 μm = 0'05 for single dish 100 m at 2 μm = 4 × 10 ^{-3"} for Interferometry λ > 200 μm: colder universe at sub-mm wavelengths High spectral resolution: velocity resolved spectra
PLATFORMS:	VLT+VLT Interferometry (λ ≤ 30 μm, λ ≥ 300 m) Large Airborne Telescope (SOFIA; 2.5 m, visible → 1 mm) Large IR/sub-mm telescope in space (FIRST, SM ³ /LDR λ = 50 → 1000 μm EDISON λ = 2 → 100 μm) Antarctica: ground-based FIR astronomy from Antarctic plateau (e.g. Vostock Station)
INSTRUMENTATION:	Large format, low-noise detector arrays for ground-based (λ = 1 → 30 μm) and space-borne (30 → 300 μm) work Quantum noise limited sub-mm heterodyne receivers
<i>Summary by R. GENZEL, Max-Planck-Institut f�ur Extraterrestrische Physik, Garching bei M�nchen, Germany</i>	

Post-VLT Optics and Telescopes

R.N. WILSON, ESO

I would like, in this brief introduction, to stimulate some thoughts and discussion on what the principal directions of optical telescope development will be after the year A.D. 2000.

Ground-based-telescopes will, I believe, continue to play a major role because of recent optics and electronics developments and the cost advantages that accrue from them. *Space tele-*

scopes will slowly gain in total reflecting area and hence in importance, the rate depending on cost, reliability and increased maintenance and user-friendliness.

1. Ground-Based Telescopes

Throughout its long development after the first manufacture about 1665, the evolution of the reflecting telescope has

been dominated by four parameters:

- Size
- Optical quality
- Tracking and pointing (mountings)
- Cost

One will always wish to build the biggest telescope one can afford which delivers high-quality images with corresponding tracking. But there are many cases in telescope history where excessive ambition on the first parameter – size – has led to failure in the technical requirement of the next two and conflict with the third – cost. These failures through over-ambition have led to products of poor cost-effectiveness. The above four parameters will not change after the year 2000: they will still be drivers a century later or, indeed, as long as ground-based telescopes are built.

For about 300 years, the line of development of conventional telescopes had been largely unchanged since the start. Its main characteristics were:

- Monolithic, stiff primaries
- Conventional figuring procedures
- Stiff tubes and mounts with absolute mechanical tolerances. After about 180 years of alt-azimuth mounts, about 130 years of undisputed triumph of the equatorial mount.

In the last 10 or 20 years, each of these aspects has undergone a revolution. These revolutions are a result – directly or indirectly – of the application of modern electronics and computers. I believe these revolutions will determine the further development after 2000 and well into the next century. They will enable the ground-based telescope not only to survive but also to thrive *because of its cost-effectiveness*.

Let us consider the four basic parameters and the impact of these revolutions on them.

Size

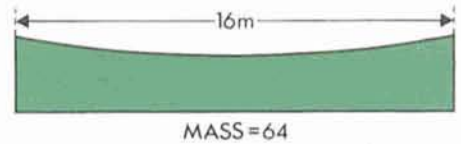
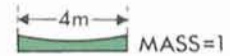
The figure shows the key to increase of size while respecting the other 3 parameters. The key is the abandonment of the full-size monolithic aperture of the primary by the principle of *segmentation* in some form. Whether the segmentation is *direct* (e.g. the Keck 10-m telescope), or *indirect* as in *MMT's* (Multi-Mirror Telescopes: several telescopes on one mount) or *Arrays* of telescopes on different mounts but linked together (e.g. ESO VLT) – this does not change their common aim of reducing the weight compared with a monolithic blank extrapolated with size in the classical way (see the figure). The important difference between these approaches is simply whether the effective aperture is undiluted (direct segmenta-

CONCEPTS FOR REDUCING WEIGHT OF PRIMARY AND EASING SUPPORT PROBLEM - SEGMENTATION

CLASSICAL EXTRAPOLATION:

e.g. RUSSIAN 6m

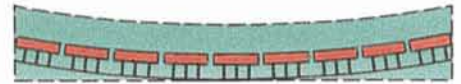
RIGIDITY 16x LESS! →



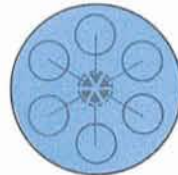
SEGMENTATION SOLUTIONS:

1. "BIG DISH" SEGMENTS:

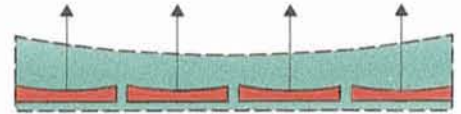
FILLED APERTURE



2. MMT "SEGMENTS": SEPARATE TELESCOPES - SINGLE MOUNT

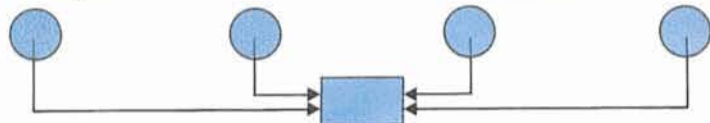


DILUTED APERTURE



EACH TELESCOPE $f/3$ - TOTAL LENGTH $f/1$

3. ARRAYS: SEPARATE TELESCOPES - SEPARATE MOUNTS - ESO VLT



MORE DILUTED APERTURE - INTERFEROMETRY (EQUIV. $\sim f/0.1!$)

tion), moderately diluted (MMT's) or very diluted (Arrays).

With possible variations and combinations, these three basic forms will dominate the aim for large size after 2000 exactly as they are dominating it today, for we are only at the beginning of the consequences of the electronic revolution.

Optical quality

The revolution is due to active optics combined with modern figuring techniques on the one hand, and adaptive optics to correct the atmospheric turbulence on the other. These two developments are complementary: *active optics* corrects classical telescope errors of manufacturing, mechanical or thermal origin which are fixed or vary slowly; *adaptive optics* corrects the rapidly varying effects originating, above all, in atmospheric turbulence. While we at

ESO see active optics as an essentially solved problem on the basis of the NTT and its routine image analysis, adaptive optics is still in its infancy and not yet available as a general system. It is incomparably more difficult than active optics because of its high frequency bandpass and because of the problems of a reference source within the isoplanatic angle.

Development of adaptive optics will undoubtedly be, together with interferometry, the principal development line in telescope optics after 2000. We shall see whether, by the year 2000, full adaptive correction (i.e. for the full effective bandpass) has been achieved for *the visible waveband and for one single isoplanatic field*. If so, it will be a great technical achievement. If not, it will be the principal area of endeavour followed by extension of the field to more isoplanatic fields. But for even modest fields, the information flow rate, apart

from the problems of correction feedback and isoplanatic angle, is formidable to say the least.

For these reasons, search for and investigation of *optimum sites* will continue at an accelerated pace: the most effective adaptive optics is a site where nature has taken as much of the load from us as possible. A further revolution has taken place here, in the scientific understanding of atmospheric optics and the means for proper evaluation of the seeing of sites.

Apart from its intrinsic advantages (see "optical efficiency" below), optimized image quality at optimum sites brings rich advantages in instrument development. The "matching problem" of instrument slit size to pixels has meant that instruments become bigger and more difficult the larger the telescope aperture for a given angular image size of a star. This dilemma is expressed by Bowen's Spectrograph Law:

$$b = S \cdot \frac{Y_1}{206265} \cdot \frac{f_{CAM}}{Y_g} = S \cdot \frac{D_1}{206265} (f/NO)_{CAM}$$

in which

- $b =$ width of the slit image on the detector
 $S =$ image size of a star in arcsec at the slit
 $Y_1 =$ radius of the telescope entrance pupil (normally, the primary mirror)
 $Y_g =$ semi-height of the spectrograph grating
 $f_{CAM} =$ focal length of the spectrograph camera
 $D_1 =$ diameter of the telescope entrance pupil (normally, the primary mirror)
 $(f/NO)_{CAM} =$ f/number of the spectrograph camera

Clearly, the smaller the value of the image S , the larger can be the f/NO of the spectrograph or the smaller the corresponding value of Y_g , determining the size of the grating. High quality imaging benefits all modes of observation, not just direct imaging.

Mounting

The alt-az mounting has returned as the standard because of the revolution in 2-axis tracking. But other forms, perhaps above all various forms of spherical mount, will certainly be further developed in the new century. The domination of the alt-az may have a much shorter life than that of the equatorial. It will be seen, too, whether non-rotational forms of mounting are technically feasible or not. Tracking will be the determinant requirement. Better image quality requires better tracking. In the NTT with its alt-az mount, it is al-

ready clear that the tracking requirement (combined with field rotation compensation) is the hardest technical specification to fill.

Buildings

The trend away from the conventional dome is clear. Cost is not in its favour, but *control of the conditions of the local air* will be the dominant reason for choosing other forms which are also favoured by the alt-az mount. The revolution here was made by the building of the MMT. Apart from external seeing, the local air will be the decisive influential factor in the final optical quality until adaptive optics is available in a general form.

The optimum size of a telescope: optical efficiency

The classical formula for the optical efficiency of a telescope has been known implicitly ever since photography was introduced into observation about 1850:

$$E = k \left(\frac{D}{d} \right)^2$$

where

- $E =$ the optical efficiency
 $D =$ diameter of the telescope pupil (normally the primary)
 $d =$ image diameter of a star
 $k =$ transmissivity

Although this formula is simplistic and only really valid assuming adequate pixel sampling and photon-limited observation in certain regimes, its general validity is proven every night by the integration times used at the NTT. More sophisticated criteria are under investi-

gation for the VLT. A general formula reflecting all different observing conditions, above all background limited, would certainly be more complex. Even if the formula above is accepted only as a rough general approximation, its conclusions are striking: if D is doubled, but d is also doubled, there is no gain in efficiency, but a tremendous amount of money and effort has been wasted: huge "light buckets" of low optical quality are not the path of the future.

After the year 2000, the struggle for bigger size will only give higher efficiency if the conditions of the local air can be adequately controlled or compensated by adaptive optics. These factors will dominate the development scene and determine what the optimum (or maximum) size can be. My colleague Richard West mentioned *cost-effectiveness* yesterday. I should like to take this up and emphasize it. The most *cost-effective* telescope (with instrumentation and detector) is the best for a given observation and size is only one of the parameters involved. The astronomical community will have to think increasingly in these terms to make the best use of its resources. Reduction of d may well be more efficient than increase of D .

It may take 50 years or more to "digest" the size range 10-20 m. Until adaptive optics is available in a fairly complete form (wavelength band, frequency band, reasonable field) the optimum size may be < 20 m or even < 10 m.

2. Space Telescopes

In the absence of an atmosphere, the specification of space telescopes is far simpler than for ground-based tele-

"Tours du Monde, Tours du Ciel"

"Around the world, around the sky" is the title of what is probably the most comprehensive documentary film about astronomy ever made. It was produced by a team of French specialists, headed by Robert Pansard Besson and supported by Pierre Léna and Michel Serres (see also the *Messenger* No. 48, page 33).

During more than three years, Mr. Pansard Besson and his crew travelled to all major observatories in the world, ancient as well as modern. The European Southern Observatory provided support during their visit to Chile and the film includes scenes from La Silla, Paranal and Garching. Many other observatories, also in the ESO member states, are shown and astronomers from all over the world have provided live commentary to various passages in the film.

The film is divided into ten "travels" in time and space: (1) The beginning (160,000 years ago); (2) Around the year 0; (3) From the other end of the world (from -500 to 1000); (4) Around the world, around the sky (1000-1600); (5) Venice, Beijing, Paris (1600-1676); (6) East, West (1642-1743); (7) The starry messenger: the light (1743-1880); (8) The visible and the invisible (1880-1950); (9) Towards the giant mirrors (1950-1970); (10) The light and other messengers (1970-1990). Each part lasts slightly less than one hour. The total playing time is therefore almost 10 hours.

The film is distributed on video cassettes (Pal, Secam, NTSC) from: HATIER, 8, rue d'Assas, F-75006 Paris, France (Tel: 49.54.49.54; Fax: 40.49.00.45). It is available with French commentary, and soon also in English.

scopes: they should be diffraction limited, also in the UV.

The real breakthrough will come when assembly and maintenance can be done in space (on the moon?). HST has made very clear the limitations of pre-assembly and control from the ground.

For individual telescopes, active optics is essential and also the simplest and cheapest solution. HST, I think, proves this clearly. Since there is no atmosphere, *no* adaptive optics is required: it is meaningless. But the harsh thermal environment makes active optics even more necessary than on earth. It also becomes easier in the absence of the disturbing effect of local air: In space, the NTT could go immediately to the diffraction limit even in the UV and be maintained there with simple technology.

Assuming the existence of bigger dif-

fraction-limited telescopes in space after the year 2000, they should be unbeatable for direct imaging of deep, faint objects until a complete solution of adaptive optics is available. Even then, the complete absence of atmospheric turbulence and absorption are bound to give the edge on space observation for direct imaging. However, cost-effectiveness will still mean many observations will be better performed by ground-based telescopes. Space is also the natural environment for interferometry whose success on earth is closely linked to, and dependent on, the advances in adaptive optics.

Wide-field telescope projects in space have been mentioned at this conference and will certainly be carried out. The quality requirements will be far higher than those of any existing ground-based Schmidt telescopes.

Ideas and technologies that will remain a phantasy for high quality ground-based telescopes may be investigated and become a reality in space, e.g. plastic film reflectors with a fixed (dc) or slowly varying active corrector for small fields. Maybe "longer" telescopes may come back since "length" in a weightless environment is of less consequence. The technical possibilities are far wider than for ground-based telescopes.

3. Optical Design Developments

Optical design solutions for telescopes are effectively worked out: it is most unlikely that new design solutions will emerge. Developments will come rather from advanced technologies to realize known designs with higher precision.

X- and Gamma-Ray Astronomy Beyond the Year 2000

G.F. BIGNAMI, IFC/CNR, Milano, and Dipartimento Ingegneria Industriale, Università di Cassino, Italy

Astronomy should progress in a balanced way. This simple statement needs no proof beyond the simple reflection, for example, on the importance for cosmology of the joint radio, optical and X-ray studies of extragalactic sources. Thus, in view of the impressive progress now being planned for the turn of the century at all wavelengths, both from the ground and from space, it is logical to think also of the goals of high-energy astronomy, in X- and gamma-rays.

Celestial objects happily carry on emitting their energy at the wavelength they please, but astronomers have to worry about how to do astronomy with photons that are widely different in their interaction/detection processes. For example, there is a basic difference between X- and gamma-ray photons: while X-ray photons can be focussed by a sufficiently smooth surface, gamma rays cannot because their wavelength is small compared to the interatomic distances in solids. Thus, X-ray astronomy can, and must, rely on focussing telescopes (of ever increasing throughput and angular resolution) and clever focal plane detectors for doing both imaging and spectroscopy of the X-ray sky. This has been the winning recipe introduced by the Einstein Observatory, currently used in the ROSAT mission, and also adopted by the "great observatories" in

X-ray astronomy of the end of this century: NASA'S AXAF and ESA'S XMM.

To speculate realistically on the future of X-ray astronomy beyond such great observatories, means to think of what more can be done using the same technique. Firstly, the optics. Of course, high throughput, essential for high sensitivity, means light-weight material, with all the technological complications involved. Very high (i.e. sub-arcsec) angular resolution will also be mandatory for matching the source positioning at other wavelengths. Such high resolution should be maintained over a wide enough field of view, in itself a big challenge, only now being seriously tackled; but not yet solved. Finally, the focal plane detectors should afford an excellent spatial resolution, so as to correctly oversample the telescope's PSF, but, most importantly, should also have a very high spectral resolution, since accurate spectroscopy will remain a key issue in the X-ray astronomy of the future.

It is difficult, at the moment, to imagine an X-ray observatory with the above characteristics without thinking of a "bigger and better" combination of AXAF and XMM: high-throughput (tens of thousands of cm^2), optics with high resolution (sub-arcsec) over square degrees FOV, suitable imaging detectors, and spectroscopy with resolving power

in the several hundreds. However, it is also difficult to imagine how such a mission could be designed and realized in the current framework of research from space, given the financial and practical constraints within which national and international Space Agencies have to move. No concrete sign for the birth of an idea of such a mission exists at present.

A possibly even more realistic approach would be to specialize missions by splitting the science objectives. For example, a pilot mission centred on high-resolution, wide-FOV imaging, dedicated mostly to extragalactic work, is currently being studied in the context of an Italy-U.S. collaboration, with manageable dimensions and reasonable budget. Complementarily, a mission dedicated to high-resolution spectroscopy of selected sources could capitalize on the wealth of imaging results presumably available in X-ray astronomy by the end of the century.

For gamma-rays, on the other hand, the situation is quite different. Because of the severe limitations posed by the physics of the detection process as well as by the intrinsically poor astronomical signal-to-noise situation, gamma-ray astronomy is only now leaving the exploratory phase, with the imminent launch of GRO, the first gamma-ray Great Observatory. On the eve of such a

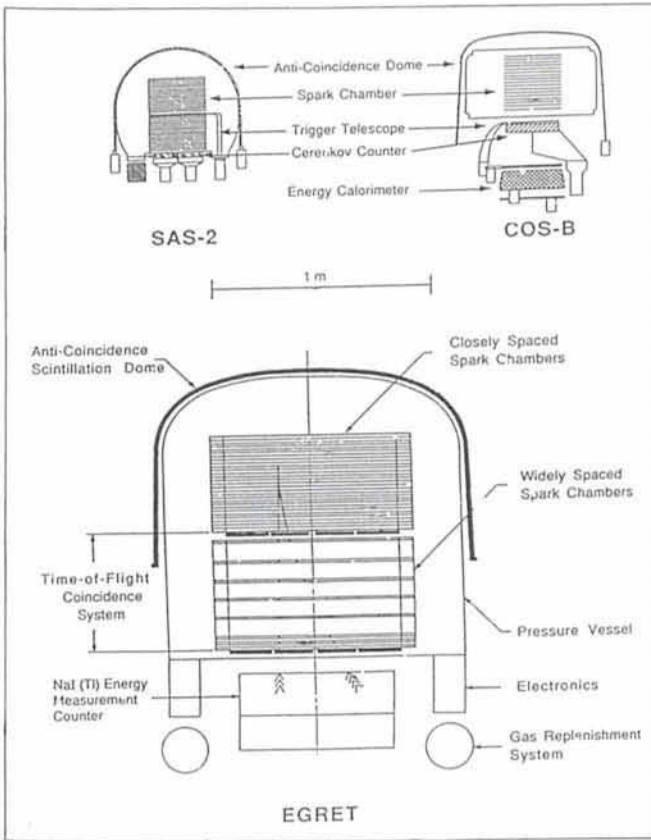


Figure 1: Schematic drawing, to scale, of the three main gamma-ray astronomy space chamber experiments: SAS-2 (1972–1973), COS-B (1975–1982), EGRET (1991–...).

launch, it is of course difficult to say precisely what GRO, with its complement of instruments, will be able to achieve. It is probably easier to speculate on what it will not, because it cannot, achieve.

Here again, as usual in astronomy, it is a matter of sensitivity, background rejection, angular resolution and spectral resolution. For gamma-rays, sensitivity can only be achieved by brute force, i.e. by increasing the exposed square centimetres. In this GRO does quite well, at least within the practical limits of what can be flown on a space mission. For the high-energy experiment (EGRET, sensitive above few tens of MeV), based on the classical spark chamber technology, a straight comparison can be made with the earlier SAS-2 and COS-B missions, showing an increase in the exposed surface of more than a factor of ten (see Fig. 1). Background rejection is also achieved very well on GRO, with different techniques according to the type of instrument and energy range.

However, it is in the field of angular and spectral resolution that the majority of post-GRO efforts will have to be done. The only way realistically applicable for increasing angular resolution in gamma-ray astronomy is the use of the coded mask technique. Conceptually,

this is an extension of the pinhole camera, i.e. of an infinitely-small-aperture collimator centred on the source to be observed. A coded mask is a collimator consisting of roughly half open spaces and half absorber elements arranged in a quasi random, repetitive pattern. A source in the sky will cast the shadow of the absorbing mask onto a detection plane, located at an appropriate distance and capable of sufficient positional resolution. By applying suitable image unfolding techniques, one can then reconstruct the real source distribution, with, of course, the limitations imposed by the instrumental and sky backgrounds. Within the payload of a near future gamma-ray astronomy space mission, a coded mask with cm-size elements could be placed at several metres from the detection plane, for which the technology is already in hand which yields positional accuracies of a few millimetres. The resulting angular resolution or, better, the instrument's source location capability can easily reach the arcminute level or better, depending on signal-to-noise and source statistics.

An ideal new-generation gamma-ray astronomy telescope should not only be able to improve dramatically (by a factor of about 100) the source positioning via the coded mask imaging, but should

also have good spectroscopic capabilities. This is especially desirable in the few MeV range, where nuclear lines promise a new tremendous potential for astrophysics, still virtually untapped.

Very good energy resolution can already be obtained with solid-state (Germanium) cooled spectrometers, reaching a resolving power of nearly 1000 at about 1 MeV. The improvement over existing, classic scintillator spectrometers, for example Na I crystals, is spectacular: Figure 2 shows the effect of Germanium-type resolution on a real spectrum in the nuclear line region. Current technology is beginning to allow the construction of Ge spectrometers in a mosaic of separate elements of dimensions of few centimetres, or less. It is thus conceivable to use such a mosaic as the detection plane for a coded mask telescope, thus coupling high angular and spectral resolution. Indeed, a mission based on the design outlined above, and with the adequate sensitivity, is currently being assessed by the European Space Agency under the name of INTEGRAL, the INTERNATIONAL Gamma-RAY Laboratory. Its timing appears good, coming as it does, just after the GRO will have exploited a maximum in the classical way of doing gamma-ray astronomy.

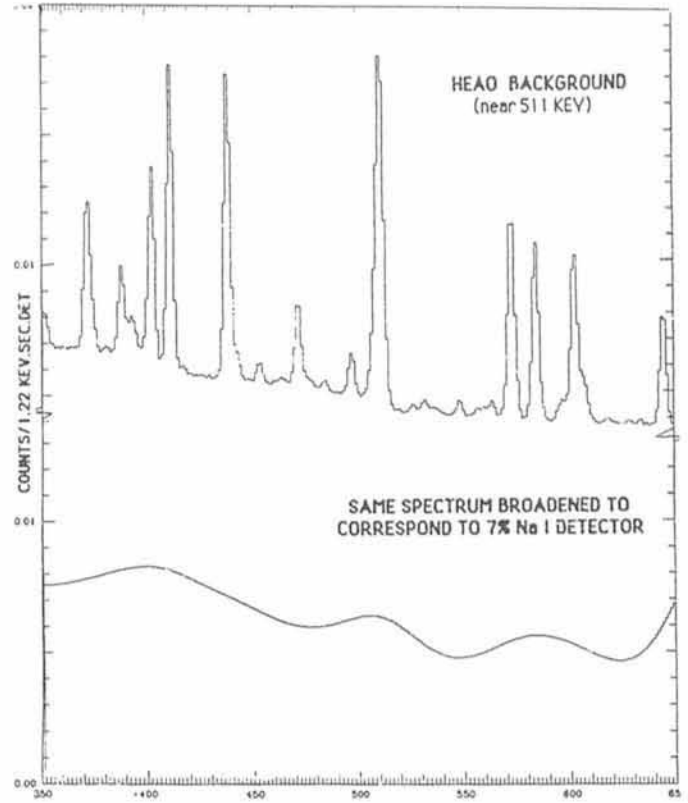


Figure 2: The effect of high spectral resolution: Upper curve: true background spectrum as seen with the HEAO-3 Germanium detector, with $\Delta E/E \sim 1/500$. – Lower curve: the same spectrum folded through the $\sim 7\%$ resolution of a "standard" Na I detector.

Astronomy and Astrophysics: To Be an Editor

J. LEQUEUX, *Astronomy and Astrophysics, Observatoire de Meudon, France*

Founded in 1969, *Astronomy and Astrophysics* has grown fast and is now one of the four leading international journals in Astronomy. It is sponsored by no less than 16 European countries. Without the Supplements, it publishes about 950 papers per year, over 8,000 pages totalling 70 millions of characters; the *Astrophysical Journal* publishes about 100 millions of characters per year while the *Monthly Notices of the Royal Astronomical Society* and the *Astronomical Journal* contain slightly more than 30 millions each. As to the Supplements of *Astronomy and Astrophysics*, they publish about 150 papers per year totalling 2400 pages, against 100 papers per year over 3000 pages for the *Astrophysical Journal Supplements*. These numbers reflect roughly the populations of astronomers in the respective countries with, however, some advantage for the American journals as a number of European astronomers who have apparently not yet discovered the merits of *Astronomy and Astrophysics* and of *Monthly Notices* still prefer to send their papers to the *Astrophysical Journal*, while the reverse is true in only a few specialized fields.

Processing all these papers is a considerable task requiring a fair amount of organization. As I have been involved in this business for more than 6 years as one of the three Editors of *Astronomy and Astrophysics*, I thought that it would be interesting to share my experience with the readers of the *Messenger*. Apparently there are no considerable differences in the way the four major astronomy journals are run, as far as the papers are processed, so that my experience should have some sort of general character.

Let me explain first how the Journal works administratively and financially. *Astronomy and Astrophysics* is directed by a Board formed of astronomers representing the 12 (soon 13 with Czechoslovakia) participating countries. The Board meets annually and takes all decisions concerning finances and policy, including the contracts with the publishers and the designation of the editors. The contributions of the member states together with the relatively small income from page charges paid by non-European authors are administered by ESO and are used to finance the running expenses of the three offices and the salaries of the secretaries. From time to time an extra issue can be paid on money drawn from the reserves of the Board, in order e.g.

to reduce the publication delay by absorbing a part of the backlog. The publication and distribution of the Journal itself is entirely subsidized by the income of the subscriptions which is received directly by Springer Verlag for the Main Journal and by Les Editions de Physique for the Supplements, respectively. The subscription rates and the number of pages published every year are fixed by a contract between the Board and the Publishers. This system is rather different from e.g. that of the *Astrophysical Journal* for which all the income comes from the subscriptions and (to a large extent) from the page charges. Both systems have advantages and inconvenients that I cannot discuss here.

Let me come back to the actual work of an Editor.

First, the authors choose to which Editor they will send their paper. The papers intended for publication as Letters are in principle sent to Stuart Pottasch in Groningen; those intended for the Supplements should go to me in Meudon and the "normal" papers either to Michael Grewing in Tübingen or to me. Many papers submitted as Letters end up as normal papers when they are not considered as very urgent (then Stuart forwards the complete file to me); the reverse is rare. There are also exchanges between the Supplements and the Main Journal. The German authors tend to send their papers to Michael and the French ones to me but there are many exceptions. At present the balance between the normal papers received on both sides is roughly even.

Then the job starts. I first eliminate at once the obvious "crackpot papers" mostly dealing with gravitation, cosmology and cosmogony. They are surprisingly rare (apparently there are not so many misunderstood geniuses in astronomy); the story ends up with a kind letter to the author. The most delicate part is the choice of the referee. We usually use only one referee, but two for the Letters. In rare cases, I referee the paper myself if I feel competent. An ideal referee should be competent, fast, honest, willing to help the author rather than to crush him, kind but firm. These qualities must be less rare than one would think as my computerized referee file contains as many as 1800 names (over some 7000 active astronomers in the world). Of course some referees are better than others and I keep in the computer my confidential evaluation of the work everyone is doing (yes, many

of you have police records in my office!). Choosing the referee is a very subjective affair requiring experience and knowledge of the community. Fortunately astronomers seem to behave better with each other than e.g. biologists, probably because there is less money involved behind their science! I would not dare to say that there are no "chapels" in astronomy but most often the problems are kept within the limits of courtesy.

The most difficult thing with the referees is to obtain their answer! We have an automatic reminder system to send them telexes, faxes or phone calls at regular intervals but this is not always efficient. If after some time we consider that the answer will not come I look for another referee, putting some pressure on him (or her) to obtain a fast reaction. Sometimes his or her comments come together with those of the first referee! The worst case (fortunately rather rare) is that of some referees who write on the acknowledgement card they are supposed to send on receipt of the manuscript that they are very interested and willing to referee, but then don't do anything. Understandably, I hesitate in such cases to contact another referee as early as in other cases and this means more time lost for the author. I hope that the readers of the present paper will sympathize with my difficulties although it is not at all pleasant to be a victim of those extra delays.

The comments of the referees come in an astonishing variety, from those who produce extremely detailed reports and even correct entirely the language of the paper, to those who say only "OK, this should be published" (or rejected) or only remark that a paper of theirs should be cited by the author! I have not been able to discover a rule for this behaviour: there are very busy people with heavy responsibilities who take their job quite seriously and are very helpful, while others do very little. The younger referees are doing somewhat better than the older, although they may be unexperienced. Surprisingly at least 3/4 of the referees allow the Editors to communicate their name to the authors, even if their report is rather harsh.

Anyway, the referees give only advice and recommendations: the Editors are taking the decision and do not necessarily follow the referee. We may call for another referee if we think that this is useful, etc. Sometimes the referee may ask to see the paper several times when this does not really seem

necessary: then we don't comply, especially if we suspect that this might be a way of delaying the publication of the paper (such cases do exist but are fortunately quite rare). In general the system works well and results in substantially improved papers. The rejection rate is only about 11 per cent (not including the papers rejected initially but eventually accepted after major changes). This may seem small in comparison to physics, chemistry or biology journals where the rejection rate oscillates between 30 and 50 per cent or more, but I must stress that the other major astronomy journals do have rejection rates similar to ours. I believe that journals in other disciplines may use different principles: they often seem to accept the paper or reject it at once, and in the latter case the authors submit it essentially unchanged to another journal until it is eventually published. This is possible because there are many journals in those fields while we have only a few, but at the end the paper is not much improved while we succeed in having many of our papers made substantially better.

I must confess that I do not actually read all the papers. This would be physically impossible (the job takes already at least 1/3 of my time). In many cases a cursory look through the paper when reading the referee's report seems sufficient. But there are cases where I have to spend many hours on a single paper. I have even rewritten a few myself to a large extent when I saw that there was something good in the science but that the author was unable to express it properly. Not unexpectedly, this is often the case with papers from Eastern countries, particularly China, due to language difficulties; I even wonder sometimes if some authors don't have a different way of thinking! This does not make me at ease as I strongly believe that there cannot be several kinds of scientific logics. In such cases there may be several iterations before coming to a publishable paper. If the paper is understandable but written in poor English, I simply send it for rewriting to a native English-speaking astronomer. I must say that since the birth of Astronomy and Astrophysics 22 years ago astronomers from Western and even Eastern Europe have made considerable progress in writing English; if not always completely correct (in particular the result is often a mixture of English and American), the language is most often quite understandable. Of course purists would like to see only papers in superb English (or American? which to choose?) but we do not have the means to achieve such a result, especially as the rewriter must necessarily be a cultivated astronomer.

At the end of the process, every

manuscript accepted by one of the Editors is seen by the other one for a check (he has a complete copy of the file): there are a few cases where we have discovered a problem at this late stage. Also, the advice of the other Editor is very welcome in marginal cases where it is better to have the responsibility shared! Then all manuscripts (except those of the Letters which are made camera-ready by the author) end up in our office in Meudon where they are prepared for edition by my two secretaries, Bernadette Perche and Monique Rougeot, and then sent either to Springer-Verlag in Heidelberg for the Main Journal or to Les Editions de Physique near Paris for the Supplements. I take the opportunity to express my appreciation of the excellent work of the two secretaries, who not only make the final preparation of the manuscripts but follow them at all stages while receiving the complaints or questions of the authors and sometimes of the referees, typing and sending innumerable letters and reminders and also adapting to the somewhat irregular schedule and changing mood of their Editor or of his occasional substitute! There are also a competent secretary in Tübingen and a half-time one in Groningen, who are not sitting idle either!

Those authors who use the Springer-Verlag T_EX or L^AT_EX macros to prepare their manuscripts are well aware of the corresponding advantages: their papers will look exactly like the manuscript (but proof-reading is still in order to check if the figures are put at the proper place and in general if there has not been a problem in the layout), but also they benefit from a substantial reduction in the publication delay (say 3–4 months after acceptance instead of 6–7 months for normal papers). Also this alleviates the burden of our secretaries and allows costs savings for publication, resulting in more pages published at the same cost for the subscribers. This is certainly the solution for the future and we are glad to see the fraction of such papers increasing (it reaches presently about 15 per cent of the total). The authors should also be aware of the *Research Note* formula. Research Notes are short papers which either contain results whose publication is not sufficiently urgent to justify a Letter, or short follow-up of previously published papers. They are used by Springer-Verlag to complete the issues which for technical reasons must have a number of pages multiple of 8. Thus Research Notes may – or may not – benefit from a reduction in publication delay.

To end, I would like to offer a few reflections concerning the future. The size of all astronomy journals is in-

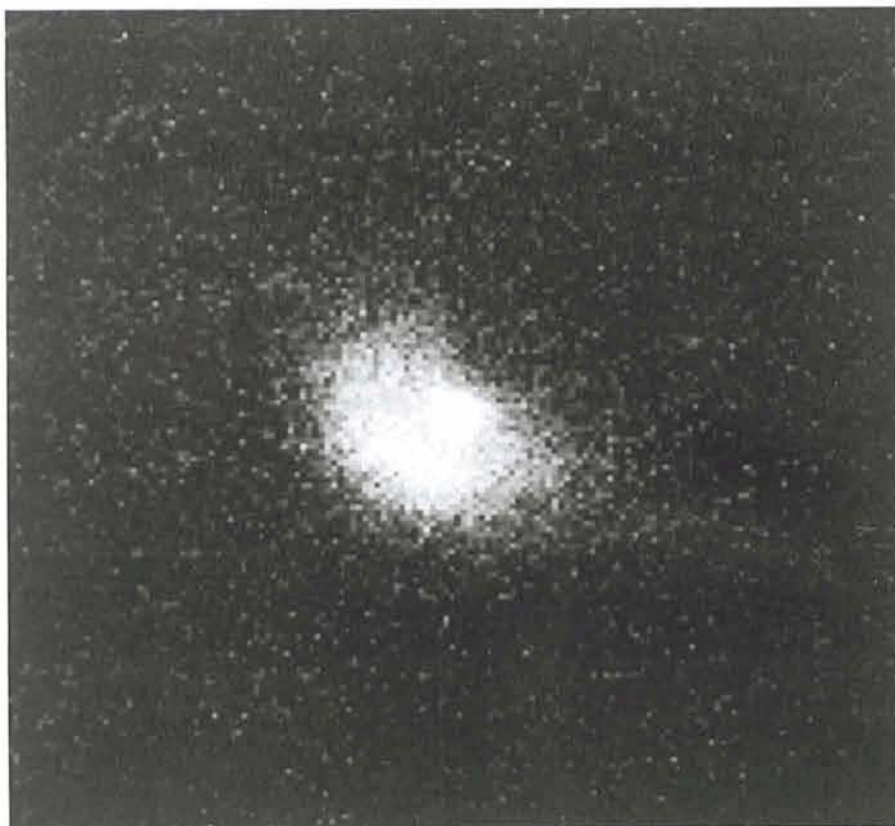
creasing continuously, not because the number of astronomers is increasing (it has been quite steady on the average during the last years) but because they have available more and faster observing means and computers, hence an increased productivity. Will the conventional way of publishing the results on paper remain appropriate? There have been many suggestions for alternatives. Microfiches is one that we use for big data sets in the Supplement Series. Data too big to be published on paper can also be stored at the Centre de Données Stellaires of Strasbourg, which distribute them on magnetic tape on request. But this is not appropriate for the normal papers. Editing all papers on microfiches is an interesting possibility for saving storage space (the *Astrophysical Journal* indeed has an edition on microfiches). However, while this can be useful for long-term archiving, it is not very practical to read microfiches of the papers just published: you need to have the microfiche reader at hand, and paper reproductions of microfiches are expensive and often not of high quality, especially for the half-tones. Moreover, the authors like to see their production printed on paper, and this is a psychological fact one cannot flatly ignore! For the same reasons, we are still a long way from a computerized journal. It is clear that papers can already be memorized in computers and can be made accessible to the community through computer networks. However, a general use of this system would mean a substantially increased charge on both the computer and the network, would require a graphic display for the figures (and what about half-tones?) while access and even reading is not going to be as fast and as convenient as for a printed issue. Moreover, even if you have a graphic terminal at home you will still not be able to read your favourite journal in the train or in the plane! Finally, this solution would be very unfair to countries and individuals whose access to a worldwide computer network is still limited or impossible. For all these reasons, I believe that there are still many good days for the conventional way of printing and distributing paper journals. I tend to believe that the substitute (which will no doubt come eventually) will be a dense individual support like an optical disk distributed by mail, that will be read on unexpensive portable lap computers with high-quality displays, of the size of a present paper issue. Perhaps such devices already exist or will be soon available. If this is the case, we have to contemplate seriously the substitution of the cumbersome paper journals by such devices. Will this be before I retire?

Dramatic Eruption on Comet Halley

This photo shows the enormous outburst of Comet Halley, as observed by ESO astronomers Olivier Hainaut and Alain Smette with the Danish 1.54-m telescope at La Silla on February 12–14, 1991. At this moment the comet was about 14.3 A.U. (2140 million km) from the Sun and 13.4 (2002 million km) from the Earth. The image is a combination of eight individual CCD Johnson-V exposures with a total exposure time of just over 7 hours.

Comet Halley's nucleus is completely hidden within a diffuse dust cloud (the "coma") that is seen as a bright light point at the centre; the magnitude is $V \sim 21.5$. From here, dust is dispersed into surrounding space; the parabolic shape of the faint, outer contour and the arc-like structure are thought to result from the complex motions of the individual dust particles. The central part of the dust cloud measures more than 30 arcseconds (300,000 km projected) across, but faint contours can be followed much further out. The total brightness of the cloud is about 19, or about 300 times brighter than the predicted magnitude of the nucleus alone, about 25.3. No outburst of a comet has ever been observed at such a large distance from the Sun.

North is up and East is to the left; 1 pixel = 0.464 arcsecond; field size: 153×153 pixels, i.e. 71×71 arcseconds or



$\sim 700,000 \times 700,000$ km at the distance of Halley. The telescope was set to follow the comet's motion (directed at 72° West of North) and several star trails crossed the image of Halley. The

projected direction to the Sun is 15° West of South. To produce this photo, the frames were individually cleaned with the ESO IHAP image processing system. The editor

Visiting Astronomers

(April 1–October 1, 1991)

Observing time has now been allocated for Period 47 (April 1–October 1, 1991). The demand for telescope time was again much greater than the time actually available.

The following list gives the names of the visiting astronomers, by telescope and in chronological order. The complete list, with dates, equipment and programme titles, is available from ESO, Garching.

3.6-m Telescope

April: van der Hucht/Thé/Williams, Courvoisier/Bouchet/Robson, Danziger/Bouchet/Gouiffes/Lucy/Fransson/Mazzali/Della Valle, Grenier/Ögelman/Gouiffes, Gouiffes/Ögelman/Augusteijn, Reimers et al. (2-009-45K), Reimers/Koester, Prieto/Benvenuti, Chincarini/Buzzoni/Molinari, Turatto et al. (4-004-45K), Danziger/Bouchet/Gouiffes/Lucy/Fransson, Mazzali/Della Valle, Hutsemékers/van Drom.

May: Malbet/Bertout/Léna/Rigaut/Merkle/Lagrange-Henri, Miley et al. (2-001-43K), van Drom/Hutsemékers, Giraud/Melnick/Steppe/Gopal-Krishna, Turatto et al. (4-004-45K), Danziger/Bouchet/Gouiffes/Lucy/Fransson/

Mazzali/Della Valle, Mathys/Maeder, Barbuy/Silk/François, Baade/Crane, Hensberge et al. (5-005-45K).

June: Gratton/Snedden, Andreae/Drechsel, di Serego Alighieri/Fosbury/Schlötelburg, Mirabel/Lutz/Dottori, Schmid/Schild, Gay/Le Bertre/Lefèvre/Lopez/Perrier, Richichi/Lisi/Di Giacomo, Vladilo/Centurion.

July: Vidal-Madjar/Ferlet/Gry, Ferlet/Vidal-Madjar/Dennefeld, Renzini/Greggio/Bragaglia, Penninx/Augusteijn/van der Klis/Kuulkers, Chambers/van Breugel/Dey, Tsvetanov/Fosbury/Tadhunter, Tsvetanov/Wilson/Fosbury, Habing et al. (5-007-45K).

August: Meisenheimer/Wagner, Turatto et al. (4-004-45K), Danziger/Bouchet/Gouiffes/Lucy/Fransson/Mazzali/Della Valle, Macchetto/Sparks, Véron/Hawkins, Danziger/Bouchet/Gouiffes/Lucy/Fransson/Mazzali/Della Valle, Cetty-Véron/Véron, Webb/Shaver/Carswell, Westerlund/Pettersson/Edvardsson, Danziger/Bouchet/Gouiffes/Lucy/Fransson/Mazzali/Della Valle.

September: Vettolani et al. (1-019-47K), Borra/Sanvico/Cristiani/Levesque/Shaver, Hammer/Petrosian/Le Fevre/Angonin, Turato et al. (4-004-45K), Danziger/Bouchet/

Gouiffes/Lucy/Fransson/Mazzali/Della Valle, Hes/Fosbury/Barthel, Gouiffes/Ögelman/Augusteijn, Danziger/Bouchet, Gouiffes/Lucy/Fransson/Mazzali/Della Valle, Habing et al. (7-008-47K).

3.5-m NTT

April: Tammann et al. (1-022-47K), Danziger/Bouchet/Gouiffes/Lucy/Fransson/Mazzali/Della Valle, Bergvall/Rönnback, Ortolani/Rosino/Renzini, Tarengi/D'Odorico/Wampler/Yoshii/Peterson/Silk, Zinnecker/Melnick/Moneti, Reipurth/Zinnecker, Moorwood/Oliva.

May: Oliva/Morwood, Danziger/Moorwood/Oliva, Danziger/Bouchet/Gouiffes/Lucy/Fransson/Mazzali/Della Valle, Dettmar/Shaw/Dahlem, Tamman et al. (1-022-47K), Danziger/Bouchet/Gouiffes/Lucy/Fransson/Mazzali/Della Valle, Bignami et al. (6-002-45K), Tammann et al. (1-022-47K), Bandiera/Della Valle, Bender et al. (1-004-43K), Tammann et al. (1-022-47K), Bandiera/Della Valle, Dejonghe/Zeilinger, Schönberner/Napiwotzki/Jordan, Tammann et al. (1-022-47K), Bandiera/Della Valle, Spite F./Rebolo/Molaro/Nissen/Spite M., Koornneef/Israel.

VACANCIES ON LA SILLA

STAFF ASTRONOMER

A position of staff astronomer will become available on La Silla in the second half of 1991. This position is open to experienced astronomers with a Ph.D. degree or equivalent and several years of post-doctoral experience in the area of high dispersion spectroscopy.

The successful applicant will be in charge of the high dispersion spectrographs on La Silla. This includes

- introducing visitors to the use of the instrumentation,
- writing and updating User's manuals,
- regularly testing the performance of the equipment, and
- interacting with the technical people regarding modifications and up-dates of the instrumentation. As members of the Astronomy Support Department on La Silla, staff astronomers are required to spend at least 50 % of their time on support activities and the remainder conducting original research.

Staff posts are tenure track positions, normally offered for an initial period of 3 years that may be renewed for a second period of 3 years. Tenure may be granted during the second term of the staff contract.

The successful applicant will have an excellent opportunity of participating in the commissioning phases of the VLT.

Applications should be submitted to ESO Personnel Administration and General Services at ESO-Garching before **31 May 1991**.

FELLOWSHIPS

Two post-doctoral fellowships are offered on La Silla starting during the second half of 1991. These positions are opened to young astronomers with an interest in Optical or Infrared observational work. The ESO fellowships are granted for a period of one year, normally renewed for a second and exceptionally for a third year.

Successful applicants will be required to spend 50 % of his/her time doing support activities and 50 % of the time on research.

Applicants normally should have a doctorate awarded in recent years. Applications should be submitted to ESO not later than 15 May 1991. Applicants will be notified by July 1991. The ESO Fellowship Application Form should be used and be accompanied by a list of publications. In addition, three letters of recommendation should be obtained from persons familiar with the scientific work of the applicant. These letters should reach ESO not later than **15 May 1991**.

The Astronomy Support Department on La Silla is composed of about 20 astronomers including staff, fellows, and students. The research interests of the members of the staff include low mass star formation, formation and evolution of massive stars and starbursts, post-AGB stellar evolution and planetary nebulae, supernovae, active nuclei, high redshift galaxies and galaxy clusters. Staff members and senior fellows act as co-supervisors for students of European universities that spend up to 2 years on La Silla working towards a doctoral dissertation.

Enquiries, requests for application forms and applications should be addressed to:
European Southern Observatory
Fellowship Programme
Karl-Schwarzschild-Straße 2
D-8046 GARCHING b. München
Germany

June: Koornneef/Israel, Käufel/Stanghellini/Renzini, Gredel, Buonanno/Fusi Pecci/Corsi/Richer/Fahlmann, Tammann et al. (1-022-47K), Bertola/Bertin/Buson/Danziger/Dejonghe/Saglia/Sadler/Stiavelli/de Zeeuw/Zeilinger, Tammann et al. (1-022-47K), Richtler/Wagner/Held/Capacciolo, Tammann et al. (1-022-47K), Haefner/Simon/Pfeiffer/Sturm/Fiedler, Glass/Moorwood/Monet.

July: Schwarz/Sahai, Ferraro/Brocato/Molaro, Murphy/Verbunt/Rutten/van Paradijs/Cohn/Lugger/Seitzer/Callanan/Charles, Borkowski/Tsvetanov/Harrington, Surdej et al. (2-003-43K), Aurière/Lauzeral/Koch-Miranda.

August: Meylan/Djorgovski/Shaver/Weir, Giallongo/Buson/Cristiani/Trevese, Mellier/Fort/Soucail/Ellis, Fort et al. (1-015-45K) Moeller/Jacobsen/Perryman, Capaccioli/Caon/Lorenz/Richter, Cappellaro/Capaccioli/Held/Ferrario, Boer/Motch/Pedersen.

September: Tarengi/D'Odorico/Wampler/Yoshii/Peterson/Silk, Wampler et al. (2-010-45K), Bergeron et al. (1-012-43K), Surdej et al. (2-003-43K), Smette/Surdej/Shaver, Christensen/Sommer-Larsen/Hawkins/Flynn, Leitherer/Drissen/Nota/Robert/Schmutz, Molano/Castelli/Bonifacio, Boisson/Joly/Moorwood/Oliva/Ward, Danziger/Bouchet/Gouiffes/Lucy/Fransson/Mazzali/Della Valle, Ögelmann/Danziger/Gouiffes/Augusteijn/Carollo / Bouchet, Danziger / Bouchet/Gouiffes/Lucy/Fransson/Mazzali/Della Valle, De Lapparent et al. (1-003-43K).

2.2-m Telescope

April: Blommaert/Habing/van der Veen, Infante/Melnick/Lucey/Terlevich/Lahav/Lynden-Bell, Surdej et al. (2-003-43K), Barucci/Fulchignoni/Harris/De Angelis/Foryta/Burchi/Dotto/Rotundi/Di Martino, Barbieri et al. (2-007-43K), Turatto et al. (4-004-45K), Zeilinger/Buson/Galletta/Saglia, MPI TIME.

May: MPI TIME.

June: Oosterloo/Prieur, Zeilinger/Bertola/Buson, Barucci/Fulchignoni/Harris/De Angelis/Foryta/Burchi/Dotto/Rotundi/Di Martino, Richtler/Kaluzny, Habing/Epchtein/Blommaert/van Langevelde/Le Berre/Winnberg/Lindqvist/van der Veen, Glass/Moorwood/Monet/Schwarz/Monet.

July: Habing/Epchtein/Blommaert/van Langevelde/Le Berre/Winnberg/Lindqvist/van der Veen, Barucci/Fulchignoni/Harris/De Angelis/Foryta/Burchi/Dotto/Rotundi/Di Martino, Surdej et al. (2-003-43K), Tosi/Focardi/Greggio/Marconi, Bertola et al. (1-008-43K), Rosa/Kinkel, De Jong/van der Kruit.

August: De Jong/van der Kruit, Giard/Bernard/Dennefeld/Verstraete, Barucci/Fulchignoni/Harris/De Angelis/Foryta/Burchi/Dotto/Rotundi/Di Martino, Infante/Melnick/Lucey/Terlevich/Lahav/Lynden-Bell, Surdej et al. (2-003-43K), Bender et al. (1-004-43K), Turatto et al. (4-004-45K), Barbieri et al. (2-007-43K), MPI TIME.

September: MPI TIME, Robert/Drissen/Leitherer/Nota/Schmutz, Mirabel/Lagage/Cesarsky, Habing et al. (7-008-47K).

1.5-m Spectrographic Telescope

April: Courvoisier/Bouchet/Blecha, Pagel/Terlevich/Diaz/Vilchez/Edmunds, Barbieri et al. (2-007-43K), Joergensen/Rasmussen/Franx, Caon/Capaccioli/Ferrario.

May: Krautter/Schmitt/Alcala/Henning, Dettmar/Krenz/Barteldrees, Bettoni/Bertola/Buson, Paturel et al. (1-017-45K), Hensberge et al. (5-005-45K), Mantegazza/Ferro.

June: Mantegazza/Ferro, Andreae/Drechsel, Goudfrooij/de Jong/Jørgensen/Noergaard-Nielsen/Hansen/van de Hoek, Courvoisier/Bouchet/Blecha, Acker/Cuisinier/Köppen/Stenholm/Terzan, Pottasch/Manchado/Garcia-Lario/Sahu K.C., Thé/de Winteler/Bibo, Sinachopoulos.

July: Sinachopoulos, Lorenz/Drechsel/Mayer, Rampazzo/Prugniel/Bica/Sulentic, de

Boer/Moehler, Habing et al. (5-007-45K), Lorenz/Drechsel/Mayer, Favata/Sciortino/Micela.

August: Luthardt/Bues, Cristiani/Giallongo/La Franca/Sanvico/Vagnetti, Barbieri et al. (2-007-43K), Iijima/Rosino, Gerbaldi et al. (5-004-43K), Ballereau/Chauville/Zorec.

September: Fouqué/Quintana/Proust, Bragaglia/Greggio/Renzini, Gerbaldi et al. (5-004-43K).

1.4-m CAT

April: Pols/van den Heuvel/Piters/Coté/Waters, Tagliaferri/Cutispoto, Giommi/Pallavicini/Pasquini, Pasquini, Gratton/Snedden, West/Sahade/Sulskij.

May: Benvenuti/Porceddu/Krelowski, Franchini/Covino/Alcalá/Chavarria/Terranegra/Ferluga/Stalio/Pasquini, Gosset, van Dishoeck/Black, Gosset, Nussbaumer/Schmutz/Schmid, Pottasch/Sahu K.C.

June: Pottasch/Sahu K.C., Pottasch/Parthasarathy, Sabbadin/Cappellaro/Turatto/Salvadori, Faraggiana/Castelli/Molaro/Gerbaldi, Pallavicini/Duncan/Randich/Tagliaferri, Pallavicini/Randich.

July: Ferlet/Vidal-Madjar/Dennefeld, Lagrange-Henri/Jaschek M./Jaschek C., Lagrange-Henri/Bouvier/Gomez/Bertout, Sembach/Crane/Danks/Savage, Pogodin, van Paradijs/Verbunt/Zwaan/Rutten/Schrijver/Schmitt/van Kerkwijk/Piters, Nussbaumer/Schmutz/Schmid.

August: Nussbaumer/Schmutz/Schmid, Bossi/Guerrero/Scardia, Favata/Sciortino/Micela, Monai/Molaro/Vladilo, Jorissen/Lambert/Tomkin, da Silva/Vasques.

September: da Silva/Vasques, Pols/van den Heuvel/Piters/Coté/Waters, Nussbaumer/Schmutz/Schmid.

1-m Photometric Telescope

April: van der Hucht/Thé/Williams, Hron, Courvoisier/Bouchet/Blecha, Tagliaferri/Cutispoto/Giommi/Pallavicini/Pasquini, Weiss/Schneider/Kuschnig/Rogl, Le Bertre et al. (5-006-45K).

May: Le Bertre et al. (5-006-45K), Courvoisier/Bouchet/Blecha, Di Martino/Mottola/Gonano/Neukum, Di Martino/Mottola/Gonano/Hoffmann/Neukum, Barucci/Fulchignoni/Harris/De Angelis/Foryta/Burchi/Dotto/Rotundi/Di Martino, Courvoisier/Bouchet/Blecha, Habing et al. (5-007-45K).

June: Habing et al. (5-007-45K), Cayrel/Buser, Fulchignoni/Barucci/De Angelis/Burchi/Dotto/Ferrari/Foryta/Roques, Richichi/Lisi/Di Giacomo, Le Bertre et al. (5-006-45K).

July: Le Bertre et al. (5-006-45K), Courvoisier/Bouchet/Blecha, Terzan, Liller/Alcaino/Alvarado/Wenderoth.

August: Augusteijn/van Paradijs, Hainaut/Detal/Pospieszalska-Surdej/Schils/Surdej/West, Habing et al. (5-007-45K), Prugniel/Rampazzo/Combes/Sulentic/Zhonggi.

September: Prugniel/Rampazzo/Combes/Sulentic/Zhonggi, Rampazzo/Prugniel/Combes/Sulentic/Zhonggi, Lorenzetti/Molinari.

50-cm ESO Photometric Telescope

April: Haefner/Pietsch/Schwarzenberg-Czerny, Arlot/Thuillot/Descamps/Vu/Colas, Surdej/Detal/Hainaut/Pospieszalska-Surdej/Schils, Arlot/Thuillot/Descamps/Vu/Colas.

May: Franchini/Covino/Alcalá/Chavarria/Terranegra/Ferluga/Stalio/Pasquini, Arlot/Thuillot/Descamps/Vu/Colas.

June: Arlot/Thuillot/Descamps/Vu/Colas, Thé/Westerlund/Fluks, Thé/de Winter/Bibo.

July: Arlot/Thuillot/Descamps/Vu/Colas, Lorenz/Drechsel/Mayer, Bruch/Schwarzenberg-Czerny, Debehogne/Lagerkvist/Magnusson/Di Martino/Zappalà/De Campos/Cutispoto.

August: Debehogne/Lagerkvist/Magnusson/Di Martino/Zappalà/De Campos/Cutispoto, Luthardt/Bues, Hainaut/Detal/Pospieszalska-Surdej/Schils/Surdej/West.

September: Poretti/Antonello/Mantegazza, Leitherer/Drissen/Nota/Robert/Schmutz.

GPO 40-cm Astrograph

April: Kohoutek/Bönnhardt.

June: Seitter/Aniol/Duerbeck/Tsvetkov/Tsvetkova, Debehogne/Machado, Caldeira/Vieira/Netto/Zappalà/De Sanctis/Lagerkvist/Mourao/Protitch-Benishek/Javanshir/Woszczyk/Lopez.

July: Debehogne/Machado, Caldeira/Vieira/Netto/Zappalà/De Sanctis/Lagerkvist/Mourao/Protitch-Benishek/Javanshir/Woszczyk/Lopez.

August: Elst.

September: Vidal-Madjar et al.

1.5-m Danish Telescope

April: Nordström/Andersen, Jørgensen/Rasmussen/Franx, Danziger/Bouchet/Gouiffes, Lucy/Fransson/Mazzali/Della Valle, Quintana/Ramirez, D'Onofrio, Caon/Capacciolo/Ferrario, Bergvall/Rönneback, Ortolani/Barbuy/Bica, Mayor et al. (5-001-43K).

May: DANISH TIME, Duquenois/Mayor, Waelkens/Mayor.

June: Moffat/Pirola, van der Klis/Penninx/Kuulkers/van Paradijs, Infante/Melnick/Lucey/Terlevich/Lahav/Lynden-Bell, Grebel/Richtler. DANISH TIME.

July: DANISH TIME, Mermilliod/Mayor, Ardeberg/Lindgren/Lundström.

August: Danziger/Bouchet/Gouiffes/Lucy/Fransson/Mazzali/Della Valle, Barbieri et al. (2-007-43K), Lindgren, Azzopardi/Lequeux/Reiberoit, Shanks/Fong/Metcalf, DANISH TIME.

September: DANISH TIME, Mayor et al. (5-001-43K), Danziger/Bouchet/Gouiffes, Lucy/Fransson/Mazzali/Della Valle.

50-cm Danish Telescope

April: DANISH TIME.

May: Mennickent/Vogt/Covarrubias, Maitzen, Leone/Catalano/Jenkner.

June: Mantegazza/Ferro, Group for Long Term Photometry of Variables.

July: Sinachopoulos, Group for Long Term Photometry of Variables.

August: Favata/Sciortino/Micela, Ardeberg/Lindgren/Lundström, Group for Long Term Photometry of Variables.

September: Group for Long Term Photometry of Variables.

90-cm Dutch Telescope

April: Rifatto/Bussoletti/Mennella/Buson/Zeilinger/Colangeli/DUTCH TIME.

May: DUTCH TIME.

June: Wendker/Heske, Houdebine/Butler/Mathioudakis/Panagi/Foing/Char/Jankov/Rodono, Augusteijn/van Paradijs.

August: Ferrari/Bucciarelli/Massone/Koornneef/Lasker/Le Poole/Postman/Siciliano/Lattanzi, Schuecker/Cunow, DUTCH TIME.

September: DUTCH TIME

SEST

May: Israel, Wu, Israel.

July: Wielebinski, Becker, Casoli, Wild, Freudling, Huchtmeier, Dupraz, van Woerden, Eckart, van der Blik.

August: F. Combes, Mauersberger, Franceschini, Andreani, Danziger, Henkel, Cas-tets, Zinnecker, Bronfman, Krügel, Pollacco, Bertout.

Minor Planet Named after Guido and Oscar Pizarro!

A minor planet in the solar system has recently been named after two night assistants at the ESO La Silla observatory as a well-deserved recognition of their great efforts to serve astronomers in the ESO member countries and beyond. In the January 30, 1991 issue of the *Minor Planet Circulars*, the following text appears on page 17658:

"(4609) Pizarro = 1988 CT3
Discovered 1988 Feb. 13 by E.W. Elst at the European Southern Observatory.

Named in honour of Guido and Oscar Pizarro, who operate the ESO 1-m Schmidt telescope and who exposed the plates on which this minor planet was discovered. For almost 20 years the two brothers have been renowned for

their patient and effective work with the telescope. They took the plates for the two ESO sky surveys and have taken several thousand plates for general programmes, including many specifically for the detection and follow-up of comets and minor planets. Citation prepared by H.-E. Schuster at the request of the discoverer."

Minor planet "Pizarro" moves in an elliptical orbit with a mean distance of 465 million kilometres, i.e. between Mars and Jupiter. One revolution takes

about 5 ½ years. Once the orbit had been established by means of the observations in 1988, it turned out that images of this minor planet had also

been measured earlier; a single observation was made already in 1969 at the Crimean Observatory. "Pizarro" measures about 10 kilometres across.

ESO'S EARLY HISTORY, 1953–1975

X. The Schmidt Telescope: Design, Construction, the ESO-SRC Agreement and the Onset of Survey Projects*

A. BLAAUW, Kapteyn Laboratory, Groningen, the Netherlands

"Erlaube mir die Anfrage, ob ihr vielleicht für Spiegelteleskope interessiren, ich --- [möchte] mal sehen, was sich mit einem Spiegel fotografieren lässt, ---"

From a letter of Bernhard Schmidt to Karl Schwarzschild of May 29, 1904 as quoted in *Abhandlungen Hamburger Sternwarte Band X, Heft 2, p. 50.*

As the last, but by no means the least, of the instruments of ESO's initial programme we turn to the Schmidt telescope. We review its history up to the time in the early 1970's when it began fulfilling its great mission: providing the astronomical community with the southern complement to the Palomar Sky Atlas. But first, a glance at its pre-history is in order.

Bernhard Schmidt and Early Developments at Hamburg Observatory

From the beginning, the planning of the Schmidt telescope was, beside the involvement of the Instrumentation Committee, very much a concern of ESO's Director Otto Heckmann himself. In the early 1950's, the Hamburg Observatory had obtained a Schmidt telescope in the acquisition of which Heckmann had been deeply involved. The observatory had special affinity to this type of telescope because it was here that Bernhard Schmidt's invention had been applied first, and thereupon it had deeply affected observational astronomy. Let me, therefore, spend a few lines on these early developments [1].

At the commemoration of Schmidt's hundredth anniversary in 1979, the President of the University of Hamburg in his opening address related that in 1904 Bernhard Schmidt approached the famous astronomer Karl Schwarzschild with the question whether his work in optics might be of interest for Potsdam Observatory and that he much impressed Schwarzschild – and that in 1916 Schmidt contacted the Director of Hamburg Observatory, R. Schorr [2].

Schmidt's ingenuity in optics led to continued association with this observatory under Schorr's direction and encouragement, and in 1931 produced the first instrument of the type we now call "Schmidt Telescope". In the *Messenger* of June 1979, Alfred Behr commemorated Bernhard Schmidt's achievements and showed a picture of the original Schmidt telescope, still at Hamburg Observatory. For the benefit of those readers who are not acquainted with the special properties of this type of telescope, the accompanying box describes its main optical features.

Considerable stimulus for Schmidt's work also seems to have been due to Walter Baade who was a member of the staff of Hamburg Observatory from 1920 to 1931. Schmidt died in 1935, and when in 1936 Baade was nominated for the succession of Schorr as Director, he made it a condition that the Observatory should be equipped with a Schmidt telescope of 80 cm aperture. The Hamburg authorities agreed, and notwithstanding the fact that Baade ultimately preferred to stay at Mt. Wilson Observatory with the prospect of utilizing the more powerful 120-cm Palomar Schmidt, the plans for the Hamburg Schmidt were realized [3]. It was to have a focal length of 240 cm, and a 120 cm diameter spherical primary mirror. In this realization Heckmann played a leading role.

It is no surprise, then, that Heckmann felt that the acquisition of the ESO Schmidt should be very much a matter of his interest and responsibility. Along with the essentially French realization of the 1.5-m telescope, the Dutch one of the 1-m telescope (both described in article IV), and the Danish role in the development of the Telescope Project Division (described in articles VIII and IX), the Schmidt-telescope project may

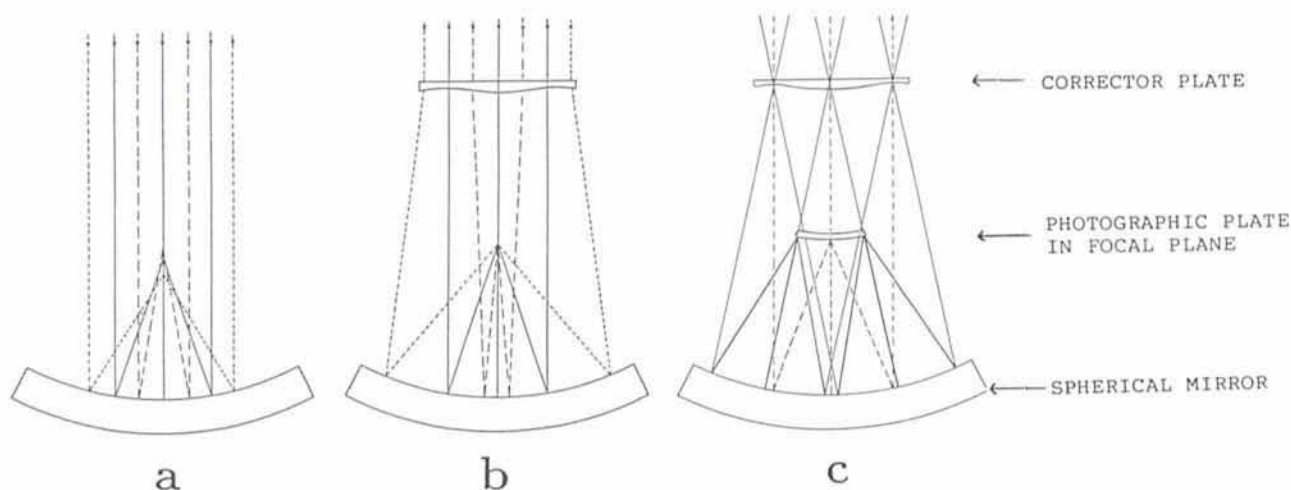
be considered as the early major instrumental contribution from German side.

Planning the ESO Schmidt

At the meeting which marked ESO's beginning, June 21, 1953, Baade suggested that ESO should acquire a copy of the Palomar Schmidt, and thus would be able to soon start its work. The Palomar Schmidt with its 120 cm aperture, fully operational since 1949, certainly met its designer's high expectation for wide-field photography. However, ESO astronomers wanted more: the facility to obtain objective prism spectra. In the 1950's, spectral surveys played an important role in galactic research at many European observatories and it was important to extend these to fainter stars than had been reached so far.

This point was raised for the first time by Heckmann at the July 1958 meeting of the ESO Committee, and taken up again when in November 1961 the Committee requested the recently created Instrumentation Committee to consider an alternative design. This differed from the Palomar Schmidt mainly in that the aperture would be 100 cm – 40 inch – instead of 120 cm, and the diameter of the spherical mirror 160 cm instead of 180 cm, however maintaining the focal length (305 cm) of the Palomar Schmidt and hence its plate scale (approximately 67" per mm). Reason for this modification were the reduced size, and hence the lower weight, of the objective prism and therefore a considerable reduction of the demand on the sturdiness of the telescope tube and lower costs, and an important additional consideration was the smaller chromatic variation that is left after the correcting plate's elimination of the principal part of the spherical

* Previous articles in this series appeared in the *Messenger* Nos. 54 to 62.



Schmidt telescopes allow astronomers to photograph large regions of the sky on one photographic plate and are therefore very suitable for making sky atlases. The sketches in this box illustrate the main optical features of the Schmidt design.

A basic element is the *spherically* shaped primary mirror, contrary to the *parabolic* mirror of regular telescopes like the ESO 3.6-m telescope. Figure a shows how this spherical mirror would work if it would receive a beam of the star light. There would be no unique focal point: marginal light rays focus on a point closer to the mirror than rays hitting the mirror nearer to its centre. This difference is eliminated by letting the light pass through a specially figured glass plate, the corrector plate, the centre of which is placed in the centre of curvature of the primary mirror, see Figure b. Given the presence of this corrector plate, we may now let the telescope receive light from stars that are at large angular distance from the central axis of the system: as shown in Figure c these rays will be focussed in essentially the same way and at the same distance from the mirror, on a spherical surface that also has its centre of curvature at the centre of the corrector plate.

Some sensitivity of the optical system to the wavelength (colour) of the infalling beam arises from the slight refraction of the light when it passes through the corrector plate. Shape and material of the corrector plate must therefore be chosen in accordance with the wavelength region of the planned survey.

As the focal plane is curved, the photographic plates are forced to have the same curvature by placing them in specially designed plate holders, a treatment that most of the (thin) plates survive.

aberration, allowing high quality objective prism spectra over a wide range of wavelengths [4]. The Hamburg Schmidt also had been provided with an objective prism.

In October 1962 the IC, upon advice from various experts, endorsed the proposal and the EC in its meeting later that year decided accordingly. A disadvantage was the reduced size of the vignetting-free field, only 5.4×5.4 , corresponding to the standard plate size of 30×30 cm, instead of the 6.5×6.5 of the Palomar Schmidt (due to the fact that the focal length was not reduced in the same ratio as the dimensions of correcting plate and mirror), and the consequent increase of the number of plates required for covering the sky in the survey programmes. However, this was accepted. This deviation from the specification of the Schmidt in the ESO Convention was confirmed at the first meeting of Council in February 1964.

Mechanical Engineer and Manufacturer

The Hamburg Schmidt had performed satisfactorily since its dedication in the year 1954, and so it was natural for

Heckmann to propose to the IC to put the realization of the mechanical parts of the ESO Schmidt in the hands of those who had been responsible for the Hamburg telescope: the firm of Heidenreich and Harbeck (precision steel constructions) at Hamburg – henceforth denoted by H&H – in collaboration with the mechanical engineer W. Strewinski. Strewinski had been an employee of H&H, but after the completion of the Hamburg Schmidt created his own, independent, engineering bureau.

On the other hand, as described in article IV, the ESO Committee that in the early days managed the affairs, preferred the creation of an engineering group to be charged with the comprehensive task of developing all major instrumentation, including the 3.6-m and the Schmidt telescopes. A preliminary agreement for a joint venture of this nature was reached with the engineers Strewinski and Hooghoudt in November 1961 [5] and contracts were signed by them in August and September 1963, respectively [6]. To what extent these covered more than just the Schmidt telescope is not clear, but in any case the arrangement did not work out satisfactorily. In August 1963 there still was a

prospect for joint effort in the design of the Schmidt [7], but in February 1964 all the ESO Directorate had at its disposal were some preliminary studies by Strewinski. Hooghoudt (whose involvement in the 1-m telescope was described in article IV) had become heavily involved in the Benelux Cross Antenna Project, a – not realized – precursor-proposal for the Westerbork Synthesis Radio Telescope.

Heckmann then decided to refrain from the joint proposition, and by the middle of 1964 proposed to IC and Council to proceed for the Schmidt exclusively with Strewinski [8]. Council agreed, although reluctantly, as it foresaw delays in view of Strewinski's simultaneous involvement in the work on the 3.6-m telescope. In June 1965, Heckmann informed Council that a draft contract with Strewinski had been drawn up. One of his first tasks was the design of the mirror cell, the mirror itself nearing completion, in 1967, at Zeiss-Oberkochen.

Some Design Features

Contrary to what has been done for the smaller ESO telescopes, no com-

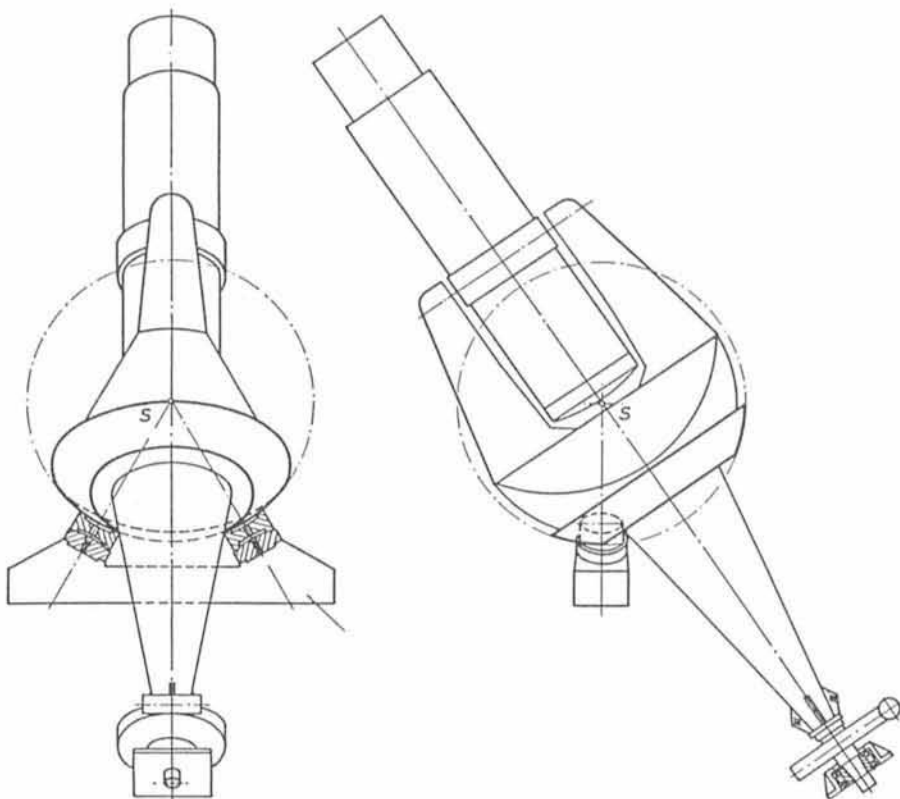
prehensive description of the design has been published for the Schmidt. A brief description by Heckmann occurs in the report on the 1972 Conference on Schmidt telescopes [9]. Specifications also occur in R. West's article on the Sky Survey project in *ESO Bulletin* No. 10 of May 1974, and later modifications have been described by A. B. Muller, see Note [16]. Quite instructive are also the proceedings of the IC meetings over the years from 1962 on. Some of the main features of the telescope are described in the following paragraph.

As in the case of the Hamburg Schmidt, a fork mounting has been chosen, and the weights of all movable parts (tube plus polar axis) are distributed in such a way that their centre of gravity coincides with the centre of the sphere which also defines the surface of the oil pads along which the upper bearing slides during its motion when the telescope is set on, or follows, a star. As one of the advantages to this construction, it allows smooth adjustment of the polar axis. The mirror is supported in its cell in such a manner that it allows maintaining exact focussing – so essential for Schmidt photography – by means of invar rods, free of thermal expansion, which keep the plate holder at constant distance from the mirror. Stiffness of the telescope tube is achieved by a double-wall construction, and an outer layer of thermal insulation helps avoiding rapid temperature changes of the interior.

A Daring Design, Not Realized

In the early 1960's, as an alternative to copying the design of the Hamburg Schmidt, Strewinski suggested for further study a rather unorthodox one, referred to as the "spherical model". It went a step farther in that not only the surface of the upper bearing that is in contact with the pads of the mounting is spherically shaped, but this spherical section is extended so as to become an almost complete sphere to which the telescope tube is directly fixed.

Fork prongs and declination axis are dispensed with. The axis of the telescope tube goes through the centre of the sphere, which is also made the centre of gravity of the sphere together with the tube including its optics. There is a short polar axis with bowl-shaped upper end to which the sphere can be clamped by means of electro-magnets fixed to the bowl. For motion around the direction towards the pole, all clamps are fixed. For adjustment in declination, two of the clamps are switched off, and the third one remains clamped but it can be displaced along a slide [10]. The concept is sketched in a drawing repro-



The Hamburg Schmidt Telescope: two drawings by W. Strewinski occurring in his article quoted in the text [18] and showing design features also adopted for the ESO Schmidt.

duced by Ch. Fehrenbach in his recent monograph "Des hommes, des télescopes, des étoiles" [11].

As advantages of this model, Strewinski pointed out that only a short and relatively light polar axis is needed, that the spherical mounting is very rigid and quite resistive against earthquakes, and that the foundation of the mounting would be simple and cheap. Manufacturing would present no difficulties and not be expensive.

The spherical model was discussed by the IC in the meetings of March, June and September 1964. The majority of its members, although appreciative of the new concept, was hesitant about applying it in the case of the ESO Schmidt. Heckmann was in favour of pursuing the idea, and reported at the September meeting that also Bruce Rule of Palomar Observatory, after a meeting in Strewinski's office, had expressed himself positively. Yet, the idea was not followed up any further, and Strewinski agreed to follow in his design essentially that of the Hamburg Schmidt.

The Optics

Following a recommendation of the IC, the ESO Committee in its meeting of February 1963 decided to order the spherical mirror with diameter 1.62 m from Schott, Mainz, to be made of low-expansion Duran 50 glass, and from the

same firm the 1-m corrector plate, to be made of ultraviolet-transparent Schott UK-50. The orders were finalized right after the ratification of the Convention. Figuring was done by Zeiss-Oberkochen, where mirror blank and corrector plate arrived by the middle of 1965 and early 1966, respectively [12]. A mishap occurred when, by unknown cause, the blank broke in the early figuring phase, but it was soon replaced so that no delay was caused. In the course of 1967 both mirror and corrector plate approached their final shape and would soon be ready for testing in the mirror cell. Unfortunately, construction of the cell and its related mechanical parts was not yet completed at that time. Provisional acceptance took place in October 1970 upon examination by Ramberg and Alfred Behr, expert in optics of Göttingen Observatory (who also made the polarimeter for the 1-m telescope). Meanwhile, also in 1967, material for the first, 4° objective prism of UBK-7 had been ordered from Schott, to be shaped by Zeiss-Oberkochen.

Mechanical Construction and First Tests

Negotiations with the firm of Heidenreich and Harbeck started in the first half of 1967 and the contract for the construction of the mechanical parts was concluded later that year. The minutes

of the July 1968 Council meeting report that manufacturing had started and – optimistically! – “A preliminary assembling – – at the factory will be possible in October. According to the plan the definitive assembling of the telescope in its building on La Silla will start in February or March 1969.” However, it was only at the December 1968 meeting that the Directorate could report that Strewinski had finished nearly all drawings for H&H. Unfortunately, changing economic conditions in the German Federal Republic by that time caused H&H to become less interested in spending their efforts on the Schmidt and to give preference to more rewarding orders, and Council – rather superfluously . . . – urged Heckmann to put strong pressure on the firm [13].

Such, then, was the situation at the time of the dedication ceremonies on La Silla in March 1969 – a time also, however, of growing discontent among Council because of the lack of progress in the large telescope and Schmidt projects. By the end of that year, according to the Annual Report, contrary to expectations of one year earlier, the drawings of the mechanical parts were not yet completely available. Even at the end of 1970, partly due to illness of Strewinski, delivery of the telescope mounting was still retarded, and it was only in 1971 that the telescope was mounted at H&H for first tests. By the end of the year it arrived on La Silla and was assembled in “its” dome where, three years earlier,

dignitaries and guests of ESO had gathered for the dedications. Final testing of the combined mechanical and optical parts could now be taken up.

After his retirement as Director General per 1 January 1970, Heckmann acted as consultant to ESO, as agreed at the Council meeting of December 1969. This concerned first of all the commissioning of the Schmidt. He was present on La Silla for prolonged stays, usually together with Strewinski and Technical Director Ramberg. After having witnessed the first satisfactory optical performances of the telescope, he returned to Europe at the end of February 1972. He would not return to La Silla again.

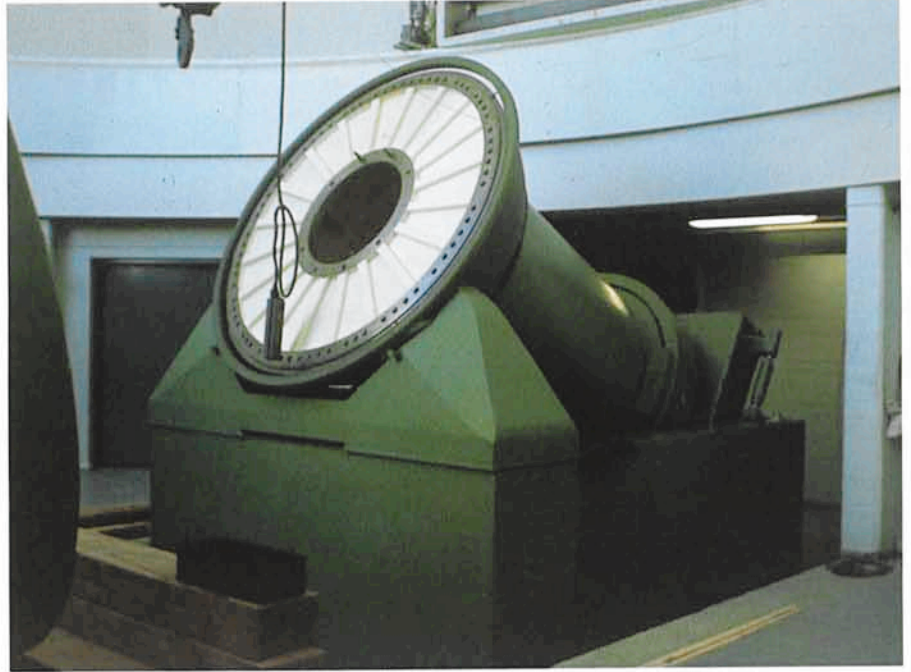
Heckmann's Concern in Retrospect

With the termination of Heckmann's consultantship in 1972 and Ramberg's retirement from ESO at the end of 1971 came the conclusion of the first stage in the Schmidt's development. By that time satisfactory photographic plates could be obtained, yet many finishing touches remained to be applied before the instrument would acquire the mature status required for the highly demanding Sky Survey programmes. A new team took over in the course of 1972 of which the achievements will be sketched below. However, let me first insert a few comments on the past, troublesome period.

For Otto Heckmann, who had iden-

tified himself so strongly with the project, bringing it to satisfactory completion had been a matter of deep concern. Worry and disappointment were caused by the failure of the engineering bureau to satisfy the high expectations he had in the beginning. His strong belief in Strewinski's qualities as an engineer made Heckmann accept the burden of Strewinski's increasingly irrational and complicated reactions. This burden grew in the course of the years when, on the one hand, Strewinski, notwithstanding the broadening scope of his assignment, persisted in remaining involved in minute details of the design whereas, on the other hand, he became more and more suspicious and distrustful and lesser and lesser communicative. As far as the author is aware – and this extends into the period of my General Directorship of ESO – Strewinski has consistently refused to sign a contract for work to be undertaken, simply referring to his honesty and professional pride.

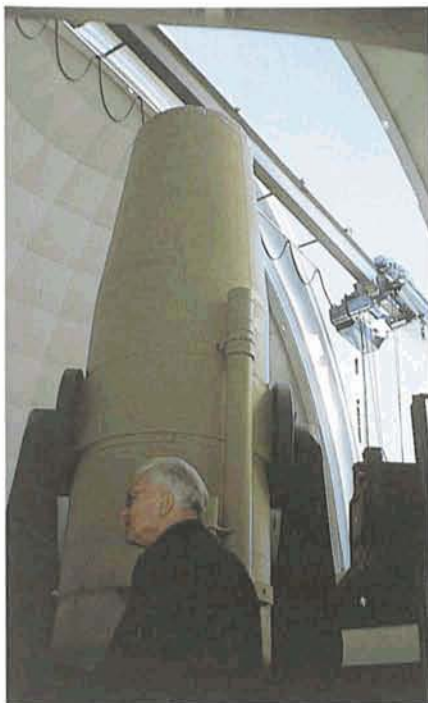
Much of this seems to be related to Strewinski's having spent years as a war prisoner in the USSR during and after World War II, where his engineering qualities and ingenuity seem to have been thoroughly exploited, even leading to continued captivity notwithstanding promises of release. He returned to Germany in 1949. Heckmann, in his book *Sterne, Kosmos, Weltmodelle*, refers at several places to their collaboration [14]. Among these references is the following, after Heckmann's mentioning



Mounting the Schmidt Telescope in the fall of 1971.

The photograph on the left shows the massive fork that would carry the telescope tube, resting on the floor of the dome. The right-hand photograph shows the polar axis already placed on its bearings. Soon after these photographs were taken, the bottom part of the fork was bolted on the flat top section of the polar axis.

Photographs by Eric Maurice in the EHPA.



December 21, 1971. Otto Heckmann in front of the Schmidt telescope during its first test period.

Photograph by Eric Maurice in the EHPA.

Strewinski's early work on the Hamburg Schmidt: "Ein Jahrzehnt später stand er uns als selbständiger Ingenieur gegenüber. Leider hatten wir erst zu einem Zeitpunkt, als seine Arbeiten bereits weit fortgeschritten waren, klar erkannt, wie starr und mißtrauisch er in der Zwischenzeit geworden war. --- Seine Unlust, sich auszusprechen oder gar zu fragen, führte leider mehrfach dazu, daß wir vor fertige Entscheidungen gestellt wurden, wo wir gerne mitbestimmt hätten. So kam es, daß später Schwierigkeiten auftauchten, weil manche Einzelheit zu geistreich, zu kompliziert gelöst worden war. ---".

As far as the ESO Council is concerned, the body where the ultimate responsibility rested, we have described their growing impatience in previous articles. Looking back, we may be surprised by their leniency; confidence in Heckmann's judgement prevailed.

The Schmidt Telescope in operation.

Upper right photograph: Oscar Pizarro, who together with Guido Pizarro was responsible for carrying out most of the extensive and delicate programme of observations for the ESO Sky Surveys, guiding the telescope during an exposure.

Lower right photograph: placing the plateholder in the telescope.

From undated slides in the EHPA.



Steps Toward Perfection

The first phase was followed by a lengthy period of finishing touches and improvements under the supervision of André Muller. Well qualified for the job by experience in optical instrumentation gathered early in his career, as well as by his acquaintance with La Silla, Muller embarked upon a series of technical improvements in collaboration with the staff on La Silla – particularly with Hans-Emil Schuster – and with the growing expertise of the staff of the TP Division, of which especially the important contributions of the engineer Jan van der Ven should be mentioned. In 1972 Muller stayed for several extended periods on La Silla where he collaborated in the middle of the year with Strewinski. The long series of improvements and modernizations which followed extended over many years, during the time of my Directorate and beyond. They will not, therefore, be recorded here in any detail; I shall only touch upon some main points, as a background for the account on the large observational projects summarized below, which developed parallel to this work.

Defects in the electronic control system as it had been delivered before the ESO TP Division became involved caused a major problem. Eventually, an entirely new system was installed, similar to the one developed by the TP Division for the 1-m telescope in 1974. Also, at the TP Division, entirely new mechanical drive systems in right ascension and declination were constructed.

A very important problem, encountered already in the beginning of the observational work, was that of the differential motion between the camera holding the plate holder and the field on the sky as seen by the guiding telescopes. The history of this problem goes back to the earliest work with Schmidt telescopes [15]. It became more and more pressing as the required exposure times became longer. For the ESO Schmidt, a major improvement was found by discarding altogether the use of guiding telescopes attached to the Schmidt tube, and introducing an offset guiding system that directly observes stars in the field of the Schmidt optics itself. And, when plates have to be taken with exposures of several hours, as is the case for the Sky Surveys, perfection even has to be carried so far that, by means of computer control, the variation in the relative position of the pointing of the plate centre with respect to that of the offset guider, caused by the changing differential refraction in the earth atmosphere, must be eliminated.

For a review of further improvements I



Otto Heckmann (23-6-1901 – 13-5-1983), painted by the artist Herbert von Krumhaar on the occasion of his retirement from the General Directorate per December 31, 1969. After his retirement, Heckmann continued to work for ESO as a consultant with particular attention to the completion of the Schmidt telescope. This consultancy was concluded when the first operational stage of the telescope had been reached in the course of 1972. The painting was donated by friends and colleagues of Heckmann.

refer to a contribution by Muller to the Bernhard Schmidt Centennial celebration mentioned before [16] and to a review by R. West "The ESO Sky Surveys" in IAU Colloquium No. 78 [17].

Finally, it is of interest to know that in 1958 Strewinski published a detailed description of the Hamburg Schmidt, which has much basic design in common with the ESO Schmidt. This work made him acquainted with the exactingness of astronomers: "*Die Wünsche der Astronomen bezüglich Genauigkeit und Zuverlässigkeit ihrer Instrumente sind sehr weitgehend. Es bedarf erheblicher Anstrengungen der Konstruktion und Fertigung --- um die gestellten Forderungen zu erfüllen*" [18].

The Sky Atlas Laboratory

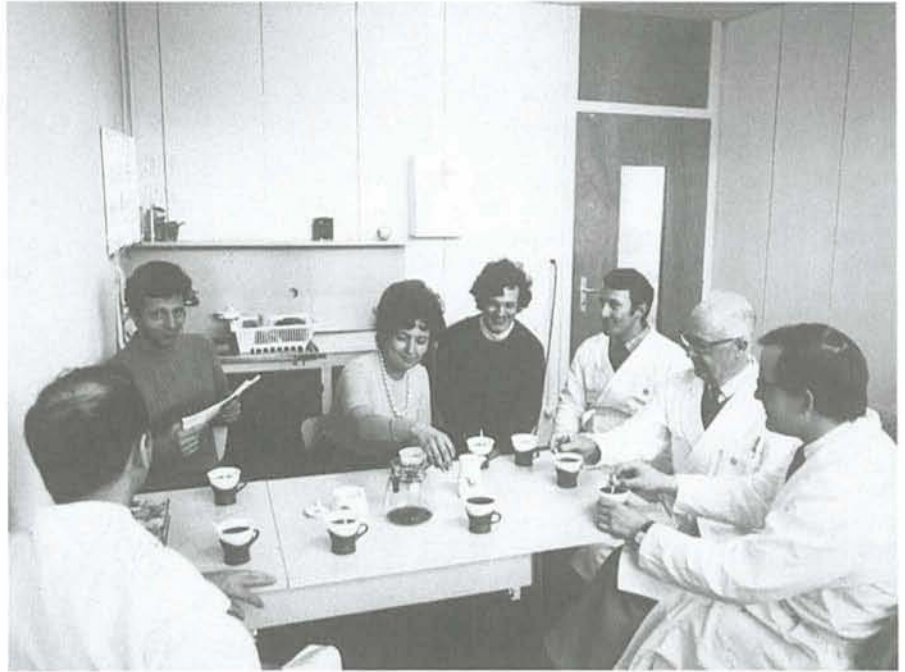
In the course of the year 1971, with completion of the Schmidt drawing nearer and the operational stage in sight, the next step to take was the creation of adequate facilities for processing the expected photographic material. The high optical performance to which the telescope was gradually brought, had to be matched by the highest possible perfection in the handling of the plates taken with the telescope. This became especially significant in connection with the planning of the sky atlas.

In the early days of the planning for ESO, the use of the Schmidt telescope

for producing sky surveys did not yet figure very prominently in comparison to, for instance, objective prism spectral work. However, by the time the instrument became ready for use, observations for the Sky Atlas were seen as the most important task for the first years of operation. The Atlas produced by the Palomar Schmidt for the northern sky had proved to be of enormous importance for research in many fields, especially for identifying candidate objects to be observed with large telescopes. Providing the southern counterpart of the Palomar Atlas became the most urgent task for the ESO Schmidt.

The extraordinary demands the photographic processing technique has to satisfy can be appreciated if one realizes that a Schmidt plate may contain some million or more stellar images, mixed with images of faint galaxies and diffuse nebulous objects, each of which may become the object of separate investigation now or in the future, and that not only all of these images should be of optimal quality, but that at the same time the plate should not contain any defect that might interfere with the research. Spurious stellar images due to inadequate processing must be avoided, and so must inhomogeneous development of the plates, scratches, etc.

Accordingly, two steps had to be taken: providing the dark room in the Schmidt telescope building on La Silla with up-to-date equipment for the processing of the plates and for prints to be made from them, and the creation in Europe of an ESO photographic laboratory for the wholesale reproduction of



The ESO Sky Atlas Laboratory on the premises of CERN.

By Council decision of December 1971 ESO established its Sky Atlas Laboratory on the premises of CERN, close to the TP Division. Before the end of 1972 it was ready to start the wholesale production of the copies of sky photographs obtained with the Schmidt telescope. The above photograph shows the laboratory's staff and visitors in March 1973. In clock-wise direction, starting from the lower left corner: Bernard Dumoulin; a visitor from TPD; Françoise Patard; another visitor from TPD; Bernard Pillet; Bill Miller from Pasadena; and Richard West. Photograph by PHOTO CERN in the EHPA.

these prints without loss of quality. These were challenging tasks, for mastering the required techniques could not be learned from experience collected in any laboratory, scientific or industrial, in Europe, and contracting out to industry would have been too expensive. It was, therefore, a most fortunate circum-

stance that ESO could profit from the know-how gathered by American colleagues involved in the Palomar Sky Atlas project. Readiness to fully share their experience with ESO was expressed at an early stage to the author by Rudolph Minkowski who supervised at that time the Atlas Laboratory at Pasadena.

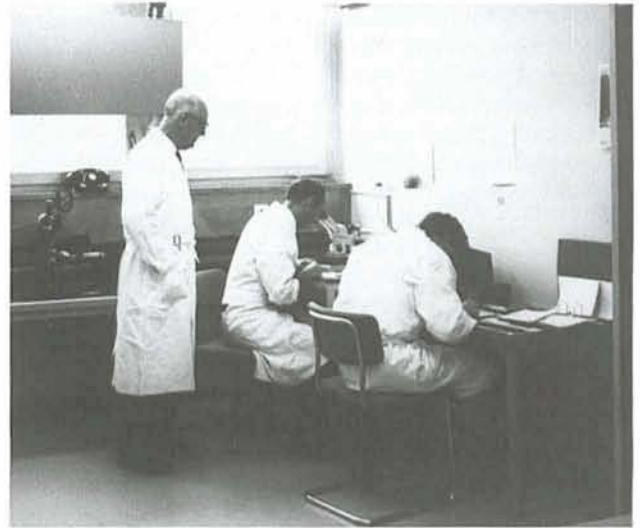


Working at the Atlas Laboratory, March 1973.

Left photograph. B. Dumoulin inspects a 30 × 30 cm copy glass plate. The special plate frames and tanks for fixing and washing were of his design.

Right photograph: William ("Bill") Miller of the Palomar Atlas Laboratory (Hale Observatories), from whose experience the ESO laboratory benefitted greatly, looking over the shoulders of B. Dumoulin and R. West.

Photographs by PHOTO CERN in the EHPA.



Consultation within ESO in the middle of 1971 led to a proposal to the Council meeting of Nov. 30–Dec. 1 for the establishment of a laboratory equipped for the production of large numbers of copies of the Schmidt plates on film or on glass. It was a major proposition, considering the space required, the personnel to be appointed, and the equipment to be purchased; on the other hand, the work to be done was a natural follow up on the completion of the telescope.

Council agreed, including the decision to establish the installation, not at the site of the administrative headquarters in Bergedorf, but on the premises of CERN, close to the TP Division which at that time had just started its work. For this project, again, strong support was received from the side of the Directorate of CERN that created space in one of its buildings adjacent to the TP Division.

As leader of the project, Richard West was appointed who since January 1970 had been an ESO employee as scientific associate to the Director General. As one of his first moves, West took up contact with the Atlas Laboratory at Pasadena and laid the foundation for close collaboration with William ("Bill") C. Miller who directed this project. Over the years, Miller's active interest and support contributed much to the work of the ESO Laboratory.

The Quick Blue Survey

Well within a year after the Council decision of December 1971, the Atlas Laboratory was ready for its first tasks. A major project was soon to be undertaken: the production of the ESO-B Atlas for which the first plates were taken in April 1973. It has also been referred to as the ESO "Quick Blue Atlas", a name derived from its aim to provide the astronomical community at an early date with an overall picture of the southern sky, pending the production of the more sophisticated ESO-SRC Atlas the origin of which will be described below. The Quick Blue Atlas was distributed on a limited scale (see also below, under ESO/SRC Agreement), yet it soon played an important role in many research projects. It covered the sky between -90° and -20° declination by means of 606 fields with exposures of one hour, reaching a limiting blue magnitude of about 21.5.

Much of the successful achievement of the Atlas project (it was completed in 1978) must be attributed to the harmonious collaboration between the staff handling the Schmidt observations at La Silla including the delicate processing and making first copies, i.e. Hans-Emil Schuster and the brothers Guido and



The Atlas Laboratory's first exhibition.

In November 1973 the Atlas Laboratory organized an exhibition of its work and of that of the TP Division in the entrance hall of the Main Office Building of CERN. Between the first and the second sky photographs from the left is a model of the 3.6-m telescope building, containing a model of this telescope.

Oscar Pizarro, and the staff of the ESO Sky Atlas Laboratory.

A British Sister for the ESO Schmidt

While ESO worked on the realization of its Schmidt project, a southern Schmidt also formed part of a project for two Schmidts to be acquired by Cerro Tololo and Kitt Peak Observatories around the year 1970. (In fact, as early as in 1960 a Schmidt for Tololo was under consideration [19].) Preliminary designs aimed at telescopes with an aperture of 1.3 m, a focal length of at least 4 m, and fields of 4.4×4.4 . These telescopes should, moreover, be convertible to Cassegrain operation. Design considerations were presented by R. Buchroeder and B. Lynds at the 1972 Hamburg Conference referred to below, but the project did not materialize.

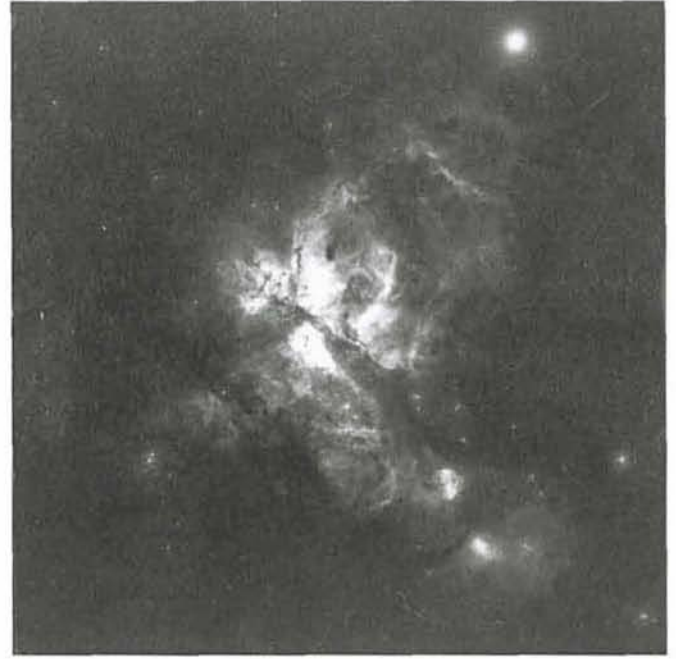
However, a sister for the ESO Schmidt was born elsewhere. Early 1971 the ESO Directorate learned about plans being developed for a southern Schmidt by the British Science Research Council (SRC) under the leadership of Vincent R. Reddish, Director of the Royal Observatory at Edinburgh. Based on a design closely similar to that of the Palomar Schmidt, this telescope became operational already in September 1973 – an outstanding achievement when compared to the tedious history of construction of the ESO Schmidt! A brief description of the SRC

Schmidt – placed at Siding Spring Mountain in Australia where also the Anglo-Australian 3.5-m Telescope is located – was presented by Reddish at the Conference on Schmidt Telescopes in 1972 mentioned below.

Obviously, with the prospect of these two powerful Schmidts in the southern hemisphere, coordination of their programmes was in order. The ESO Directorate therefore approached Dr. Reddish and found him agreeable to joint planning, and this was soon followed by parallel consultation between the President of the ESO Council and the Chairman of the SRC. From these first steps, a very fruitful collaboration emerged.

The Hamburg Conference on Schmidt Telescopes

A first result of this collaboration was the Conference on The Role of Schmidt Telescopes in Astronomy, held at Hamburg Observatory on March 21–23, 1972. This observatory joined in the organization of the conference, and the proceedings were edited by Ulrich Haug of Hamburg Observatory [20]. The conference surveyed fields of applications of large Schmidts, and in particular served for looking ahead in connection with the extensive Sky Surveys to be carried out in the coming years. It profited much from the participation of astronomers involved in the work with the Palomar Schmidt. On the day following the conference, March 24, a session of



Two of the early photographs taken with the Schmidt telescope.

Left: The central part of the constellation Orion including the Orion Nebula, a 20-minute exposure taken by Schuster on February 2, 1972.

Right: The Carina Nebula, a 45-minute exposure taken by Schuster on February 28, 1973.

specialists discussed in detail the specifications for the surveys.

The ESO-SRC Agreement

After the Hamburg Conference, consultation between ESO and the SRC gradually shaped the final agreement [21]. A first draft was made by Reddish in April 1972, and the final text was signed in January 1974 by Reddish as Project Officer of the U.K. 48-Schmidt Telescope Unit, and the ESO Director General. From ESO side the correspondence was conducted mostly by Richard West, whose task as Head of the Sky Atlas Laboratory henceforth would also embrace this collaborative project. The agreement has been of far-reaching importance for astronomical research. We shall outline here its main features. For a more detailed account reference is made to R. M. West's article on the ESO-SRC Sky Atlas and related items in *ESO Bulletin* No. 10 of May 1974, and to accounts in the ESO Annual Reports.

The agreement consisted of four parts. The first one defined a general framework for collaboration "— — — considering that ESO and SRC have previously expressed their interest to cooperate in carrying out southern sky surveys and publishing the results, — — —". The second part was an arrangement "governing the production, publication and sale of a two-color atlas of the southern sky", to be printed on film. The third part concerned arrangements "governing

the production and distribution of initial [glass] copies of the ESO (R) and the SRC (IIIaJ) surveys". The fourth part dealt with "the production and distribution of initial copies of the ESO "B" Survey".

In this fourth part, principal item was the number of copies of the Quick Blue Survey to be distributed by ESO among ESO countries and a few US observatories and by SRC among observatories in the UK (and the price to be paid for the latter by SRC). 20 glass copies and 20 film copies were to be made, of which SRC acquired 6 on glass and 14 on film. Taking the plates for the Quick Blue Survey had started in April 1973. By the end of 1973, 40 acceptable plates (out of 80 taken) were available. We note that the earliest plate used for this survey carries the number 299 [22]; plates taken previously served many other purposes.

The second part specified the most substantial component of the collaboration: the joint production of the two-colour Atlas for which the SRC Schmidt would provide the ESO Sky Atlas Laboratory with the "blue" plates on IIIaJ emulsion, and the ESO Schmidt the "red" plates on 094-04 emulsion. Other items of this agreement included market exploration, selling prices, the number of copies to be made, etc., and the fact that the Sky Atlas Laboratory would handle the production, distribution and sale on a non-profit basis. The Atlas referred to here, containing 606 fields between declinations -20° and -90° ,

was made on film.

The third part specified the production of a small number of copies of the Atlas on glass: 6 for SRC and 4 for ESO.

The ESO-Uppsala Faint Galaxies Survey

As a last item in this early history of the Schmidt telescope, I shall briefly dwell on the birth of the ESO-Uppsala faint galaxies project. When early 1973 the first Schmidt plates of atlas quality became available, astronomers' thoughts naturally went to the many research projects for which they might be used. As mentioned before, a most important field of application would be the study of extragalactic stellar systems. Was there a task for the ESO Directorate beyond just providing the astronomical community with the Atlas?

A comparison may be drawn with an earlier situation in astronomy when, in the beginning of this century, wholesale spectral classification by means of objective prism plates became possible. Harvard Observatory then initiated the systematic cataloguing of the spectral types of all bright stars, resulting in Annie Cannon's monumental Henry Draper Catalogue. With its more than 200000 stars it has been a basic reference in stellar research since then. Now, with extragalactic research being opened up in the southern sky, shouldn't it be a task for ESO to promote the provision of the community with a basic catalogue of galaxies, down

to a well-defined observational limit and specifying main characteristics such as Hubble type and apparent magnitude? Many considerations pointed to answering "yes", including the important side effect of ensuring uniformity in the identification numbers to be used in the future.

Since the task would be far beyond what might be done by the ESO staff itself, collaboration with an astronomical institute, preferably in one of the ESO countries, would be the solution and this led the ESO Directorate to approach in the spring of 1973 the Director of Uppsala Observatory, Eric Holmberg. Uppsala Observatory was one of the few in the ESO countries with an established tradition in extragalactic work, including work of statistical nature. A major project published in 1973 was P. Nilson's Uppsala General Catalogue of Galaxies, containing data for nearly 13,000 galaxies north of declination $-2^{\circ}30'$ and based on the Palomar Sky Survey [23]. In reply to a formal letter of May 16, 1973 of the ESO Director General, Holmberg expressed his interest in the proposition and sketched first outlines for the collaboration in a letter of May 27. Further correspondence and meetings between ESO and Uppsala staff led to a formal agreement between the two institutes of February 8, 1974 [24].

In the course of the negotiations, for ESO the Head of the Sky Atlas Laboratory, Richard West, became more and more involved, and soon took this project, too, under his wings. The agreement specified, among other items, that the Uppsala search was to be made by an astronomer at Uppsala Observatory on copies of the original plates of the Quick Blue Survey especially made for this purpose; an Annex, apart from giving technical details, stated that besides galaxies satisfying certain observational criteria, also a selection of stellar clusters and planetary nebulae were to be included. The criteria to be adopted for the selection of the galaxies were the same as those used by Nilson so that homogeneous coverage of the northern and southern parts of the sky would be assured.

In a letter of February 20, 1974 to the Director General of ESO, Holmberg wrote that, since November 1973, the work had been going full force by Andris Lauberts, and a first batch of 20 plates were under survey. A comprehensive description of the project was published in 1974 by Holmberg, Lauberts, Schuster and West [25].

Acknowledgement

I am indebted to Drs. A. B. Muller and R. M. West for helpful comments on a draft of this article.

References and Notes

Abbreviations used:

EC = ESO Committee, the committee that preceded the ESO Council.

EHA = ESO Historical Archives. See the description in the *Messenger* No. 54 of December 1988.

FHA = Files belonging to the Office of the Head of Administration of ESO.

EHPA = ESO Historical Photographs Archive. Heckmann Sterne = O. Heckmann, *Sterne, Kosmos, Weltmodelle*, Verlag Piper and Co., München - Zürich, 1976.

- [1] I am indebted to Prof. U. Haug of Hamburg Observatory for providing me with the references [2] and [3] below.
- [2] *Abhandlungen Hamburger Sternwarte* Band X, Heft 2, p. 50, 1979.
- [3] See O. Heckmann, in *Nature*, Vol. 76, p. 805, 1955 and in *Mitteilungen Astron. Gesellschaft* 1955, p. 57, 1956.
- [4] See Fehrenbach's report in the minutes of the 9th meeting of the Instr. Comm., Oct. 18, 1963, p. 10 in FHA. Reference is also made to the minutes of the EC of Nov. 1961, Oct. 1962, in FHA, and to the ESO Annual Rep. 1964.
- [5] Minutes of the 6th meeting of the Instr. Comm., p. 3, in FHA.
- [6] Minutes Instr. Comm. June 25, 1964, p. 7, in FHA.
- [7] Minutes of the 13th meeting of the Instr. Comm., p. 4; Minutes 2nd Cou Meeting, May 1964, both in FHA.
- [8] See also, in EHA-I.A.2.10, relevant correspondence between Oort and Heckmann in June and July 1964 and March 1965.
- [9] Proceedings of the Conference on "The Role of Schmidt Telescopes in Astronomy", Ed. U. Haug, published jointly by ESO, SRC and Hamburg Observatory, 1972, p. 137-139.

- [10] A more extensive description is in the minutes of the Instr. Comm. of March 1964, in FHA.
- [11] Editions du Centre National de Recherche Scientifique, Paris 1990, p. 404.
- [12] See ESO Annual Reports 1964-1966 and minutes Cou Meetings 1965 and 1966, in FHA.
- [13] FHA-Cou minutes Dec. 1968, p. 4.
- [14] Heckmann *Sterne*, p. 216 and 321-322.
- [15] In a letter of January 10, 1990, Prof. U. Haug of Hamburg Observatory points out to me, that in the case of the Hamburg Schmidt, whereas Strewinski was responsible for the mechanical design of the mounting, the combination optics-telescope tube was primarily handled by Zeiss-Jena, including a solution for the alignment telescope-tube/guiding-telescopes.
- [16] Ref. [2], p. 79.
- [17] "*Astronomy With Schmidt Telescopes*", Ed. M. Capaccioli, Reidel, 1983, p. 13.
- [18] *Mitteilungen Ver. Drehbank-Fabriken* No. 15, March 1958, p. 1, in EHA-III.
- [19] According to a letter by D. Shane to J. H. Oort of August 22, 1960; in EHA-I.A.1.13.
- [20] See note [9].
- [21] Documentation pertaining to the development of the ESO-SRC collaboration is contained in FHA-2.8.3, "Cooperation with SRC", including copies of correspondence between West, Blaauw and Reddish and the legal advisors of ESO and SRC from April 20, 1972 and draft texts for the Agreement from November 1972 till the final version of January 1974.
- [22] See, for instance, the internal Memo ref. SK/74/186/RW/FP of October 10, 1974 from West to various ESO Officers: "List of plates which have been distributed" in EHA-III.
- [23] *Uppsala Astron. Obs. Ann.*, Vol. 6, 1973.
- [24] I am much indebted to Prof. E. Holmberg and Dr. A. Lauberts for providing me with copies of the early correspondence in the files of Uppsala Observatory: letters of May 27 and Sept. 26, 1973. The ESO FHA-2.8.6. contain, for the period reported here, copies of correspondence and drafts as well as the final contract, beginning Sept. 26, 1973. See also the ESO Annual Reports.
- [25] E. B. Holmberg, A. Lauberts, H.-E. Schuster and R. M. West, The ESO/Uppsala Survey of the ESO (B) Atlas of the Southern Sky. I., in *Astron. Astrophys. Suppl* 18, p. 463-489, 1974.

Open Clusters Under the Microscope

B. NORDSTRÖM and J. ANDERSEN, Copenhagen University Observatory, Denmark

Stellar Evolution Models

Our use of, and faith in, stellar evolution models underlie much of contemporary astrophysics. Stellar evolution

theory has provided a framework within which, in broad terms, we can fit the apparently bewildering variety of single and double stars into a logical order described by a physical theory.

Stellar evolution models are used to calculate the ages of observed stars and their lifetimes in various evolutionary phases. They also describe the transformation of lighter to heavier chemical

elements within the stars, and the amounts of processed material returned to the interstellar environment at various stages during their evolution. Thus, stellar evolution models are an essential basis for models of galactic chemical evolution, a subject of much current interest.

How well do these models correspond to the real stars? Open clusters are an excellent place to make the comparison, but care is required in interpreting what one sees. We have attempted to look a bit deeper into this question than is often done.

Weak Points

Among the weak points of current stellar evolution models is their treatment of the energy transport in the stellar interior.

At the microscopic level, the effect of the absorption, reemission, and scattering processes encountered by a photon on its way towards the surface of the star is described by *opacity tables*. Here, the 1970 Cox-Stewart (C-S) opacities have now been superseded by the more recent Los Alamos Opacity Library (LAOL). The LAOL opacities are, on average, significantly larger than those by C-S, leading to cooler and less luminous stellar models (see Guenther et al., 1989).

At the macroscopic level, the treatment of convective energy transport in stellar interiors has long been recognized as one of the weakest points in stellar evolution theory. Standard models use the classical mixing-length approximation, but it has long been argued that the convective motions will "overshoot" into the classically stable, radiative regions. Overshooting from the convective cores of massive stars increases the amount of hydrogen fuel available in the main-sequence stage. Hence, main-sequence models with convective overshooting are brighter than standard models, and the stars leave the main sequence with higher ages and larger helium cores, modifying their later evolution.

Models vs. Real Stars

As no satisfactory physical overshooting theory exists (Renzini, 1987), its existence and eventual importance must be ascertained by comparison with real stars (Chiosi, 1990; Maeder, 1990). So let us assume that we have a real star of known mass, composition, and age, and use our favourite evolution code to construct a computer model of this star. How well do the observable properties, radius, effective temperature or luminosity, and surface composition

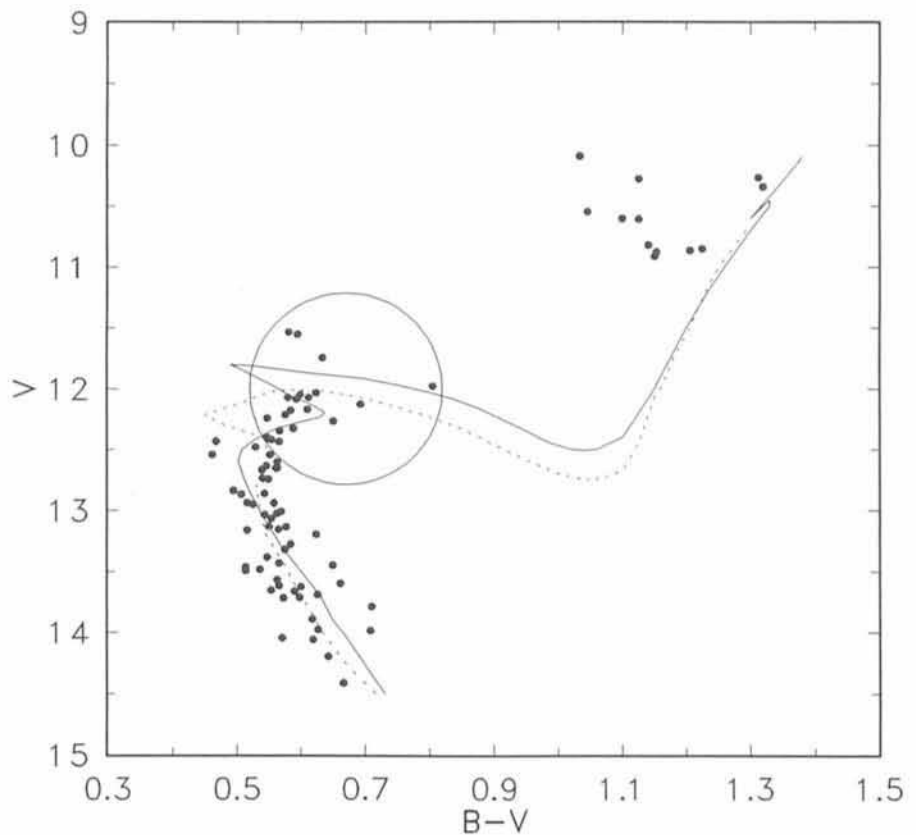


Figure 1: CM diagram of IC 4651, from Anthony-Twarog et al. (1988). Isochrones from Maeder (1990) are shown, for the observed reddening and metal abundance: Dotted: No overshooting, $2.2 \cdot 10^9$ yr. Solid: With overshooting, $4.0 \cdot 10^9$ yr.

(which might also have evolved) match those of the observed star?

Well, for which real stars do we know the mass, radius, effective temperature, chemical composition, and age, accurately and *without reference to stellar models*? The answer is: Only for one star, the Sun. So, the minimum requirement for a trustworthy evolution code is to produce a satisfactory solar model. In fact, no set of standard solar models has been found to account for all of the observations mentioned above and for the observed solar neutrino flux, oscillation spectrum, and surface lithium abundance as well (Sackmann et al., 1990). But how about stars of other masses and ages?

The Binary Test

Apart from the Sun, two alternative kinds of test object exist: eclipsing binaries and star clusters. The former have the great advantage that their masses, radii, and effective temperatures can be determined with great accuracy in a fundamental manner. Metal abundances can be determined by standard spectroscopic methods. The ages are not known, but must be the same for both components. Thus, one binary system provides us with two points of known mass (the key param-

eter determining the evolution of a star) on a model isochrone, the locus for models of different mass, but the same age.

Precise masses and radii of eclipsing binary stars for such comparisons have long been a pet subject of ours. Here, we shall just quote a couple of relevant recent results: Standard models (VandenBerg, 1985) gave a superb fit to the evolved system AI Phe at 1.2 solar masses when LAOL (but not C-S) opacities were used (Andersen et al., 1988). However, at just slightly larger masses (1.5–2.5 solar masses), binary stars near the top of the main sequence can only be fitted reasonably by overshooting models (Andersen et al., 1990).

Later precise studies of additional binaries in this mass range confirm this conclusion. But what do the clusters tell us?

The Cluster Test

As test objects for stellar evolution models, star clusters have the advantage of populating the entire isochrone, defining its shape much more precisely than possible with the mere two points supplied by a binary system. For this reason, cluster colour-magnitude (CM) diagrams have been compared extensively with theoretical model isochrones

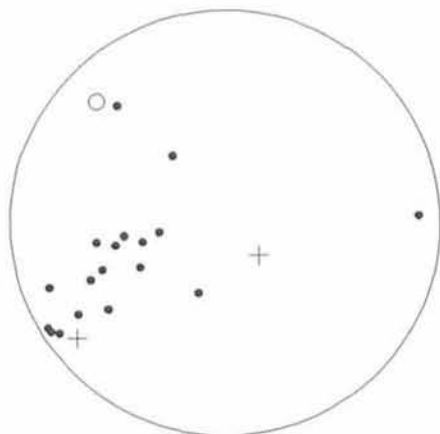


Figure 2: Close-up of the circled region of Figure 1, where CORAVEL radial-velocity observations have been made. Dots: Likely single members. Crosses: Established non-members. Circle: Uncertain (broad-lined star).

(e.g. VandenBerg, 1985), and quite precise age determinations have been reported (e.g. Mazzei and Pigatto, 1988). We concentrate in the following on the age range covered by the open clusters.

As tools for testing stellar models, CM diagrams of star clusters also have a number of drawbacks: First, of course, the true masses of the stars are in principle unknown. Second, defining the correct effective temperature and luminosity scales in the cluster requires that the reddening and distance of the cluster have been accurately determined. Next, the metal abundance must be accurately measured by photometric and spectroscopic observations of cluster stars. Then, some cluster stars will be unresolved binaries and appearing brighter and generally redder than the more luminous component by itself (if both are main-sequence stars). Finally, most cluster CM diagrams also contain a significant number of non-member or field stars.

All of these effects combine to produce more ambiguity in fitting theoretical isochrones to observations than often meets the eye in published diagrams. If reddening, metal abundance, and distance have not been determined separately, but included in the fit, any systematic errors in the model colours or luminosities will be hidden, but reappear as systematic errors in the derived ages. Errors will also occur if reddening or metal abundance determinations were based partly on non-member stars.

Further uncertainty in the interpretation of details in the isochrones is introduced if, in addition, one can pick and choose which stars to exclude from the fit as presumed binaries and non-members. We have examined this point

closely in two open clusters of intermediate age, IC 4651 and NGC 3680. Our results show that these "nitty-gritty details" are far from inconsequential when one wishes to actually *test* stellar models: The purpose of a critical test is not to play with enough free parameters to fit the data with one's favourite model, but to see whether at least *some* of the competing models are in fact excluded by the data.

IC 4651

IC 4651 is a fairly rich open cluster with turnoff stars of mid-F type. The most recent photometric studies of it are by Anthony-Twarog et al. (1988) and Nissen (1988), who found its age to be about $2.5 \cdot 10^9$ yr, based on the VandenBerg (1985) standard models. Mazzei and Pigatto (1988) derived an age of $1.3 \cdot 10^9$ yr with models incorporating strong overshooting, which they found to be superior to standard models. Maeder (1990), on the other hand, derived ages of $4 \cdot 10^9$ yr and $2.2 \cdot 10^9$ yr, respectively, from models with and without overshooting – from the same CM diagram!

Which of all these wildly conflicting estimates can one believe? And, to ask the underlying key question, does the CM diagram of IC 4651 provide unambiguous evidence for significant overshooting in the cluster stars, or does it not?

The CM diagram of IC 4651 is shown in Figure 1. The isochrones are those by Maeder (1990), fitted with the reddening and (solar) metallicity determined directly by Nissen (1988). Clearly, the main differences between the two curves are in the upper part of the turnoff: The overshooting isochrone extends significantly higher above the turnoff than the standard isochrone, and also curves gently towards the red before reaching the "red hook".

The issue is decided by the true nature of the encircled group of stars: Are they all binary and field stars which should be disregarded? If so, the standard models without overshooting and the associated (low) age are to be preferred. Or are they mostly single cluster members? In that case, the standard isochrone is clearly not an acceptable match to the observations, and the high age estimate must prevail.

IC 4651 under the Microscope

Let us look for the answer by putting the turnoff region of IC 4651 under the microscope. Our "microscope" in this case is the radial-velocity scanner CORAVEL (Mayor, 1985), mounted on the Danish 1.5-m telescope at La Silla.

For distant clusters such as IC 4651, accurate radial velocities (1 km s^{-1} or better) are the most reliable indicator of membership: If repeated observations show a constant velocity equal to the cluster mean, there is a very strong probability that the star is both single and member of the cluster.

Figure 2 shows what the "microscope" reveals after two seasons of observations: The large majority of the stars do indeed appear to be single cluster stars. Granted, a couple may turn out to be long-period binaries in the cluster, which we happened to observe just when they were close to the mean velocity. Sure, one or two may be field stars with nearly the same velocity as IC 4651. But certainly not *all* the stars in Figure 2 are binaries and non-members, as would be required for the standard isochrone to be the appropriate choice. *IC 4651 does appear to show unambiguous evidence for the presence of convective core overshooting.*

NGC 3680

NGC 3680 is a cluster very similar to IC 4651 in age and metal abundance (both marginally higher than IC 4651). We show its CM diagram in Figure 3, assembled from the photometry of Anthony-Twarog et al. (1989), Nissen (1988), and Eggen (1969). The CM diagram is less neat than that in Figure 1, due to the larger influence of field stars. A striking feature is the apparent dichotomy of the main sequence into two parallel sequences, the so-called "bimodal turnoff" discussed extensively by both Nissen (1988) and Anthony-Twarog et al. (1989). No credible explanation for a real feature of this type could be found.

Again, we have focused our CORAVEL "microscope" on the encircled stars in Figure 3. Although our 1989–1990 observations of NGC 3680 are much more complete than those of IC 4651, what we see is not quite as clear-cut as that in Figure 2. This is because the fraction of stars with broad lines and/or variable or slightly discrepant velocities is much larger. More data are needed to clearly separate the various categories of stars. We expect to obtain these during the 1991 observing season. However, several robust conclusions are already emerging:

First, about 2/3 (!) of the stars in Figure 3 appear not to be members of NGC 3680 at all. Also, binaries are rather frequent among both cluster and field stars. Then, when binaries are identified and field stars removed, the "bimodal turnoff" dissolves into a single sequence of stars. Interestingly, this sequence shows the shallow slope on the

upper main sequence and the large vertical extent and redward curvature of the turnoff which distinguish the overshooting isochrone in Figure 1: Overshooting seems definitely present in NGC 3680 also.

Some Lessons

One lesson is immediately obvious: If significant conclusions on stellar models or cluster age depend on the correct interpretation of minor features of a cluster CM diagram, careful star-by-star identification of non-members and binaries is essential. The microscope may reveal that initial, and perhaps biased, impressions are in fact wrong.

Then, together with the binary evidence, the cluster data seem to show that convective overshooting does exist as an observable phenomenon in stars of these masses. Future stellar evolution models will have to take this into account. With their precise photometry and membership data, clusters such as IC 4651 and NGC 3680 will be very valuable in helping to calibrate the model parameters used in the convection prescription. We hope to extend this type of work to clusters of other ages, and subject new generations of stellar models to tests based on both binary and cluster data.

A third significant consequence of accepting the validity of overshooting models is that higher ages ($\sim 4 \cdot 10^9$ yr) are estimated for the stars in IC 4651 and NGC 3680 than with standard models, by almost a factor of two (cf. Fig. 1). This result appears to be typical for evolved main-sequence stars (cf. Table 1 in Andersen et al., 1990), and should be of some significance for models of the evolution of the Galactic thin disk population.

Why did Mazzei and Pigatto (1988) derive ages a factor of three lower from their overshooting models, when they considered their ages accurate to $\sim 10\%$? Their determination of reddening in the isochrone fit itself is a likely reason: Their values of $E(B-V)$ are ~ 0.15 mag larger than those observed directly,

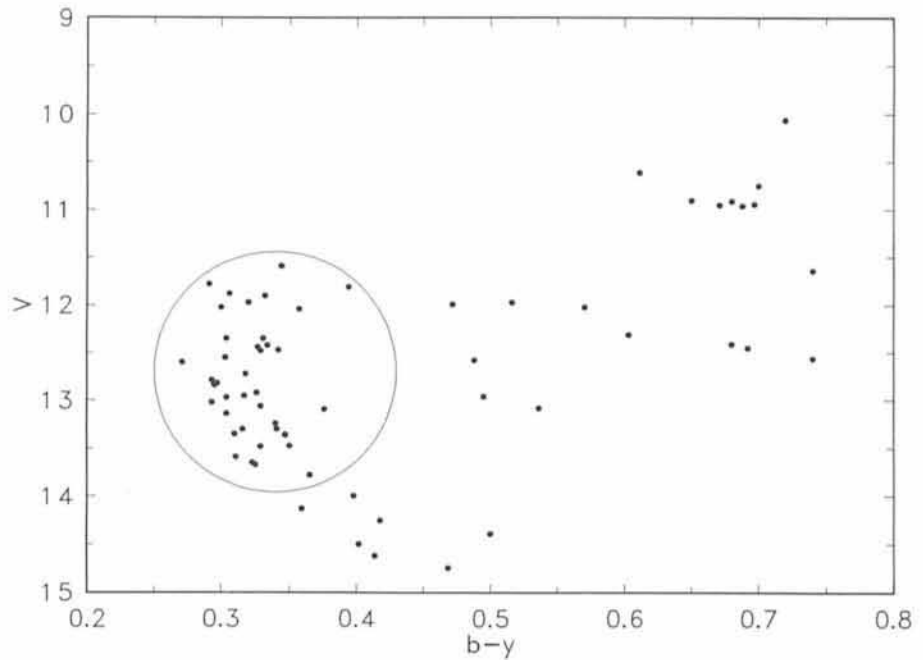


Figure 3: CM diagram of NGC 3680 from Anthony-Twarog et al. (1989), Nissen (1988), and Eggen (1969, transformed to $b-y$). Note the apparent bimodality of the main sequence; CORAVEL data for the circled stars show this to be an artifact of binary and non-member contamination.

maybe because the C-S opacities lead to their models being too hot. Overcorrecting for reddening by 0.15 mag will, of course, lead to significantly lower age estimates.

Acknowledgements

We thank Drs. B. Anthony-Twarog, M. Mayor, B. Twarog, and D. Vandenberg for helpful conversations and correspondence, and ESO, the Danish Board for Astronomical Research, the Danish Natural Science Research Council, and the Carlsberg Foundation for financial support.

References

Andersen, J., Clausen, J.V., Gustafsson, B., Nordström, B., Vandenberg, D.A.: 1988, *Astron. Astrophys.* **196**, 128.
 Andersen, J., Nordström, B., Clausen, J.V.: 1990, *Ap. J.* **363**, L33.

Anthony-Twarog, B.J., Mukherjee, K., Caldwell, C.N., and Twarog, B.A.: 1988, *A.J.*, **95**, 1453.
 Anthony-Twarog, B.J., Twarog, B.A., and Shodhan, S.: 1989, *A.J.*, **98**, 1634.
 Chiosi, C.: 1990, *Publ. Astr. Soc. Pac.* **102**, 412.
 Eggen, O.J.: 1969, *Ap. J.* **155**, 439.
 Guenther, E.B., A. Jaffe, Demarque, P.: 1989, *Ap. J.* **345**, 1022.
 Maeder, A.: 1990, in *Astrophysical Ages and Dating Methods*, eds. E. Vangioni-Flam, M. Cassé, J. Audouze, J. Tran Thanh-Van, Ed. Frontières, Paris, p. 71.
 Mayor, M.: 1985, in *Stellar Radial Velocities*, IAU Colloq. No. **88**, eds. A.G.D. Philip, D.W. Latham, L. Davis Press, Schenectady, p. 35.
 Mazzei, P., Pigatto, L.: 1988, *Astron. Astrophys.* **193**, 148.
 Nissen, P.E.: 1988, *Astron. Astrophys.* **199**, 146.
 Renzini, A.: 1987, *Astron. Astrophys.* **188**, 49.
 Sackmann, I.-J., Boothroyd, A.I., Fowler, W.A.: 1990, *Ap. J.* **360**, 727.
 Vandenberg, D.A.: 1985, *Ap. J. Suppl.* **58**, 711.

The Oldest Stars

A. ARDEBERG¹, H. LINDGREN² and I. LUNDSTRÖM¹

¹Lund Observatory, Sweden; ²European Southern Observatory

Introduction

Traditionally, young stars have been favourite objects for investigations of galactic structure and dynamics. Among

the reasons for this preference, the generally high luminosity of hot stars has played a major role. As a result, our knowledge of the young population in the Galaxy is relatively advanced. The

same is definitely not true for the oldest populations in the Galaxy. The major reason for our limited insights into the early generation of galactic stars is their low luminosities and generally incon-

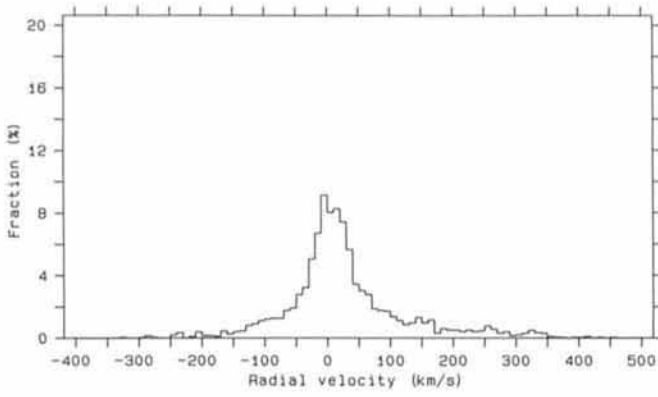


Figure 1: Fractional histogram of radial velocities obtained for the 1300 objects selected for our present study. Bin size is 10 kilometres per second.

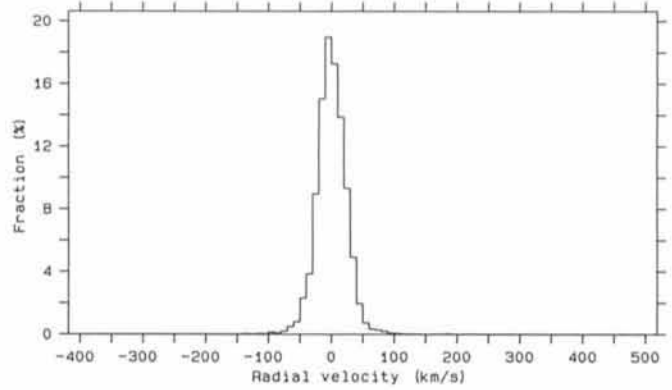


Figure 2: Fractional histogram of radial velocities for stars included in the Bright Star Catalogue. Bin size is 10 kilometres per second.

spicuous appearance. Simply speaking, these stars have not been able to raise the same enthusiasm among observers as their hotter and more recent counterparts. Consequently, our knowledge of the first generations of galactic stars has long been rather limited. This is a definite weakness in the understanding of our own galaxy, its structure and evolution. It is also, in a corresponding manner, a limitation to our understanding of the evolution of stars and of the Universe.

Stars of Interest

For a study of the earliest phases of the evolution of the Galaxy, we are interested in stars with lifetimes comparable to, or longer than, that of the system itself. In practice, this means that we are limited to stars of roughly solar temperature and cooler. At the same time, there is a special advantage in studying stars which are reasonably similar to the Sun in their basic properties, as this largely improves our possibilities to interpret observing data through direct comparisons with corresponding solar data. Taking into consideration both the age and the similarity to the Sun, we are limited to stars of spectral types from late F to late K. Among these, those with higher surface gravities are the most interesting ones.

What Do We Want to Know?

Nobody embarking on a project concerned with the earliest generations of galactic stars should have difficulties in identifying interesting topics for studies. Such topics are as numerous as important. Largely depending on our present lack of suitable data, a major problem is to arrive at some basic understanding of early star formation and its governing processes.

In general, we want to obtain a picture of the early Galaxy, its structure and

dynamical behaviour. At the same time, the evolution of star-forming processes as a function of time is an important target for our studies. In addition to parameters describing structure and dynamics as a function of time, we are highly interested in the chemical evolution of the Galaxy. This involves the chemical composition of the very young Galaxy and the subsequent composition evolution.

The structure, the dynamics and the chemical composition may be seen as parameters describing the Galaxy as an entity or, in other words, as seen by an outside observer watching our galaxy at low spatial resolution.

In our case, it is natural to include parameters describing the Galaxy more in detail. Such parameters concern star-formation processes. How were the first stars formed? Did first-generation star formation occur mainly in groups or clusters, or did it give preference to individual stars? Are there a number of galactic stellar components well or at least reasonably well distinguishable or is the distribution of such components

generally smooth? Is the total history of star formation marked by explosive events or does it present overall continuity? Does star formation present a largely isotropical pattern or is the picture of a more patchy nature? Are early and more recent star formation processes approximately comparable or are the mechanisms significantly different?

From the dynamical point of view, a detailed approach provokes a number of questions. How did the early Galaxy behave dynamically? Can we determine galactic rotation as a function of age of the Galaxy? How are orbital parameters depending on age? Can stars have high space velocities but still not show significant underabundance of heavy elements?

Is there a smooth transition between stars with high space velocities and those with modest and low velocities? Is space velocity a large-scale characteristic only, or can isolated groups of stars break an otherwise smooth velocity distribution? Can we derive a well-defined velocity of escape for the solar neigh-

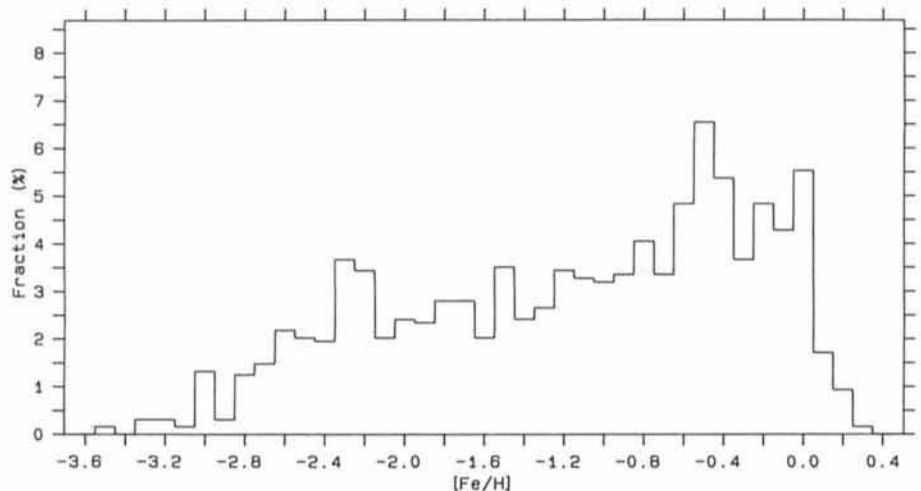


Figure 3: Fractional histogram of heavy element abundance for the 1300 objects selected for our present study. Bin size is 0.1 dex.

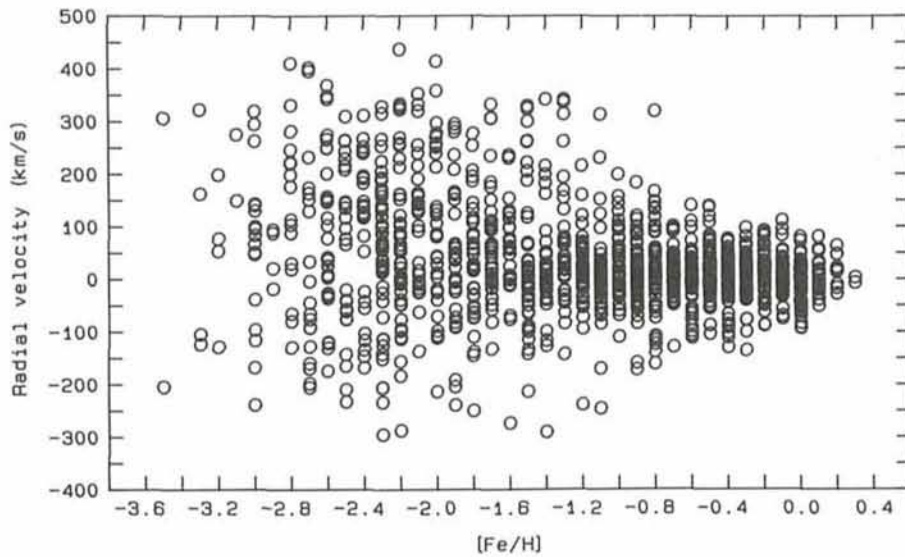


Figure 4: Radial velocity, expressed in kilometres per second, vs. abundance of heavy elements, expressed in dex, for the 1300 objects selected for our present study. In the right-hand central part of the diagram, plot crowding is substantial.

bourhood and thereby obtain an estimate of the mass of the Galaxy outside the solar orbit?

In addition to our concerns regarding the chemical evolution of the Galaxy, we are interested in the general chemical picture presented by the early Galaxy as well as by its more recent counterparts. Is there a metallicity gradient in the Galaxy? If so, what is the nature of this gradient? Is metallicity a parameter with smooth variations, or does it present an uneven pattern?

Both for a study of large-scale parameters of the early Galaxy and for investigations of star formation processes, data on binary and multiple stellar systems with high ages are highly valuable. Among other things, such data can contribute to our understanding of early-generation protostellar matter. Further, we are highly interested in the ratios of binary and multiple objects as a function of stellar age. From a sample of old binary systems, the circularization time for short-period systems can be estimated. From data on period cut-off, abundance of heavy elements can be inferred. A study of binary systems permitting mass determinations should provide crucial information concerning the mass-luminosity function for the oldest stars. Such data would significantly improve our possibilities to understand early stellar evolution and also provide an estimate of the production of helium in the first phases of galactic evolution as well as, possibly, an estimate of the primordial abundance of helium. Finally, with a solid material for binary systems, it should be feasible to identify components with very small masses, possibly down to the mass range occupied by brown dwarfs and planets.

Observations

Our weak knowledge of the oldest stars has been and is still emphasized by the fact that observational samples of such stars are normally seriously affected by selection bias. Such bias has been exceedingly hard if not impossible to avoid. Nevertheless, it is a significant limitation concerning almost all our knowledge of the first generations of galactic stars. For this reason, we have endeavoured to obtain an observing material which is, firstly, as free as possible from selection bias and for which we can, secondly, study possible effects of existing unavoidable bias. To this extent, we have chosen to include both a primary observing sample and sub-samples supporting the primary one and our possibilities to study sample bias.

The primary observing sample is based on photometric criteria. It includes stars with spectral types between F5 and M0, observed on the Strömgren uvby system. Our photometric data give us effective temperature, surface gravity and abundance of heavy elements (Crawford, 1978; Nissen and Gustafsson, 1978; Nissen, 1981; Ardeberg and Lindgren, 1981; Ardeberg et al., 1983; Olsen, 1984; Ardeberg and Lindgren, 1985a). In addition to general stellar parameters, this provides us with a sensitive selection criterion regarding metallicity. In this way, we define the sample of stars for which we subsequently obtain radial velocity data. This basic set of programme stars is, in parallel, supported by samples of stars defined entirely from kinematical data (Stock and Wroblewski, 1972; Giclas et al., 1971, 1978).

For the total sample of programme

stars selected for radial velocity observations, we have used the photoelectric radial velocity scanner CORAVEL. The major part of this work has been made with the Danish 1.54-metre telescope at La Silla, with a minor part made with the Swiss telescope at the Haute-Provence Observatory in France. Our present report refers exclusively to data obtained at La Silla.

From our photometric data, we have identified around 3000 stars as belonging to Population II. For approximately 2400 of these stars, we have obtained radial velocity data. In addition, we have made spectroscopic studies of some of the most interesting objects. Finally, astrometric data are forthcoming for many of the stars, partly obtained with the Carlsberg Automatic Meridian Circle at La Palma, partly with the HIPPARCOS satellite. These data will furnish both distances and tangential velocities.

Some Tentative Results

As described above, a search for binary and multiple systems among our programme stars is an essential part of our project. For this reason, we have scheduled our observations, of photometric quantities as well as of radial velocities, to cover adequate time intervals. In practice, these intervals depend on the periods of the systems we want to include. At the same time as our observations have to cover relatively large intervals in time, there is a corresponding need for data of high accuracy. This is especially emphasized for radial velocity data, as we want to be able to detect also components with small masses.

From the total of 2400 objects which are classified as belonging to Population II, and for which we have obtained photometric as well as radial-velocity data, we have selected approximately 1300 objects, including also a smaller number of reference stars, mainly belonging to the younger galactic population. For the latter objects, the data now available and reduced are solid enough to permit some tentative conclusions, even if additional data are needed for conclusions of a more definite nature.

In Figure 1, we present a fractional histogram of the radial velocities obtained for the 1300 objects selected. For the systems with variable radial velocity, we have used best available estimates of system radial velocities. As a comparison, Figure 2 shows the corresponding data for stars included in the Bright Star Catalogue. While a difference in the fractional distributions is to be expected, we think that the observed difference clearly indicates the need for systematic surveys, as unbiased as

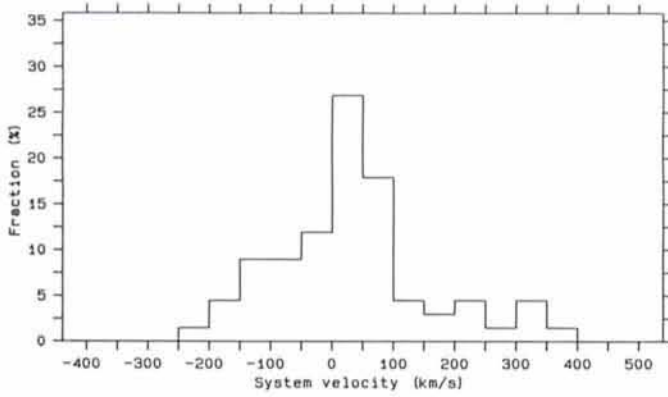


Figure 5: Fractional histogram of system radial velocities for our sub-sample of binary and multiple systems. Bin size is 50 kilometres per second. About 70 systems are included.

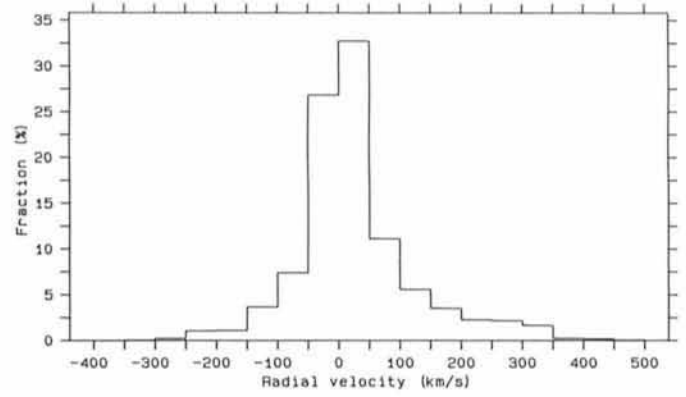


Figure 6: Same as Figure 1 but with a bin size of 50 kilometres per second for convenient comparison with data shown in Figure 5.

possible, of stars belonging to the old galactic population.

For the stars studied, the abundance of heavy elements is a key parameter. Formally representing this parameter as $[Fe/H]$, we display, in Figure 3, the fractional distribution of this parameter. The result most immediately obvious from Figure 3 is the large range in $[Fe/H]$, covering an abundance interval including objects typical for populations ranging from that of the solar neighbourhood disk stars to values normally described as indicative of an Extreme Population II or even a Population III.

Some discussion concerning galactic stellar populations has concentrated on the internal relations between these populations. From the distribution of metallicity (Fig. 3), some tentative comments may be made. First of all, an Intermediate Population II seems indicated. The extension of the range of the metallicity for this population has been subjected to extensive debate. We mention the conclusions drawn by Strömgren (1966) and by Eggen et al. (1962). From our data, we find a relatively strong indication of an Intermediate Population II being rather restricted in $[Fe/H]$. As a matter of fact, our data indicate a range in this parameter even more narrow than that proposed by Strömgren (1966). At the same time, there is some suggestion of a split in metallicity between Intermediate Population II and Population I, although this should be more carefully studied when more data are available.

Whereas it appears possible to delimit tentative ranges in $[Fe/H]$ for Population I and for an Intermediate Population II from our data, stars with more extreme underabundance of heavy elements seem to have a comparatively smooth distribution with respect to $[Fe/H]$. Whether this fact should be taken as an argument against the existence of a Population III cannot be decided from the present status of our material. At any

rate, the substantial range of Extreme Population II seems verified beyond doubt.

Judging from the distribution in Figure 1 only, it is difficult to distinguish between stars belonging to Intermediate Population II and those pertaining to Population I. Rather, these two populations merge in the radial velocity domain. At the same time, the difference between Population I and Intermediate Population II, on the one side, and Extreme Population II, on the other side, seems rather pronounced. This fact, as well as the large width of this Population in radial velocity, tends to confirm the impressions based on the distribution of metallicity. As was the case in the metallicity distribution, it is not clear whether or not separation of a Population III can be made by means of the present radial velocity material.

The data on abundance of heavy elements and on radial velocities have

been combined in Figure 4. The separation of stars belonging to Intermediate Population II and to Population I is confirmed, especially when compared to Figure 3. From the distribution of data, both populations show kinematical characteristics defining them as disk populations. At the same time, there is a significant indication of a thick disk (Gilmore and Wyse, 1986). This thick disk is most clearly defined by stars whose metallicities show that they belong to Intermediate Population II. However, the presence of a thick disk seems also well indicated in the range ascribed to Population I.

From the width of the distribution of radial velocities, Extreme Population II is clearly present over a range in $[Fe/H]$ from around -1.0 to beyond -3.0 . Over a major part of this metallicity interval, this population appears to be rather homogeneous. However, at its high metallicity end, Extreme Population II

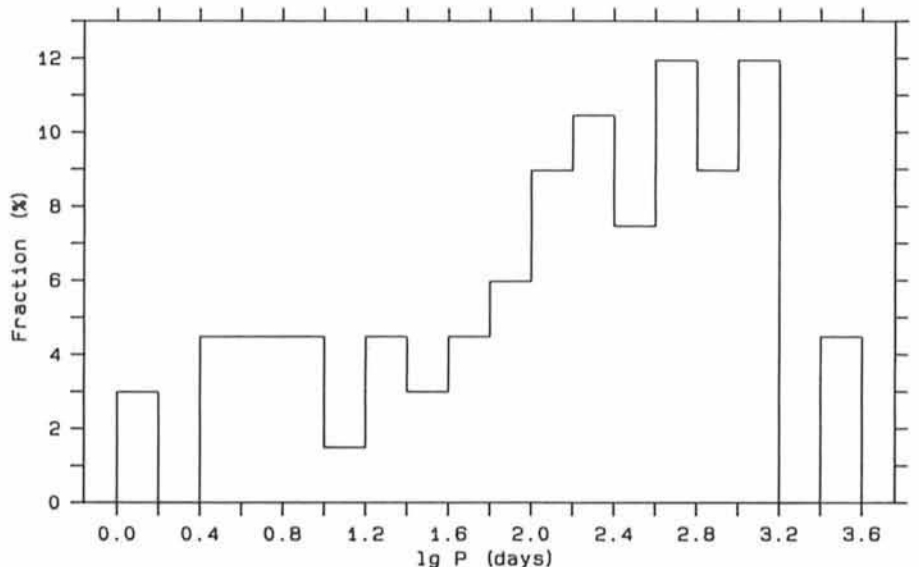


Figure 7: Fractional histogram of orbital periods, expressed in days, for our sub-sample of binary and multiple systems. No attempt has been made to correct for selection effects, which are probably highly significant. See the text.

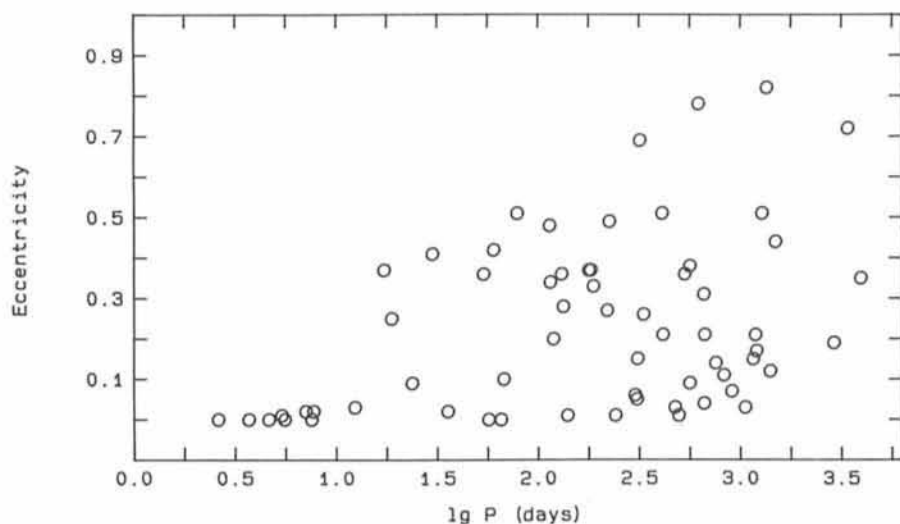


Figure 8: Orbital eccentricity vs. orbital period, expressed in days, for our sub-sample of binary and multiple systems.

seems to display considerably smaller radial velocity dispersion than more metal poor stars. Whether this should be interpreted in evolutionary terms is a problem that merits a closer study with more complete data. As judged from Figure 4, the reality of a Population III seems possible, but is not confirmed. More data are necessary, before this question can be addressed in a fully adequate manner. Very tentatively it might be suggested that, if real, Population III is in evolutionary terms rather firmly coupled to Extreme Population II.

From the sample of objects classified as binary and multiple systems (Ardeberg and Lindgren, 1985b, c; Lindgren et al., 1987, 1989; Ardeberg and Lindgren, 1990), we have selected those for which system radial velocities and orbital periods are determined with accuracies which, although not sufficient for definite conclusions, allow some reasonably well-defined statistical conclusions. This gives us a sub-sample of close to 70 binary or multiple systems. In all but a few cases, eccentricities have also been determined to an accuracy that allows tentative statistical conclusions.

For this sub-sample of binary and multiple systems, Figure 5 shows the fractional distribution of system velocity with a bin size of 50 km s^{-1} ; a rather wide distribution is noted. In order to compare it to the distribution in radial velocity of the total sample of stars under present study, we have, for the data presented in Figure 1, made a rebinning resulting in the fractional distribution of radial velocities presented in Figure 6.

A comparison of Figures 5 and 6 indicates that the distribution of system radial velocities for binary and multiple systems is as wide as that defined by the distribution of radial velocities for the total sample

of stars presently under discussion. This is a result of special interest, in particular with reference to the long-standing controversy about the relative incidence of binary and multiple systems among the oldest stellar generations as compared to the corresponding incidence among younger stars. We refer to studies by Abt and Levy (1969), Crampton and Hartwick (1972), Lucy (1977), Peterson et al. (1980), Griffin (1989), Lucke and Mayor (1982), Mayor and Turon (1982), Lindgren et al. (1987), Carney and Latham (1987) and Latham et al. (1988). The fact that our data, with their low bias, indicate a fractional radial velocity distribution for binary and multiple systems comparable to that of our total sample of stars, speaks clearly in favour of the absence of a significant dependence on galactic age of processes determining stellar multiplicity. At the same time, this is obviously a question that merits a more stringent treatment with a better data base. Given the importance of the topic, we will endeavour to revisit this field as solidly as possible.

In Figure 7, we have displayed the fractional distribution of orbital periods for our sub-sample of binary and multiple systems. In order to interpret such a distribution in an adequate manner, we have to consider effects of selection as well as of other bias. We mention the difficulties to derive non-spurious selections of the systems with the shortest periods, due to the high resolution necessary in the radial velocity data, and, equally, of the systems with longer periods, in this case due to the large time coverage needed for detection and determination of radial velocity variability of systems. Nevertheless, it is of considerable interest to note the presence of systems with very short as well as with rather long periods.

The distribution of orbital eccentricity, versus orbital period has been shown in Figure 8. Except for a general trend of the upper and lower envelopes for periods longer than around 15 days, the existence of a cut-off period seems strongly indicated. This is another topic that needs further study.

References

- Ardeberg, A. and Lindgren, H. 1981: *Rev. Mexicana Astron. Astrof.* **6**, 173.
 Ardeberg, A. and Lindgren, H. 1985a: in Proc. IAU Symp. No. 111, p. 509.
 Ardeberg, A. and Lindgren, H. 1985b: in Proc. IAU Coll. No. 88, p. 151.
 Ardeberg, A. and Lindgren, H. 1985c: in Proc. IAU Coll. No. 88, p. 371.
 Ardeberg, A., Lindgren, H. 1990: *Astron. Astrophys.* in print.
 Ardeberg, A., Lindgren, H. and Nissen, P.E. 1983: *Astron. Astrophys.* **128**, 194.
 Crawford, D.L. 1978: *Astron. J.* **83**, 48.
 Eggen, O.J., Lynden-Bell, D. and Sandage, A. 1962: *Astrophys. J.* **136**, 748.
 Giclas, H.L., Burnham, R., Jr. and Thomas, N.G. 1971: *Lowell Proper Motion Survey of the Northern Hemisphere*, Lowell Obs., Flagstaff, Arizona, USA.
 Giclas, H.L., Burnham, R., Jr. and Thomas, N.G. 1978: *Lowell Obs. Bull.* No. **164**.
 Gilmore, G. and Wyse, R.F.G. 1986: *Nature* **322**, 806.
 Lindgren, H., Ardeberg, A. and Zuiderwijk, E. 1987: *Astron. Astrophys.* **188**, 39.
 Lindgren, H., Ardeberg, A. and Zuiderwijk, E. 1989: *Astron. Astrophys.* **218**, 111.
 Nissen, P.E. 1981: *Astron. Astrophys.* **97**, 145.
 Nissen, P.E. and Gustafsson, B. 1978: in *Astronomical papers dedicated to Bengt Strömberg*, Copenhagen University Observatory, P. 43.
 Olsen, E.H. 1984: *Astron. Astrophys. Suppl. Ser.* **57**, 443.
 Stock, J. and Wroblewski, H. 1972: *Publ. Dep. Astron. Univ. Chile* **11**, 59.
 Strömberg, B. 1966: *Ann. Rev. Astron. Astrophys.* **4**, 433.

The Proceedings of the ESO Workshop on

RAPID VARIABILITY OF OB-STARS: NATURE AND DIAGNOSTIC VALUE

have just become available. The volume, edited by D. Baade, contains about 380 pages and is offered at a price of DM 45,- (including packing and surface mail).

Payments have to be made to the ESO bank account 2 102 002 with Commerzbank München or by cheque, addressed to the attention of

ESO, Financial Services
 Karl-Schwarzschild-Straße 2
 D-8046 Garching bei München.

Please do not forget to indicate your complete address and the title of the Proceedings.

Dust and Extended Ionized Gas in NGC 5044 and its Fellow Radio Elliptical Galaxies

P. GOUDFROOIJ, *Astronomical Institute "Anton Pannekoek", University of Amsterdam, the Netherlands*

Introduction

A remarkable discovery of recent years is the detection of cool interstellar matter in a surprisingly large number of apparently "normal" elliptical galaxies. In particular, the technique of co-adding IRAS survey scans has led to the detection of more than half of all ellipticals brighter than $B_T^0 = 11$ mag. in the *Revised Shapley-Ames Catalog of Bright Galaxies* [1] (hereafter referred to as RSA). The far-infrared radiation is most likely explained by thermal emission of heated interstellar dust [2]. In addition, CCD multi-colour surface photometry effectively shows dust patches in some 30% of the cases studied to date [3]. Thorough study of the gas and dust in elliptical galaxies is important to: (1) determine its origin (mass-loss from late-type stars, merging collisions with other galaxies or accretion inflows from cooling X-ray gas), and (2) investigate the three-dimensional shape of elliptical galaxies (oblate, prolate or triaxial) as can be derived from the orientation of the dust lanes and the two-dimensional velocity field of the gas.

Extended ionized gas has been detected in a number of elliptical galaxies. Kinematical studies have shown [4, 5] that the kinematical major axes of gas and stars generally do not coincide. This strongly suggests that the gaseous material has an origin external to the galaxy itself, i.e. brought in during an interaction or merging collision with another galaxy. Moreover, a number of dominant cluster ellipticals containing hot, X-ray emitting gas have been found to contain irregularly distributed dust patches and associated ionized gas in their central regions [6, 7]. Also in these cases, the interstellar matter evidently has an external origin. However, the presence of dust is surprising, since the life time of dust grains exposed to erosion by "sputtering" in hot gas is only of order $10^6 - 10^7$ yrs. To resolve this dilemma, it has been suggested in some recent studies that the dust is replenished by evaporation of cool gas clouds brought in by a recent merging collision [8, 9]. Transfer of heat through electron conduction from the hot X-ray gas to the cooler gas can provide both the excitation for the emission-line gas and the heating of the dust responsible for the far-infrared emission.

To study the global occurrence and properties of dust and gas in elliptical galaxies, we (P. Goudfrooij and T. de

Jong from the University of Amsterdam, H. E. Jørgensen and L. Hansen from the Copenhagen University Observatory

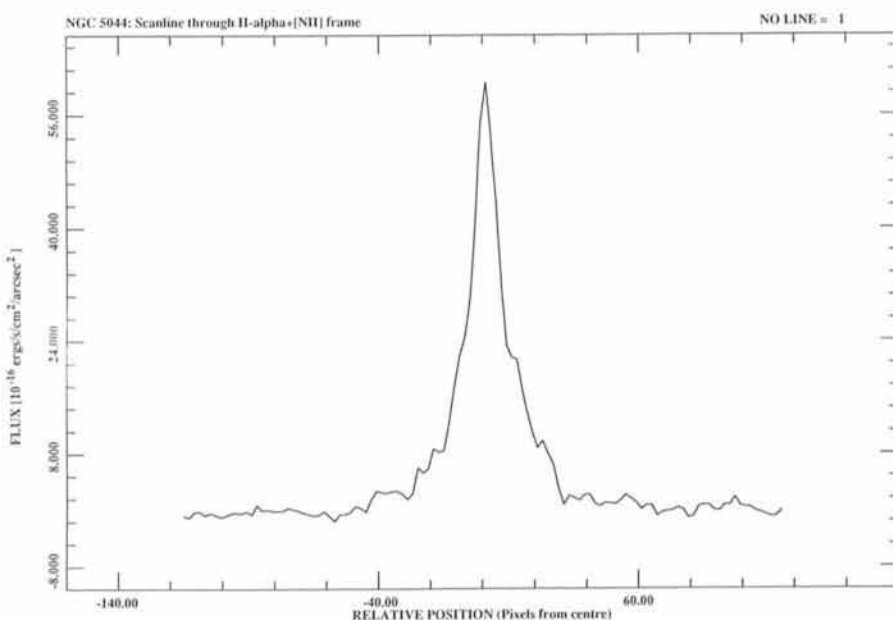
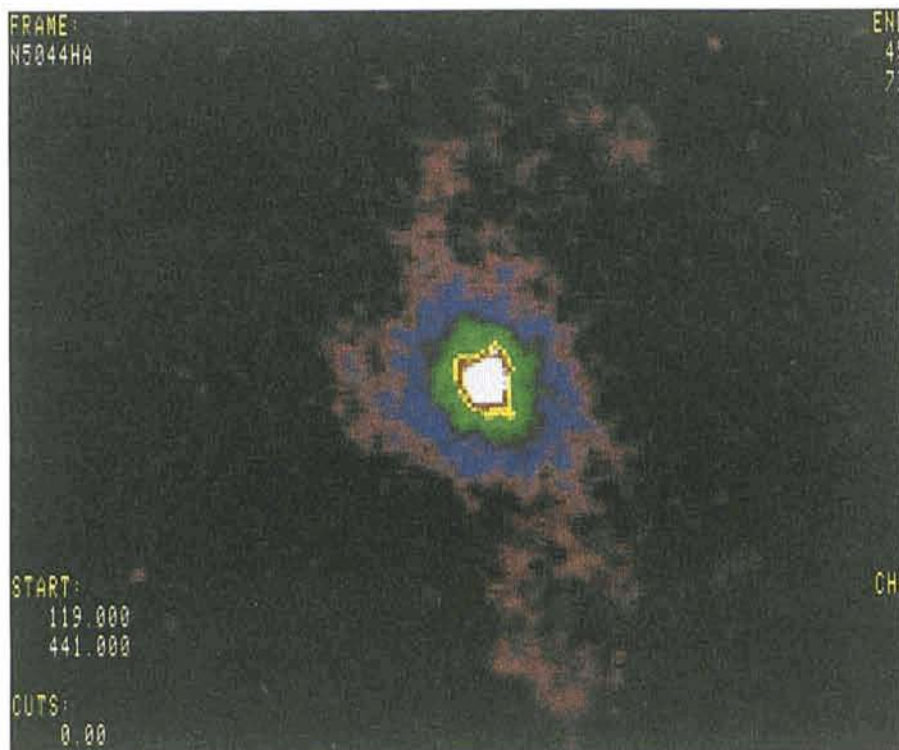


Figure 1 (a): False-colour plot of the $H\alpha+[NII]$ emission-line flux in the central $1:31 \times 1:31$ of NGC 5044. North is up and east is to the left. Spiral-like features are present at a low level. The frame has been smoothed by a rectangular box of 3×3 pixels. This causes the "boxy" appearance of the central region. (b): Scanline running through the centre of NGC 5044, in the same orientation as in Figure 2b.

and H. U. Norgaard-Nielsen from the Danish Space Research Institute) are currently undertaking an optical survey of a complete, *apparent*-magnitude selected sample of elliptical galaxies, containing all such objects (58 in number) with $B_T^0 < 12$ mag in the RSA catalog. We have performed deep CCD imaging with B, V, and I broad-band filters to study dust patches, and with narrow-band filters centred on the $H\alpha + [NII]$ emission lines to derive the amount and distribution of ionized gas. The project also involves long-slit spectroscopy at two resolutions. Low-resolution spectra (covering the whole optical region) are used to study the properties of the underlying stellar populations. Template (stellar) spectra will be made using measurements of metallic absorption lines in these spectra. Subtraction of an appropriate template from the spectrum of each object in which the presence of ionized gas has been established by our CCD imaging will reveal the pure emission-line spectrum which can be used to investigate the ionization mechanism of the gas [10]. High-resolution spectra in the wavelength region around $H\alpha$ are used to determine the kinematics of the gas. Comparison with the stellar kinematics provides information about the origin of the gas. For the southern sample objects, the bulk of the imaging data have already been obtained with the Danish 1.54-m, while the spectra are being taken with the Boller & Chivens spectrographs attached to the 1.52-m and 2.2-m telescopes on La Silla.

Careful Reduction Essential

Since the amounts of dust and ionized gas in ellipticals are very small (generally of order $10^4 - 10^6 M_\odot$) compared to the total mass of the galaxy (in most cases one cannot distinguish any sign of it on the "raw" CCD frames), the image processing has to be done carefully. To produce satisfactory B-V, B-I and $H\alpha + [NII]$ emission-line frames it is essential that the point-spread function is of uniform width and shape in each frame before one can be subtracted from the other. If, for example, the seeing in the I frame is better than in the B frame, then a B-I frame will contain an artificially "red" nucleus, since the I profile contains proportionally more intensity in the central few pixels of the galaxy. An additional problem in producing colour-index frames is the subtraction of the sky background. The "normal size" CCD frames of 320×512 pixels are not large enough to include an empty region of sky background when observing these giant elliptical galaxies, and an error as small as 1% in the background

subtraction can already lead to unusual elliptical ring-like features with anomalous colours in the colour-index frame. We have therefore made separate sky frames in each (broad-band) filter just before and after each object frame. After elimination of the stellar images in the sky frames we have subtracted these from the object frames. The result is generally very good.

Some Striking Examples: Radio Ellipticals

During the time-consuming routine reduction process, it is quite stimulating when one of the galaxies turns out to be more peculiar than the others. A recently published example of such a galaxy is IC 1459, which exhibits a striking spiral-like disk of ionized gas accompanied by

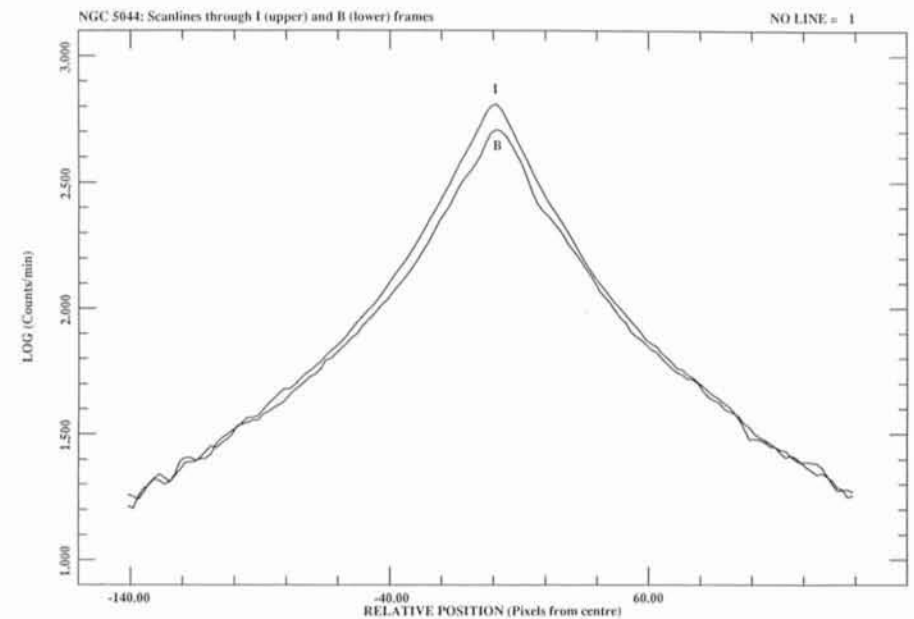
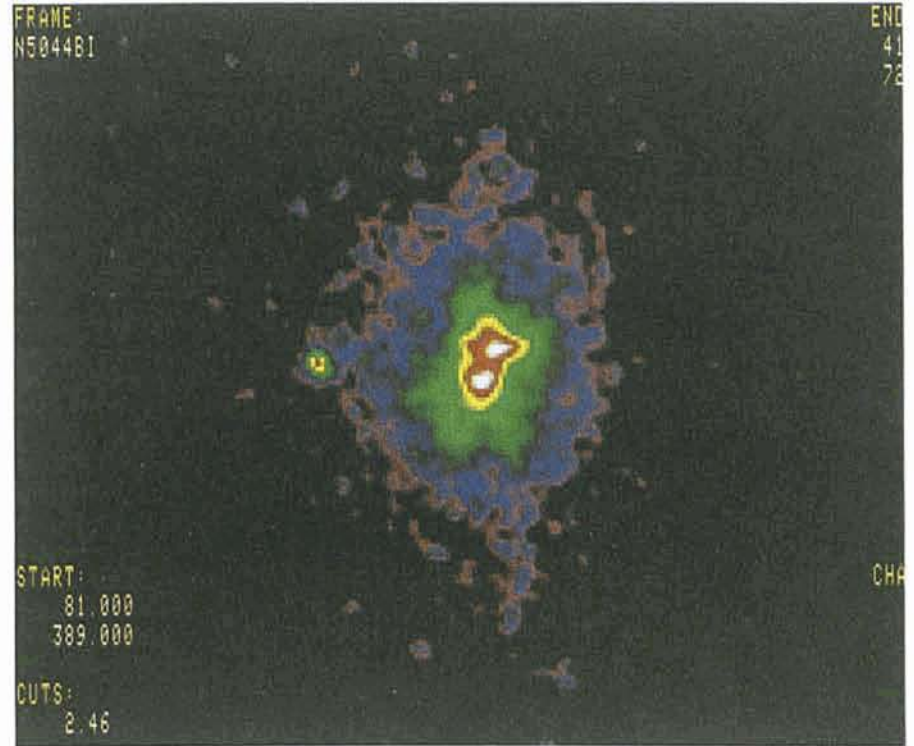


Figure 2(a): False-colour plot of the B-I colour index in the central $1:31 \times 1:31$ of NGC 5044. Orientation and colour lookup table as in Figure 1a. The two "blobs" near the nucleus are reminiscent of an almost face-on dust ring. The faint spiral-like features (see Fig. 1a) can just be recognized. The source to the east of NGC 5044 is probably a foreground star. (b): Scanlines running through the centre and the two dusty "blobs" in the centre of NGC 5044, both for the I and B frames. It can be seen that the B light profile shows "dips" at the positions of the blobs, whereas the I profile is much smoother. The I profile has been shifted to agree with the B profile in the outer parts of the galaxy.

dust patches [11]. Other interesting features of IC 1459 are: (1) it is a compact, powerful radio source with a flat radio spectrum (the latter feature is an indication of “activity”, since most quasars also show it; we hereafter refer to this feature as CNFRS [from Compact Nuclear Flat-spectrum Radio Source]), and (2) it contains a (stellar) core which is kinematically decoupled from the outer body of the galaxy (a “counter-rotating core”) [12].

Here we want to point out that these features may be quite common to ellipticals with a CNFRS. All of the southern ($\delta < 0^\circ$) ellipticals in our sample which are listed in the literature as having a CNFRS [13] are found to exhibit extended $H\alpha$ + $[NII]$ emission, most of the time associated with dust patches.

As another striking example of the class of peculiar ellipticals with a CNFRS we present here results of our observations of the E0 galaxy NGC 5044. This giant elliptical ($B_T = 11.92$, $M_B = -21.61$) is a member of a small group at a distance of 56 Mpc ($H_0 = 50 \text{ km s}^{-1} \text{ Mpc}^{-1}$), containing 3 galaxies. Hot X-ray gas has not been detected, but the presence of dust is indicated by a (marginal) detection of NGC 5044 by the IRAS satellite at 60 and 100 μm . Figure 1a shows the distribution of the ionized gas. This frame has been produced using background-corrected exposures by subtraction of a scaled frame containing purely stellar continuum light from a frame containing both stellar continuum and $H\alpha$ + $[NII]$ emission. Just like in the case of IC 1459, spiral-like structure can be seen at a low level. These features are probably tidal tails which reflect the response of the gas in the gravitational potential of NGC 5044 after the capture of a gas-rich galaxy. The emission is dominated by the nuclear region, as can be seen in Figure 1b. Associated with the ionized gas, dust patches are revealed by the B-I colour frame (Fig. 2a). The spiral-like extensions to the north and south can just be recognized. In addition, two “blobs” of high reddening are present near the centre. In Figure 2b we show a scan line running through these two “blobs” in both the B and I frames. It can be seen that the blobs correspond to a local deficit of light in the B frame relative to that in the I frame, and the reddening is therefore assumed to be caused by absorbing dust. A possible interpretation of the two blobs is that we are observing a small nuclear dust ring seen almost edge-on, but to be more convinced of this we must await kinematical data on NGC 5044, which will be obtained during ESO observing Period 47.

We emphasize that, in addition to

IC 1459 and NGC 5044, other ellipticals with CNFRS have been shown to have extended ionized gas which is generally kinematically decoupled from the stellar velocity field, e.g. NGC 5077 [5], NGC 6868 [14], NGC 1052 and NGC 6958 [15]. This strongly suggests that this phenomenon is linked to the presence of a CNFRS. In addition to this we note that a number of dust-lane ellipticals show extended radio emission, usually in the form of twin antiparallel “jets”. In these cases it has been shown [7, 16] that the radio jets are aligned perpendicularly to the dust lane. A possible interpretation of this is discussed below.

Building Ellipticals by Mergers

Summarizing the case of elliptical galaxies with a CNFRS, we note that all (at least in our sample) exhibit extended ionized gas, and in all cases but one (NGC 1399), dust is seen associated with the ionized gas. Apart from that, we remind the reader that an elliptical galaxy is recognized by the characteristic way in which its surface brightness falls off with distance from the centre, generally called the de Vaucouleurs or $R^{1/4}$ law. At this point we would like to draw a parallel between ellipticals and the so-called “Luminous Far-Infrared Galaxies” (hereafter LFIRGs), which are evidently involved in mergers [17]. In optical images, LFIRGs are irregular (and often multiple) systems, dominated by chaotic patterns of dust. It has recently been reported that several LFIRGs also follow the $R^{1/4}$ law when imaged in the near infrared, where the light is largely radiated by old stars which were formed well before the merger [18]. Apparently, the old stars in these galaxies have already settled into a distribution typical of an elliptical galaxy. The nuclei of LFIRGs generally exhibit optical emission-line spectra which are reminiscent of active Seyfert nuclei, heavily reddened by dust which is also responsible for the high far-infrared luminosities of these galaxies.

There is much observational evidence that nuclear activity can be triggered by a merging event. From a theoretical point of view, the mechanisms that could transport gas and dust involved in the merger from about one hundred parsecs (which is the scale of a typical nucleus) down to scales ten orders of magnitude smaller where the gas can feed the active “monster” [19] are poorly understood. The main question is how the gas can lose its angular momentum during infall. However, it has recently been shown that interactions and mergers can be quite effective in redistribut-

ing angular momentum in galaxies. Numerical simulations of interacting galaxies containing gas and dark matter show that the interactions can generate strong gravitational torques that remove angular momentum from the gas so that it can sink to the centre (e.g., [20]). If an active nucleus is formed, it may destroy the surrounding dust and subsequently reveal a nuclear “monster” of non-thermal radio emission. We emphasize that these features are just what is observed in ellipticals with CNFRS like IC 1459 and NGC 5044.

In view of the evidence mentioned above, we may attempt to draw the parallel between LFIRGs and radio ellipticals somewhat further. The near-infrared imaging results of LFIRGs support the idea that some ellipticals are forming in the present epoch as a result of mergers. Indeed, the radio ellipticals could well be analogues to LFIRGs, but in a more advanced stage of evolution after the merging collision. In this view, the radio ellipticals have either almost blasted away the dust surrounding the monster or the dust and gas have meanwhile settled in one of the possible preferred planes in the galactic potential, whereby the radio jets could develop perpendicular to this plane. In analogy, the active radio source in an elliptical with CNFRS may be expected to develop jets. High-resolution radio observations of the southern ellipticals with CNFRS using the new Australian Telescope array would therefore be quite valuable.

As to the ionization of the extended ionized gas in e.g. NGC 5044, this is most probably due to shock heating in cloud-cloud collisions which are expected during the process of gas infall. In this respect we note that a 60 $\text{\AA}/\text{mm}$ spectrum of NGC 5044 in the wavelength region around $H\alpha$ [21] shows emission-line intensity ratios $[NII]/H\alpha$ and $[SII]/H\alpha$ typical for the class of Low-Ionization Nuclear Emission-line Regions (LINERs) [22], which are well fitted by models of shock waves moving at $\sim 100 \text{ km s}^{-1}$ through a medium with densities of $10\text{--}100 \text{ atoms cm}^{-3}$. We will study the behaviour of the doublet ratio of the $[SII]$ lines (which is a measure of the density of the ionized gas) along the slit of a high-resolution spectrum to check if there is a density gradient in the gas. We note that all bright galaxies in the sample of Heckman [22] containing a LINER and a CNFRS are early-type galaxies.

Our extensive dataset of elliptical galaxies may soon tell us what fraction shows lurking active nuclei; the spectroscopic data will help relating the observed characteristics of gas and stars to the merger picture.

References

- [1] Sandage, A., Tammann, G.A.: 1981, *A Revised Shapley-Ames Catalog of Bright Galaxies*, Carnegie Institution of Washington. (RSA).
- [2] Jura, M., et al.: 1987, *Astrophys. J.* **312**, L11.
- [3] Véron-Cetty, M.P., Véron, P.: 1988, *Astron. Astrophys.* **204**, 28.
- [4] Bertola, F., et al.: 1988, *Nature* **335**, 705.
- [5] Bertola, F., et al.: 1990, preprint.
- [6] Jørgensen, H.E., Nørgaard-Nielsen, H.U.: 1982, *The Messenger*, No. 30.
- [7] Kim, D.-W.: 1989, *Astrophys. J.* **346**, 653.
- [8] Sparks, W.B., et al.: 1989, *Astrophys. J.* **345**, 153.
- [9] de Jong, T., et al.: 1990, *Astron. Astrophys.* **232**, 317.
- [10] Baldwin, J.A., et al.: 1981, *Publ. Astr. Soc. Pacific* **93**, 5.
- [11] Goudfrooij, P., et al.: 1990, *Astron. Astrophys.* **228**, L9.
- [12] Franx, M., Illingworth, G.D.: 1988, *Astrophys. J. (Letters)* **327**, L55.
- [13] Sparks, W.B., et al.: 1984, *Monthly Notices Roy. Astron. Soc.* **207**, 445.
- [14] Hansen, L., et al.: 1991, *Astron. Astrophys.*, in press.
- [15] Forbes, D.A., et al.: 1991, in proceedings of IAU Colloquium No. 124: *Paired and Interacting Galaxies*, Ed.J. Sulentic, in press.
- [16] Kotanyi, C.G., Ekers, R.D.: 1979, *Astron. Astrophys.* **73**, L1.
- [17] Sanders, D.B., et al.: 1988, *Astrophys. J.* **325**, 74.
- [18] Wright, G.S., et al.: 1990, *Nature* **344**, 417.
- [19] Gunn, J.E.: 1979, in *Active Galactic Nuclei*, eds. C. Hazard and S. Mitton, Cambridge University Press, p. 213.
- [20] Barnes, J.E.: 1988, *Astrophys. J.* **331**, 609.
- [21] Véron-Cetty, M.P., Véron, P.: 1986, *Astron. Astrophys. Suppl. Series* **66**, 335.
- [22] Heckman, T.M.: 1980, *Astron. Astrophys.* **87**, 152.

Spiral Galaxies on the Chess Board

E. A. VALENTIJN, ESO and Laboratory for Space Research, Groningen, the Netherlands

1. Introduction

Last summer I published a Letter in the scientific journal *Nature* in which evidence was presented for a relatively high content of obscuring dust in spiral galaxies. This work, together with a more detailed analysis of the properties of the light absorbing bodies (ESO preprint 730) and a study of the rotation curves of some dusty spiral galaxies with González-Serrano (ESO preprint 731) was highlighted in an ESO press release (PR 07/90 No "Missing Mass" in Opaque Spiral Galaxies?). Here, I will address some comments and frequently asked questions related to this work.

The new analysis of the dust content of spiral galaxies is based on data from *The Surface Photometry Catalogue of the ESO-Uppsala Galaxies* (by Lauberts and myself, in short ESO-LV), a project which was described in the *Messenger* (LV 1983, 1989). In the Introduction to this catalogue, which contains about 180 parameters for 16,000 galaxies, an extensive discussion is given of the photometric accuracy (thought to be better than 0.15^m in surface brightness) and the completeness and selection effects of this galaxy sample and its various sub-samples. Today, after two years of intense research on this data base, it is a great pleasure to say that only a very minor amount of errors have been found so far and I would like to use this opportunity to express my deep appreciation for the enormous dedication of my co-author Dr. Andris Lauberts, who worked full-time on this project for so many years.

The basic idea to study the dust content and hence the degree of transparency in spiral galaxies by means of photo-

metric data is very simple. We think of spirals as flattened round disks that contain dust and stars. Stars emit light; dust particles absorb and scatter light (together called "extinction"). When such a disk is seen from the top it appears round and we see the integrated star light attenuated by the dust along the line of sight. When we see the same disk at a tilted viewing angle, the line of sight will have a larger path-length through the disk, hence it will meet more stars, but also more dust. The tilt angle of the intrinsically round disk can be deduced from its observed axial ratio a/b .

The basic steps to study the transparency are then: (i) to select a *sample* of spiral disks with supposedly similar intrinsic properties, (ii) to make *models* of the spatial distribution of both the dust and the stars in a disk, (iii) to make an analytical solution for these models, describing how for a certain dust content, various *photometric parameters* are expected to change with viewing angle or a/b and, eventually, (iv) to fit these models to the photometric parameters of the sample galaxies.

Although, in theory, these steps appear rather simple and straightforward, in practice the choice of samples and its effect on the other steps is quite delicate. The discussion in the literature is extensive and complicated, not only by the different photometric parameters used for the analysis, but also by the wildly different properties of the different sub-samples used. Table 1 summarizes a few of the most popular photometric parameters used (horizontal direction) while, vertically, different employed sub-samples are listed. Basically, each of the 64 boxes in the table can provide

information on the effective transparency, but for each box one has to evaluate the *intrinsic distribution* of the particular parameter used and its relation to the observed distribution, both as a result of *selection effects* and effects of incompleteness. The selection effects are so much dependent on both the type of parameters used and on the selection criterion employed, that each box constitutes its own story. Most selection effects are distance dependent and the degree of complication is further quadrupled when the particular parameter used for the test is in itself distance dependent. In Table 1 distance dependent parameters and sample cuts have been shaded, high-lighting the 'doubly difficult' boxes.

Related to the distance dependent selection effects is the so-called Malmquist bias, an effect that puts categories of objects into a sample even while their average intrinsic parameter value would have prohibited them to pass the selection criterion. This is because of the dispersion around that average value, either due to a cosmic dispersion or due to measurement errors. Since there exist more faint than bright galaxies, the Malmquist bias has some amplification and lets more faint galaxies enter a sample than bright ones drop out. A similar effect is well known in radio astronomy, when counting radio sources close to the noise level of the observations.

To complicate matters even further, one has to care about the possible presence of spheroidal bulges that off-set the assumption of disky objects. Fortunately, the effect of bulges can be shown to be very minor for Spirals of type ≥ 3 (Sb, Sc, Sd). This has also

TABLE 1: The 'chess board' of selected samples and parameters for transparency studies

SAMPLES	Diameters		Magnitude	Surface brightness			Axial ratio	Dia. ratio
	D_e	D_{26}	B	μ^{proj}	μ_0	μ_e	a/b	D_{26}/D_e
Magnitude: $B < 14.5$	–	De Vauc.-Fig. 1 a	–	Holmberg	–	–	–	–
Diameter: $D_{26} > 80''$ Diameter: $D_{26} > 60''$	–	–	–	Holmberg	–	–	Spiro	–
Surface brightness	–	–	•	–	•	• Fig. 2	–	•
Volume: $< cz <, B$ Volume: $< cz <, D_{26}$ Volume: $< cz <, \mu_0$ Volume: V/V_{max}	–	Choloniewski Burstein, L Fig. 1 b Fig. 1 c	– • – –	– – – –	– – – –	– – – –	– – – –	– – – –

• Key-tests on ESO-LV data presented in the *Nature* paper.

been confirmed, amongst others, by a recent compilation (also using Kent's data) presented by Simien (Observatoire de Lyon) at an ESO seminar.

2. The Analysis in Various Boxes (Sample, Parameter)

The ESO-LV data can be used and have been used for analyzing the effec-

tive transparency in almost all of the boxes in Table 1, since each of the photometric parameters (including the intensity weighted axial ratio a/b) have been determined by the computer programmes. Especially, the homogeneous acquisition of the data allows a very detailed evaluation of the selection effects involved. But, a paper that would describe all this, including a full analysis

of each box would become rather unreadable. After all, one would be tempted to discuss the result of one box in comparison with that of another and eventually the degree of complication might remind us of the chess-board.

How tricky the selection effects can be is illustrated by the test in the box ($B < 14.5^m, D_{26}$). When isophotal diameters of a magnitude selected sample are

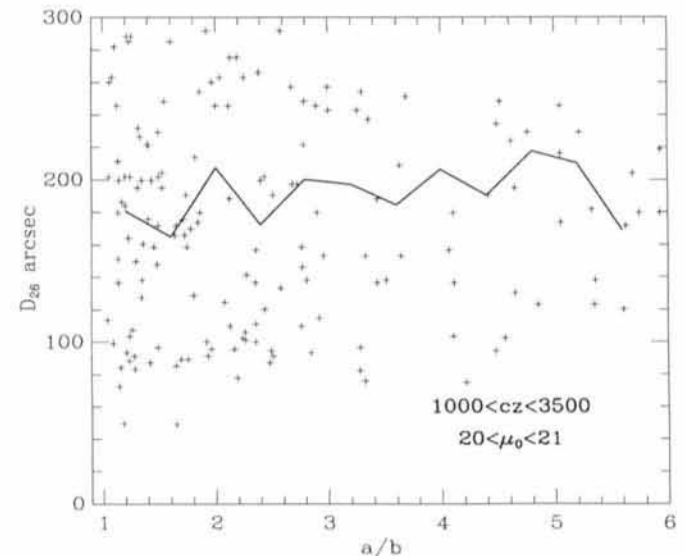
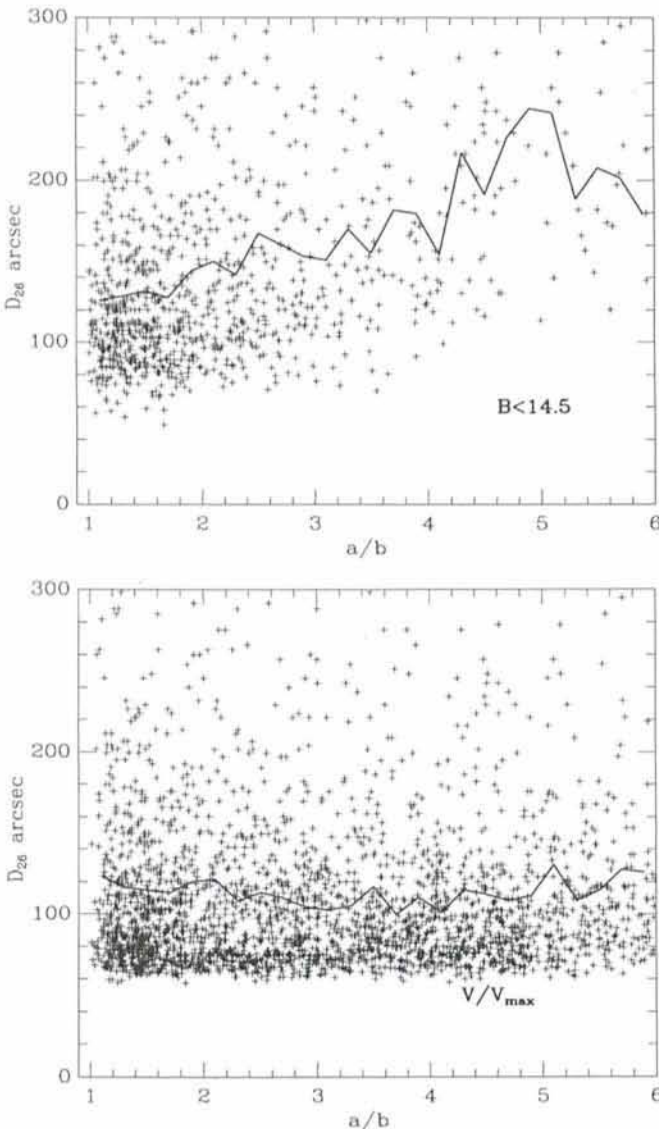


Figure 1: The isophotal diameter at the Blue 26th isophote of ESO-LV Sb galaxies versus axial ratio a/b for three different subsamples drawn from the same parent sample. Magnitude limited (upper left), redshift limited (upper right) and V/V_{max} limited (lower left). While the average regression with a/b (line) for the magnitude limited sample indicates fully transparent galaxies, the other two, more proper spatial volume representative samples, indicate extremely dusty conditions.

plotted versus a/b , a clear increase ($\sim 45\%$) with increasing a/b (1 to 5) can be noted – see Figure 1a. In fact, this is also the case for diameter selected samples. The amplitude of this increase conforms to the expectation of fully dust free – i.e. *transparent* – galaxies and such data provided the motivation for adopting fully transparent models for the outer regions of spirals in numerous

papers (e.g. de Vaucouleurs, RC2). But this box represents one of the doubly distant dependent cases, where all distance dependent selection effects cooperate. When a subset of the same sample is taken for which redshifts have been measured, and subsequently only a particular *volume* of space is used in which galaxies have been selected in a more representative way (galaxies with radial velocities $cz < 3500$ km/sec and limited range of central surface brightness, μ_0) the increase of the diameters is reduced to 9%. But the redshifts have been measured for only a limited number of not necessarily randomly chosen objects. An alternative way – not using redshifts – to construct spatial volume representative samples is provided by the application of the V/V_{\max} test, which is detailed in the Introduction to ESO-LV. The last panel of Figure 1 shows that the diameter increase with a/b virtually disappears for such a V/V_{\max} complete subsample of 2047 galaxies, and is now consistent with *fully opaque* models for the outer regions of spiral galaxies. The V/V_{\max} sample deserves a more extensive discussion, but this example demonstrates how the distance dependent selection effects can conspire to mimic transparent systems and how dangerous it is to draw conclusions from ‘doubly difficult’ boxes. In a paper in press in *Monthly Notices*, Chotomiewski (Warsaw) concludes from a different galaxy sample (CfA), for which redshifts have been obtained in a complete fashion, that isophotal diameters do not increase with a/b , confirming an earlier suggestion by Burstein and Lebofsky (1986). The example of the

isophotal diameter test demonstrates how critical the definition of the sample is for the type of result one obtains.

In the *Nature* paper, I outlined that the classical test (box B < 14.5^m, μ^{proj}) presented by Holmberg, which highly influenced the view that spiral galaxies are transparent, could be equally well interpreted with simple fully opaque galaxy models. Similar worries have been raised by Disney et al. (1989). The basic reason for this ambiguity was the definition of the average projected surface brightness μ^{proj} , which was such that its regression with a/b does not discriminate between different models. Holmberg most clearly described what he did, but for some (unclear) reason his results later propagated in the literature as *evidence* that spiral galaxies are essentially transparent.

Now, if both the ‘classical techniques’ that formerly led to the notion of transparent spiral galaxies are ambiguous, how can we proceed without introducing similar ambiguities? The key to this problem is the availability of actually measured surface brightness profiles in ESO-LV. In itself surface brightness (s.b.) is a *distance independent* parameter, which leaves only the worry about distance dependent selection effects in the sample definition itself. When verifying the axial ratio distribution of the samples used with the expected distribution of randomly projected axial ratios and by carefully screening the results with the diameter selection procedure, it is possible to perform a complete, unambiguous analysis of the problem. However, this is greatly due to the fact that the ESO-LV data can give

us a rather good description of the *input* (i.e. cosmic) distribution of the s.b. of the target galaxies. The amazingly small spread of 0.6^m of the central s.b. (Freeman, 1970) has been confirmed (average 21–22 mag/arcsec²), albeit with the refinement that it becomes fainter for later type galaxies. That this in itself is *not* a result of distance dependent selection effects, could be demonstrated by computing the average central s.b. of the V/V_{\max} samples, which are supposedly representative for particular volumes of space. The average central s.b. from the V/V_{\max} samples agreed within 0.25^m with that of the total samples, which confirms the results of van der Kruit (1976). Davies et al. (priv. comm.) recently pointed out that if, conversely, the narrow range of observed s.b. was caused by selection effects, then the s.b. tests would be more ambivalent. This might be partly true in theory, but the ESO-LV data appear to constrain the cosmic distribution of s.b. to an amazingly narrow range, which greatly facilitates its application to studying transparencies.

In Figure 2 the s.b. at the half total light radii are plotted versus a/b for Sb and Sd systems. While the regression with a/b for the Sd’s conforms to simple semi-transparent models ($C=0.5$), the data of the Sb’s are consistent with opaque models, i.e. s.b. hardly decreasing with a/b . Also, in the central parts the s.b. does not appear to depend on a/b , but the greatest surprise to most of us was the result at the half total light radius, which seems to indicate that large parts of the disks of spiral galaxies are very obscured by dust. This result

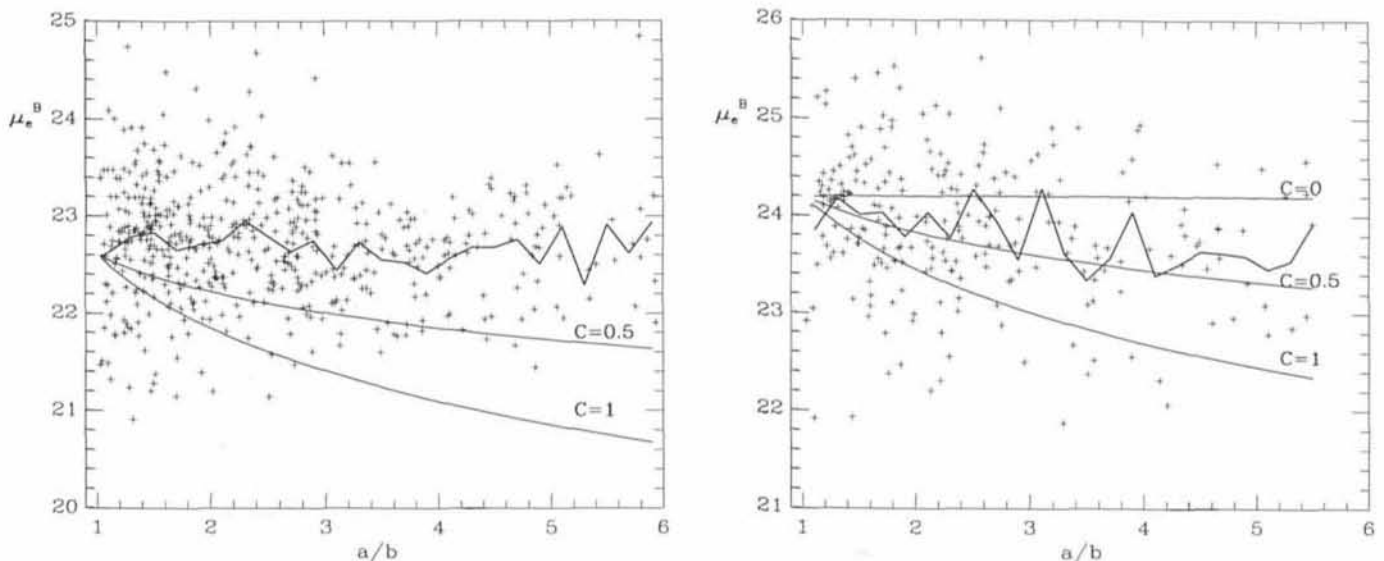


Figure 2: The local surface brightness at the effective radius of ESO-LV galaxies that exhibit a pure exponential luminosity profile ($N-1$) on both the Blue and the Red plates. These galaxies are thought not to contain any significant bulge component. The left panel shows the very small decrease of the s.b. with a/b of \sim Sb galaxies-conform very dusty scenarios-, while the right panel shows similar data for apparently much more transparent, very late type spirals (type > 7.5 , \sim Sd’s). The curves correspond to simple fully transparent ($C=1$) and semi-transparent ($C=0.5$) models.

could be further extended to the outer regions of the disks by analysing the distance independent ratio D_{26}/D_e and by several tests that operated on the total magnitudes.

In the *Nature* paper I argued that these results are most consistent with the view that spiral galaxies are opaque over large parts of their disks. While Burstein (1990) apparently agrees with these conclusions, he wonders whether attention had been given to the effects caused by the sample definitions (without discussing the actual work presented on this). Well, as a matter of fact, this was what most of the work was about. In Figure 2 of the *Nature* paper it was demonstrated that the prime selection effect that operates in a diameter selected sample could be only understood in terms of opaque spiral disks, while that same basic selection criterion would lead to a serious inconsistency in the case of transparent systems.

So, in other words: by carefully evaluating *how* galaxies were selected, it could be shown that the result of that selection procedure could be best understood in terms of opaque systems. In addition, a *control* sample was designed for the brightest galaxies, to evaluate any remaining distance dependent selection effects. The a/b distribution of this control sample is representative for a random projection of axial ratios and reproduced the results of the total sample. Indeed, it is not *a priori* the large size of the ESO-LV sample that permitted to obtain the new results, it is merely the very strict selection and homogeneous acquisition in combination with the possibility to create various sorts of smaller subsamples (types, s.b. redshift, etc.) to perform a variety of verifications.

At a session at CERN, Spiro (CEN-Saclay) presented some of his findings in the box ($D_{26}>80''$, a/b), which refers to studying the *frequency* distribution of axial ratios. This is one of the 'doubly difficult' boxes since, although axial ratio is principally distance independent, it is subject to a Malmquist-like distance dependent selection effect, which operates as follows: Sb-c galaxies with transparencies as indicated by the s.b. tests will undergo an increase of the isophotal diameter by about 9% when seen with an a/b of 5. This implies that around the diameter cut-off limit, highly inclined objects will enter a diameter limited sample in some cases even while their face-on diameters would have prohibited that. The fact that there are *more* fainter (smaller) galaxies than brighter ones strongly amplifies this effect, which was ignored by Spiro when he concluded that the noted excess of high a/b galaxies must

result from intrinsically transparent systems. In fact, by analysing the $D_{26}>80''$ sample, the same effect that has been described in the *Nature* paper at fainter magnitudes for the $D_{26}>60''$ sample has been transferred to brighter galaxies. No wonder that I dedicated this article to the chess board! In fact, if Spiro had inspected a control sample with central s.b. <20.5 , he would have noted that the excess of high axial ratios is entirely eliminated, which cannot be explained by his 'transparent model', but is well understood in the descriptions I gave.

This example again illustrates how dangerous it is to embark on double difficult boxes, and that one can then obtain results that look clean and good, but are dictated by selection effects, as with the data presented in Figure 1a. Using the frequency distribution of axial ratios to directly deduce transparencies can only be done when one knows *a priori* the luminosity function of the galaxies studied. In my work I used the frequency distribution only as a check on the representative nature of samples.

At a session of the Dutch Astronomers Club, van Albada questioned whether the effect of the physical thickness of disks could influence the results of the s.b. test as shown in Figure 2. While my studies of axial ratio frequency distributions indicated that the effect of the disk thickness is only evident at $a/b>5$, he suggested that this might already be the case at $a/b>2-2.5$ and he presented results of fits to the small range of $a/b<2-2.5$, which essentially represent face-on systems. In spite of the fact that the increase of the line of sight with axial ratio goes linearly with a/b , he presents the data versus b/a , which masks the very strong degradation of the resolution of the test when cutting off the sample at $a/b=2-2.5$. By applying detailed axial ratio deprojection algorithms, it could be deduced that the spiral structure of our target galaxies causes the intrinsic face-on axial ratio distribution to peak at $a/b\sim 1.4$. So, in practice the fits presented by van Albada correspond to $a/b=1.4:2-2.5$ or a nominal 43-70% increase of the line of sight, opposed to the fits presented in my work $a/b=1.4--5$ corresponding to 257%. This implies that they degraded the resolution of the test by a factor of about 6-4 and not surprisingly, the data are then less conclusive and could represent semi-transparent situations.

Anyway, a more elegant way to assess the effect of the disk physical thickness is by comparing the results of other parameters that are supposedly much less affected (like total magnitudes and the mean s.b. within the effective radius) with

those of 'suspected' parameters. Both the tests using total magnitudes and especially the s.b. test using the mean surface brightness within the effective radius, reproduced the results of the tests using local s.b. values, demonstrating that it is quite unlikely that the disk thickness is affecting the outcome of the tests for $a/b<5$.

3. Opaque, Optically Thick, $\tau > 1$, $\tau \gg 1$

The observed dependency of the s.b. on a/b could be well fitted with simple models of single layers of light emitting stars mixed with light absorbing bodies, which can either represent scattered dust particles (cirrus) or compact opaque clouds. For Sb and Sc galaxies these layers are then found to have, *on average*, a face-on optical depth τ (i.e. ratio between disk metric thickness and mean free path of a photon) of, respectively, 2 and 1.3 for the outer parts and higher values for the central parts. Since these values do not include the effects of scattering and a possible small contribution of fully transparent layers on top of the disks, they represent lower limits. This means that on average we miss *at least* half of the emitted light when a galaxy is face-on and that values of $\tau>5$ must be common for inclined galaxies with $a/b\sim 2.5$. In this regime of optical depth, the photometric properties of spiral galaxies are entirely like opaque systems, which is the basic justification to call them opaque as opposed to transparent or even semi-transparent.

On the other hand, the term is slightly confusing since it does not discriminate between $\tau=2-5$ and $\tau\gg 1$. We simply miss the vocabulary to separate $\tau>1$ and $\tau\gg 1$. Although, both in the central areas and along the spiral arms most likely $\tau\gg 1$ and even in the inter-spiral arm region of nominally inclined spirals the data indicate $\tau=5$, both implying that we are essentially seeing stars from the front side, we must remember that we are here discussing average properties integrated over large parts of these systems. The deduced range of τ can very well allow us to see through the disks occasionally; for instance a typical face-on $\tau=2$ can imply that we can detect on average about half of the quasars behind such a disk when the obscuring material is composed out of compact molecular clouds, or see them attenuated by 1 magnitude, when the dust is in the form of well-distributed cirrus.

Both predictions are in practice very difficult to verify. The big geometrical difference between these two examples illustrates the probably most dramatic

aspect of the results. Our interpretation of observational data will heavily depend on the spatial structure of the light absorbing components, and much more refined models than those applied in the tests should be constructed. The simple models used in the test serve to provide some first constraints. How complicated the real situation might be is illustrated by a recent paper by Dickman et al., 1990, in which the spatial structures of some molecular cloud complexes were proposed to be best described by fractals! I for one will be reading with great interest any future papers on this subject.

4. Why Relating to Dark Matter?

The notion of the 'missing mass' in spiral galaxies originates from a comparison of the rotational velocities with the amount of observed light and its spatial distribution. If studies of transparency indicate a drastic re-interpretation of the detected light, then it seems natural to reflect how that would affect such missing mass analyses. Recently, Davies (1990) published a paper anticipating $\tau \gg 1$ in the central parts of spiral galaxies, which, as he argued, could lead to a dramatic underestimate of the amount of stellar matter in the bulges of spirals. By accordingly increasing the contribution of the bulges, he computed flat rotation curves, which did not require any additional missing mass. However, as Simien pointed out, $\tau \gg 1$ in combination with heavy bulges would inevitably lead to an asymmetric light distribution of such bulges, when the disks are seen under a tilted angle. Such an asymmetry has never been observed and, as he says, would have been noted in the detailed bulge to disk decompositions performed for large numbers of galaxies. Note, that for $\tau = 2$ disks this asymmetry would be much less dramatic.

My own results seem to indicate that at least half of the star light of face-on galaxies is obscured by dust, implying that the true luminosities are at least a factor of two higher. Consequently, the mass-to-light ratios M/L of the stellar populations that resulted from the 'missing mass analyses' should be divided by at least a factor of two. The point is, however, that the 'missing mass' analyses that incorporated haloes of dark matter already resulted in quite low maximum M/L ratios for the material in the disks. Moreover, most of the studied objects are inclined, which facilitated the mapping of the velocity field. When the new extinction results are applied to the luminosities of these disks the resultant M/L values drop well below 1 for almost all cases, which values are sig-

nificantly lower than found in well studied stellar populations. In other words, the current disk-halo solutions combine an *overluminous* disk with an *underluminous* dark component, and become less credible. This fact, together with the suggestion from the absorption studies that the absorbing medium is more widely distributed over the disks than the stars (implying that the observed M/L decreases with radius from the centre) simply calls into question the evidence for dark haloes, as inferred from a comparison with optical light profiles.

This triggered I. González and myself to compute a new category of mass models, now without dark haloes, to fit the observed rotation curves. Indeed, we could find good fits to the rotation curves, but a substantial fraction of the mass that was labeled as discrepant in previous studies, should now be identified with the obscuring component itself! This has been often misquoted in the press, where it was wrongly said that all the discrepant mass was found to be in the obscured prime stellar component with the same spatial distribution as the observed radial luminosity profile. It can be shown in several ways that such a solution would not work and would not resolve the mass discrepancy at larger radii. To our surprise, we found that if the obscuring component was composed of compact molecular clouds, that they would precisely have the correct mass as required by the fits and at the same time perform the amount of absorption required by the optical extinction studies.

Is this implying that the dark mass in spiral galaxies has been found? The extinction results certainly weaken the evidence for dark haloes, and they directly point to the presence of a baryonic component that has the correct spatial distribution to resolve the discrepancy. But can the agreement with molecular cloud mass be circumstantial? Yes it could, and this suggestion needs verification.

On the other hand, an evaluation of the situation in the Galaxy seems not to contradict this suggestion; recently, a number of papers showed that the CO luminosity $-H_2$ mass conversion factor, on which most of our understanding of the molecular mass is based, might be a factor 4 larger in the outer regions. Apart from a few very nearby galaxies, we can only guess the conversion factor in external galaxies. Next to this, several reports reveal a factor 4 higher virial mass of molecular clouds than deduced from the CO luminosities. It also remains to be seen how many molecular clouds are hidden in the noise of the observations. One team of observers that already ob-

served a quite high spatial density of molecular clouds claim that the deflection of the noise distribution of their observations indicates that 68% of their signal is below their detection limit (Lee et al., 1990).

The final word has certainly not yet been said and the current results only form a starting point. The great number of very interesting studies of molecular gas that are presently conducted at many observatories might shed some light on these very cold and dusty regions of the universe. Or, do we have to wait for the launch of the Infrared Space Observatory in 1993, when new windows will be opened that will allow the attempt to detect some lines of the H_2 molecule?

References

- Burstein, D. and Lebofsky, M.J.: 1986, *Astrophys. J.*, **300**, 683.
 Burstein, D. 1990, in *Morphological and Physical Classification of Galaxies*, Busarello et al., Astrophysics and Space Science Library, Kluwer.
 Davies, J. 1990: *Monthly Notices Roy. Astron. Soc.*, **245**, 350.
 Dickmann, R. L., Horvath, M.A., Margulis, M.: 1990, *Astrophys. J.*, **365**, 586.
 Disney, M., Davies, J., Phillips, S.: 1989, *Monthly Notices Roy. Astron. Soc.*, **239**, 939.
 Holmberg, E.: 1958, *Medd. Lunds Astr. Obs.*, Ser. II. Nr. 136.
 Holmberg, E.: 1975, *Stars and Stellar Systems*, Volume IX, University of Chicago.
 Freeman, K.C.: 1970, *Astrophys. J.*, **160**, 811.
 Kruit, P.C. van der: 1987, *Astron. Astrophys.*, **173**, 59.
 Lauberts, A., Valentijn, E.A.: 1983, *The Messenger*, **34**, 10.
 Lauberts, A., Valentijn, E.A.: 1989, *The Messenger*, **56**, 31.
 Lauberts, A., Valentijn, E.A.: 1989, *The Surface Photometry Catalogue of the ESO-Uppsala Galaxies = ESO-LV*, ESO.
 Lee, Y., Snell, R.L., Dickmann, R.L.: 1990, *Astrophys. J.*, **355**, 536.
 Valentijn, E.A.: 1990, *Nature* **346**, 153.
 de Vaucouleurs, G., de Vaucouleurs, A., Corwin, H.G.: 1976, *Second Reference Catalogue of Bright Galaxies = RC2*, Univ. Texas Press, Austin.

New ESO Scientific Preprints

(December 1990 – February 1991)

- 743: J. Choloniewski: Inclination Dependence of Galaxy Brightnesses, Diameters and Average Surface Brightnesses. *M.N.R.A.S.*
 744: F. Bertola et al.: Testing the Gravitational Field in Elliptical Galaxies: NGC 5077. *Astrophysical Journal*.

745. D. Hutsemékers and E. Van Drom: HR Car: a Luminous Blue Variable Surrounded by an Arc-Shaped Nebula. *Astronomy and Astrophysics*.
746. G. Bertin, R.P. Saglia and M. Stiavelli: Elliptical Galaxies with Dark Matter. I. Self-Consistent Models. *Astrophysical Journal*.
747. H.M. Adorf, J.R. Walsh and R.N. Hook: Restoration Experiments at the St-ECF. Proc. Workshop "The Restoration of HST Images and Spectra", STScl, Baltimore, 21–22 August 1990.
748. P. Bouchet, J. Manfroid and F.-X. Schmider: JHKLM Standard Stars in the ESO System. *Astronomy and Astrophysics*.
749. P. Bouchet, I.J. Danziger and L.B. Lucy: The Bolometric Light Curve of SN 1987A: Results from Day 616 to 1316 After Outburst. *Astronomical Journal*.
750. G.A. Tammann: Commission 28: Galaxies. IAU Transactions, Vol. XXI A, 1991.
751. B. Reipurth and M. Olberg: Herbig-Haro Jets and Molecular Outflows in L 1617. *Astronomy and Astrophysics*.
752. B. Reipurth and S. Heathcote: The Jet and Energy Source of HH 46/47. *Astronomy and Astrophysics*.

Supermassive Disk Galaxies

L.M. BUSON, *Osservatorio Astronomico, Padova, Italy*

G. GALLETTA, *Dipartimento di Astronomia, Padova, Italy*

R.P. SAGLIA, *Department of Astrophysics, Oxford, United Kingdom*

W.W. ZEILINGER, *ESO*

Introduction

Supermassive disk galaxies (SDGs hereinafter) are characterized by a high rotational velocity of their gas component ($V_{\max} > 350 \text{ km s}^{-1}$). NGC 1961 (Shostak et al., 1982), UGC 2885 (Burstein et al., 1982) and UGC 12591 (Giovanelli et al., 1986) are the best known examples. As Saglia and Sancisi (1988) pointed out, these galaxies lie at the extreme upper end of the Tully-Fisher relation and are on the average less luminous than expected from their rotational velocity. Their mean mass-to-luminosity ratio M/L is 15 (with $H_0 = 75 \text{ Mpc km s}^{-1}$), i.e. 1.6 times the value for Sa galaxies (Rubin et al., 1985). In addition, their optical sizes appear to be on the average smaller than those of the normal galaxies.

SDGs have been discovered only recently, since in the past the technical limitations of the 21-cm spectrometers have rendered impossible the detection of the very wide HI profiles that characterize such systems. In effect, none of the galaxies in the Roberts (1978) sample has a rotational velocity greater than 350 km s^{-1} . SDGs are still poorly known: it is not even clear whether supermassive galaxies really form a distinct category of galaxies with definite properties or whether they simply represent the extreme tail of the distribution towards the largest masses. These questions have deep implications on the formation and evolution of galaxies and the amount of dark matter. The observed properties indicate that in supermassive galaxies dark matter may dominate even inside the R_{25} radius, in contrast to what seems to happen in normal spirals (Sancisi and van Albada, 1985).

Observations and Data Reduction

In order to investigate further these properties we have started an extensive optical survey of SDG candidates in the southern hemisphere, using the 2.2-m ESO/MPI telescope at La Silla. In particular, we would like to understand

whether SDGs have in general an unusual high content of dark matter in the inner regions or, perhaps, an unusual stellar population. It is important to study SDGs optically, since the distribution of HI often has a hole in the centre and is also affected by a severe beam

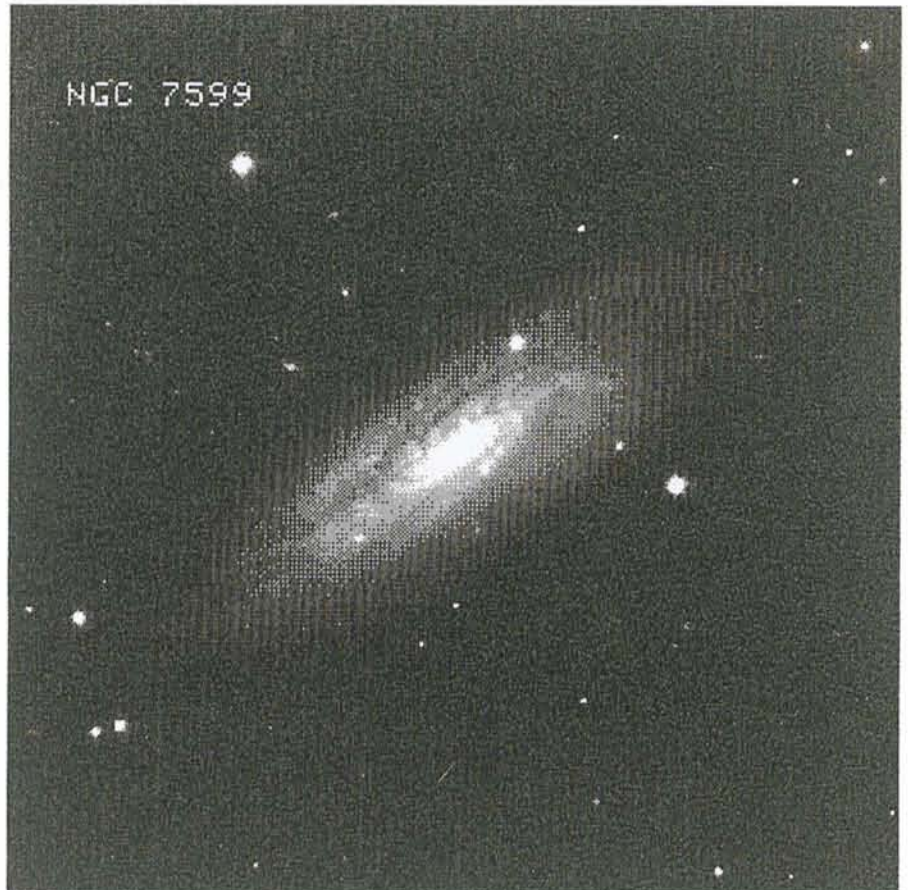


Figure 1: Red image of NGC 7599 obtained with EMMI at the NTT (kindly taken for us by S.D'Oodorico). The field is 6×6 arcmin. North is at the top and East to the right.

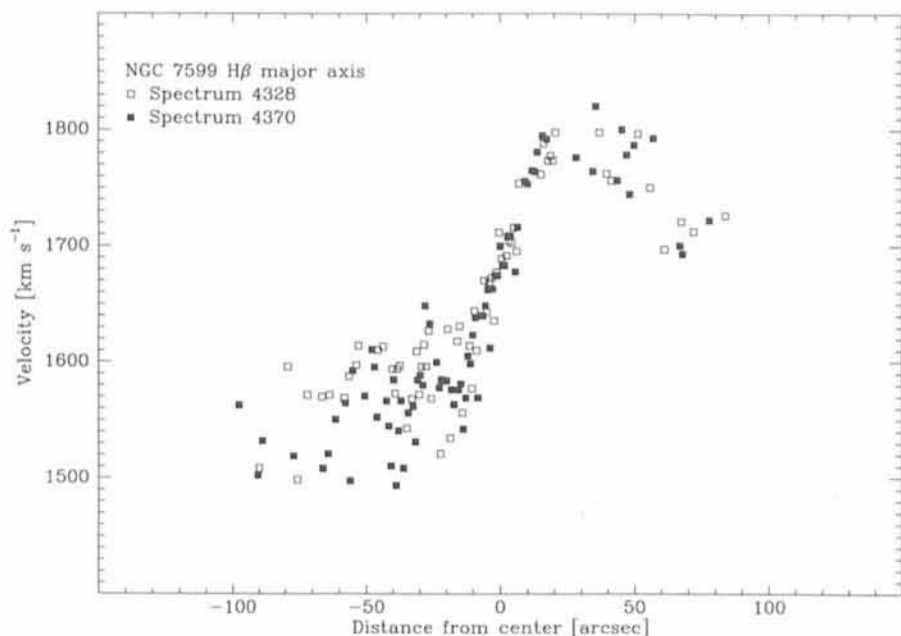


Figure 2: Rotation curve of the gaseous component of NGC 7599 derived from the measurements of the H β line at P.A. = 57°. The exposure time of each spectrum was 120 minutes.

smearing. Moreover, for the case of southern galaxies, high resolution HI observations are still lacking. A candidate list was produced using the HI catalogue of Huchtmeier and Richter (1989) and the following selection criteria: (i) a rotational velocity $V_{\text{max}} \geq 350 \text{ km s}^{-1}$, deduced from the HI line width at 20% height. (ii) a HI line profile quite regular and double-horned, indicating circular motions.

Our observations of SDGs started with NGC 5084, which was observed in May 1987 and July 1988 as a feasibility test of this programme. The results (Zeilinger, Galletta and Madsen, 1990) were so encouraging that we decided to start this work more systematically. CCD images in different colours, deep Schmidt plates and long-slit spectroscopy of four additional galaxies (NGC 1350, NGC 1398, NGC 7038, and NGC 7599) were then obtained in October 1990. A CCD image of NGC 7599 is presented in Figure 1 as an example. Other galaxies will be observed next April using again the 2.2-m telescope. The data reduction has been performed using IHAP and other specific programmes developed in Padova (Fourier-Quotient package). A sample rotation curve of the ionized gas, obtained by means of Gaussian fitting of the emission lines is shown in Figure 2 for the galaxy NGC 7599. Surprisingly the gas rotation curve of NGC 7599 has values which are too low for SDG. This may have two reasons: (i) we are looking only at the inner region of the galaxy and the rotation curve rises outside; (ii) the very wide HI profile is influenced by the presence of a companion galaxy or has too low an

S/N ratio. The analysis of the stellar rotation curve and the stellar velocity dispersion profile may clarify this point.

In order to analyse the luminosity distribution outside the region covered by the CCD frames we used ESO Schmidt plates and the calibrated images, extracted from the ESO-LV catalogue on optical disk (Lauberts and Valentijn, 1989). The inner parts of the galaxies have been calibrated in surface brightness using the aperture photometry values reported in the catalogue of Longo and de Vaucouleurs (1983).

The M/L Ratio: Models and Results

The relevant kinematical information comes from stellar and ionized gas rotation curves. Rotational velocities must be corrected for the inclination; the stellar rotation curves (obtained from absorption lines) also require a correction for the asymmetric drift, if a non-negligible velocity dispersion is present. In addition, the effect of integration along the line of sight must be taken into account (in the hypothesis of negligible absorption). More accurate corrections, taking into account the presence of internal absorption (Holmberg, 1958, Disney, 1990, Valentijn, 1990) will be included in the final paper. These corrections are accomplished with a three-component model (Zeilinger, Galletta and Madsen, 1990) representing the bulge, disk and halo component. A Young density law (Young, 1976) is used to reproduce the bulge halo $R^{1/4}$ component, an exponential law to simulate the disk, and a power law of the type discussed by van Albada et al. (1985) for the dark halo. This model yields a circular velocity curve (related to the mass density profile assuming that the luminous components of the galaxies have constant M/L ratios) and a light density profile. For NGC 5084 the corrected stellar rotation curve is in agreement with the velocities measured at 21-cm wavelength by Gottesman and Hawarden (1986) at a distance (400") twice the optical size of the disk. The global M/L profile of the galaxies can be derived from the above density profiles.

Figure 3 shows for NGC 5084 the decomposition of the observed rotation

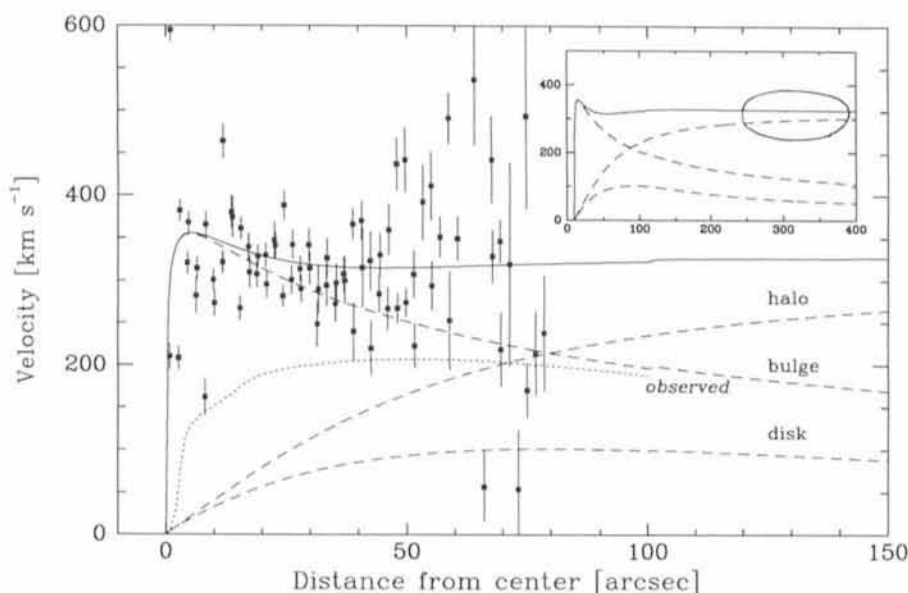


Figure 3: Rotation curve on NGC 5084 presented as the sum of bulge, disk and halo (dashed lines) in order to fit both the circular rotation curve (full line) and the velocities of the outer HI ring (shown in the inset as ellipse). The dotted line represents the observed rotation curve. The individual observed values (full points) are corrected for the asymmetric drift and integration along the line-of-sight.

curve into the contributions of bulge, disk and halo component. Combining these results with existing HI data, the extension of the halo component and its contribution to the total galaxy mass can be calculated. For instance, in the case of NGC5084, a massive halo is required to explain the M/L profile. This is found to vary from about $19 M_{\odot}/L_{\odot}$ ($H_0=100 \text{ Mpc km s}^{-1}$) in the inner regions increasing outwards to $45 M_{\odot}/L_{\odot}$, with a possible central peak of $> 30 M_{\odot}/L_{\odot}$. Following the model, a total mass of $7.28 \times 10^{11} M_{\odot}$ ($R < 30 \text{ kpc}$), 80% of which contained in the halo component, is derived. The presence of the massive halo could also explain the tilted lane observed in this galaxy in terms of a stabilized warped disk (Binney, 1978).

NGC5084 is an S0 galaxy, but nevertheless has an enormous quantity of gas. This observed gas can hardly derive from a single accretion event, since such a large mass would probably leave the gas in an inclined configuration due to the effect of self-gravitation

(Sparke and Casertano, 1988), but this configuration is not observed. If the picture of the external origin of the gaseous material should still hold, one has to assume that the time scale of the accretion process is very short with respect to the life time of the galaxy.

A possible picture for the formation of SDGs is then that they are the result of a series of accretion events, possibly induced also by the progressive deepening of the galaxy potential well.

References

Binney, J., 1978. *Mon. Not. R. Astr. Soc.*, **183**, 779.
 Burstein, D., Rubin, V.C., Thonnard, N. and Ford, W.K.Jr., 1982. *Astroph. J.*, **253**, 70.
 Disney, M., 1990. *Nature*, **346**, 105.
 Giovanelli, R., Haynes, M.P. and Chincarini, G.L., 1986. *Astroph. J.* **301**, L7
 Gottesman, S.T. and Hawarden, T.G., 1986. *Mon. Not. R. Astr. Soc.*, **219**, 759.
 Holmberg, E., 1958. *Medd. Lund Astr. Obs. Ser.*, 2, n. 136.

Huchtmeier, W.K. and Richter, O., 1989. *A General Catalog of HI Observations of Galaxies* (New York, Springer).
 Lauberts, A. and Valentijn, E.A., 1989. *The Surface Photometry Catalogue of the ESO-Uppsala Galaxies* (ESO, Garching).
 Longo, G. and de Vaucouleurs, A., 1983. *A General Catalog of Photoelectric Magnitudes and Colors in the U,B,V Systems*, Univ. Texas Monogr. Astron. n. 3.
 Roberts, M.S., 1978. *Astron. J.*, **83**, 1026.
 Rubin, V.C., Burstein, D., Ford, W.K.Jr. and Thonnard, N., 1985. *Astroph. J.*, **289**, 81.
 Saglia, R.P. and Sancisi, R., 1988. *Astron. Astrophys.*, **203**, 28.
 Sancisi, R. and van Albada, T.S., 1985. *IAU Symp.* **117**, 67.
 Shostak, G.S., Hummel, E., Shaver, P.A., van der Hulst, J.M. and van der Kruit, P.C., 1982. *Astron. Astrophys.*, **115**, 293.
 Sparke, L.S. and Casertano, S., 1988. *Mon. Not. R. Astr. Soc.*, **234**, 873.
 Valentijn, E.A., 1990. *Nature*, **346**, 153.
 van Albada, T.S., Bahcall, J.N., Begemann, K. and Sancisi, R., 1985. *Astroph. J.*, **295**, 305.
 Young, P.J., 1976. *Astron. J.*, **81**, 807.
 Zeilinger, W.W., Galletta, G. and Madsen, C., 1990. *Mon. Not. R. Astr. Soc.*, **246**, 324.

On the Origin of the Continuum Radiation at Optical and Ultraviolet Wavelengths in AGN/Quasars

M.-H. ULRICH, ESO

It is generally proposed that the energy source in quasars and Seyfert galaxies is accretion onto a massive object. Since angular momentum appears in most astrophysical situations, it has been further proposed that the accreted gas is assembled in a disk (Lynden-Bell, 1969; Shields, 1978; for reviews see Pringle, 1981; Collin-Souffrin and Lasota, 1988). For a given model, the spectrum of the radiation emitted by a pure viscous flow can be calculated. Comparison of this continuum spectrum with the observed optical/UV/soft X-ray spectrum can, in principle, give the mass of the central object M_{BH} and the accretion rate \dot{M} (e.g. Sun and Malkan, 1989). However, not only are the models still uncertain but also, as we shall see below, the rapid variations of the UV and optical continuum of AGN suggest that the origin of this continuum is more complex than previously realized.

Let us examine the flux variations data available for one of the best studied AGNs: NGC 4151 (Ulrich et al., 1990).

NGC 4151 has been observed with IUE on 125 days mostly grouped in campaigns of typically 20 to 40 days,

the interval between observations being 4 to 5 days. No ground-based optical observations were systematically done simultaneously with the UV observations but we have at our disposal the flux measured with the fine error sensor (FES) on-board IUE before each spectral exposure. The optical FES flux, which is recorded with an S20 photocathode, is contributed by variable components

(broad emission lines + continuum) and a nonvariable component including stellar light and narrow emission lines.

The contribution of the Balmer continuum in the FES band is negligible. That of the broad emission lines is estimated to be $< 20\%$ of the total flux.

Figures 1 and 2 show that the optical (FES) and UV fluxes undergo variations which are simultaneous within our time

TABLE 1: NGC4151 = Selected episodes: observing dates

1983	IUE EXOSAT	October 30; November 4, 7, 11, 15, 19 November 7, 11, 15, 19
1984	IUE EXOSAT	December 16, 19, 24, 28 December 16, 20, 22, 24, 28
1985	IUE EXOSAT	January 2, 8, 14 January 2
1988	IUE	November 29 December 10, 14, 20, 24, 28, 31
1989	IUE	January 5, 9, 13, 17, 21, 25, 30
1990	IUE	February 25 March 1, 5, 9, 13, 17, 21 April 1, 12, 17

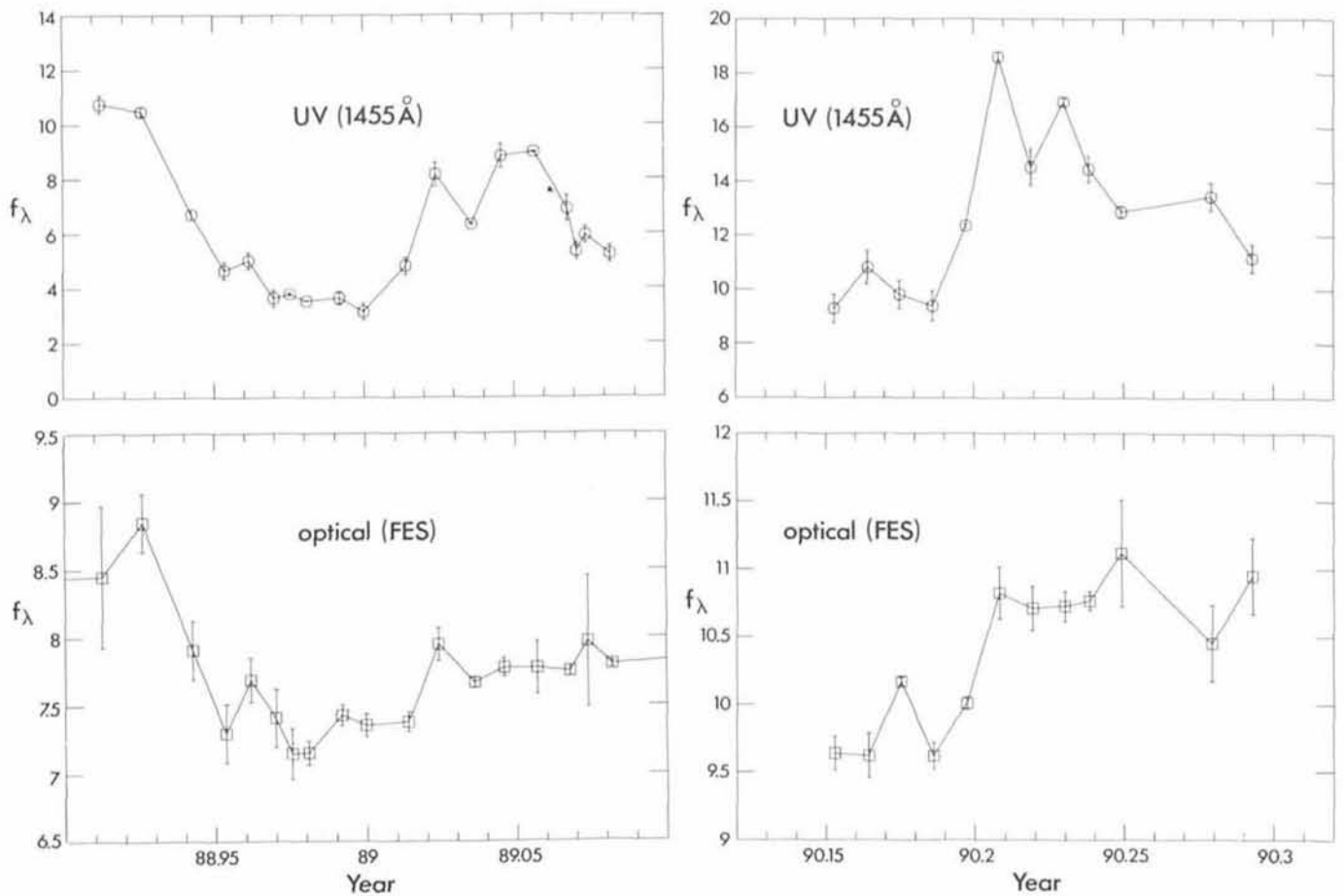


Figure 1: UV/optical flux variations in NGC 4151: The flux at 1455Å and in the FES for 2 episodes, November 29, 1988 – January 30, 1989, and February 25 – April 17, 1990. Ordinates in 10^{-14} erg cm^{-2} s^{-1} Å $^{-1}$. Abscissae, year minus 1900.

sampling. The data taken as an example are those of the 2 most recent campaigns of observations, November 1988 – January 1989 and February–April 1990. The maximum delay between the UV and the optical variations is < 2 days in either direction as compared to a viscous time scale of a few years. Moreover the time scale of the continuum variations is of the order of days. This rules out the possibility that the observed continuum variations are due to variations of the accretion rate (Pringle, 1981; Clarke, 1988).

We propose two processes for the rapid and simultaneous optical and UV continuum variations (Ulrich et al., 1990):

1. The variations are due to local instabilities in the inner part of the disk which produce small hot regions emitting mostly in the far UV but which contribute to the optical flux through the low energy tail of their spectrum. This results in a nearly perfect modulation of the UV and optical flux. The time scale and the amplitude of the variations at different wavelengths have the potential to give strong constraints on the dimensions, temperature and location of these instabilities.

2. Alternatively, the UV/optical varia-

tions could be due to irradiation of the disk by a central variable X-ray source. Such a model has been proposed by Czerny, Czerny and Grindlay (1986) for low mass binaries. The irradiation heats the disk surface which then emits a spectrum different (hotter) from that of a pure accretion flow. The modulation of the UV and optical fluxes is caused by the X-ray variations. In this case, one expects the UV/optical variations to be correlated with the X-rays variations.

Our simultaneous IUE/EXOSAT observations of NGC4151 (Fig. 2) of 7–19 November 1983 and 16 December 1984 – 2 January 1985 (Perola et al., 1986) give results consistent with irradiation: There is an excellent linear correlation (probability of 2.5×10^{-6} of being due to chance) between the 2–10 keV flux and the continuum at 1455Å during the 2 periods of simultaneous observations.

Figure 3 shows the correlation between the X-ray flux in the ME range and the UV flux at 1455Å (same data as Fig. 2). We note that each value of the ME flux is the average of the flux measured during an EXOSAT observation. During each observation (which lasted several hours) the flux drifted smoothly by about $\pm 15\%$ around the mean for this observation. The extremely good

correlation of Figure 3 suggests that similar variations must have occurred in the UV range but the timing of our IUE observations (2 consecutive spectra within 2 hours, every 4 to 5 days) is not adequate to verify this point.

We stress that at other isolated dates of simultaneous UV/X-ray or optical/X-ray observations, the UV (or optical) and X-ray fluxes do not follow this correlation but scatter at larger values of the UV (or optical) flux and lower values of the X-ray flux. See, for example, the point representing the simultaneous IUE/Einstein observations of 19–21 May 1979 which falls on the right hand side of Figure 3 (Perola et al., 1986; Penston, 1986). We suggest that in November 7–19, 1983 and December 16, 1984 – January 2, 1985, the X-ray variations overrode and masked the effects of the inner disk instabilities; the latter are, in general, the dominant process producing the UV/optical variations when the X-ray source is not particularly strong.

The determination of M_{BH} and \dot{M} from fitting of the UV/optical spectra with theoretical models of an accretion disk spectrum have not so far included the effect of irradiation or of the instabilities discussed here. Further modelling in-

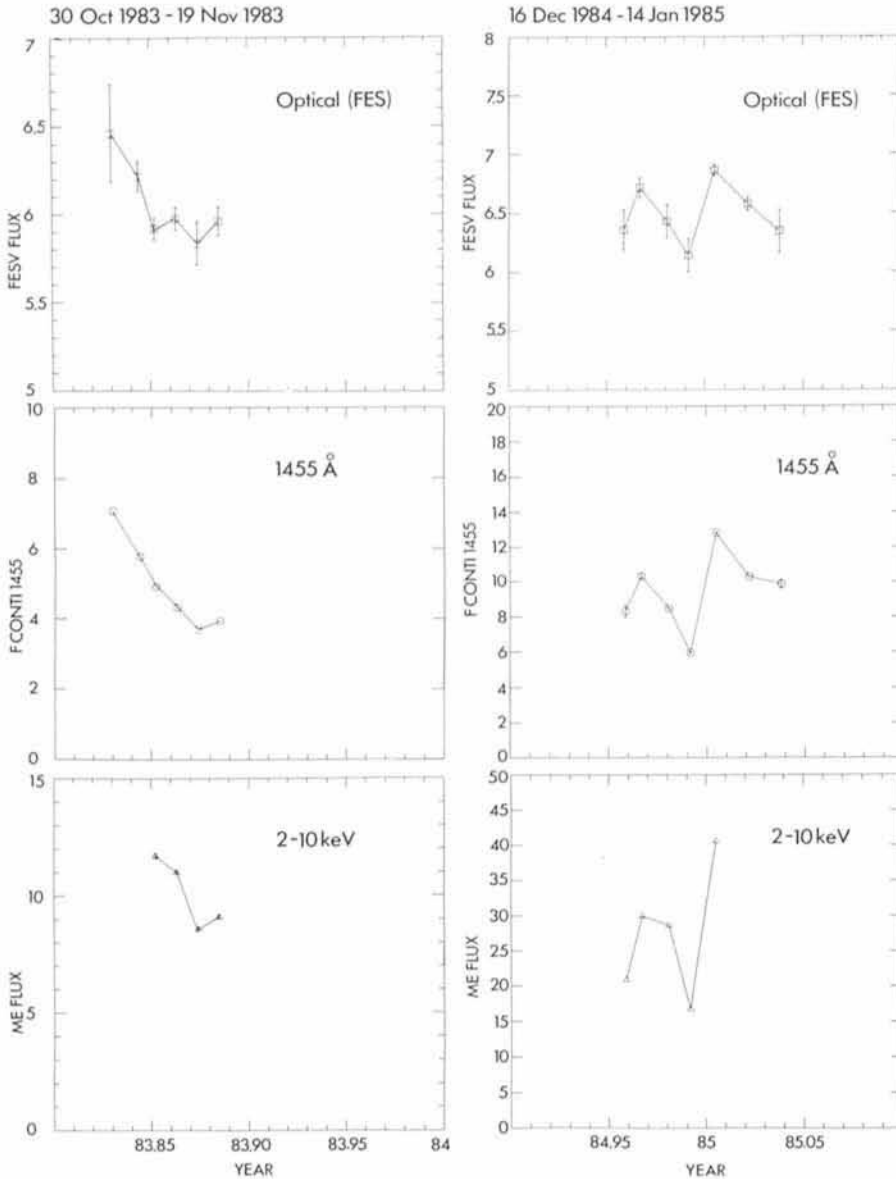


Figure 2: UV/optical/X-ray flux variations in NGC4151: The FES flux, UV flux at 1455Å and 2 – 10 keV flux during two campaigns with simultaneous observations with IUE and EXOSAT (Perola et al., 1986).

cluding these effects will lead to better estimates of \dot{M} and especially M_{BH} than presently available.

We note that there is no clear correlation between the UV (or optical) flux and the X-ray flux in other AGN/quasars which have been adequately observed in different energy bands (NGC4051: Done et al., 1990; 3C 273: Courvoisier et al., 1990). The good UV/X-ray correlation observed in NGC 4151 in November 1983 and December 1984 – January 1985 is exceptional for NGC4151 as well as among the other AGN/quasars.

Evidently, a good estimate of the time delay between UV and X-ray variations provides constraints on the relative location of the different emission regions. This time delay in NGC 4151, at the epochs when the correlation was ob-

served, is less than 2 days. Considering that the mass of the central object in NGC 4151 is likely to be less than $5 \times 10^7 M_{\odot}$, which corresponds to a

A New Jet in M87?

B.J. JARVIS, ESO

The giant elliptical galaxy M87 (NGC 4486) has been the subject of intense study over the past two decades for a number of reasons. Firstly, it is large and bright, centrally placed in the Virgo cluster and also because of its bright optical

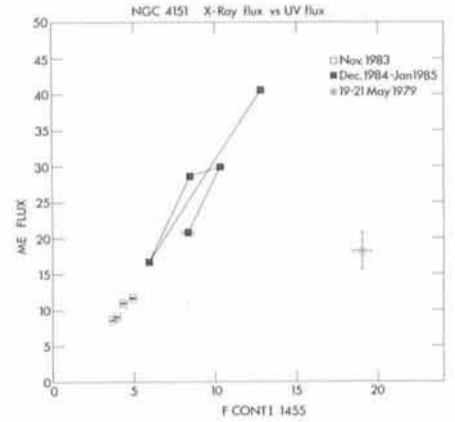


Figure 3: The 2 – 10 keV flux vs the flux at 1455 Å for the dates of Figure 2, plus the point representing the X-ray and UV flux on May 19 – 21, 1979. The optical/X-ray data taken at isolated dates do not follow the correlation X-ray vs UV flux or X-ray vs optical flux defined by the November 1983 and December 1984 – January 1985 data. Altogether the data suggest that irradiation by the X-ray source produces the quasi simultaneous optical/UV flux variations at some epochs. But in general, it is the instabilities in the inner disk which modulate simultaneously the optical and UV fluxes.

Schwarzschild radius $r_s \leq 2 \times 10^{13}$ cm, the upper limit on the time delay available now is not very constraining.

References

Clarke, C.J., 1988. *Mon. Not. Roy. Astron. Soc.* **235**, 881.
 Collin-Souffrin, S., and Lasota, J.-P., 1988. *Publ. Astr. Soc. Pacific* **100**, 1041.
 Courvoisier, T.J.-L., et al., 1990, *Astron. Astrophys.* **23**, 73.
 Czerny, B., Czerny, M., and Grindlay, J.G., 1986, *Ap. J.* **311**, 241.
 Done, C., et al., 1990, *Mon Not. Roy. Astron. Soc.* in press.
 Lynden-Bell, D., 1969, *Nature* **223**, 690.
 Penston, M.V., 1986, *Physics of Accretion onto Compact Objects*, ed. K.O. Mason, Springer, Berlin.
 Perola, G.C., et al., 1986, *Ap. J.* **306**, 508.
 Pringle, J.E., 1981, *Ann. Rev. Astr. Ap.* **19**, 137.
 Shields, G.A., 1978, *Nature* **272**, 706.
 Sun, W.-H., and Malkan, M.A., 1989, *Ap. J.* **346**, 68.
 Ulrich, M.-H., et al., 1990, preprint.

synchrotron and radio jet emanating from the nucleus. The jet has been studied at all wavelengths from X-ray to radio. An understanding of these jets is important for probing the physical processes in active nuclei and their interac-

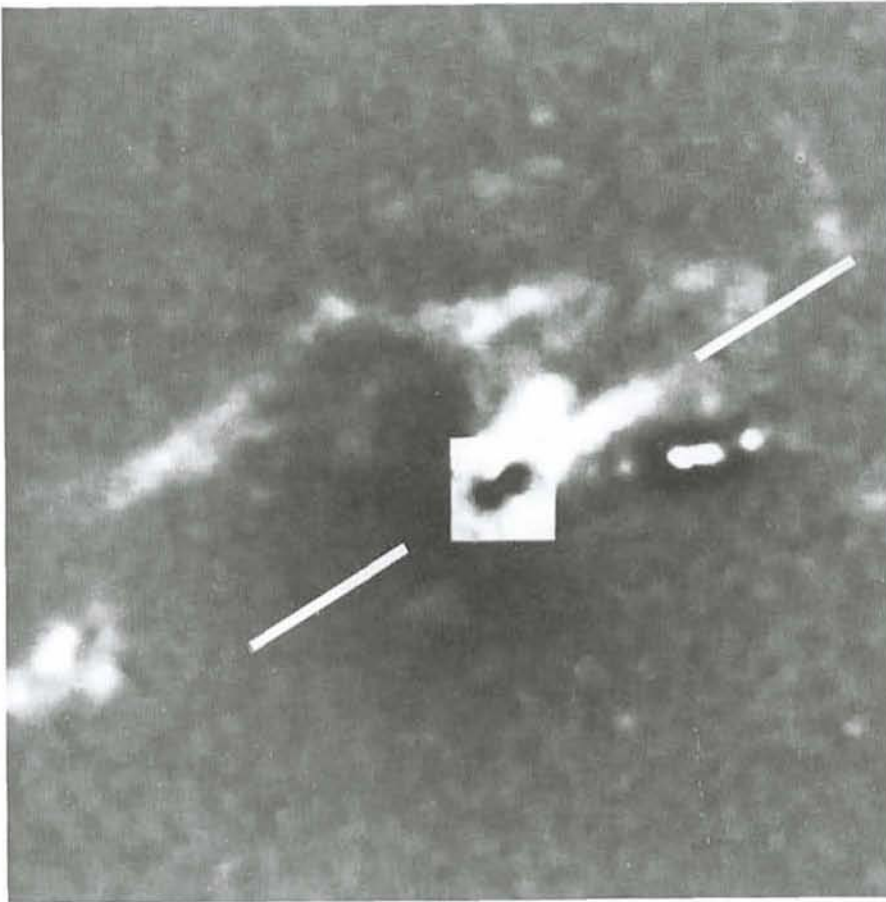


Figure 1: Narrow-band continuum subtracted image (slightly smoothed) of the central region of M87 through a redshifted (70\AA FWHM) $H\alpha$ filter. The insert at the centre shows the [O III] emission concentrated in the core region. The $H\alpha + [\text{N II}]$ jet (PA = $317^\circ.5$) extends towards the upper right-hand corner, inclined about 25° from the radio synchrotron jet. Note the alignment of the $H\alpha + [\text{N II}]$ jet with the [O III] feature. The dimensions of the image are 4.8×4.8 kpc for an assumed distance of 15 Mpc.

tions with the surrounding matter.

The nucleus of M87 is also interesting for other reasons since it is believed to

contain a supermassive object, possibly a black hole, first proposed by Sargent et al. (1978) and Young et al. (1978). Very

recent observations of the Calcium triplet absorption lines in the core of M87 by Jarvis and Melnick (1990) indicate a mass of about $5 \times 10^9 M_\odot$ within a radius of $r = 3''$. Surrounding the nucleus is a complex system of $H\alpha + [\text{N II}]$ gas, loosely concentrated on the nucleus. This is clearly seen in narrow-band imaging by Ford and Butcher (1979) and more recently by van den Bergh (1987) and Jarvis (1989). We report here the kinematic observations of a "jet-like" $H\alpha + [\text{N II}]$ feature, shown between the white lines in Figure 1, emanating from the nucleus at an angle of 25° northward of the optical synchrotron jet.

Narrow-band $H\alpha + [\text{N II}]$ imaging observations, shown in Figure 1 were made on La Silla in August 1989 with the New Technology Telescope during its commissioning phase. Kinematic observations of the elongated emission feature aligned with the nucleus were made in March 1990 with the ESO 3.6-m telescope and Boller and Chivens spectrograph. The RCA CCD detector had pixels of dimension $1''.1 \times 1.68\text{\AA}$ with a spectral range of $5776 \text{\AA} - 7510\text{\AA}$. Four 60-minute exposures were co-added together with the slit aligned along the elongated emission feature and passing through the nucleus. Figure 2 shows an image of the reduced long-slit spectra in the region of the $H\alpha + [\text{N II}]$ and [S II] emission lines. Gaussian profiles were least-squares fitted to the lines to determine their radial velocities. The results are plotted in Figure 3.

All five emission lines in Figure 2 show identical kinematic behaviour indicating that the emission-line regions are mov-

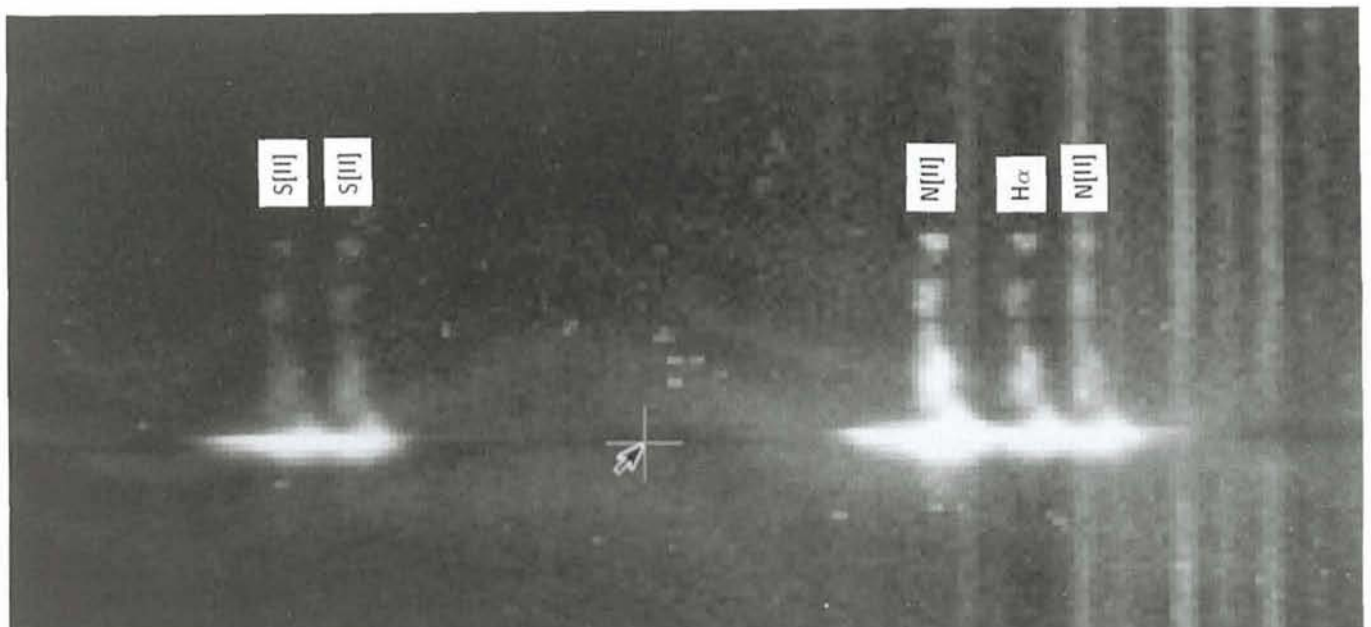


Figure 2: Long-slit spectra of the $H\alpha + [\text{N II}]$ jet feature in Figure 1. The vertical lines extending to the edges are night-sky emission lines and were included to show how the galactic emission lines are clearly inclined. All five galactic emission lines show the same rotation curve. The cursor marks the centre of the galaxy and the image is $94''$ in height.

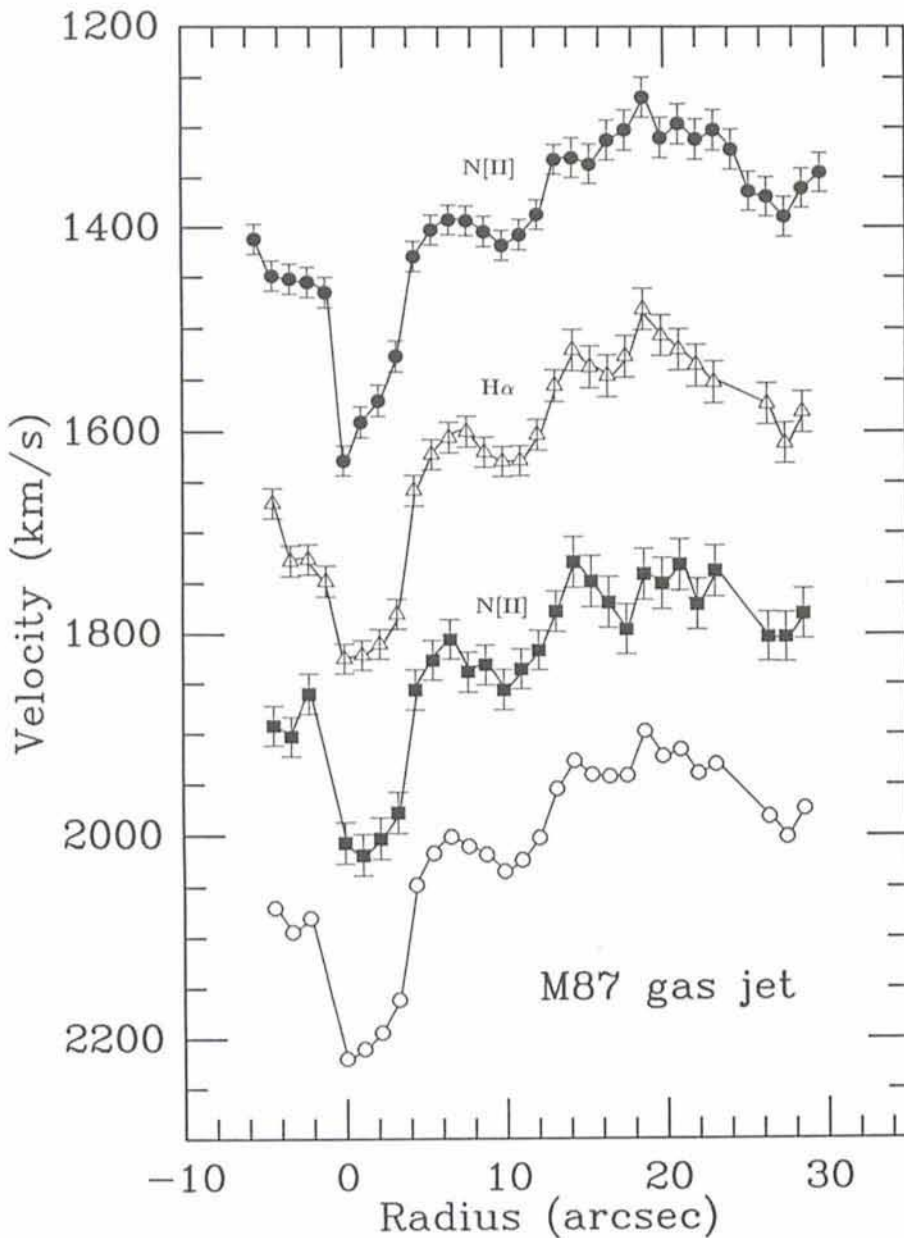


Figure 3: Observed radial velocities, from long-slit spectra, of the $H\alpha$ and two $[NII]$ lines shown in Figure 2. The bottom curve shows their mean. The velocity scale is arbitrary.

ing together. Their behaviour is characterized by a rapid increase in velocity of more than 200 km s^{-1} within the first $6''$ from the nucleus. Between six and ten arcseconds, a small decrease is observed followed by another rapid increase to a maximum velocity of about 320 km s^{-1} relative to the core at $20''$. Beyond $20''$ there is a slow but smooth decrease for as long as there is measurable gas. It is interesting to compare the morphological characteristics of this "jet-like" feature with Keel's (1985) criteria for optical jets. Keel proposed four criteria for a jet, i.e. it must contain less than 10% of the host galaxy's luminosity, be one sided (with respect to the nucleus), have an aspect ratio greater than 10, and be straight to within the limits of its width. The optical feature

studied here clearly satisfied all these conditions. With also a clearly defined velocity gradient we believe that this is a true jet, albeit gaseous and not stellar.

Could we be looking at a rotating, nearly edge-on disk of gas instead of a real jet of material? This possibility can be immediately rejected by the velocities measured on the opposite side of the nucleus from the jet. Figure 3 shows that this gas also shows a rapid rise in velocity away from the nucleus *in the opposite sense that would be expected if it were a disk of gas seen nearly edge-on*. Unfortunately, however, it is not possible to conclude from the velocities alone if this material is falling into the core or being expelled from it.

Morphologically, the jet is not continuous along its length since the outer

emission-line regions are closely linked kinematically to the main body of the jet because those regions which lie on the slit also have velocities consistent with those of the inner continuous part. This suggests that the $H\alpha + [NII]$ gas may share a common origin or fate depending upon whether it is being expelled from or falling into the nucleus. For an assumed distance of 15 Mpc, the continuous part of the jet is approximately 1 kpc in length.

Heckman et al. (1989) also observed the kinematics of the $H\alpha + [NII]$ gas in M87 although not along the jet. However, their $PA = 0^\circ$ velocities are in close agreement with those here. Even though the Heckman et al. data extend to only about $10''$ from the core, both data sets show the same amplitude of about 320 km s^{-1} and the sharp decrease approaching the core from both sides. They concluded that this gas is *infalling* at about the free-fall velocity. These observations suggest that *all* of the gas in the immediate vicinity of the nucleus is kinematically similar. Walker (1968) observed a fan-shaped distribution of $[OII]$ emission ($3726\text{-}29\text{\AA}$) between position angles $310^\circ\text{-}65^\circ$ to which he also reported an increasing velocity with radius. However, very little $[OII]$ emission was observed at the position angle of the $H\alpha + [NII]$ jet reported here. The velocity amplitude and maximum radial extent of the $[OII]$ emission is very similar to that observed for the $H\alpha + [NII]$ jet, i.e. about 1 kpc. The distributions, however, of the $H\alpha + [NII]$ and $[OII]$ emission-line regions are quite different. Contrary to Heckman's conclusions, he believed that this material was being *ejected* from the nucleus in which case an increasing velocity with radius means that the outflow is being ejected away from us. It would be worthwhile to repeat these observations with CCD's to obtain better S/N ratios than Walker obtained photographically.

Of particular interest is the very close alignment of the nuclear $[OIII]$ emission with the optical $H\alpha + [NII]$ emission-line jet. This is indeed curious in view of recent work by Haniff, Wilson and Ward (1988) and also Wilson and Baldwin (1989). Haniff et al. found that in a sample of 10 galaxies with "linear" radio sources, all showed alignment (within measurement errors) of the $[OIII]$ emission-line region and the radio structures. Wilson and Baldwin's observations of another Seyfert galaxy, 0714-2914 showed the same effect. Moreover, Whittle et al., showed from a sample of 11 Seyfert galaxies that several also had clear evidence for double-lobe substructure in the $[OIII]$ emission. This is also clearly seen in M87, except that the circumnuclear $[OIII]$ is aligned with the

H α + [NII] jet and *not* the well-known radio jet as in all other cases.

The nuclear spectra also show a complex structure: the H α and two [NII] emission lines are multiple with at least three observable components. This is probably due to flows of gas in other directions, e.g. towards the north where other emission can be seen in Figure 1. The [OIII] (5007 Å) emission line is double peaked in the core. This can be clearly seen in Figure 4. The emission lines then merge at about $r = \pm 2''$, reminiscent of an expanding shell of gas. The velocity of expansion is measured to be about 300 km s^{-1} .

In summary, the jet nature of the H α + [NII] emission-line feature seems well established. The origin of the entire H α + [NII] gas is not. Moreover, of particular interest is the alignment of the [O III] core emission with this jet since it is not seen in any other radio galaxy with emission-line activity. This gas and other species will merit more detailed study in the future.

References

- Ford, H.C., Butcher, H., 1979, *Astrophys. J. Supp. Ser.*, **41**, 147.
 Haniff, C.A., Wilson, A.S., and Ward, M.J., 1988, *Astrophys. J.*, **334**, 104.
 Heckman, T.M., Baum, S.A., van Breugel, W.J.M., and McCarthy, P., 1989, *Astrophys. J.*, **338**, 48.
 Jarvis, B.J., 1989, *The Messenger*, **58**, 10.
 Jarvis, B.J., and Melnick, J., 1990, *Astron. Astrophys. Lett.*, in press.
 Keel, W.C., 1985, *Astron. J.*, **90**, 2207.
 Sargent, W.L.W., Young, P.J., Bokseberg, A., Shortridge, K., Lynds, C.R., Hartwick, D.A., 1978, *Astrophys. J.*, **221**, 731.
 van den Bergh, 1987, IAU Symposium

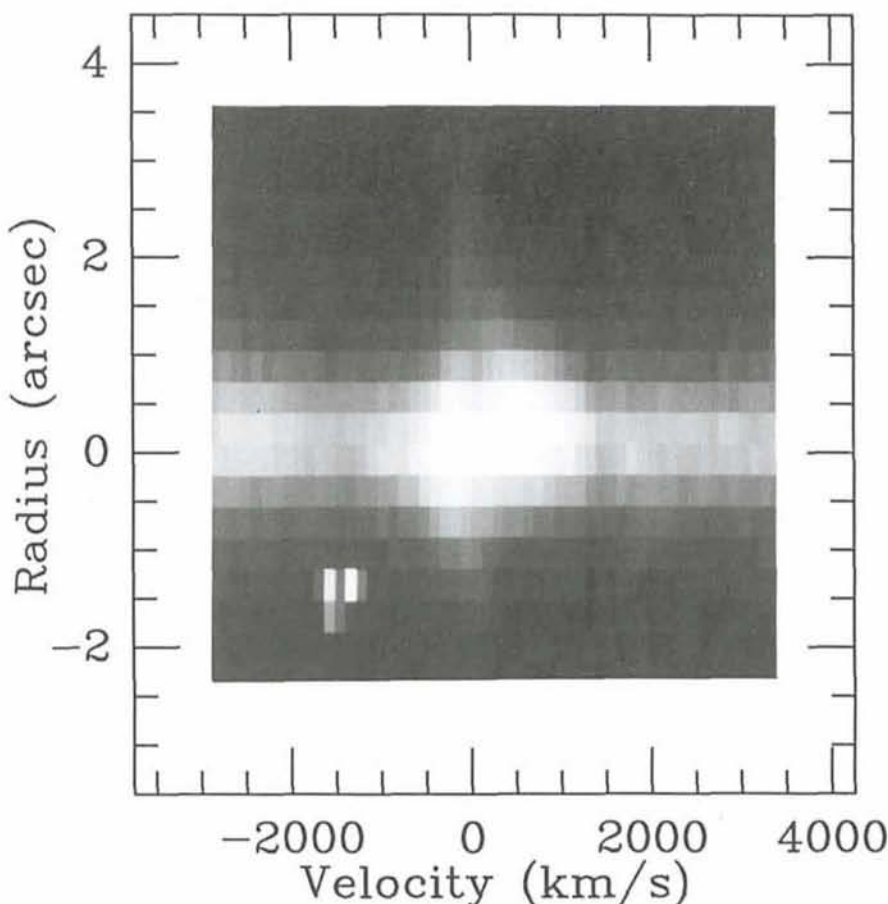


Figure 4: The [OIII] (5007 Å) emission line in the core of M87. Note the double peak at the centre.

- No. 117, 217.
 Walker, M.F., 1968, *Astrophys. J. Lett.*, **2**, 65.
 Whittle, M., Pedler, A., Meurs, E.J.A., Unger, S.W., Axon, D.J., and Ward, M.J., 1988, *Astrophys. J.*, **326**, 125.

- Wilson, A.S., Baldwin, J.A., 1989, *Astron. J.*, **98**, 2056.
 Young, P.J., Westphal, J.A., Kristian, J., Wilson, C.P., Landauer, F.P., 1978, *Astrophys. J.*, **221**, 721.

Infrared Coronal Lines in Active Galaxies

A.F.M. MOORWOOD, ESO

E. OLIVA, Osservatorio Astrofisico di Arcetri, Italy

1. Introduction

Coronal lines are forbidden fine-structure emission lines from highly ionized heavy metals. Although the best known are probably those of [FeVII]–[FeXIV], which fall in the visible, many more coronal lines from a large number of elements fall in the infrared spectral range but have received little attention so far. These include transitions of [CaVIII], [AlV], [AlVI], [SiVI], [SiVII], [MgVIII], [AlIX], and [SiIX] at wavelengths between 1.96 and $3.92 \mu\text{m}$ which, although mostly falling in regions of poor atmospheric transmis-

sion, have now been observed from the ground in several novae. Discovery of these lines in novae was completely unexpected and their identification was controversial for some time until confirmed by subsequent work.

The [Si VI] ($^2P_{1/2}$ – $^2P_{3/2}$) $1.96 \mu\text{m}$ and [SiVII] (3P_1 – 3P_2) $2.48 \mu\text{m}$ lines are also present in spectra of the extremely high excitation planetary nebula NGC 6302 and represent the highest ionization stages (ionization potentials of 167eV and 205eV respectively) observed in PN.

2. Infrared Lines

As further evidence that infrared spectroscopy is still in its exploratory phase, the first reported measurement of an infrared coronal line in an extragalactic object was our somewhat serendipitous detection of the [SiVI] $1.962 \mu\text{m}$ line in the Seyfert galaxy NGC 1068 while using IRSPEC at the ESO 3.6-m telescope to explore bright galaxies in previously unobserved portions of their infrared spectra lying outside the high transmission 'window' regions (Oliva and Moorwood 1990).

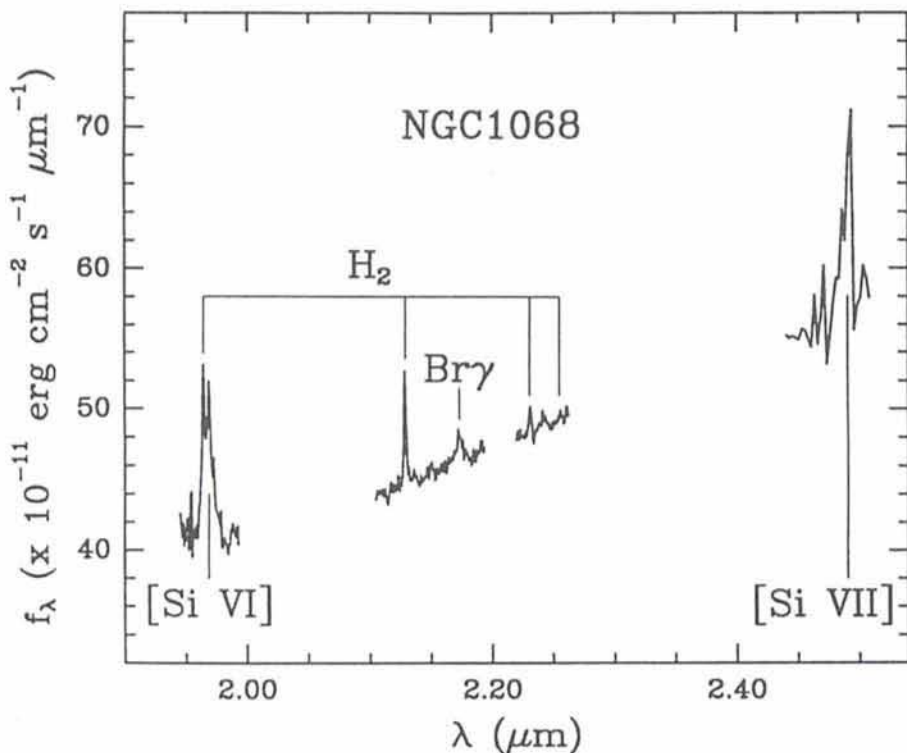


Figure 1: Discovery spectrum of the [SiVII] 2.48 μm line in the Seyfert galaxy NGC1068 obtained with IRSPEC at the NTT plotted together with the previously obtained spectrum at the 3.6-m telescope showing [SiVI] 1.962 μm blended with the H_2 1-0S(3) line. Residual noise in the [SiVII] spectrum is dominated by imperfect cancellation of strong atmospheric absorption lines in this region of the spectrum which lies to the long wavelength side of the K band window.

Following this discovery we have subsequently searched specifically for the [Si VI] line in several other galaxies with detections in the Seyfert galaxies A1409-65, NGC5506 and IC4329A and, as anticipated, no evidence for this line in several starburst nuclei included for comparison.

Following the transfer of IRSPEC to its new home at the NTT in October 1990 we have also now observed the [SiVII] line at its expected rest wavelength of 2.48 μm in NGC 1068 to confirm the line identifications and obtain additional diagnostic information. Apart from their potential as a new technique for investigating the origin of coronal lines, simply the presence of these lines is of considerable interest as potential infrared tracers of Seyfert activity and their intensities should provide a valuable check on models now being used to predict the likely strengths of longer wavelength coronal lines which are unobservable from the ground but should be accessible to the spectrometers to be flown on the ESA Infrared Space Observatory scheduled for launch in 1993.

Both lines exhibit extremely large equivalent widths as can be seen in Figure 1 which shows the calibrated spectrum of NGC1068 around [SiVII] plotted together with our previously

published discovery spectrum of [SiVI]. Estimated fluxes are ~ 7.5 and $9.0 \cdot 10^{-13} \text{erg. cm}^{-2} \cdot \text{s}^{-1}$ in a 6×6 arcsec aperture for the [SiVI] and [SiVII] lines respectively, although accurate determinations are difficult because the [Si VI] line is blended with the H_2 1-0S(3) line and lies shortward of the K(2.2 μm) window, where the transmission is poor and varies rapidly with wavelength, while the [Si VII] line lies in an even worse atmospheric region longward of the K window. This line, being broad (~ 1000 km/s), is clearly visible in the raw spectra. In order to improve cancellation of the many strong and narrow H_2O absorption features, however, the spectrum shown was obtained by combining spectra measured with the 32-pixel array at four grating positions selected to yield a 128 point spectrum with half pixel spacings which was then re-binned over four pixels (~ 300 km/s) before dividing by interleaved measurements of a nearby standard star treated in the same way. The resulting noise is, nevertheless, still dominated by imperfect cancellation of these lines.

3. Origin of the Lines

As infrared coronal lines result from transitions between low lying levels, they are easy to excite collisionally even

in relatively low temperature gas. Formation of the ions themselves, however, requires a highly energetic process and is generally attributed to collisional excitation in hot ($\sim 10^6 \text{K}$) gas or photoionization by UV/X-ray photons. The relative importance of these mechanisms in active galaxies is still a matter of debate as is the actual location and density of the coronal line gas.

Initially, therefore, it appeared highly significant that both the ratios [SiVI]/ $\text{Br}_\gamma \sim 6$ and [SiVII]/[SiVI] ~ 1.2 measured for NGC 1068 are almost exactly as predicted very recently for photoionization of the low density interstellar medium by the central continuum source in active galaxies (Korista and Ferland, 1989 and results presented in the ISO Long Wavelength Spectrometer Consortium GT Proposal obtained using the same code). Accepting the apparent support for this model at face value, however, would imply that the Br_γ emission within the central 6×6 arcsec region observed is dominated by the coronal line gas which appears improbable. Following conventional reasoning, the fact that the [SiVI] and [SiVII] lines are broader than other forbidden lines of lower excitation, e.g. [FeII] have widths comparable to the He I 1.083 μm line, also indicates an origin in high- rather than low-density gas.

Comparison of our results for NGC 1068 with those obtained on novae and the planetary nebula NGC6302 also reveals the more perplexing fact that, whereas the [SiVII]/[SiVI] ratio should be sensitive to details of the ionization mechanism, its measured values are essentially identical in all the objects so far measured.

In novae, the coronal lines are believed to arise in relatively high density gas ($< 10^6 \text{cm}^{-3}$) excited by both photoionization and collisions in hot gas and the remarkable similarity in conditions implied by the constancy of the [SiVII]/[SiVI] ratio in the four novae in which this has been measured has already been drawn attention to by Greenhouse et al. (1990). In the planetary nebula NGC 6302 it appears to be consistent with lower density (10^4cm^{-3}) gas photoionized by a central star at $T \sim 5 \cdot 10^5 \text{K}$ (Ashley and Hyland, 1988) and the same ratio now observed in NGC 1068 is consistent with photoionization of low density gas by an active nucleus. At the moment the detailed implications of this result are not clear.

As the [Si] line critical densities are similar and much higher ($\sim 2 \cdot 10^8 \text{cm}^{-3}$) than the model densities considered in NGC6302 and NGC1068 their line ratios should exhibit a relatively weak density dependence and the similarity of the observed ratios may simply reflect

the fact that the ionizing spectrum of a star as hot as that invoked in the planetary nebula does closely mimic an active nucleus (thus at least providing support for photoionization rather than collisional excitation in active nuclei). The more difficult problem is accounting for the similarity with novae if collisional excitation really does play an important role in these objects.

As the other galaxies mentioned above which show the [SiVI] line have not been observed around [SiVII], the constancy of this ratio in galaxies cannot yet be tested. These and other galaxies for which [SiVI] upper limits have been obtained do, however, appear to exhibit lower [SiVI]/Br_γ ratios (≤ 2) except perhaps for the Seyfert 1 galaxy IC4329A (≥ 1.7). The [SiVI]/

[FeVII] line ratio in this galaxy is also larger than in NGC1068 – consistent with higher excitation conditions as already indicated by its larger [FeX]/[FeVII] ratio. Further tests of the correlation between [Si] and [Fe] lines are of interest but presently limited by the small sample of galaxies observed to date and uncertainties in the extinction corrections to be applied to the visible lines.

Following the planned upgrade of IRSPEC with a 2D array detector, it is now hoped in the near future to be able to extend our observations of the [Si] lines to a larger sample of galaxies; to utilize the new long-slit capability to measure their spatial distribution and to search for coronal emission from other species in order to investigate further

the location and excitation of these lines.

Acknowledgement

We are grateful to Livia Origlia for her assistance during the data reduction.

References

- Ashley, M.C.B., Hyland, A.R.: 1988, *Ap. J.*, **331**, 552.
 Greenhouse, M.A., Grasdalen, G.L., Woodward, C.E., Benson, J., Gehrz, R.D., Rosenthal, E., Skrutskie, M.F.: 1990, *Ap. J.*, **352**, 307.
 Korista, K.T., Ferland, G.J.: 1989, *Ap. J.*, **343**, 678.
 Oliva, E., Moorwood, A.F.M.: 1990, *Ap. J.*, **348**, L5.

New NTT Discoveries on Distant Galaxies and Gravitational Lensing

F. HAMMER, DAEC, Observatoire de Paris-Meudon, France

O. LE FÈVRE, Canada-France-Hawaii Telescope Corp., Hawaii, USA

Since the discovery of the double lensed QSO 0957+561 by Walsh et al. (1979), gravitational lensing effects are being identified in a steadily increasing number of sources. Indeed, detector improvements in the 1980s have led to the detection of features as faint as a few thousandths of the sky signal. This has resulted in the identification of radio galaxies at high- z , which are much more numerous than QSOs and also potentially affected by gravitational lensing.

We know today about 50 radio galaxies at $z > 1$, and these sources are likely to be affected by gravitational lensing, because they lie at the bright end of the Radio Luminosity Function (RLF). This is the steepest part of the RLF – the slope is equal to -3.5 – and hence is strongly subjected to statistical gravitational lensing. Let us recall that the latter influences much more steeper luminosity functions than the normal galaxy luminosity function which, with a slope equal to -1 , cannot be statistically affected by lensing. We have predicted (Hammer and Le Fèvre, 1990; Hammer and Wu, in preparation) that there should be 5 to 10 times more bright radio sources behind rich lensing clusters of galaxies than in the rest of the sky and therefore, maybe that all 30 known high- z galaxies are part of the 3CR catalog because their radio luminosity has been sufficiently mag-

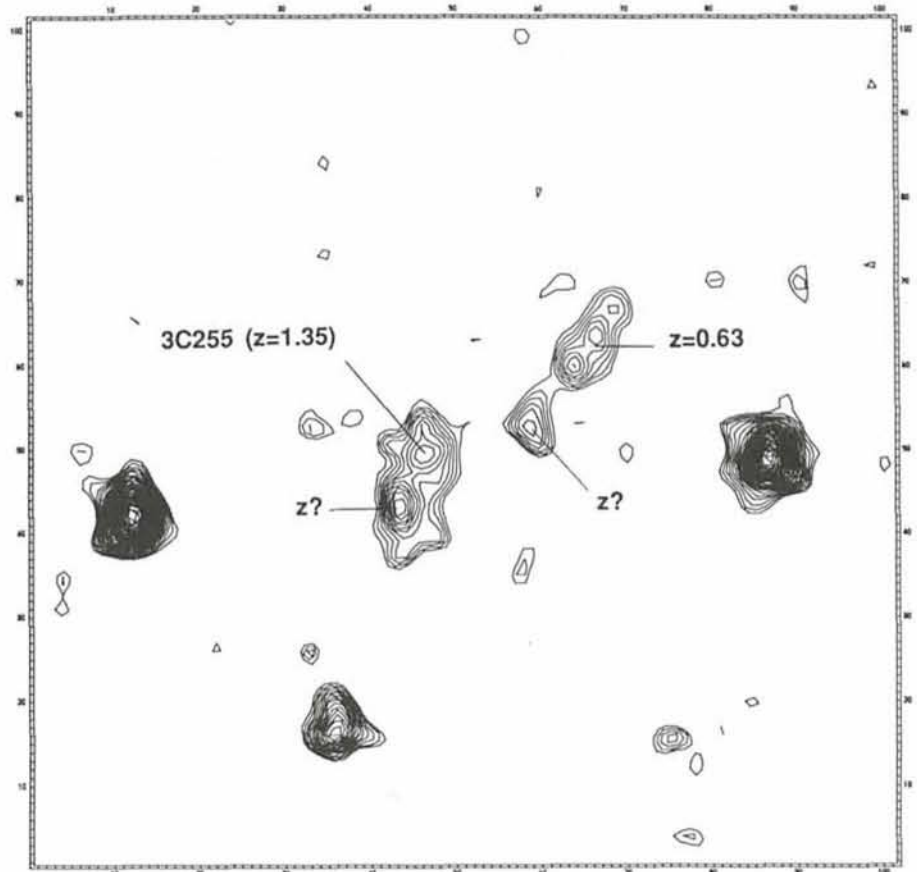


Figure 1: 3C255 ($z=1.35$), R, FWHM=0".9, CFHT prime focus. The field is 20×20 arcsec, North is up and East to the left.

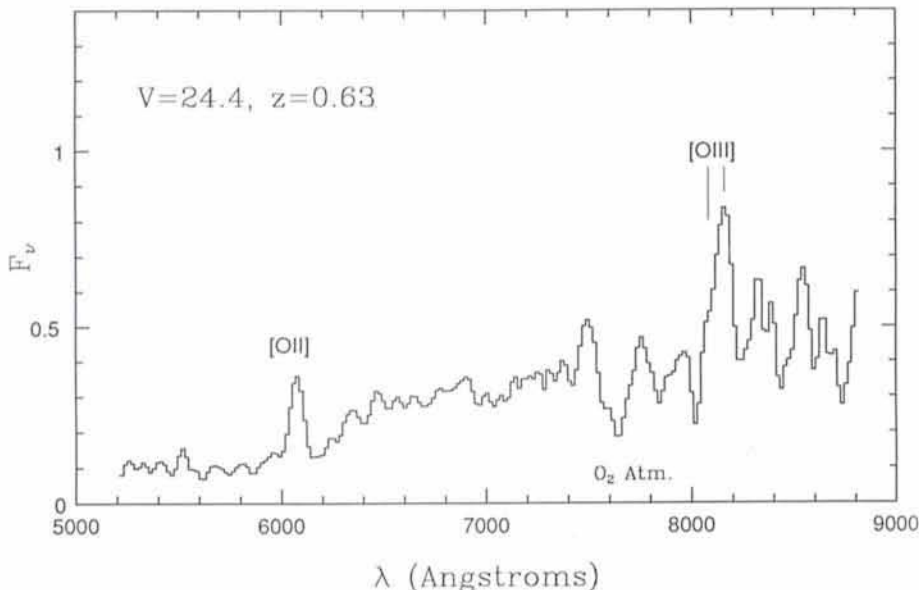


Figure 2: ESO/NTT spectrum of a $B=25$ ($V=24.4$) galaxy identified at $z=0.63$ from [OII] 3727 Å and [OIII] at 4959 and 5007 Å. It is only 4.5 away from the radio galaxy 3CR255 ($z=1.35$).

nified by foreground deflecting matter. Identification of foreground matter and search for possible gravitational mirages among these sources are part of an ESO Key Programme (Surdej et al., 1989) jointly with similar searches for bright multiple lensed optical QSOs and additional observational studies of known lenses.

There are few doubts that gravitational lensing greatly helps us in detecting the most distant galaxies. Discoveries and studies of giant luminous arcs (Soucaill et al., 1987; Lynds and Petrosian, 1987; Hammer and Rigaut, 1989) have led to a new sample of galaxies which would have $B=24-25$ if they were not lensed and which probably lie at relatively moderate z ($\langle z \rangle = 0.8$ for 6 sources). Radio rings are the result of gravitational lensing of a distant radio lobe or jet by a massive foreground galaxy (Hewitt et al., 1988). They also potentially allow studies of distant galaxies which are much more "normal" than the extremely peculiar radio galaxies in the 3C and 4C surveys which are dominated by radio emission.

In the following sections, we present several results obtained during five very good nights at the NTT in February 1990. Weather conditions were good (seeing $\langle FWHM \rangle = 0.9$ and stable, best seeing 0.7 FWHM, photometric sky) while the telescope, the EFOSC2 instrument and the Thomson 1024² CCD performed almost flawlessly. This combination has provided us with very good data. There was no instrumental failure, which is remarkable since it was only the 2nd month of official use of the NTT. We first report on the spectroscopic discovery of foreground galaxies close to the 3CR 255 line of sight including the record

spectroscopic identification of a $B \sim 25$ galaxy. Another high z 3CR galaxy, 3CR 297, is found to be a good gravitational mirage candidate from its spectroscopy. Deep spectroscopy of the well-known high- z galaxy, 3CR368 ($z=1.13$) reveals that the brightest and central component

is a Galactic M star, and elucidates the nature of this source. Finally, direct imaging in several broad-band filters of M1131+0456 identifies the lens and the lensed/distorted optical counterpart of the radio ring, while the physical nature of the lens and a possible redshift are tentatively derived from the spectroscopy. These results emphasize the importance of gravitational lensing in our understanding of the distant Universe.

Contaminating Foreground Galaxies in the Field of 3CR255

3CR255 was identified with an extremely complex optical system including at least five components (Fig. 1). The redshift was previously obtained by Giraud (1989) and we confirm its value of $z=1.35$ from our detection of the strong [OII] 3727 emission line and [NeIII] 3869 which are to be added to the previously detected CIII, CII and MgII. However, only one component, indicated on Figure 1, shows emission lines at this redshift.

Four arcseconds away there is a $B=25$ ($V=24.4$) galaxy for which we have derived a redshift $z=0.63$ (5.5 hours of total integration time) from the observed [OII] 3727 and [OIII] 5007 and 4959 emission lines (Fig. 2). Apart from

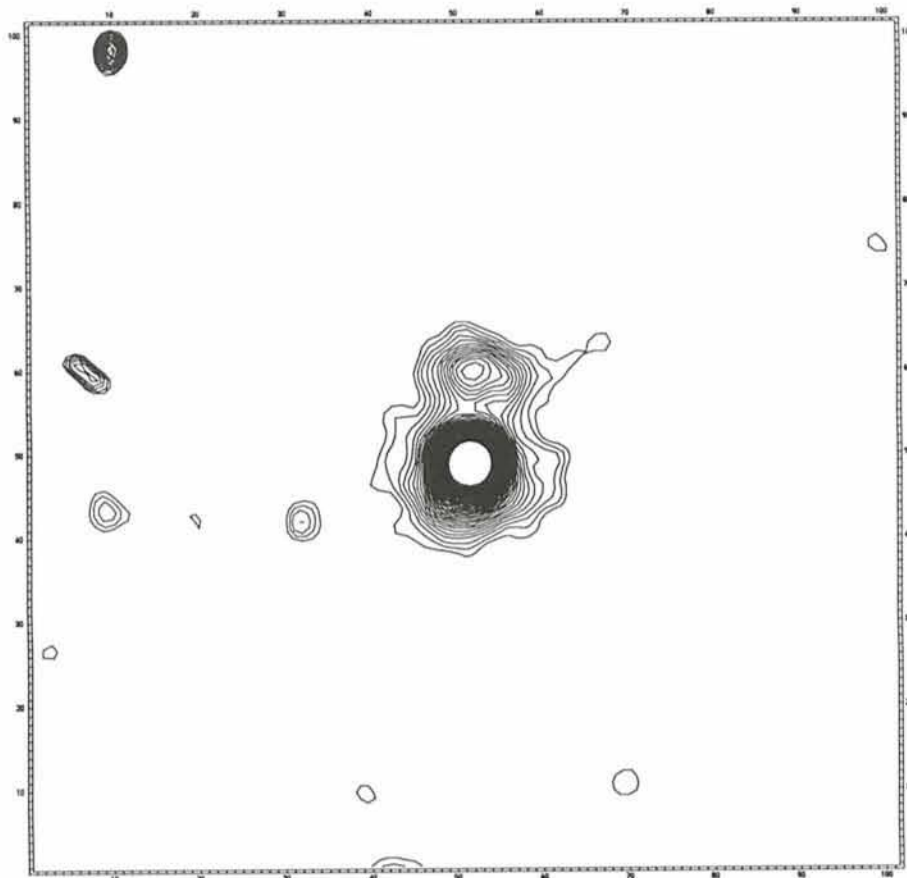


Figure 3: 3CR297 ($z=1.4$), R , $FWHM=0.9$, CFHT prime focus. The field is 20×20 arcsec, North is up and East to the left.

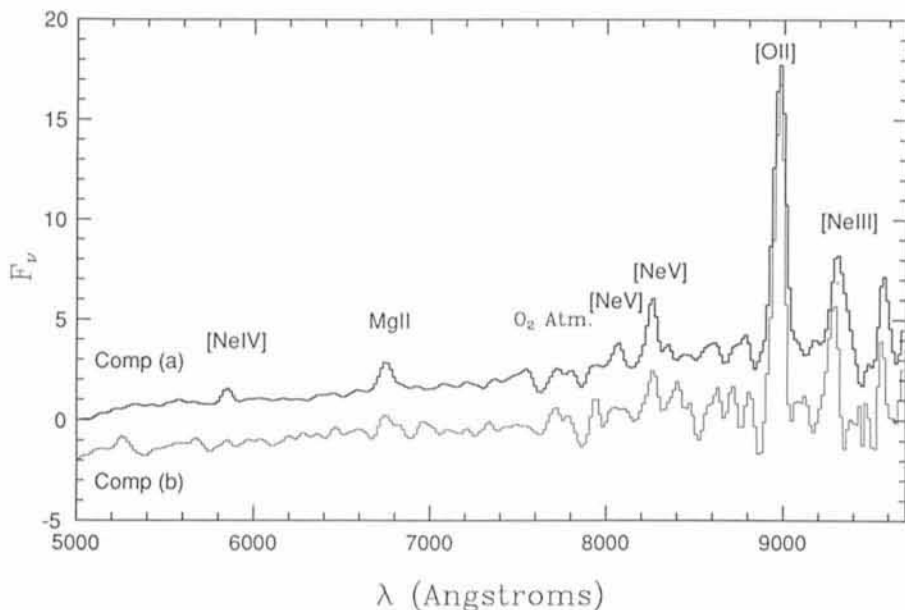


Figure 4: ESO/NTT spectra of the 2 components of 3CR297. The emission lines show the same velocity at less than 100 km/s difference.

the detection record in faint object spectroscopy, this is a field galaxy selected at random which should be compared with similar detections up to $B=24$ (Cowie, Ellis and Koo, in a workshop on galaxies at high z , Oxford, July – August 1990) and to the $B=24-25$ sources forming the giant luminous arcs. Our $B=25$ galaxy is also intrinsically faint – several tenths of L^* (see e.g. Efstathiou et al., 1988) – similar to galaxies belonging to the main population of the $B=22.5$ redshift survey (Colless et

al., 1990) with $\langle z \rangle = 0.32$. Taken together, these results indicate that no luminosity evolution is required for galaxies up to $z \sim 0.8$, and that counts up to $B=27$ (Tyson, 1988; Lilly et al., 1990) might be dominated by galaxies at moderate z . There are also indications that component (c) is a foreground object, and possibly again at $z=0.63$.

The 3CR 255 optical counterpart is probably gravitationally magnified by this foreground matter, and its complexity and intrinsic luminosity would be

largely decreased by removing the foreground objects. A more detailed analysis of these data will be reported elsewhere.

A New Gravitational Lens Candidate: 3CR 297

The optical counterpart of 3CR 297 ($z=1.4$) is dominated by two components (Fig. 3). Spectroscopy with EFOSC at the 3.6-m and EFOSC2 at the NTT have provided the spectra shown in Figure 4. The two components have the same emission lines [NeIV], MgII, [NeV], [OII], [NeIII] and there is no velocity discrepancy between them down to our measurement accuracy of 100 km/s. Moreover, [OII] 3727, the strongest emission line, has a blueshifted wing in both spectra. The continuum of the faintest component however is bluer than the brightest one, which could be due to the presence of the deflecting object. New radio data (van Breugel, private communication) show very distorted structures but do not confirm or infirm at this stage the lensing hypothesis.

3CR 368: a Well-Known High- z Galaxy Dominated by a Galactic M Star!

This source has been considered by several authors as a prototype of the high- z radio galaxies from its luminosity, its colour, its morphology (Fig. 5 (a)) and the alignment between radio and optical axis. It has been the source of a large

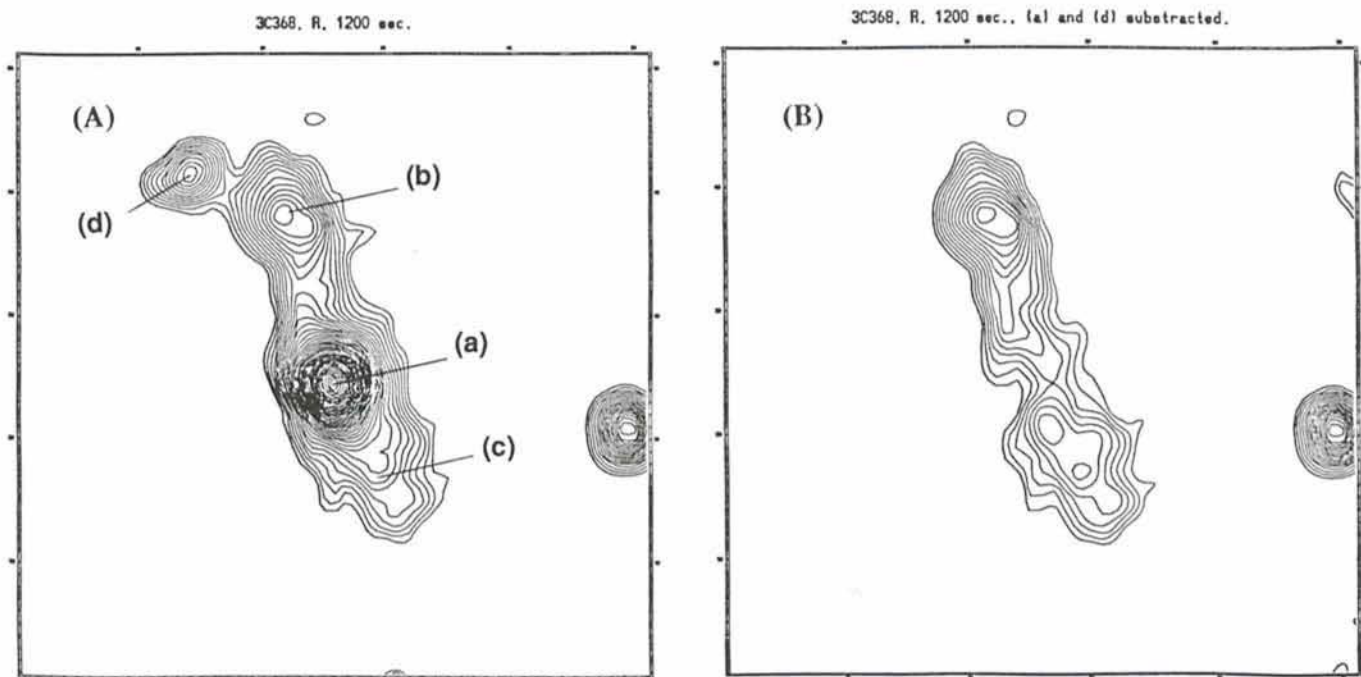


Figure 5: 3CR368, R image, $FWHM=0.8$, CFHT prime focus: (a) before "decontamination", (b) after "decontamination" by a foreground Galactic M star. The fields are 10×10 arcsec, North is up and East to the left.

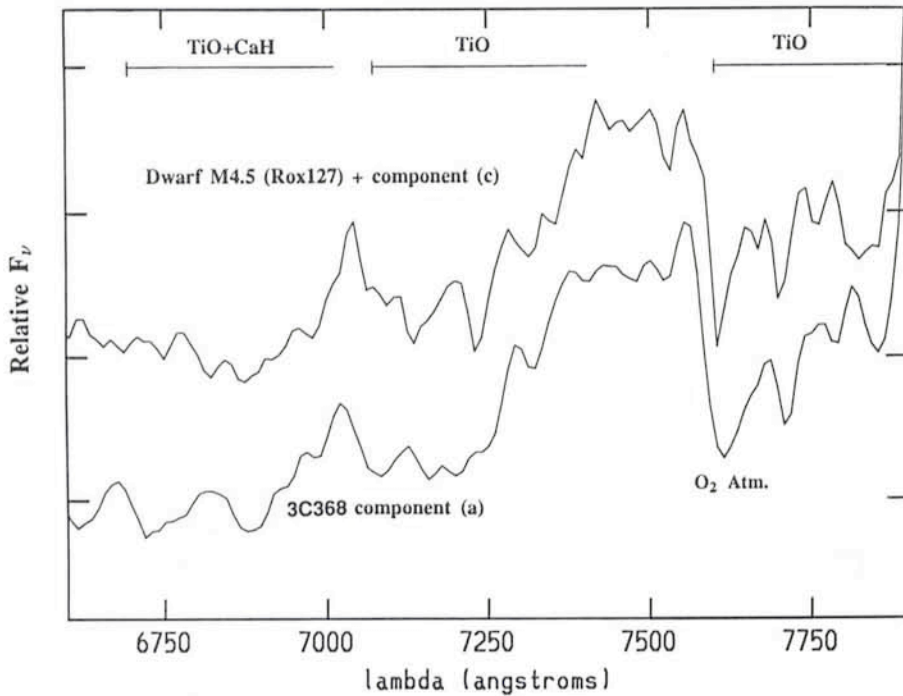


Figure 6: ESO/NTT spectrum of component (a) of 3C368, sum of 3 spectra 45 min each. It shows the TiO and CaH bands typical of M5 stars.

number of studies at all wavelength (Djorgovski et al., 1987; Chambers et al., 1988; di Seregho Alighieri et al., 1989; Chambers and Charlot, 1990; Scarrott et al., 1990, etc . . .). Our new spectroscopic measurements obtained with the CFHT and the NTT have revealed that the brightest and reddest central component is a Galactic star – probably an M5 dwarf – rather than a foreground galaxy as we first believed or a $z=1.13$

source as stated prior to our measurements (Fig. 6 and Hammer, Le Fèvre and Proust, 1990). Removing the foreground object decreases the 3CR368 luminosity several times, especially at red and infrared wavelength (up to 1.4 mag in the K band). We believe that the superposition of the M star may also alter the radio properties and the previously reported optical polarization. The residual 3CR368 at $z=1.13$ (Fig. 5

(b)) actually shows an almost flat continuum associated with very strong and somewhat broad emission lines. Its appearance is therefore strongly modified and it could be an AGN associated with an extended emission line region rather than a distant galaxy dominated by stellar emission. Similar results on other distant radio galaxies, namely 3CR 238 and 3CR 297, have also been found from the same run at the NTT (Hammer and Le Fèvre, in preparation). We emphasize again the danger of interpreting such peculiar and rare distant radio sources as multiple-component galaxies without paying attention to the possible contamination by foreground objects, such as Galactic stars or faint galaxies.

MG 1131+0456: Discovery of the Optical Lensed Source and Spectroscopy of the Lens

This radio source has been discovered by Hewitt et al. (1988) in the frame of a large radio survey with the VLA. Its radio morphology consists of an almost complete ring accompanied by a pair of compact sources nearly diametrically opposed. This is probably the result of a radio jet well aligned with a foreground massive galaxy and then highly lensed, while the associated radio core is gravitationally multiplied.

We have obtained deep broad band images in the B, V, R and I bands. Nothing has been detected in B, while we have measured the optical object at other wavelengths, with $V=23.4$,

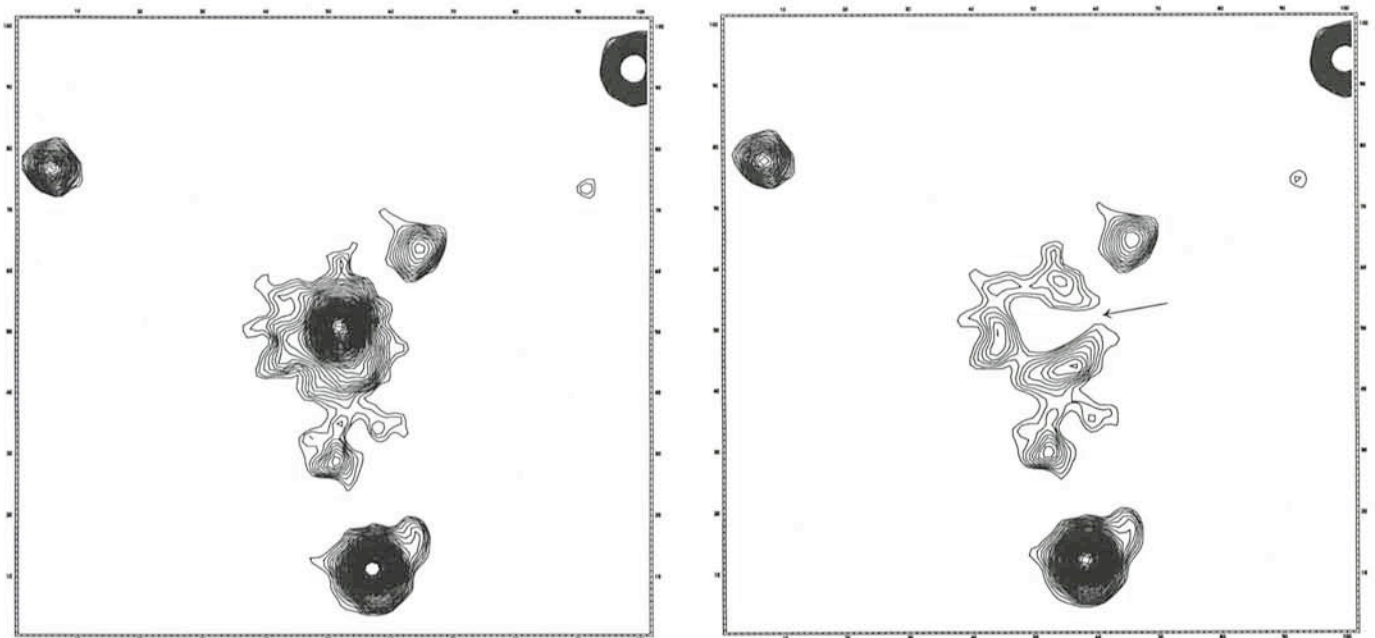


Figure 7: (a) NTT image of the optical object detected at the radio location of the M1131+0456 Einstein ring (2 h 30 total integration R+I bands, seeing 0".9 FWHM); (b) same after removal of a $L_{\text{eff}}=5 \text{ kpc } r^{1/4}$ profile. The residual is believed to be the optical emission associated with the lensed object and radio ring (see text). The field is 16×16 arcsec, North is up and East to the left.

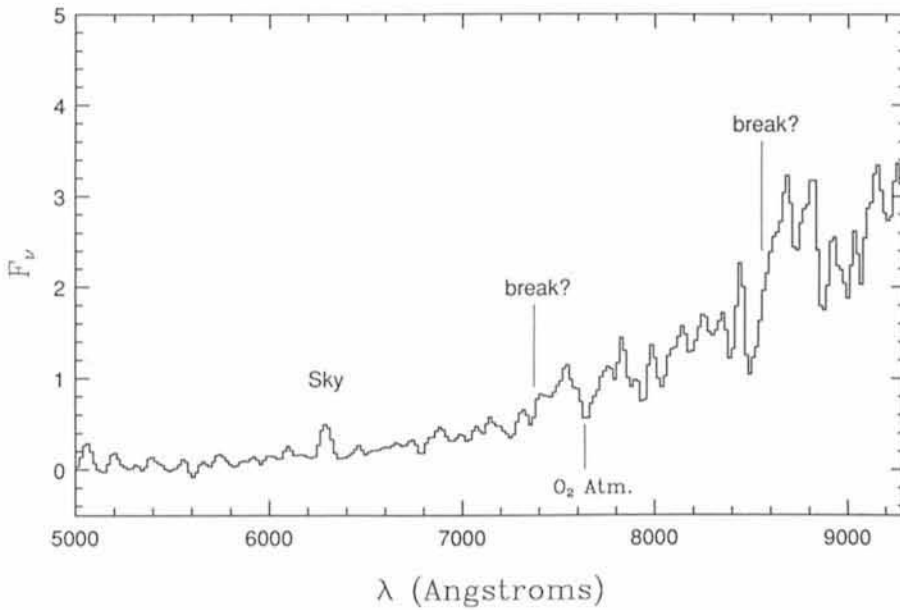


Figure 8: ESO/NTT spectrum of M 1131+0456 ($R=22.15$), note the very red continuum and two possible breaks at 7400\AA and 8550\AA .

$R=22.15$ and $I=20.67$. It is located just at the centre of the radio ring and constitutes most probably the lens (Fig. 7 (a)). The red colours deduced have led us to the hypothesis of a 4000\AA break between V and R or between R and I. Moreover, the I image looks more extended than that of an elliptical galaxy. Indeed, if we assume that the lens is an elliptical galaxy, the R and I images cannot be fitted by any reasonable $r^{1/4}$ profile, which indicates an additional source of light. After removal of a $r_{\text{eff}}=5$ kpc $r^{1/4}$ profile, one can see a residual ring-like emission that follows the radio ring fairly closely (Fig. 7 (b)); note the gap indicated by the arrow in both the optical and radio images); profiles with r_{eff} up to 15 kpc have also been tried but none was successful in removing this extra emission. It is therefore likely to be the optical counterpart of the background radio source, i.e. the first example of an optical ring.

We have then obtained spectra of the optical object and Figure 8 reveals a featureless spectrum without any emission line. This is however extremely red with two breaks ($S/N \sim 2$), one located at 7400\AA and the other at 8550\AA . There are at this stage two alternatives: either we have spectroscopically detected the lens alone which has a spectrum very similar to the one of an elliptical redshifted at $z=1.13$ or we have found the blend of the lens at $z=0.85$ with the source at $z=1.13$. In both cases the lens is identified with a rather unevolved elliptical galaxy for which the absence of [O II] 3727 emission indicates no strong star-formation activity. The source is the counterpart of a radio emission at mJy

level, far below the radio luminosity of the 3CR high- z galaxies. It is likely to be an elliptical galaxy gravitationally distorted by the foreground lens, and if it lies at $z=1.13$ it should also be a non evolved elliptical at least 3 magnitudes fainter than the powerful radio galaxies (Hammer et al., in preparation).

Conclusions

The NTT has convincingly shown us its outstanding capabilities in terms of the detection of very faint objects and features in crowded environments, in both imaging and spectroscopy.

The results presented above should be interpreted in the frame of extragalactic research and more especially in the sampling of the high- z Universe by distant galaxies. A key problem was open by deep counts of galaxies up to $B=27$: if they were dominated by high- z sources ($z=1.4$), this would favour strong luminosity evolution and a low value for the baryonic density, while a major contribution by small and dwarf galaxies at moderate z ($z=0.6-1.2$) implies no or small luminosity evolution plus a number density evolution and then a higher value for the baryonic.

Spectroscopic results on distant 3CR galaxies show them to be extremely peculiar and without evidence to be dominated by stellar content. Indeed, most of their properties seem to be closely linked with their active nucleus (Hammer, Le Fèvre and Sol, in preparation). Interpretations of these sources should be made carefully, also because they are expected and found as being affected by contamination due to foreground

matter and/or resulting gravitational lensing (Hammer and Le Fèvre, 1990). The use of these extremely peculiar sources to test galaxy evolution is therefore particularly dangerous. Moreover, we know now some massive and high- z ellipticals considerably fainter than the high- z radio galaxies and rather non evolved. These are for instance the lens of QSO 2016+112 identified at $z=1.01$ by Schneider et al. (1986) or the lens and/or the source of the system M 1131+0456 detected by us. On the other side, there are the spectroscopic identifications of very faint sources found at moderate z , such as sources associated with the giant luminous arcs or the $B=25$ galaxy presented here. Again they show no or little luminosity evolution. Strong luminosity evolution seems to be rejected both for intrinsically bright and faint galaxies.

References

- Chambers, K.C., Miley, G.K., Joyce, R.R., 1988, *Astrophys. J.* **329**, L75.
- Chambers, K.C., Charlot, S., 1990, *Astrophys. J. Letters*, **348**, L1.
- Colless, M., Ellis, R.S., Taylor, K., Hook, R.N., 1990, *M.N.R.A.S.* **244**, 408.
- Djorgovski, S., Spinrad, H., Pedelty, J.A., Rudnick, L., Stockton, 1987, A., *Astron. J.*, **93**, 1307.
- Efstathiou, G., Ellis R.S., Peterson, B.A., 1988, *M.N.R.A.S.*, **232**, 431.
- Giraud, E., 1989, *The Messenger*, **56**, 63.
- Hammer, F., Rigaut, F., 1989, *Astron. Astrophys.*, **226**, 45.
- Hammer, F., Le Fèvre, O., 1990, *Astrophys. J.*, **357**, 38.
- Hammer, F., Le Fèvre, O., Proust, D., 1990, *Astrophys. J.* in press.
- Hewitt, J.N., Turner, E.L., Schneider, D.P., Burke, B.F., Langston, G.I., Lawrence, C.R., 1988, *Nature*, **333**, 537.
- Lilly, S.J., Cowie, L.L., Gardner, J., 1990, *Astrophys. J. Sup. Ser.* in press.
- Lynds, R., Petrosian, V., 1986, *Bull. Amer. Astron. Soc.* **18**, 1014.
- Scarrott, S., Rolph, C., Tadhunter, C., 1990, *M.N.R.A.S.*, **243**, 5p.
- Schneider, D.P., Gunn, J.E., Turner, E.L., Lawrence, C.R., Hewitt, J.N., Schmidt, M., Burke, B.F., 1986, *Astron. J.*, **91**, 991.
- di Seregho Alighieri, S., Fosbury, R., Quinn, P., Tadhunter, C., 1989, *Nature*, **341**, 307.
- Soucail, G., Mellier, Y., Fort, B., Picat, J.P., 1987, *Astron. Astrophys.*, **172**, L14.
- Surdej, J., et al., 1989, *The Messenger*, **55**, 8.
- Tyson, T.A., 1988, *Astron. J.*, **96**, 1.
- Walsh, D., Carswell, R.F., Weymann, R.J., 1979, *Nature*, **279**, 381.

Ultraluminous Infrared Galaxies

I.F. MIRABEL, *Service d'Astrophysique, CEN-Saclay, France*

The Infrared Astronomical Satellite (IRAS) revealed a class of luminous galaxies that emit almost all the energy ($\geq 95\%$) in the far-infrared. The most extreme galaxies of this type radiate as much as $10^{12} L_{\odot}$ in the $8\ \mu\text{m}$ – $1000\ \mu\text{m}$ wavelength band, which is equivalent to the accepted minimum bolometric luminosity of quasars. These objects are called "ultraluminous infrared galaxies". Although the space density of ultraluminous infrared galaxies exceeds that of optically selected quasars of the same bolometric luminosity, there are only a few tens of galaxies of this type in the Local Universe ($z \leq 0.13$).

The study of "luminous infrared galaxies" has now become a key area in extragalactic research for two reasons: (1) We have come to the realization that above $10^{11} L_{\odot}$ the infrared luminous galaxies are the dominant population of objects in the Universe, being as numerous as Seyferts, and more numerous than quasars of the same bolometric luminosities^[1]. (2) There is increasing evidence that luminous infrared galaxies may represent an early and brief phase

in the evolution of galaxies, and that their study will provide clues for our understanding of the genesis of the most energetic – quasars and radio galaxies – and most massive – giant elliptical galaxies – in the Universe.

Most of the far-infrared emission from galaxies is due to the absorption and re-emission of light by dust. Although the luminosity density in the Local Universe seems to be evenly split between cool disk emission and warmer starburst emission, from the IRAS colours we know that the infrared emission from ultraluminous infrared galaxies is mostly radiated by warm dust. At present it is not known if the source of the light that heats the dust consists solely of large amounts of massive stars, or if in addition, the formation of gigantic black holes with X-ray emitting accretion disks are also required to explain the colossal amounts of thermal energy radiated by the dust in the far-infrared.

To reveal the nature of the host galaxies and to understand the origin of the greatly enhanced infrared radiation, we are carrying out at ESO, optical, infrared

and radio observations of a flux limited sample of the nearest luminous infrared galaxies, selected from a survey^[2] of bright IRAS galaxies in the southern hemisphere.

NTT Images

The optical morphology of ultraluminous infrared galaxies has recently been a subject of controversy. Whereas from observations with the Palomar 1.5-m telescope some authors^[3] had concluded that nearly all ultraluminous infrared galaxies are strongly interacting mergers, from studies at La Palma, other authors^[4] conclude that galaxy interactions are far from being an ubiquitous factor among this type of galaxies. In view of the contradictory reports on the morphology of ultraluminous infrared galaxies, optical imaging with the most advanced technology had become necessary. The excellent optics of the New Technology Telescope (NTT) and the good seeing conditions on La Silla were fully exploited to arbitrate on the question of the optical morphology.

CCD images of the 16 nearest ultraluminous infrared galaxies in the southern hemisphere^[5] were obtained using the second ESO Faint Object Spectrograph and Camera (EFOOSC2) attached to one of the Nasmyth foci of the NTT. The observations were carried out during the commissioning period of these instruments. The detector used was a low resolution ($320 \times 512, 30\ \mu\text{m}$ pixels) RCA CCD. The exposures were obtained through a Bessel R filter. Typical exposure times were of 2 minutes. The diameters of stellar images on these exposures allowed the resolution of faint features with sizes ≥ 2.5 kpc, for this nearby sample ($z \leq 0.13$) of objects.

A clear result from the NTT images is that none of the sample galaxies show either the spiral or the elliptical shapes that are characteristic of isolated galaxies. On the contrary, the NTT images reveal a wide variety of morphologies that can be interpreted as resulting from gravity in strongly interacting merger systems (e.g. Fig. 1). Tails, bridges and/or double nuclei are apparent in all galaxies $cz \leq 25,000\ \text{km s}^{-1}$ (e.g. Fig. 2). However, in the images of galaxies at higher redshifts, the faint extended features that are characteristic of tidal interactions are less ostensible, and become increasingly blurred with increasing distance.

From the detailed optical inspection of the 16 nearest ultraluminous infrared sources made with the NTT it is concluded that ultraluminous infrared galaxies are colliding galaxies that have profoundly penetrated each other. In fact, we find a critical separation of

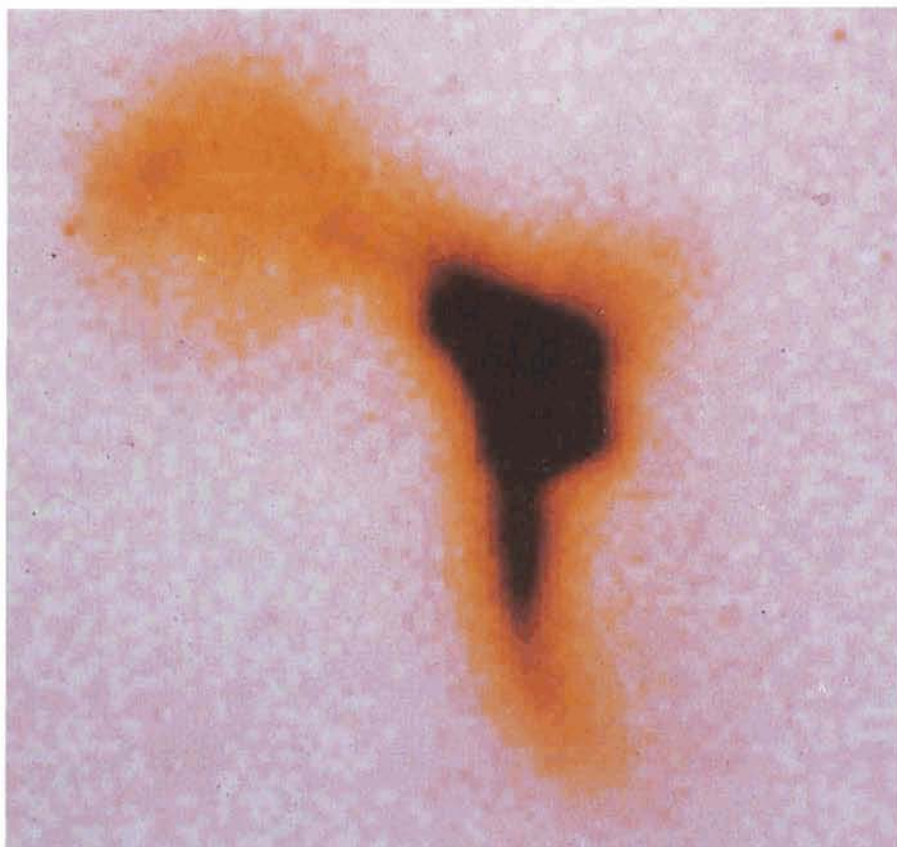


Figure 1: R band CCD image of the "South America" galaxy obtained with the NTT. This galaxy is receding from the Sun at $23,200\ \text{km s}^{-1}$ and radiates 10^{12} solar luminosities in the far-infrared.

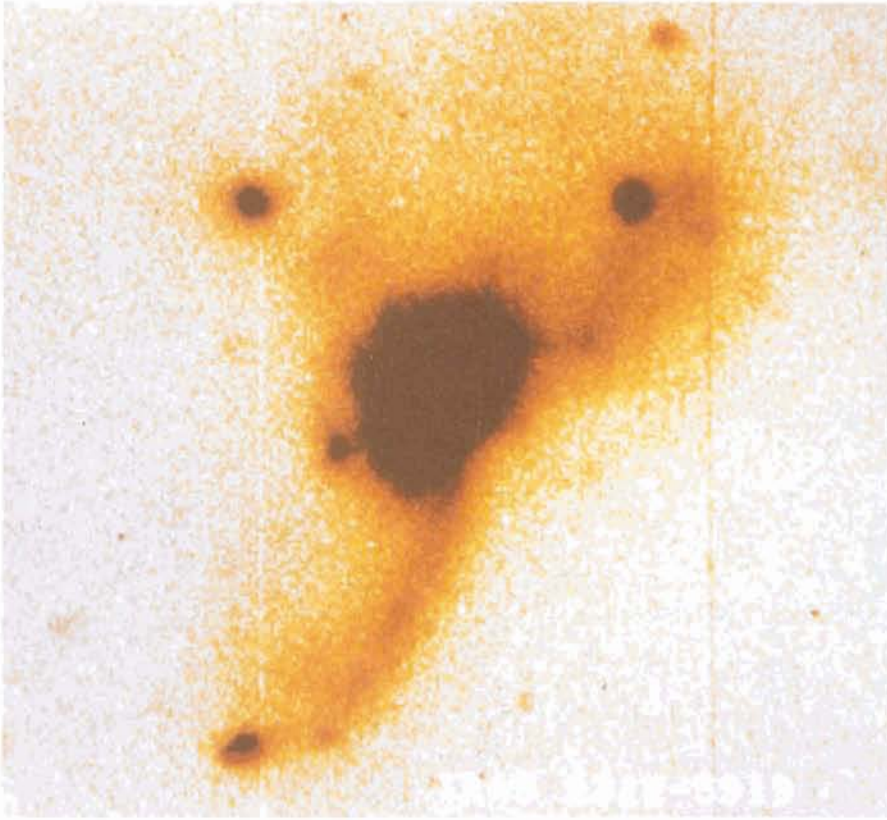


Figure 2: R band CCD image of the galaxy IRAS 23128-5919 obtained with the NTT. Computer simulations show that the elongated features emanating from the central object are the result of tidal interactions between merging disk galaxies. At the distance of IRAS 23128-5919, the condensations seen at the end of the tails would have the luminosities of star forming dwarf galaxies.

about 10 kpc between the nuclei of the colliding galaxies (e.g. Fig. 3). In other words, advanced merging seems to be a necessary condition for the greatly enhanced infrared luminosity.

SEST Observations

Since cold interstellar gas is the fuel for intense massive star formation, studies of the molecular gas in IR luminous galaxies are important for our understanding of the ultimate source of the energy radiated by these systems. The Swedish programme committee allocated the observing time needed to carry out a survey of the CO(1→0) emission from an IRAS flux limited sample of 33 galaxies with $L_{\text{IR}} \geq 10^{11} L_{\odot}$. CO(1→0) emission was detected from most of the galaxies of this sample up to a redshift of 0.1^{[6],[7]}.

From the SEST observations it was found that IR luminous galaxies are extremely abundant in turbulent CO. The emission profiles show velocity widths of up to 1000 km s⁻¹ (e.g. Fig. 4). Using a galactic CO→H₂ conversion factor one derives total masses of H₂ in the range of 6-60 10⁹ M_⊙, namely 2-20 times the mass of molecular gas in the Milky Way. The infrared luminosities per nucleon of

molecular gas, $L_{\text{IR}}/M(\text{H}_2)$, are in the range of 10-80 L_⊙/M_⊙. This is 5-40 times the global value of this ratio in the Galaxy averaged over the whole disk. This ratio is also larger than the average ratio found in starburst galaxies like M82. From the NTT and SEST observations it is then concluded that luminous infrared galaxies represent colliding, and in the most extreme cases, mergers of giant gas-rich galaxies.

In deriving H₂ masses from the ¹²CO(1→0) emission one should keep in mind that there may be systematic biases that depend on the physical properties of the molecular gas, such as the mean temperature, density, and metallicity. To study the physical properties of the molecular gas in luminous infrared galaxies, CO(2→1) and ¹³CO observations of the five brighter galaxies were carried out. The analysis of these observations will provide an important test of the use of the galactic ¹²CO→H₂ conversion factor in this type of galaxies.

Infrared Observations

One of the most relevant questions that remain open about these intriguing systems is if in addition to bursts of

massive star formation, compact non-thermal sources (AGN) are really needed to produce the extraordinary infrared luminosities above 10¹² L_⊙. Because of heavy optical obscuration along the line of sight to the central regions, infrared imaging is one observational approach to this question.

Observations with IRAC in the J(1.25 μm), H (1.65 μm), K (2.2 μm), and L(3.6 μm) will be conducted in the near future. Imaging in the N(10 μm) band is also planned with the TIMMI camera being constructed at CEN-Saclay under contract with ESO. These infrared observations will substantially improve our knowledge of the central morphology of these galaxies. Through the large amounts of obscuring dust they may be able to reveal the presence of multiple nuclei. Furthermore, the infrared colours will provide essential information to discriminate between different components of the central energy source, namely, starlight from red supergiants formed during super-starbursts, thermal emission from hot dust, and possible emission from an accretion disk surrounding an AGN. By comparing the ratio of the 10 μm to thermal radio emission found in the central regions of ultraluminous infrared galaxies, with the ratio found in galactic HII regions we will test the controversy "Starburst-AGN's".

Optical Spectroscopy

Low and high dispersion optical spectroscopy of the 20 most luminous objects at $z \leq 0.13$ was carried out with the 4-m Tololo telescope^[8]. Na D absorption lines and strong Balmer decrements are common features in the spectra of the nuclei. Despite the strong absorption, it is found that about 50% of the nuclei are Seyfert 2's, the other 50% liners or starbursts. The [OIII] emission lines show asymmetric shapes with extended blue wings, that may result from an attenuation of the emission from the far side of outwardly moving line-emitting gas mixed with dust.

An interesting possibility is that merging disk galaxies may not only trigger nuclear activity, but also eject dwarf galaxies into intergalactic space. We became interested in this idea after a close inspection of the NTT images of these galaxies. Patches of luminous material usually appear at the tips of the tidal tails (e.g. Fig. 2). Another specially interesting feature is a blue knot found in the Superantennae^[9] at a projected distance of 200 kpc from the merging nuclei. If these objects are actually associated to the merging disks, their luminosities are comparable to star forming dwarf galaxies.

At present we do not know why bursts

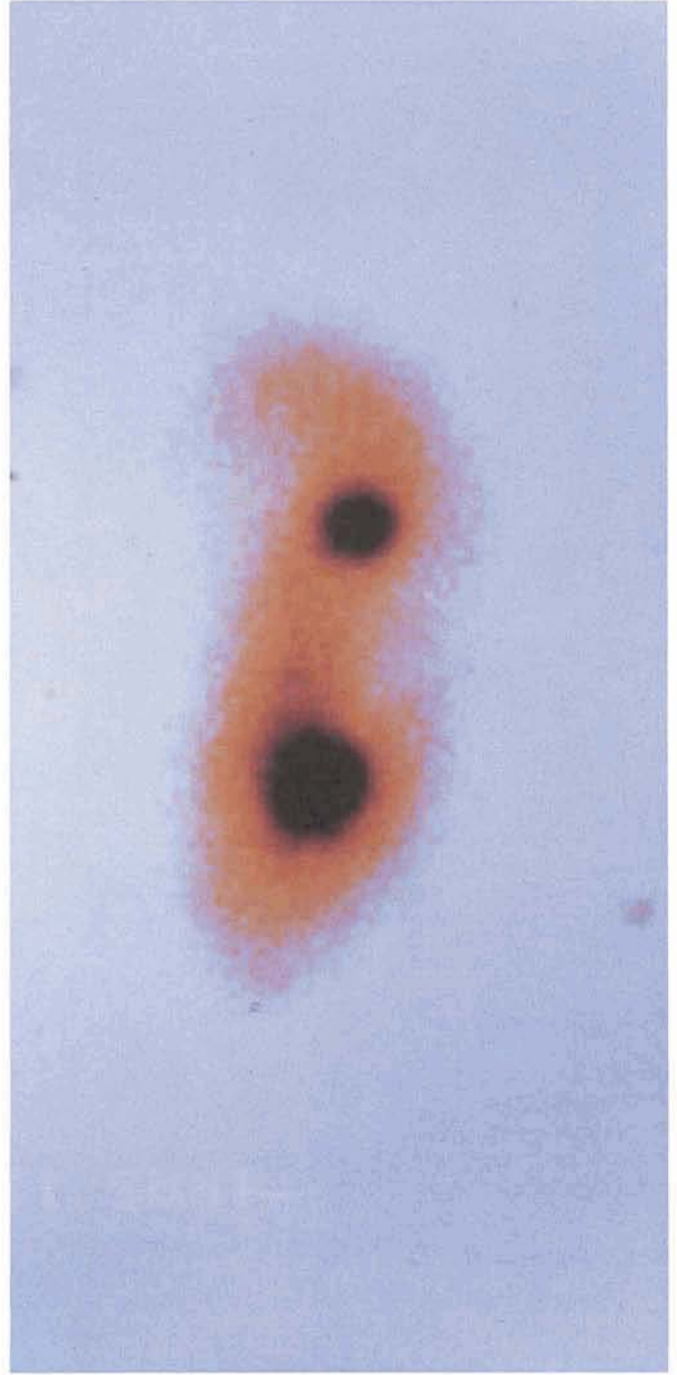
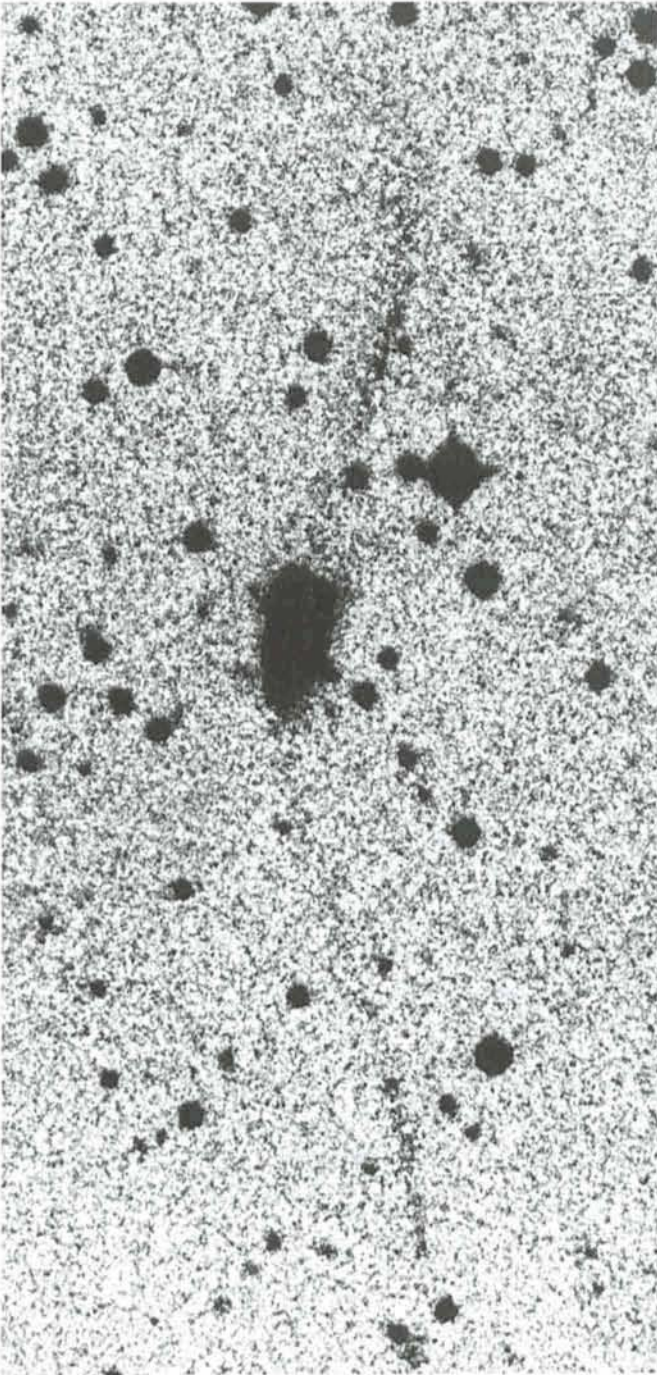


Figure 3: "The Superantennae", a remarkable galaxy at a distance of 250 Mpc^[9]. The colossal tails seen in the black-and-white reproduction of an ESO survey plate stretch to an unprecedented total extent of 350 kpc. The false-colour CCD image obtained with the NTT reveals inside the central body from which emerge the gigantic tails, two galaxy nuclei separated by only 10 kpc.

of star formation should occur at the ends of tidal tails. Furthermore, it is not clear how massive stars could be formed in intergalactic space out of the scattered debris of galaxy-galaxy collisions. We have proposed to carry out spectroscopy of these condensations with EFOSC on the 3.6-m to: (1) confirm their physical association to the merging disks, (2) determine the chemical composition of the HII regions in the tidal tails, and (3) probe a mechanism that returns metal-enriched gas into intergalactic space.

The IRAS view of the sky led to the discovery of a few tens of ultraluminous infrared galaxies in the Local Universe. Since in an expanding Universe, galaxy-galaxy collisions must have been more frequent in the past, it is likely that the several hundred times more sensitive Infrared Space Observatory (ISO), a European space mission to be launched in the year 1993, will reveal a large population of this type of objects in earlier epochs. To look back into the history of the Universe, and to inspect in detail the directions signalled by ISO, we will

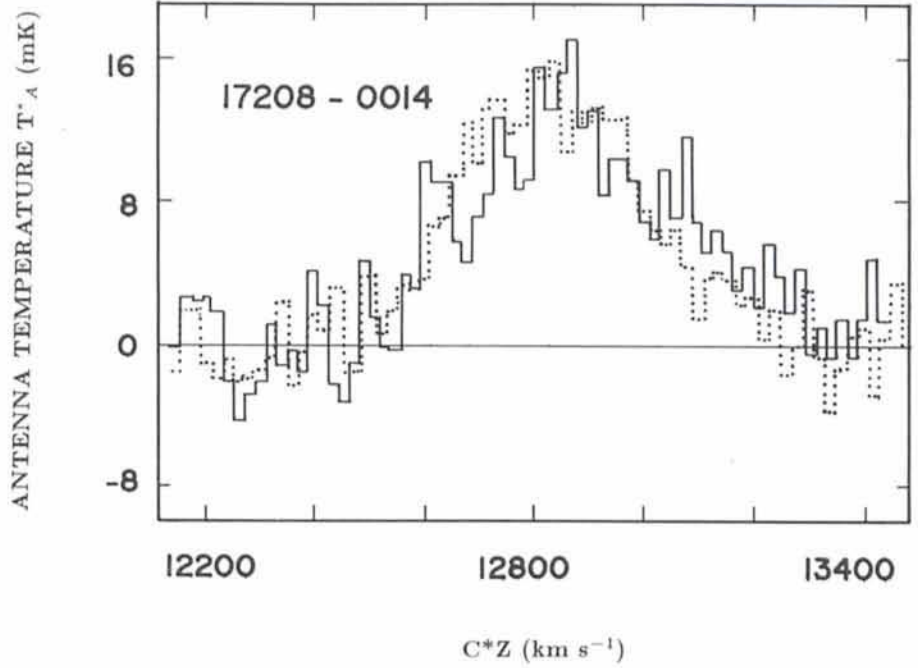
need terrestrial telescopes more powerful than the NTT, telescopes like the 16-m Very Large Telescope to be installed in Chile by ESO.

References

- [1] Soifer, B.T., Sanders, D.B., Madore, B.F., Neugebauer, G., Danielson, G.E., Elias, J.H., Lonsdale, C.J., Rice, W.L. 1987, *Astrophys. J.* **320**, 238.
- [2] Sanders, D.B. and Mirabel, I.F. 1991, in preparation.
- [3] Sanders, D.B., Soifer, B.T., Elias, J.H., Madore, B.F., Matthews, K., Neugebauer,

- G., Scoville, N.Z. 1988 *Astrophys. J.* **325**, 74.
- [4] Lawrence, A., Rowan-Robinson, M., Leech, K., Jones, D.H.P., Wall, J.V., 1989, *Mon. Not. Roy. Astr. Soc.* **240**, 329.
- [5] Melnick, J. and Mirabel, I.F. 1990 *Astron. Astrophys.* **231**, L19.
- [6] Mirabel, I.F., Booth, R.S., Garay, G., Johansson, L.E.B., Sanders, D.B. 1988, *Astron. Astrophys.* **206**, L20.
- [7] Mirabel, I.F., Booth, R.S., Garay, G., Johansson, L.E.B., Sanders, D.B. 1990, *Astron. Astrophys.* **236**, 327.
- [8] Maza, J. and Mirabel, I.F. 1991, in preparation.
- [9] Mirabel, I.F., Lutz, D., Maza, J. 1991, *Astron. Astrophys.* in press.

Figure 4: CO(1→0) emission profile of an ultraluminous infrared galaxy as observed with SEST (solid line) and the NRAO 12-m telescope (dotted line). This type of observation shows that luminous infrared galaxies are extremely rich in interstellar molecular gas.



Blue Galaxies in the Field of the Quasar PKS0812+02

E. GIRAUD, ESO

1. Introduction

Some galaxy clusters at $z=0.3-0.4$ have a higher frequency of galaxies with signs of recent star formation or nuclear activity than their nearby counterparts. The most luminous red galaxies in these clusters, however, do not show any evidence of evolution. At higher redshift ($z=0.7$) there seems to be a significant variation in the 4000Å break amplitude of the reddest galaxies (Dressler, 1987; see also Giraud, 1990), suggesting that evolution of the most passive galaxies has also been detected.

Low-redshift quasars ($z \leq 0.4$) are not found in very rich clusters of galaxies. Nevertheless they appear to be located in regions of higher-than-average galaxy density (Yee and Green, 1984). The environment of quasars at $z \sim 0.6$ is sometimes radically different. Some of them are found in environments as rich as those of Abell class 1 clusters (Yee and Green, 1987). While at higher redshift field contamination is necessarily large, Tyson (1986) and Hitzen, Romanishin and Valdes (1991) have also reported an apparent excess of galaxies near quasar at $0.9 \leq z \leq 1.5$.

These sets of observations indicate that there has been a rapid evolution of clusters in the range $z=0.2$ to 0.7 .

The nature of the population of clusters containing quasars is not well known. Results on two of these have

shown that they have a large blue population (Yee, 1988). In fact, the cluster which is apparently associated with PKS0812+02 at $z=0.403$ (Fig. 1) has a fraction of blue objects larger than any of the ten clusters at $z=0.3$ observed so far in the GC3 programme. According to Yee, this structure is compact and centrally concentrated and has a richness between that of class 0 and 1.

Observing the population in the field of PKS0812+02 is important for the following reasons:

(a) the cluster membership has to be carefully checked since a quasar in a cluster is a rare event, and because the population in this probable cluster appears to be photometrically different;

(b) its redshift is in the range where there seems to be a dramatic evolution of clusters.

Obtaining spectra of blue galaxies is important for understanding the nature of this intriguing population.

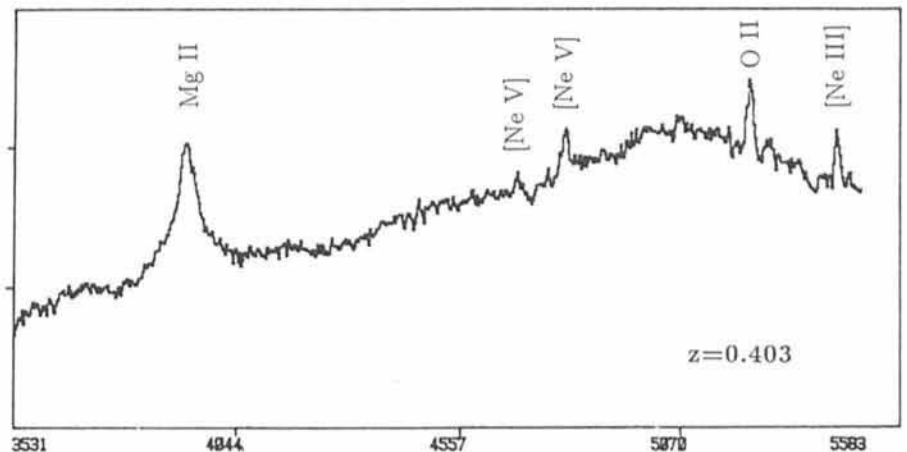


Figure 1: A blue spectrum of PKS0812+02 obtained with the NTT and EFOSC2 at a resolution of 2Å per pixel (Grism No. 3). The observation was done to check the feasibility of blue spectroscopy with a TH CCD (January 30, 1990; exp.:1800 s).

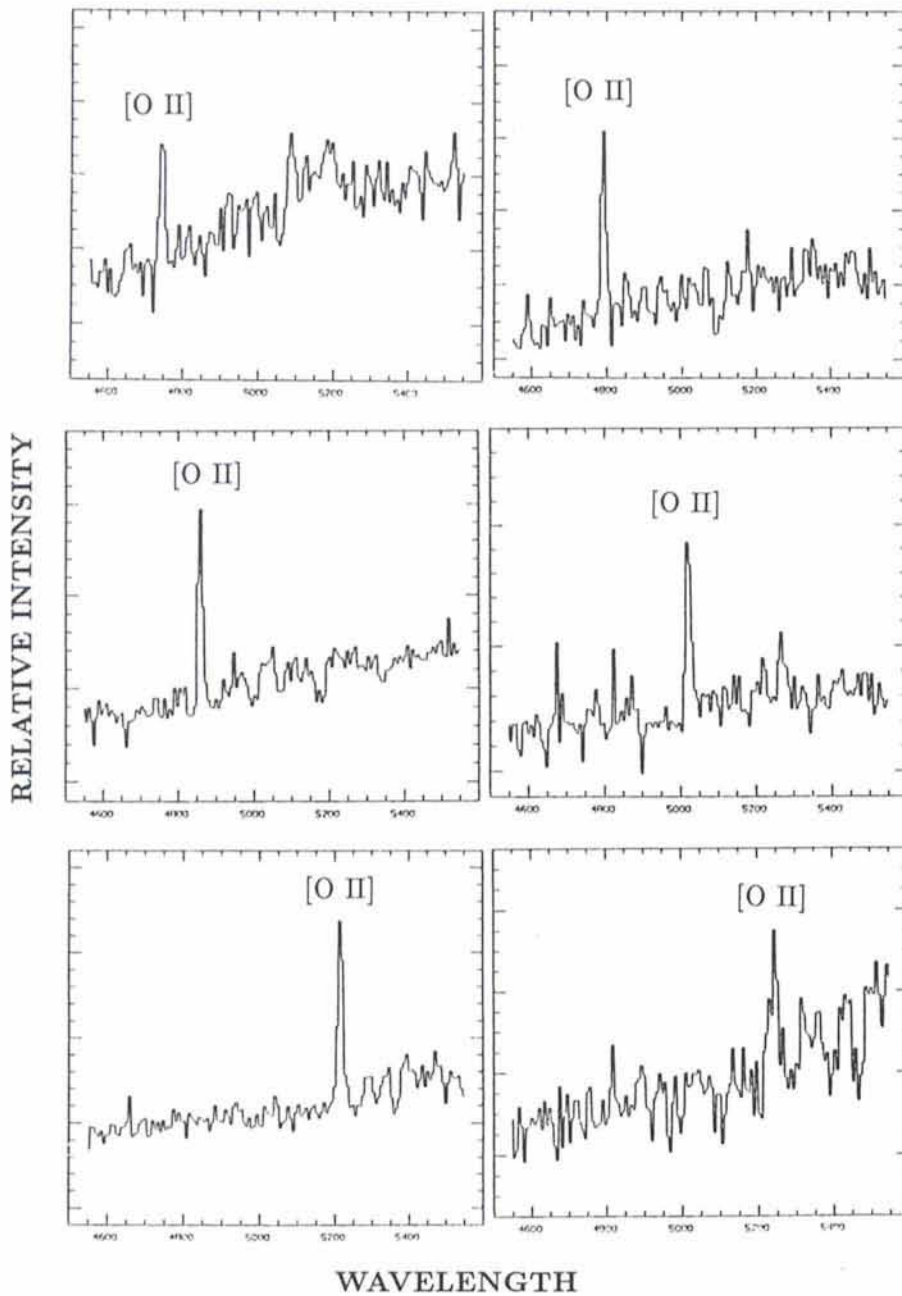


Figure 2: Spectra in the region of the [O II] λ 3727 Å emission line of 6 blue galaxies in the field of PKS0812+02. Redshifts range between $0.273 \leq z \leq 0.406$.

TABLE 1: Data for galaxies in the field of PKS0812+02

Ident.	V	B-V	z	EW(Å)
(1)	(2)	(3)	(4)	(5)
PKS	17.10*	0.18*	0.403	**
No.1	20.7	1.35	0.305	-
No.2	22.2	1.05	0.285	50
No.3	21.6	1.15	0.347	40
No.4	21.3	0.95	0.303	30
No.5	21.2	1.35	0.307	-
No.6	21.0	1.05	0.399	28
No.7	21.1	1.45	0.325	-
No.8	21.2	1.15	0.406	15
No.9	21.2	1.00	0.273	12

Notes: * from Véron's catalogue (1989)
 ** not measured

2. Blue Galaxies in the PKS0812+02 Field

The spectroscopic observations were made at La Silla with EFOSC mounted at the 3.6-m telescope. One multislit exposure (7200 s) was obtained through cirrus on December 18, 1990, and repeated (3600 s) the next night. Six blue galaxies with V magnitudes between $21.0 \leq V \leq 22.2$ and three red galaxies have been selected. All blue galaxies are

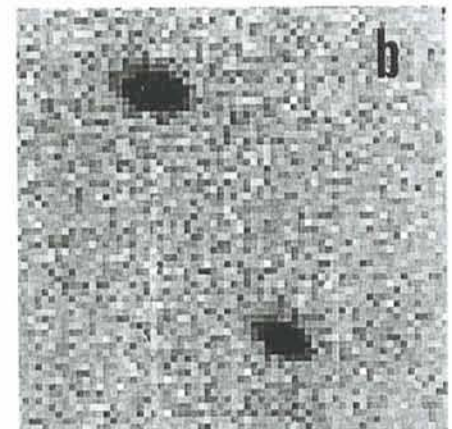
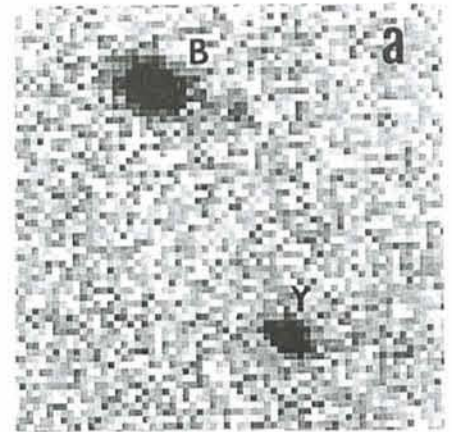


Figure 3: (a) A V-band image of an emission-line galaxy at $z=0.2$ (B) and of a yellow galaxy at $z=0.3$ (Y) obtained with EFOSC2 at the NTT (seeing 0".81), (b) Same as (a) but in the I-band (seeing 0".85), (c) the ratio of the V/I images showing that the region close to the nucleus of the blue galaxy is very blue. The objects are in the field of CI0500-24.

found to have a well visible [OII] λ 3727 Å emission line (Fig. 2) and the red objects have a rather large 4000 Å break amplitude.

The redshift of the galaxies show that we are not observing a cluster at the same redshift as the quasar. Seven objects out of nine could be in a cluster or a loose structure at $z \sim 0.3$ and two blue objects have the same redshift as the quasar (Table 1). Galaxy No. 6 is physically linked by an OII bridge to the quasar (Guzzo et al., 1988).

Perhaps the most surprising point is not that the cluster and the quasar are at different redshifts. The singularity is that this apparent cluster has such a peculiar population. Firstly it has a large blue excess, secondly it does not contain a core of very bright elliptical galaxies, thirdly the velocity spread is higher than expected. If giant elliptical galaxies were born in high density peaks of the initial density distribution, their absence suggests that there is not here a strong gravitational potential. There are indeed 10 red galaxies in the range $20.7 \leq V \leq 22$, implying the presence of a cluster. But the

velocity range of the blue galaxies and the apparent compactness of the structure also suggests that we are observing a filament in the line-of-sight. Understanding the geometry of this structure would require more spectroscopic work.

The measurements of the [OII] λ 3727 Å equivalent width $E(W)$ show that four of the blue objects have $E(W) > 25 \text{ \AA}$ indicating that they are "bursting" objects or have nuclear activity. The absolute magnitudes of these galaxies are similar to those of the 6 "bursting" objects in CI0500-24. But in that case the redshift range $0.314 \leq z \leq 0.333$ is compatible with that of a rich cluster at $z = 0.32$. Possible explanations on the nature of these objects include galaxy interactions, environment dependent bursting, nuclear processes. Good spatial resolution imaging can tell us whether the star formation is across the entire disk, nuclear, associated with companions.

An example of an emission-line galaxy at $z = 0.2$, observed with EFOSC2 at the NTT (March 1990), is shown in Figure 3. Also shown is a red galaxy at

$z = 0.3$. The V image (Fig. 2a, seeing 0".81) is slightly more extended than the I band image (Fig. 2b, seeing 0".85) indicating that the star-forming region is larger than the old component. A grey scale of the V-I colour (Fig. 2c) shows that the bluest part is in the central region implying that activity close to the nucleus plays a role in this object.

References

- A. Dressler, 1987, in *Nearly Normal Galaxies* ed. S. Faber, Springer, p. 276.
- E. Giraud, 1990, in *The Messenger* No. 62, p. 45.
- L. Guzzo, J. Danziger, S. Cristiani, P. Shaver, 1988, in IAU Symposium No. 130 *Large Scale Structures of the Universe* p. 573.
- P. Hitzten, W. Romanishin, and F. Valdes, 1991, *Ap. J.*, **336**, 7.
- J. Tyson, 1986, *A. J.*, **92**, 691.
- M.-P. Véron-Cetty and P. Véron, 1989, *A Catalogue of Quasars and Active Nuclei (4th Edition)*, ESO Scientific Report No. 7.
- H. Yee, and R. Green, 1984, *Ap. J.*, **280**, 79.
- H. Yee, and R. Green, 1987, *Ap. J.*, **319**, 28.
- H. Yee, 1988, in *High Redshift and Primeval Galaxies*, eds. Bergeron et al., Frontières, p. 257.

Artificial Intelligence for Astronomy

ESO course held in 1990

H.-M. ADORF, ST-ECF/ESO

Introduction

To many people "Artificial Intelligence" is as fascinating as astronomy, to some it is a mystery and to some simply an annoyance. By constructing appropriate computer software, researchers in artificial intelligence laboratories around the world attempt to solve a variety of tasks generally considered to require some form and degree of intelligence. Among these tasks we find natural (written) language processing, speech processing, vision, symbolic computation (as opposed to numeric computation), various forms of formal reasoning such as theorem proving and uncertainty reasoning, learning, game playing and so on. A number of interesting results have been obtained in the past, but progress has been generally slower than anticipated by early enthusiasts, a phenomenon not unknown in other scientific areas.

A formal definition of artificial intelligence cannot be provided, but for our purpose it suffices to say that "AI", as it

is often simply called, consists of the science of processing symbols by computers. What exactly is subsumed under the AI umbrella changes with time, a fact which has nicely been summarized in Tesler's law: "AI is whatever hasn't been done yet."

A Brief Excursion Into History

The roots of today's AI adventure can be traced back several centuries. The ancient Greeks already explored the rules governing our everyday logic. In the 17th century Blaise Pascal and Gottfried Wilhelm Leibniz dreamt of machines that could perform intellectual tasks. Boole and DeMorgan in the 19th century devised "the laws of thought" (i.e. propositional calculus) and developed rules for formal reasoning by manipulating symbols. Early in our century the eminent German mathematician David Hilbert posed several difficult problems, among them the question whether mathematics could eventually

be completely formalized using a logical calculus. This conjecture was refuted through subsequent important discoveries by the logicians Kurt Gödel (1931) and Alonzo Church (in the 1930s) and one of the legendary fathers of computers, Alan Turing (1930s-50s).

Gödel, for instance, found the then shocking "Incompleteness Theorem" (see e.g. Hofstadter, 1979) which essentially says that within every formal theory there will be some conjecture which is *undecidable*; using predicate logic, neither its truth nor its falsity can be proved within the set of notions and axioms used for their formulation. This discovery ended speculations about the possibility of doing mathematics solely by mechanical theorem provers.

Turing made a number of important contributions to the general field of computing. In 1936, before the invention of 'real' computers, he posed the *halting problem*: "Is it possible to (mechanically) prove for every computer programme whether it will eventually stop?" His an-

swer was “no”, i.e. there are “undecidable” computer programmes, a result closely related to Gödel’s incompleteness theorem. During World War II Turing participated in the very successful British endeavour of breaking the code of the German Enigma machine by developing and using the first real computers. Turing, a broad-minded mathematician, was the first to programme computers to play chess. In 1950, he attempted to define artificial intelligence by an operational test, which later became known as the “Turing test”.

It took eight further years until the American computer scientist John McCarthy called for the first conference solely devoted to the subject of artificial intelligence. (It was actually at this conference that the notion “artificial intelligence” was coined.) Around this time McCarthy had conceived the LISP computer language, which was particularly suited for symbol manipulation. One of the founding principles of LISP is “recursion”, a concept previously explored by Church in his so-called lambda calculus of recursive functions.

Another important result relevant to AI was discovered not too long ago by the computer scientist Steven Cook, who in 1971 showed that proving theorems using propositional logic is computationally intractable; in practice it takes exponential time (see e.g. Garey and Johnson, 1979). This result was generalized by others who showed many important practical problems (e.g. scheduling) to be as difficult as theorem proving.

This brief excursion into history provides us with two insights: Firstly, the AI-endeavour is deeply rooted in history and secondly, AI builds upon – and conversely is restricted by – many solid results obtained in neighbouring disciplines.

AI Methods and Techniques

Artificial intelligence researchers have always been very creative in inventing new tools and techniques in order to facilitate their work towards far reaching and ambitious goals. I will concentrate on three of these, namely languages, expert systems and artificial neural networks.

Languages. A basic tool for any computer scientist is an appropriate formal *language*. We already came across the LISP language, which actually is (after FORTRAN) the second-oldest high-level programming language still in use. However, contrary to other pioneering languages, LISP did not calcify, since it was not widely used and not standardized early on. Instead it underwent a continuous development by a breed of

young enthusiastic computer specialists. LISP, a language built around the concept of manipulating lists (of symbols), has remained amazingly modern. Its simple syntax – every statement is itself a list of an operator followed by zero or more operands – allowed the easy construction of language sensitive text editors and comprehensive programme development environments. Another feature which is a direct consequence of LISP’s syntactical simplicity

```
(defun factorial (n) ;define function
  (if (= n 0) ;if argument equals 0
      1 ;then return 1
      (* n (factorial (- n 1))))) ;else recurse with n-1
```

The programme works as follows: when called with some numerical argument *n*, the argument is first tested whether it is equal to zero (2nd line). If it is, the value 1 is returned (3rd line), since factorial of 0 is 1. Otherwise the factorial function is recursively called, but with an argument decremented by 1, and the result is multiplied by *n* (4th line).

```
(defun wondrous (n) ;define function
  (print n) ;output value of n
  (cond ((= n 1) t) ;if n = 1 then stop
        ((evenp n) (wondrous (/ n 2))) ;if n even, rec. with n/2
        (t (wondrous (+ 1 (* 3 n))))) ;else recurse with 3n+1
```

This programme prints a series of integers and, at least for all positive integers tested so far, eventually stops at 1. But, simple and short as the programme code looks, it is an open mathematical problem, whether for every positive integer *n* the programme will eventually halt.

Expert systems. One of the practical applications of AI-research in theorem proving and symbolic reasoning are *expert systems*. These programmes have been devised for a variety of different fields, the paramount example being medicine. Expert systems, in their traditional and widespread form, combine a body of knowledge, which is coded in form of facts and rules, with an “inference engine”, which allows the deduction of new facts from the known ones with the help of the rules. Some expert systems use exact logic, others use “fuzzy” inference indicating how to combine uncertain knowledge.

Quite enthusiastically greeted when they first arrived on the scene, expert systems are not the panacea which they have sometimes unduly been taken for. Particularly, they will not replace the “how to do” of procedural programming by the “what to do” of logic programming. Expert systems for sizeable real world problems often suffer from serious performance problems. But when applied to tasks which they are suited

is the ability of programmes to manipulate themselves. The language is also easily extensible and allows quick emulation of other special purpose computer languages.

For those who have never seen a statement in LISP (and may never have a chance to see one again), here is the complete recursive definition of a function which, when called, will calculate “*n* factorial”, i.e. the product of the first *n* integers:

Here is another interesting LISP programme, which calculates the “wondrous” function, defined as follows: Take an integer. If it is divisible by 2, divide; otherwise multiply by 3 and add 1. Continue with the division test. If you encounter the value 1, stop. The corresponding recursive LISP programme reads:

to, the reasoning techniques developed for expert systems are useful tools in the programmer’s toolbox.

Artificial neural networks. Another area of artificial intelligence, which has already flourished several times, is associated with the notion of neural networks. Networks of neurons, axons and dendrites govern the functioning of mammalian brains. They are held responsible for performing the complex cognitive tasks which allow animals to survive in a hostile environment. The amazing speed performance of neural networks is seen to be a consequence of the huge number of neurons and their high interconnectivity, allowing a form of massively parallel computing unchallenged even by modern serial supercomputers. Another advantage of natural neural networks, when compared with traditional computers, is their ability to learn and generalize. Computers almost invariably need to be programmed in every detail.

These are some of the incentives which have lead AI-researchers to distil the essentials out of natural neural networks and to construct *artificial neural networks*, usually comprised of software models. The concept of artificial “threshold logic neurons” was conceived as early as in 1943 by W. McCulloch and W. Pitts. The recent upsurge of interest was spurred by two influential papers

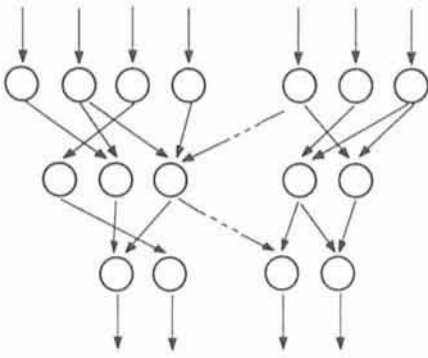


Figure 1: Schematic view of a feed-forward neural network with three neuron layers, a topology frequently used for pattern recognition and classification. Input signals stimulate the neurons of the top layers. Their output is channelled through the middle layer and the bottom layer neurons finally produce the recognition/classification results.

written by the physicist J.J. Hopfield in 1982 and 1984. Artificial neural networks are applied to a variety of tasks, among which we find adaptive control, image processing, natural language processing, scheduling, speech synthesis, and unsupervised and supervised classification (Fig. 1). For more details on the history and application of neural networks, consult the interesting book by Arbib (1987) and my own recent review (Adorf 1989).

Astronomical Applications of Artificial Intelligence

A few years ago, artificial intelligence entered astronomy. The prime account of current ideas and applications of AI in astronomy is the book *Knowledge-Based Systems in Astronomy*, initiated and edited by André Heck and Fionn Murtagh, to whom we all should be very grateful. As can be seen from the contributions to this book, AI has reached the fringes of astronomy, but barely the core.

Proposal processing and scheduling. The Hubble Space Telescope has served as a focal point for AI-oriented applications in the US and in Europe. A few years ago the Space Telescope-European Coordinating Facility launched its "Artificial Intelligence Pilot Project" with the aim of exploring AI opportunities and to apply these new software techniques to a few selected areas of interest.

At the Space Telescope Science Institute, Baltimore, the leading centre for the application of AI to astronomy, a number of successful AI-based computer programmes have been developed and are in operational use within the complex ground system of the Hubble Space Telescope. The TACOS natural language front end, for instance, provides easy access to the data base of proposals used by the HST time allocation

committee. The "same science" duplication checker effectively acts as a stopgap for similar proposals from different research groups. A cornerstone in the sequence of proposal processing operations (see Adorf 1990 and references therein) is the "transformation" expert system, which disassembles observing proposals into scheduling units and re-merges them from a pool into larger entities for subsequent placement onto the observational timeline.

The most prominent example of the set of STScI's proposal processing tools is certainly SPIKE, a programme system written by Mark Johnston and his group for long-term scheduling of HST-observations (Johnston, 1989, 1990; Miller and Johnston, 1991 and references therein). After the science verification phase, HST is supposed to deliver the large quantity of some 10,000 exposures per year, which are subject to a variety of (partially interacting) scientific, political, operational, spacecraft and environmental constraints. Placing these exposures onto an observational timeline is a complex task – insurmountable, if it were tried manually. SPIKE (Fig. 2) combines a novel uncertainty reasoning mechanism with a very fast neural network-inspired, stochastic scheduling algorithm (Johnston and Adorf, 1989; Adorf & Johnston, 1990) to achieve an unparalleled performance, even on ordinary serial computers. The

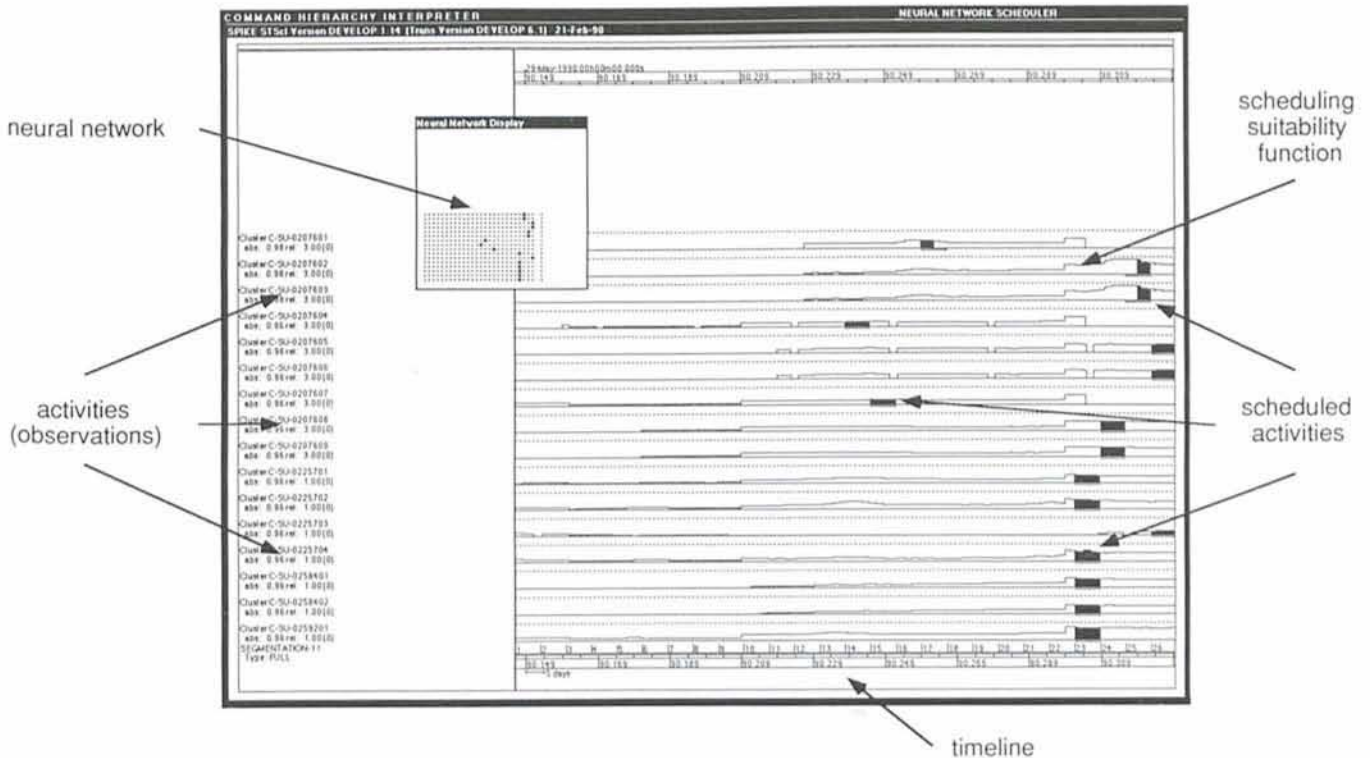


Figure 2: Example screen from the long-range scheduler SPIKE showing the scheduling of HST observations. A number of activities (along the y-axis of the large window) have to be scheduled within a six-month scheduling interval (along the x-axis). For each activity the scheduling suitability function represents scheduling opportunities as a function of time. The small window in the upper left shows an artificial neural network used for the computation of the displayed schedule.

SPIKE scheduler is not restricted to HST scheduling problems and has successfully been applied on a trial basis to schedule observations for the International Ultraviolet Explorer (IUE), the Extreme Ultraviolet Explorer (EUVE) and ESO's 3.6-m telescope.

Full-text retrieval. Retrieval of astronomical bibliographic full-text information is another area, for which the application of AI-techniques has been proposed originally for the machine-readable version of Astronomy & Astrophysics Abstracts (Adorf and Busch, 1988) and is now being realized within the American Astrophysical Data System (ADS), a distributed database system which incorporates all major astronomical space-borne databases.

Symbolic computation. Symbolic computations are required e.g. in the process of solving integrals or differential equations. For quite some time, there exist computer programmes which can assist in carrying out such tasks. In physics, these programmes are mainly being used for elementary particle or general relativity computations. One of these programmes, available at ESO, is Mathematica, a comprehensive system for doing mathematics. It allows one to easily solve algebraic equations, to multiply matrices, to integrate complex formulae, etc., all on the symbolic level. Results can be cast into FORTRAN-, C- or T_EX-form, or can be graphically represented. Arbitrary precision arithmetic can be used to solve problems, which can only be computed numerically. A convenient interface allows easy access to the functionality provided by this modern research tool. Mathematica has successfully been applied at ESO to optical design problems.

Classification. This seems to be a natural area for the application of artificial intelligence techniques to astronomy. Already in 1986 a rule-based classifier for the morphological classification of galaxies was devised by the French computer scientist Monique Thonnat (see Heck and Murtagh, 1989). Other classifiers have been designed for the classification of IUE low-dispersion spectra and of low-resolution spectra from the Infrared Astronomical Satellite (IRAS). Trainable neural networks offer some potential for difficult classification tasks such as the detection and discrimination of cosmic ray hits on images from solid-state detectors in space.

The Future

Artificial intelligence in astronomy has neither as bright a future as some see it, nor as dark a future as some others do. It is easy to imagine a number of areas, still outside the core of astronomy,

where AI-techniques may play a role in the future.

The increased complexity of computer systems will require better human-computer interfaces. The operation of ground-based observatories also seems to increase in complexity, and may reach a stage beyond the level which can quickly and reliably be handled by humans. Absentee and split-schedule observing modes will become more common. Coordinated multi-frequency observations, which require the synchronization of several ground-based and satellite observatories, could be facilitated by the help of sophisticated schedulers. Planned planetary missions, if ever financed, will require autonomous observing capabilities. Retrieval by content of data from large image databases, adaptive control of "flexible" telescope optics or the optimization of arrays of telescopes may be possible using neural networks (see the discussion after Merkle, 1988, and Angel et al., 1990). There are already approved plans to provide assistance in the reduction and analysis of astronomical data by a computerized expert system (Miller, 1990). All these areas may (and in the long run will) benefit in one way or other from methods and techniques developed in AI-research labs.

Conclusion

By considering a few examples we have seen that artificial intelligence techniques have already made an inroad into astronomy. The achievements described above have been established by few, dedicated people without monetary reasons as driving forces (as opposed to other areas such as geological oil exploration). It is fairly safe to expect more AI in astronomy in the future, related, of course, to the interest by the astronomical community and the amount of resources devoted to AI-research and astronomical application development.

References and Further Reading

- Adorf, H.-M., Busch, E.K.: 1988, "Intelligent Access to a Bibliographical Full Text Data Base", in: *Proc. ESO Conf. on "Astronomy from Large Databases: Scientific Objectives and Methodological Approaches"*, Garching, Oct. 1987, F. Murtagh and A. Heck (eds.), pp. 143–148.
- Adorf, H.-M., Johnston, M.D.: 1990, "A discrete stochastic 'neural network' algorithm for constraint satisfaction problems", in: *Proc. IEEE Intern. Joint Conf. Neural Networks (IJCNN 90)*, San Diego, 17–21 June 1990, Vol. III, pp. 917–924.
- Adorf, H.-M.: 1989, "Connectionism and Neural Networks", in: "Knowledge-Based Systems in Astronomy", *Lecture Notes in Physics* 329, A. Heck and F. Murtagh (eds.), Springer-Verlag Heidelberg, pp. 215–245.

Adorf, H.-M.: 1990, "The processing of HST observing proposals", *ST-ECF Newsletter* 13, 12–15.

Angel, J.R.P., Wizinowich, P., Lloyd-Hart, M., Sandler, D.: 1990, "Adaptive optics for array telescopes using neural-network techniques", *Nature* 348, 221–224.

Arbib, M.A.: 1987, *Brains, Machines, and Mathematics*, Springer-Verlag, New York.

Garey, M.R., Johnson, D.S.: 1979, *Computers and intractability – A Guide to the Theory of NP-Completeness*, W.H. Freeman and Co., New York.

Heck, A., Murtagh, F. (eds.): 1989, "Knowledge-Based Systems in Astronomy", *Lecture Notes in Physics* 329, Springer-Verlag Heidelberg.

Hofstadter, D.R.: 1979, "Gödel, Escher, Bach: An Eternal Golden Braid – A Metaphorical Fugue on Minds and Machines in the Spirit of Lewis Carroll", Vintage Books, New York.

Johnston, M.D., Adorf, H.-M.: 1989, "Learning in stochastic neural networks for constraint satisfaction problems", in *Proc. NASA Conf. on "Space Telemetry"*, Pasadena, 21 Jan.–2. Feb. 1989, G. Rodriguez and H. Seraji (eds.), JPL Publ. 87-7, Vol. II, 367–376.

Johnston, M.D.: 1989, "Knowledge Based Telescope Scheduling", in: "Knowledge-Based Systems in Astronomy", *Lecture Notes in Physics* 329, A. Heck and F. Murtagh (eds.), Springer-Verlag Heidelberg, pp. 33–49.

Johnston, M.D.: 1990, "SPIKE: AI Scheduling for NASA's Hubble Space Telescope", in *Proc. 6th IEEE Conference on "Artificial Intelligence Applications"* (CAIA), Santa Barbara, CA, 5–9 March 1990.

Merkle, F.: 1988, "Adaptive Optics Development at ESO", in *Proc. ESO Conf. on "Very Large Telescopes and their Instrumentation"*, Garching, 21–24 March 1988, M.-H. Ulrich (ed.), Vol. II, p. 639–656.

Miller, G., M.D. Johnston: 1991, "Long range science scheduling for the Hubble Space Telescope", in: *Proc. 1991 Goddard Conference on "Space Applications of Artificial Intelligence"*, (to appear).

Miller, G.: 1990, (priv. comm.).

Editorial Note

The present *Messenger* issue exceptionally contains 84 pages, due to a late, unexpected influx of articles, reflecting an ever-increasing level of astronomical activity in and around ESO. It is, however, our intention to revert to the normal size (60–68 pages). This may mean that we will in the future be unable to accept contributions which are submitted after the stipulated deadlines, i.e. January 20, April 20, July 20 and October 20, for the March, June, September and December issues, respectively.

Multi Object Spectroscopy with the ESO Multi Mode Instrument at the NTT

First successful test of the MOS mode of EMMI using a new plate punching unit operating under computer control inside the instrument

H. DEKKER, S. D'ODORICO, H. KOTZLOWSKI, J.-L. LIZON, A. LONGINOTTI, W. NEES, ESO and

V. DE LAPPARENT-GURRIET, Institut d'Astrophysique de Paris, CNRS, France

1. Low Dispersion Spectroscopy with EMMI

EMMI, the ESO Multi Mode Instrument recently installed at the 3.5-m NTT (D'Odorico, 1990, Dekker, D'Odorico and Melnick, 1990) is a dual-channel focal reducer/spectrograph designed for high efficiency observations and for a wide range of resolving powers. Figure 1 shows the instrument layout. Low dispersion spectroscopy ($R \leq 1600$ for a 1-arcsec slit) is possible in the red arm ($\lambda\lambda 4000-10000 \text{ \AA}$, upper right part of Figure 1) with a choice of 6 grisms which can be inserted in the parallel beam space of the focal reducer. In this observing mode, where EMMI operates like EFOSC1 and EFOSC2, the two focal reducer/low dispersion spectrographs mounted at the ESO 3.6-m and 2.2-m telescopes. The corrected field of view is 10×10 arcmin. The scale in the telescope and in the detector focal planes

are $186 \mu\text{m}$ and $43 \mu\text{m}$ per arcsecond respectively. At the time of this test a 1024×1024 , $19 \mu\text{m}$ square pixels THX 31156 CCD was used as a detector. This CCD is characterized by a peak quantum efficiency of 50% at 7000 \AA , very high cosmetic quality and a read-out noise of $4-5 e^-/\text{pixel}$. With this detector the field in imaging is 7.6×7.6 arcmin.

2. Multi Object Spectroscopy in EMMI

As in the EFOSC-type instruments, EMMI has an aperture wheel in the focal plane of the telescope where 4 long slits of different width are usually mounted and one position is left free for direct imaging. For MOS observations with EFOSC1 at the 3.6-m telescope, special aperture plates can be prepared from punching files derived from direct im-

ages of the target fields. The punching machine PUMA2 located in the telescope control room generates round holes with a minimum diameter of 2.1 arcsec, and these can be combined to make rectangular slitlets. The aperture plates are later mounted in the instrument and, after a proper alignment procedure, used for MOS observations.

When designing the MOS unit for EMMI (usually identified as *starplate unit*) we took into account the experience with EFOSC1 and tried to improve some aspects of the observing procedure. It was decided to install the plate punching on the instrument itself with the aim of simplifying the plate alignment procedure and to have a fully hands-off procedure for this observing mode. Secondly, a punching device of new design was conceived to improve the reliability and the quality of the slitlets in the aperture plates. A further ad-

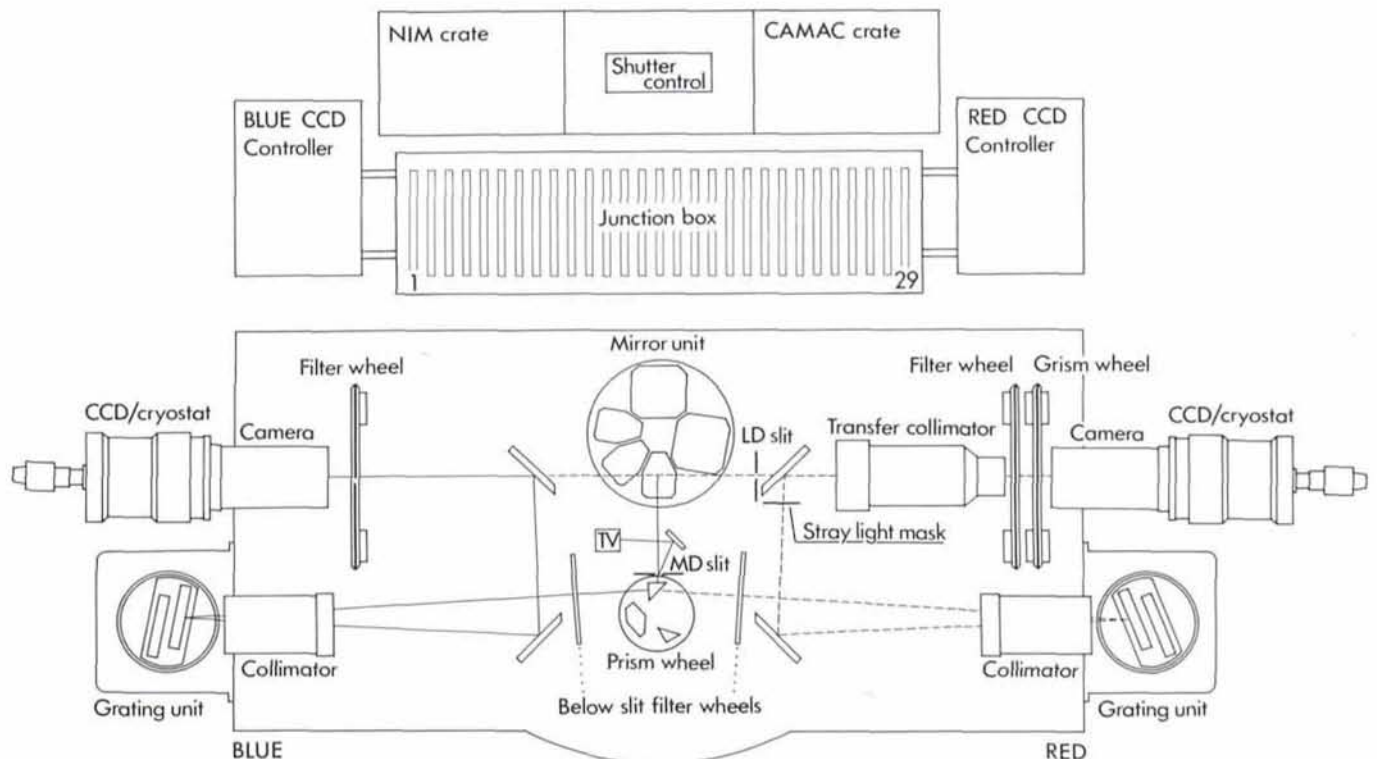


Figure 1: An overview of the main components of EMMI. Multiple Object Spectroscopy at low resolution is carried out as explained in the text by using MOS plates inserted in the aperture wheel of the focal reducer mode (identified as LD slit in the drawing). The punching of slitlets in the plates is carried out in EMMI itself by an ad-hoc designed "starplate unit".

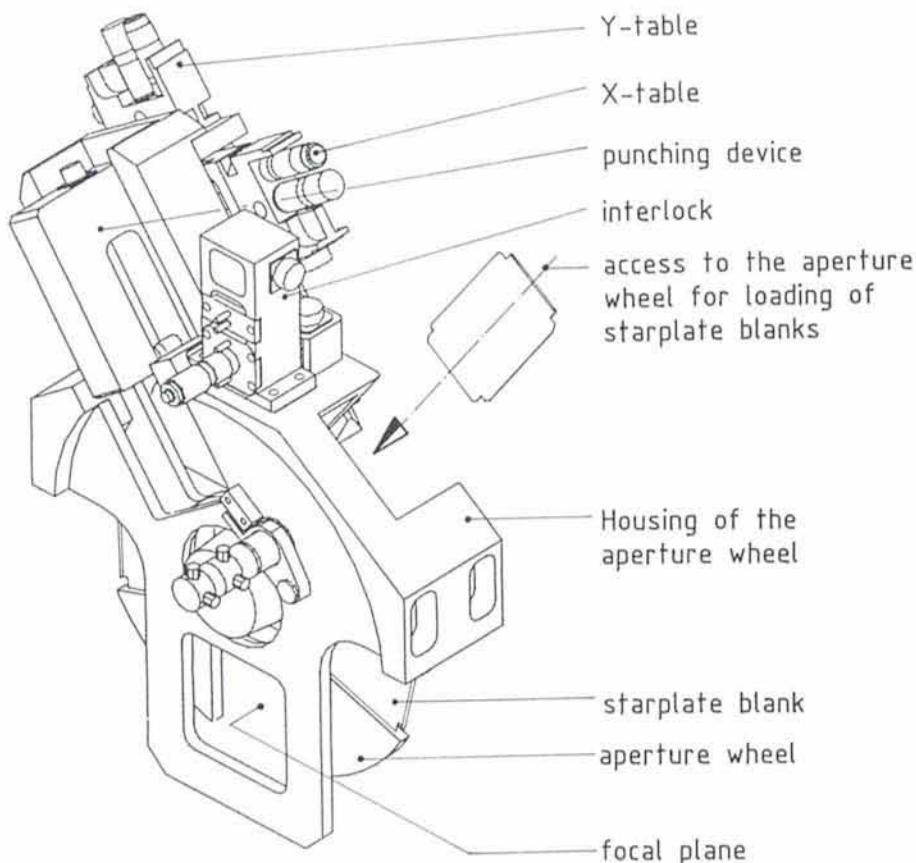


Figure 2: A CAD drawing of the starplate unit with identifications of the main components.

vantage of MOS in EMMI is the field of view which is 5×8 arcmin approximately, an area 3–4 times larger than in EFOSC1.

For the MOS work up to four of the long-slit plates in the aperture wheel can be replaced by starplate blanks of identical geometry. A punching device, mounted on a cross-table fixed on the EMMI structure, is then used to punch short slits in the blanks. The punching units are equipped with tools which determine the minimum slit width and length. While the slit length can be increased by multiple punching along the slit, the slit width can only be changed by replacement of the complete punching unit (equipped with tools of the desired slit width). Figure 2 is an isometric view of the starplate unit of EMMI showing the subunits: aperture wheel, interlock, x-table, y-table and punching device.

The *aperture wheel*, mounted in the focal plane of the low-resolution mode of EMMI, is driven by a DC-motor with tachogenerator and positioned by an incremental encoder like all servo-controlled units in EMMI. The selected plate is placed in the optical path of the instrument by the proper software instruction. For loading or removal of starplates the aperture wheel is easily accessed to form the EMMI service platform.

The *interlock* has a dual function. Mounted on the aperture wheel housing

it mechanically locks the aperture wheel during punching of the slits and prevents an inward motion of the punching device when the starplate is not in the

punching position. The positioning of the punching device across the slit (direction of the spectral dispersion) is provided by the *x-table*. The range of its movement is 56 mm which corresponds to a field width of 5 arcmin. The positioning accuracy is ± 8 microns or ± 0.04 arcsec. The limited space available for the starplate unit did not allow a clamping system for the x-table. Therefore, during punching, EMMI should not be rotated and the x-table should always be in the same orientation with respect to the gravity, preferably in the horizontal position with the punching device on top.

The movement of the punching device into the punching field of the starplate, positioning of the punch along the slits and elongation of the slits, is provided by the *y-table*. The movement range is 116 mm of which only 90 mm (8 arcmin) can be used for punching in EMMI.

The most complex part of the starplate unit is the *punching device*. It required some development effort and the application of new technologies. Figure 3 shows the punching device with tools in its final version. From outside it looks like a miniature sewing-machine. Inside its light-weight but stiff body are the punch-motor with control switch, the linear guide and support of the punch, a cross-table to support and adjust the die, and a clamping system to lock the device distortion-free and stable on the x-table. The punching tools are fabricated from

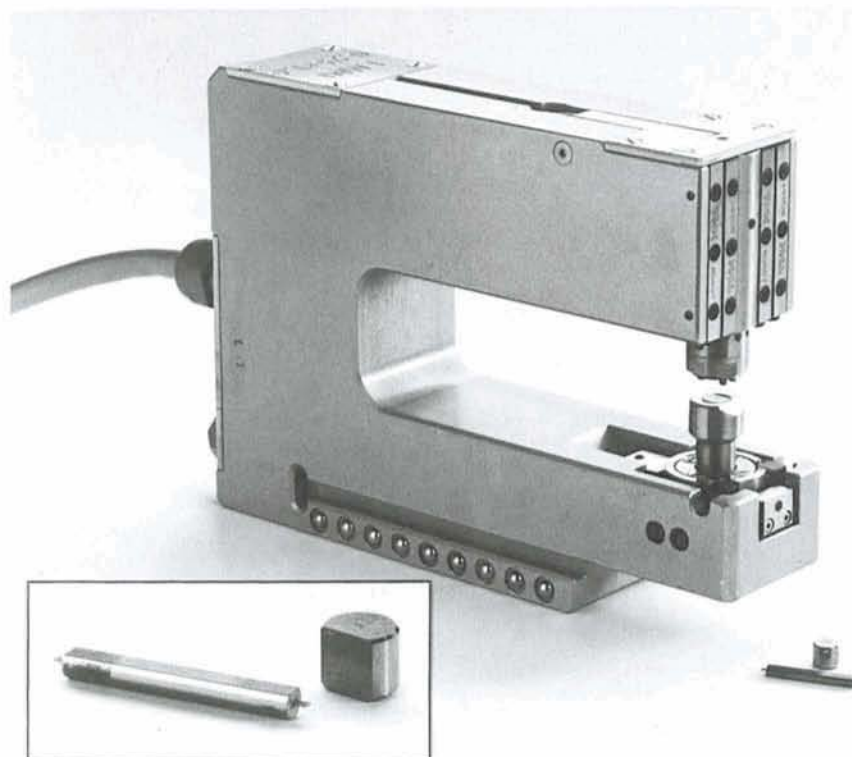


Figure 3: The plate punching device, with the insert showing a magnification of the punching tool. The dimensions of the device are $170 \times 120 \times 40$ mm, the weight is 1.6 kg.

carbide using the spark erosion technique. The chips produced during the punching are stored in a container below the die, sufficiently large for approximately 10,000 punches.

The starplates are consumables and designed therefore for cheap manufacture in small series. This is achieved by wire-cutting of approximately 50 plates at once. After the cutting, one side of the starplate is reinforced by a bend to achieve better flatness in the unsupported region when mounted in the aperture wheel. An anti-reflecting black painting of the starplate surface is used to avoid ghosts in the spectrum. Table 1 summarizes the characteristics of the MOS mode of EMMI.

3. First Astronomical Results

A first test of the MOS mode of EMMI and in particular of the operation of the starplate unit was carried out during the EMMI commissioning period in October. First we obtained one 1-minute direct image of a field from the Key Programme "A Redshift Survey of galaxies with $z \leq 0.6$ " (de Lapparent et al., 1989). The goal of this programme is to obtain a complete catalogue of 700 galaxies brighter than $R=20.5$ over 0.4 deg^2 near the south galactic pole for studying the large-scale structure at $z=0.3$. All galaxies in the catalogue will have BVR photometry and low-resolution spectroscopy for redshift measurements. The direct image in the red arm of EMMI did show several galaxies with angular sizes up to $\sim 6 \text{ arcsec}$ and R magnitudes in the range 17–21. Eight galaxies were selected for the preparation of the punching file, using an improved version of the software which is used for the same purpose in EFOSC1. The actual punching in the starplate unit took about 2 minutes, the dimension of the tool used corresponded to $1.3 \times 8 \text{ arcsec}$. The plate was then moved to the optical path of the instrument and used in combination with the EMMI grism No. 3 for two 1-hour exposures on the eight galaxies. Figure 4 shows one of these exposures. No alignment of the galaxies with the slitlets was needed for the first exposure. A minimal telescope offset ($\leq 1 \text{ arcsec}$) was needed for optimal centring before the second exposure.

A preliminary reduction of these data has been carried out to estimate the capability of this observing mode. After bias subtraction, the two 1-hour MOS exposures were flatfielded with a halogen lamp used as source through the grism and aperture plate. This procedure is necessary to remove non-uniformities up to 10% of the transmission along the slitlets. This effect has been traced to remnants of the black paint

TABLE 1: MOS in EMMI

Punching area on the starplates:	56 × 90 mm (5 × 8 arcmin)
Minimum slit width:	150 microns (0.8 arcsec)
Minimum slit length:	1.2 mm (6.5 arcsec)
Maximum number of slits/starplate:	52
Flatness of punched starplates:	< 0.3 mm peak-to-peak
Punching time of 40 slits:	approx. 5 minutes
Life-time of the punching tools:	> 10.000 punches
Thickness of the starplates:	120 to 200 microns, depending on the desired slit-width
Material of the starplates:	copper alloy with 2% beryllium

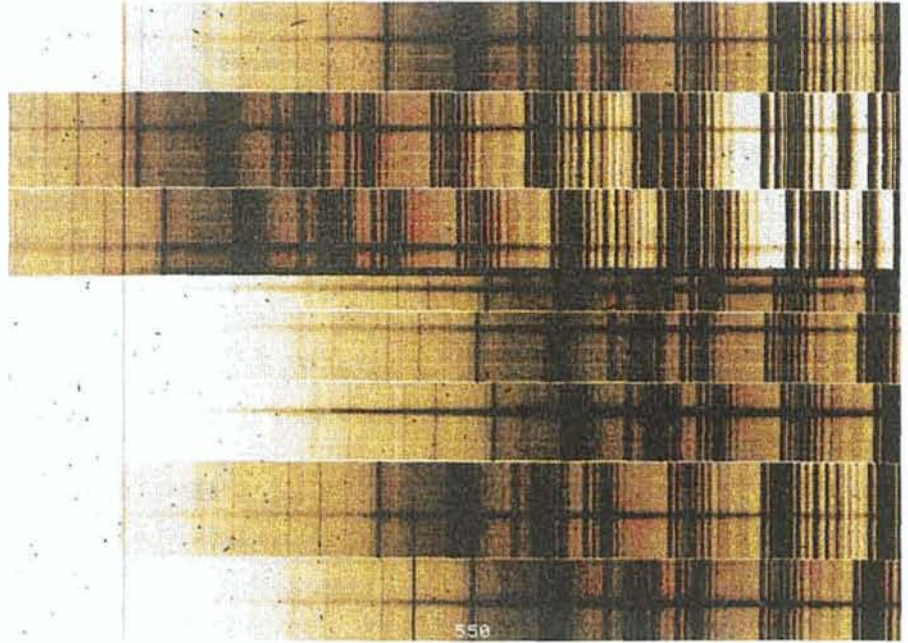


Figure 4: A one-hour MOS exposure on a galaxy field obtained with EMMI at a resolution $\sim 10 \text{ \AA}$. The eight targets are galaxies with 2–6 arcsec in size and integral R magnitudes between 17.5 and 19.5.

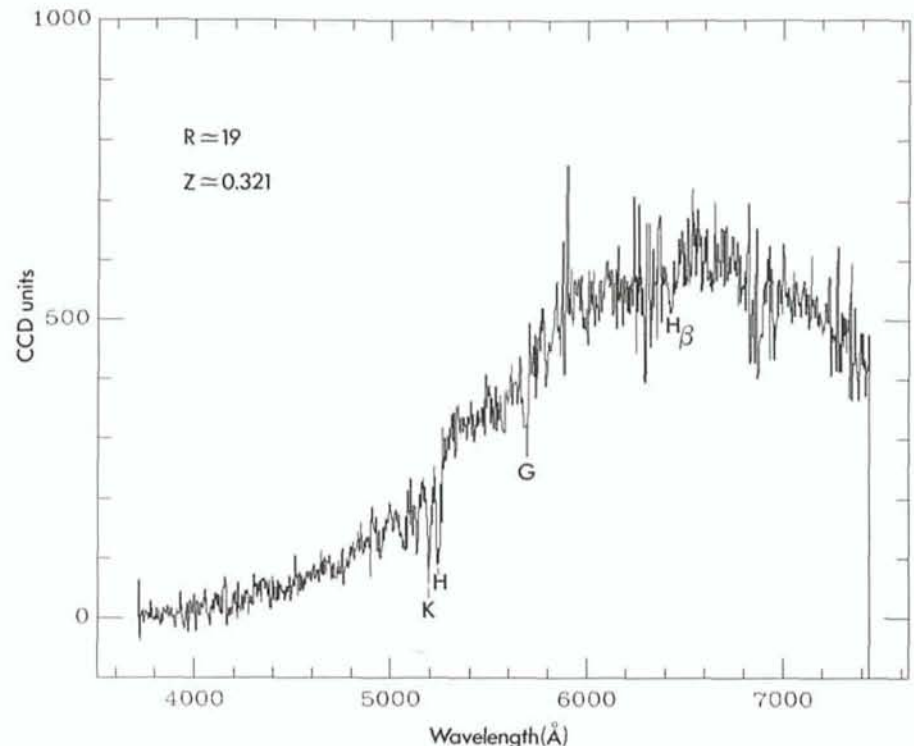


Figure 5: The sum of two one-hour reduced spectra of a galaxy of $R=19$ (the first spectrum from the bottom in Figure 4).

used on the plates in the punched slits and it should hopefully be eliminated in the future by the use of a different paint.

Removal of radiation events on the CCD (of the order of one per row) was done by a two-step filtering procedure which does minimal damage to the data. First, all pixels exceeding by more than a factor of 2 the value of the pixel at the same position on the other 1-hour exposure were replaced by the pixel value from the other exposure. Second, a median filtering over a few pixels perpendicular to the dispersion direction with a high threshold for data modification was applied and further removes all but a couple of events. This second filtering was necessary for removing the cosmic rays affecting identical pixels in both exposures.

Each object spectrum was finally extracted using all rows within the half width of the object profile along the slit, and was calibrated in wavelength using He and Ar calibration exposures. The resulting dispersion is $\sim 3.7 \text{ \AA}/\text{pixel}$, the resolution $\sim 10 \text{ \AA}$. As much sky as available in each slit was independently

wavelength calibrated and then removed from the corresponding object spectrum. A long slit calibration procedure with a signal-weighted extraction procedure will clearly yield a cleaner sky subtraction, a crucial problem for faint and extended objects, and a better S/N ratio in the extracted data but it has not yet been applied to this set of data. Figure 5 shows the sum of the two 1-hour spectra for a galaxy with $R \sim 19$. The H and K lines, the G band and the $H\beta$ absorption line are clearly identifiable and yield $z = 0.321$. The S/N ratio of the spectrum at 5500 \AA is ~ 15 .

The eight galaxies observed in this first MOS field with EMMI have R magnitudes ranging from ~ 18 to ~ 20 . The derived redshifts range from $z = 0.120$ to $z = 0.431$. The sum of the two 1-hour exposures is sufficient in all objects for rough ($\Delta z \sim 0.001$) but reliable redshift measurement using the positions of the H and K lines or the [OII] and other emission lines. Cross-correlation analyses with a reference spectrum will yield smaller uncertainties in the redshift measurement.

In conclusion, the first tests of the MOS mode of EMMI have proven that the multi-slitlet plates can be prepared at the instrument with the required quality and immediately used for astronomical observations without manual intervention.

The results from the quick reduction of the data from the October run can be used for an estimate of the capability of the system. Assuming an optimal extraction procedure of the spectra, it should be possible with EMMI to measure the redshift of as many as 15 objects down to an R magnitude of 21–22 in a field of 5×8 arcmin with three 1-hour exposures.

The MOS mode of EMMI will be released to visiting astronomers in the course of Period 47 (April–September 1991).

4. References

- De Lapparent V., Mazure A., Mathez G., and Mellier Y. 1989, *The Messenger*, **55**, 5.
Dekker H., D'Odorico S., and Melnick J., 1991, *ESO Operating Manual No. 14*.
D'Odorico S., 1990, *The Messenger*, **61**, 44.

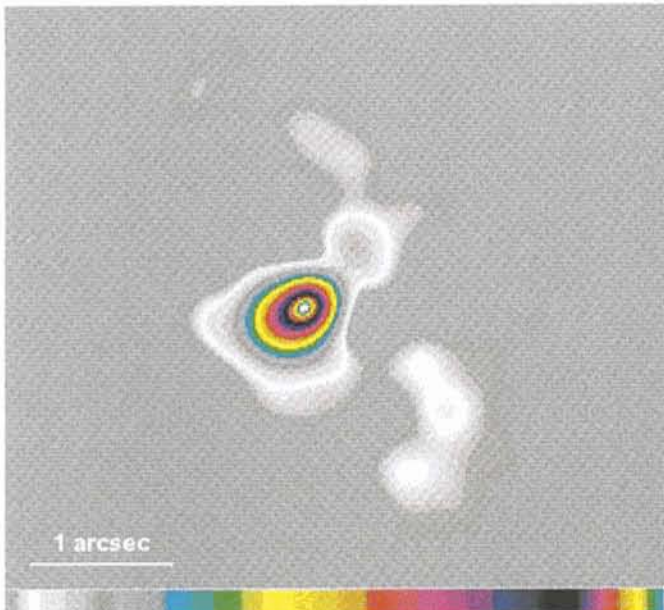
New Year's Eve with Adaptive Optics

From December 31, 1990 through January 8, 1991 a second observing run with the VLT adaptive optics prototype system – fully devoted to scientific programmes – took place. During this period, astronomers could benefit not only from diffraction-limited images

which are now given routinely by the adaptive optics system, but also from new features like a coronagraph, designed and built at Observatoire de Meudon, and an infrared wavefront sensor. For standard observation the Electron-Bombarded CCD (EB-CCD) of the

visible wavefront sensor (see *The Messenger* No. 62, p. 64) is used for wavefront sensing, allowing objects up to the 13th magnitude to serve as reference sources.

The observations with the adaptive optics prototype system started with the



η Carinae in the L- (left) and M-band (right). Both images are composed of five sub-images (four quadrants and additional frame in the centre) like a mosaic. The scales for both images are the same. The two mosaics have been deconvolved with the measured point spread function at the corresponding wavelength. These observations show new features around the central object (some people say it looks like a carrot-eating vizcacha).

initial set-up of the system which required half of the first night. As for the previous scientific observing run (November 1990) the system worked for the astronomers in a fully reliable and reproducible way. During these observations the seeing conditions varied from good to excellent. Unfortunately, during part of the observing time the programme suffered under cloud coverage.

The scientific goals of the November 1990 run concentrated on the solar system (i.e. Pallas), extragalactic astronomy (i.e. NGC 1068), and the search for brown and red dwarfs (i.e. G29-38, G1866). For this run the major interests were in the area of circumstellar features (i.e. Z CMa, FU Ori, VY CMa), jets (Red Rectangle), and ejected material from

luminous blue variables (i.e. η Car, AG Car). Out of this list of objects one of the most exciting was η Carinae, where new amazing structures of arcsecond scale have been revealed around the central object in the L- (3.8 μm) and M-band (4.5 μm) (see Figure).

In addition, during the test and set-up, night images were taken in the visible wavelength band with a commercial CCD. These experiments demonstrated that even in this range a significant improvement in image quality (corrected image FWHM ~ 0.4 arcsec for an initial seeing of ~ 0.7 arcsec) was possible with the current prototype system.

The last and final run with the current prototype system is planned for April this year. Extensive technical tests will be performed before the system goes

back to Europe for a major upgrade programme (Called COME-ON PLUS). It will be equipped with a fifty actuator mirror and a modified wavefront computer to reach 40 Hz closed-loop bandwidth. This will allow to produce diffraction-limited images at shorter wavelengths, typically down to 1.7 μm . All optical parts will receive new, more efficient coatings, pushing the limiting magnitude for the reference star up to magnitude 14. This upgrade will make the VLT adaptive optics prototype system a very powerful tool for higher angular resolution observation of the southern sky.

G. GEHRING, ESO

F. RIGAUT, Observatoire de Paris-Meudon

New 2D Array Detectors Installed in IRSPEC and IRAC

A. MOORWOOD, ESO, Garching

A. MONETI and R. GREDEL, ESO, La Silla

IRSPEC at the NTT and IRAC at the 2.2-m telescope were equipped with new SBRC 58 \times 62 InSb and Philips Components 64 \times 64 Hg:Cd:Te arrays respectively during late January and early February. In the case of IRSPEC the new array has not only brought more than an order of magnitude s/n gain at $\lambda < 2.5 \mu\text{m}$ but also provides a long-slit capability which both extends the scientific capabilities of the instrument and simplifies its operation compared with the old 1D array which it has replaced. The present upgrading of these instruments has, at some risk, been done between normally scheduled observing runs in order to keep them available for visitors and so that they can benefit from any improved performance as soon as possible. Due to the need to complete this article within a few days of the end of both test runs we are only able at this stage to present a few preliminary results based on partially reduced data at the telescope but will report more fully in a future issue of the *Messenger*. In the present evolutionary stage of infrared arrays, however, the situation can change rather rapidly. New InSb arrays have already been received and will be tested as soon as possible in Garching and a 256 \times 256 Hg:Cd:Te array should be delivered later this year. Visitors planning to apply for observing time are therefore encouraged to contact Alan Moorwood in Garching or the astronomers responsible on La Silla – Roland

Gredel and Andrea Moneti for IRSPEC and IRAC respectively for the latest information. (EMail: @DGAESO51 or ESOM-C1::ALAN or RGREDEL or MONETI).

IRSPEC

New Features at the NTT

In its new home at the NTT IRSPEC is attached permanently to the telescope structure (and hence free of instrumental flexure effects) and employs an optical de-rotator in front of the slit to counter the field rotation at the telescope Nasmyth focus and to permit orientation of the slit at any position angle on the sky. The detector pixels of 76 μm are a factor of 2.7 smaller than in the old array, corresponding to $\sim 2''.2$ on the sky, and the maximum slit length using all 58 pixels in the cross dispersion direction would therefore correspond to $\sim 2'$. Unfortunately only the central $1'$ at present is free of vignetting – believed to be mainly due to a radiation stop installed several years ago when the slit was only 6" long! This will be removed as soon as possible. Alignment of the slit and de-rotator to the telescope optical axis (rotation axis) was achieved within $1''$ and combined telescope/de-rotator tracking errors in the worst case of objects transiting within 1° of zenith were measured to be less than $1''$. For objects with accurately known coordinates the excellent NTT pointing does

pose a small problem in that they usually disappear in the slit which then has to be closed in order to see them!

For calibration purposes the slit can be illuminated by an integrating sphere equipped with spectral line lamps plus a halogen lamp and black body source for flat fielding which is mounted in the telescope adapter and viewed via a retractable diverter mirror.

During the recent test the IRSPEC functions were controlled via an HP1000 computer using the existing software while the detector integration parameters were set by form filling on the A900 instrument computer with status display on a RAMTEK monitor which is also used to control the measurements (start, stop, repeat, etc.) by 'mouse' clicking on a menu bar. In future all parameters will be set via the A900. IHAP is available on-line with a RAMTEK monitor for image display and a graphics terminal for obtaining 1D spectrum plots, traces, etc. In addition, images and 1D traces can be displayed in real time on a monitor connected directly to the pre-processor in the detector acquisition system. Cut levels and any averaging desired for the 1D display, e.g the spectrum averaged over n pixels along the slit can be easily set via the A900 terminal and the monitor automatically displays the coordinates and value of the pixel (plus values of the surrounding pixels) indicated by a mouse driven arrow.

From the observers point of view the new system now resembles much more closely an optical spectrograph. Neither sky chopping nor a chart recorder were used during the test (although the possibility of retaining sky chopping to improve the cancellation of sky lines is being considered). Visible objects were normally centred (or generally found to be centred) using the slit viewing camera while invisible ones were centred either by blind pointing or offsetting from a nearby star. If necessary, the real time monitor can be used in place of the chart recorder for infrared 'peaking-up'. In order to perform sky subtraction, sufficiently compact objects were observed alternately at two positions along the slit thus yielding positive and negative images after subtraction and hence no loss of on-object integration time. For very extended regions it was necessary to choose appropriate sky positions at larger distances.

Performance

The SBRC 58×62 pixel InSb array now installed has a quantum efficiency ~ 0.8 around $2 \mu\text{m}$, exhibits its nominal read noise of $\sim 500\text{e}$ and dark current of $\sim 200\text{e/s}$ at 30 K and has 17 bad pixels. As the pixel pitch of $76 \mu\text{m}$ is a factor of 2.7 smaller than in the old 1D array, the resolving power is effectively higher by the same ratio, i.e. $\sim 2500\text{--}5000$ depending on wavelength and grating order. However, this definition corresponds to a slit width equal to one pixel whereas most of the test observations were made with two pixel matching to a slit of 4.5 yielding resolving powers of half these values i.e. close to the values defined with the old detector but now with adequate sampling, at least for extended sources.

Figure 1 shows a sky subtracted 'image' obtained with the slit oriented across the Orion bar as an example of what can be displayed on-line at the telescope on the real time monitor and/or the RAMTEK display. The slit is in the Y direction and dispersion in the X direction. In the upper part of the image the diffuse band is continuum emission from ionized gas behind the ionization front which also shows He I and some 1-OS(1) H_2 line emission which then increases in intensity into the molecular cloud ahead of the front. A more compact continuum source which also exhibits He I emission can be seen in the lower part and could be a compact H II region in or in front of the molecular cloud. Total on-source integration time was $5 \times 60\text{s}$ and the peak intensities/pixel on the He I and H_2 lines in the upper ionized region are comparable and $\sim 5 \cdot 10^{-22} \text{ W.cm}^{-2}$.

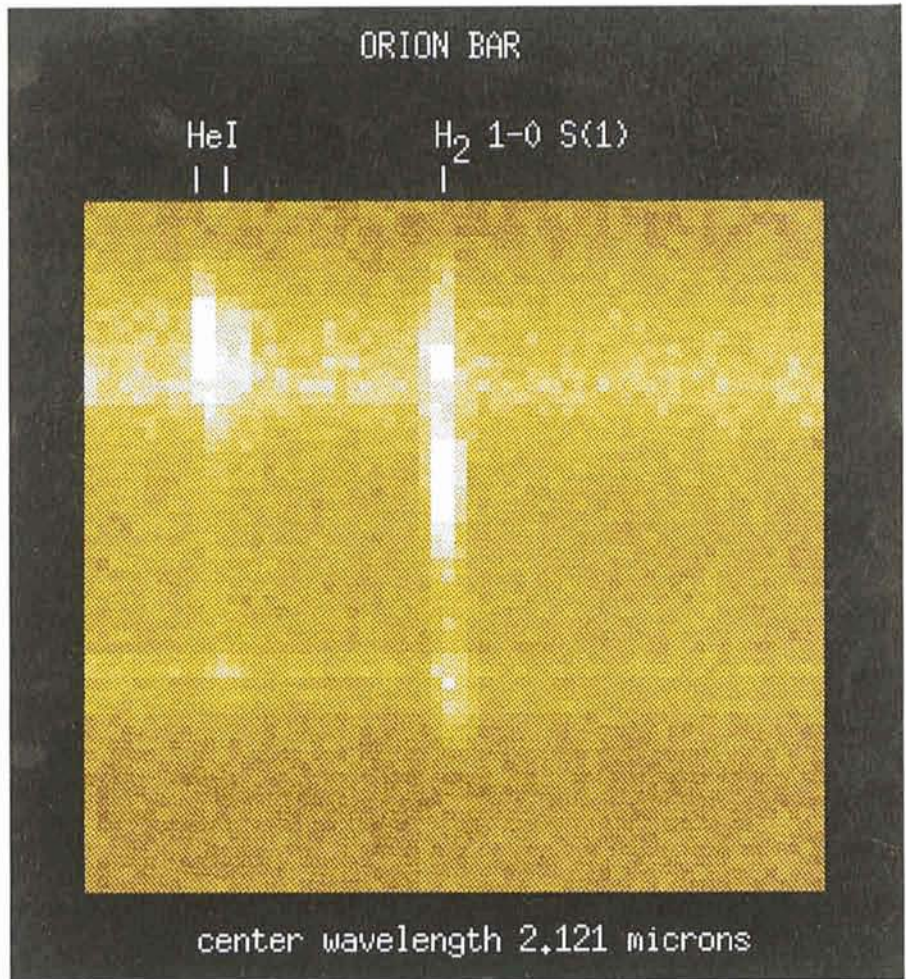


Figure 1: Sky subtracted IRSPEC 'image' with the slit oriented across the Orion bar. Towards the top can be seen both extended continuum and He I line emission from ionized gas behind the ionization front plus H_2 1-OS(1) line emission which then extends downwards into the molecular cloud and increases in strength. Another continuum source exhibiting He I emission, which could be an ultracompact H II region within or in front of the molecular cloud, is also visible towards the bottom. Total on-source integration time was $5 \times 60\text{s}$ and the peak intensities/pixel on the He I and H_2 lines in the upper ionized region are comparable and $\sim 5 \cdot 10^{-22} \text{ W.cm}^{-2}$.

Except for standard stars the typical on-chip integration times used for measurements at $\lambda < 2.5 \mu\text{m}$ were typically 60s and after subtraction of a sky frame corresponding to the same integration time the 1σ noise corresponded to $J \sim 13.25 \text{ mag.} = 3 \cdot 10^{-22} \text{ W.cm}^{-2}/\text{pixel}$, $H \sim 14.25 \text{ mag.} = 8 \cdot 10^{-23} \text{ W.cm}^{-2}/\text{pixel}$, $K \sim 13.75 \text{ mag.} = 7 \cdot 10^{-23} \text{ W.cm}^{-2}/\text{pixel}$ and $L \sim 8 \text{ mag.} = 3 \cdot 10^{-21} \text{ W.cm}^{-2}/\text{pixel}$. Except at L, where photon noise on the sky emission dominates, these limits are about a factor of 15 fainter than quoted in the old IRSPEC manual for the same integration time! If the sky frame also contains the object at a different position along the slit it is possible to gain a further factor of 1.4 whereas integrating over the same aperture as subtended by the old pixels will, in principle, lead to a factor of 2-3 increase in the effective noise. Although this already represents a large sensitivity gain relative to the old detector it is still hoped to improve on this substantially in the future. At pres-

ent the noise for 60s integrations is a combination of the nominal detector read noise and shot noise on the thermal background in the instrument which was found to be much higher than expected - partly due to the instrument itself running warmer than usual (following an obviously unsuccessful attempt to simplify the cryogenic system!) and partly due to insufficient shielding close to the detector. As a next step therefore it is planned to (i) implement multiple non-destructive sampling of the detector which can substantially reduce the read noise and has been tried briefly in the laboratory but was not ready for implementation during this first telescope test and (ii) introduce a number of measures to reduce the internal thermal background.

In addition to the s/n considerations discussed above it should be borne in mind that other factors such as flat fielding and cancellation of sky emission lines can, depending in detail on the

nature of the observation, also effect the overall system performance. During this first test, the halogen lamp at $\lambda < 2.5 \mu\text{m}$ and the sky at longer wavelengths were used for flat fielding. A few checks made on line indicate that these techniques provide correction to better than 1% but more analysis of the data is required in order to establish the actual limits and optimum procedures. No attempt has been made so far either to connect frames at different grating settings to produce continuous spectra. (In this latter regard, the old 'vignetting' problem should be considerably reduced because of the possibility of integrating over several pixels along the slit if necessary.) Residual sky lines (mainly OH at $\lambda < 2.5 \mu\text{m}$ and H₂O at longer wavelengths) were still found to be present in some regions on object/sky difference frames separated in time by 5-10 min. Depending on the programme this may or may not be a problem but if it is, the sky reference can be measured more often or it should be possible to further suppress the residuals using 'sky' measurements within the flat fielded frames themselves. In this regard, however, it should be noted that due to the Littrow mount used in IRSPEC, spectral lines are observed to be parallel to the array at wavelengths corresponding to the grating blaze angle but can be tilted by up to 8 degrees at the extreme ends of the grating range.

In summary, IRSPEC now has both considerably improved sensitivity, which it is hoped to increase further in future, and extended scientific capabilities (due to the long slit). It is also simpler to operate but whether this is also true of the data reduction remains to be seen.

IRAC

As the new Philips Components 64×64 Hg:Cd:Te array only arrived about 10 days before the planned test there was relatively little time available to characterize and optimize it before it was installed on the 2.2-m telescope. Nevertheless, some laboratory measurements were made and yielded a read noise ~ 400 e, a dark current of ~ 1000 e/s (at 50K), about 20-100 bad pixels depending on integration time in the range 1 to 60s and an efficiency (q.e \times fill factor) of $\sim 20\%$. Although fewer bad pixels would have been nice, the only real disappointment in these numbers was the efficiency which was expected to be closer to 50%. Overall, however, the larger format together with the fact that this array operates out to $4.2 \mu\text{m}$ (with a large well capacity $\sim 10^7$ e) and appears to be rather uniform and stable represents a consid-

erable improvement compared with the 32×32 array which it replaces.

At the telescope the 'warm' (i.e. high dark current) pixels are obvious in the raw images and also exhibit 'tails' presumably indicative of some charge transfer problem in the CCD readout chip to which the Hg:Cd:Te array is bonded. Sky subtraction leads to good cancellation of the tails and the warm pixels themselves can be removed with a high cut median filter either on-line or later. (By adjusting the drive voltages it is also possible to substantially reduce the number of warm pixels at the expense of creating a roughly equal number of 'cold' ones which are preferable because they are less visually obvious and do not create tails). Where the tails do potentially cause some problems is for observations of bright stars which also show this effect at least in the J and H bands.

It is not possible here to give reliable limiting magnitudes for the various modes (IRAC is equipped with broadband filters and CVF's which can be combined with on-line selectable magnifications of 0'3, 0'5, 0'8 and 1'6/pixel). As a guide however, based on measurements with a detector integration time of 60s and with 0'8 pixels, it appears possible to do photometry at $s/n=5$ in a 50 pixel synthetic beam down to $K=15$ and $J \sim H \sim 15.5-16$ on frames obtained with a total integration time of 1 hr equally divided between object and sky. For broadband L ($3.8 \mu\text{m}$) imaging the corresponding value is $L=9$ mag using 1 sec integrations and 0'5 pixels. Based on the actual detector parameters and overall efficiency measured on stars, the overall performance should actually be better, and this discrepancy is still not fully understood. It appears however that the actual read noise at the telescope was probably 2-3 times higher than measured in the laboratory and that this may have followed changes to settings to the acquisition system. The sky/telescope background also appeared to be high and, at least at K and L, could be attributable to the extremely high telescope temperature ($\sim 16\text{C}$) during the test run. It is therefore likely that the above figures are, if anything, on the pessimistic side. In addition to broad-band imaging, some tests were also made with the CVF and the K band Fabry Perot. As several people have expressed interest in $3.28 \mu\text{m}$ feature observations, the CVF performance at this wavelength was tested specifically by observing the planetary nebula IC 418 which, unfortunately, could not be detected in 15 min. This is presumably due to the relatively low transmission of our CVF in this region and means that, for the time being, we would not

encourage people to propose specifically for such observations.

In summary, IRAC is now both much better and much easier to work with than before and its performance can probably be improved beyond the preliminary guide given here once we have more experience in how to best optimize this particular array. It is also not excluded that this array could be replaced in the future with one of the InSb arrays still to be tested in Garching if this would lead to a substantial improvement in the overall performance. As this would require technical effort, however, this decision also depends on the future progress of IRAC2 and the actual delivery of its 256×256 Hg:Cd:Te array which is now ordered and expected before the end of the year.

Acknowledgements

At the risk of omitting to mention several people who contributed to the work described here we would like to specially thank P. Biereichel, M. Comin, G. Finger, H. Gemperlein, J.-L. Lizon, M. Meyer and U. Weilenmann for their technical support during these two parallel test runs and also our night assistants J. Miranda and M. Pizarro at the NTT.

MIDAS Memo

ESO Image Processing Group

1. MIDAS Environment Document

The first official version (1.0) of the MIDAS Environment document is now available. It contains complete documentation about the development of MIDAS application software for both FORTRAN and C. Besides a revision of the document, a chapter about Coding Standards for MIDAS applications and a table example programme have been added. This document will be the reference for anybody wanting to contribute software to MIDAS. Copies will be sent to all MIDAS sites automatically. Additional copies can be obtained from the Image Processing Group at ESO, contact Resy de Ruijscher.

2. MIDAS Directory Structure

A revision of the MIDAS directory structure has been made to provide a clear separation between the Core system and all other application software. A standard directory structure for contributed packages is defined to enable

easy implementation of software into MIDAS. See the MIDAS Environment Document for a detailed description of the new directory structure.

3. Installation Procedure

A new extended installation procedure will be available with the 91MAY release of MIDAS. It provides an easy question and answer session during which a customized version of MIDAS, only including the application packages required, can be installed. The procedure is available for both UNIX and VMS systems.

4. Application Developments

The Table File System has been extended in order to store arrays at table items. This upgrade was required to provide compatibility with the Binary 3-D table format being proposed as a FITS extension. This format is expected to be used by a number of projects (e.g. ROSAT for event tables) due to the high efficiency of the format. Only the very basic table applications can currently manipulate such arrays. The command syntax of the previous versions is still valid but the upgraded syntax includes some additions.

An old table can be read and processed by the new Table File System. A command RETRO/TABLE is provided to convert a 3-D table to the old format.

5. MIDAS Newsletter

The Image Processing Group intend to start a MIDAS-Newsletter with two annual issues. In order to make an inventory of the MIDAS usage at ESO and the various other MIDAS sites we passed a ques-

tionnaire to the participants of the Data Analysis Workshop last year. Although not everybody reflected on the questionnaire, from the forms which have been returned it became clear that many users find the information about MIDAS published in the *Messenger* (the MIDAS Memo) insufficient. A large majority would like to obtain more detailed information, for example in the form of a separate newsletter.

In order to serve the user community better, the Image Processing Group of ESO will start a MIDAS newsletter. We hope to publish the first issue in the month of May, shortly after the release of the 91MAY version of MIDAS. At first, we will start the newsletter with a periodicity of two issues per year.

The newsletter will contain various kinds of information, e.g.:

- new commands or command modifications/improvements;
- new packages or upgrades;
- MIDAS installation and performance;
- bugs found and bug fixes;
- experiences and results obtained;
- suggestions, criticism;
- plans for the future.

It is not the intention of the ESO-IPG to be the only group that provides contributions to this newsletter. We would like to encourage all MIDAS users to make contributions as well. Obviously, such contributions should be of interest for the general MIDAS user. Clearly, the emphasis in the newsletter will be on MIDAS and on its software. However, since MIDAS is made for data analysis in astronomy, the inclusion of some astronomical results obtained by using the MIDAS software is welcome.

We would hereby like to invite you to contribute to the MIDAS newsletter. Since the first issue will probably appear

in the course of May, we would be happy to receive contributions before April 1. The contributions should be submitted as a computer readable ASCII file in $L_A T_E X$ format using the article style with an 11 pt font. Contributions must be submitted to the editor Rein Warmels, ESO Image Processing Group (E-mail addresses EARN: REIN@DGAESO51 or SPAN: ESO::REIN).

6. Personnel

We are happy to announce that Resy de Ruijsscher has joined the Image Processing group as technical secretary. She is responsible for documentation and distribution of MIDAS and will be your prime contact person for these matters.

7. MIDAS Hot-Line Service

The following MIDAS support services can be used to obtain help quickly when problems arise:

- EARN: MIDAS@DGAESO51
- SPAN: ESO::MIDAS
- Eunet: midas@eso.uucp
- Internet: midas@eso.org
- FAX.: +49-89-3202362, attn.: MIDAS HOT-LINE
- Tlx.: 52828222 eso d, attn.: MIDAS HOT-LINE
- Tel.: +49-89-32006-456

Users are also invited to send us any suggestions or comments. Although we do provide a telephone service we ask users to use it in urgent cases only. To make it easier for us to process the requests properly we ask you, when possible, to submit requests in written form either through electronic networks, telefax or telex.

Automatic Photometry at La Silla

C. STERKEN, Astrophysical Institute, University of Brussels (VUB), Belgium

J. MANFROID, Institut d'Astrophysique, Université de Liège, Belgium

1. Automatic Telescopes and Photoelectric Photometry

Automatic telescopes represent a novel concept leading to a radically new way of planning and conducting observations. This is best illustrated in photoelectric photometry where the human factor is responsible for errors and for degraded accuracy. Man, with his slow reaction time and high tendency to fatigue, certainly cannot compete with a computer and with ultrafast equipment.

In manually conducted photometric observations, most of the time is spent with the photometer in idle status, when the observer moves the telescope to the next star, when the observer is identifying or centring the object, or when he or she is planning the rest of the night. Above all there is the problem of manpower: for each telescope in operation a skilled observer is needed all year round, and this is a major limitation on the total number of measurements that can be made.

Especially in differential monitoring of variable stars, short integration time and short time intervals between successive measurements are essential for high-accuracy photometry. Fast speed of measurement also means that a lot of measurements can be made each night, and this means that it is much easier to incorporate many more standard and constant star measurements. This in turn leads to more consistent reductions and higher accuracy and homogeneity in the data.

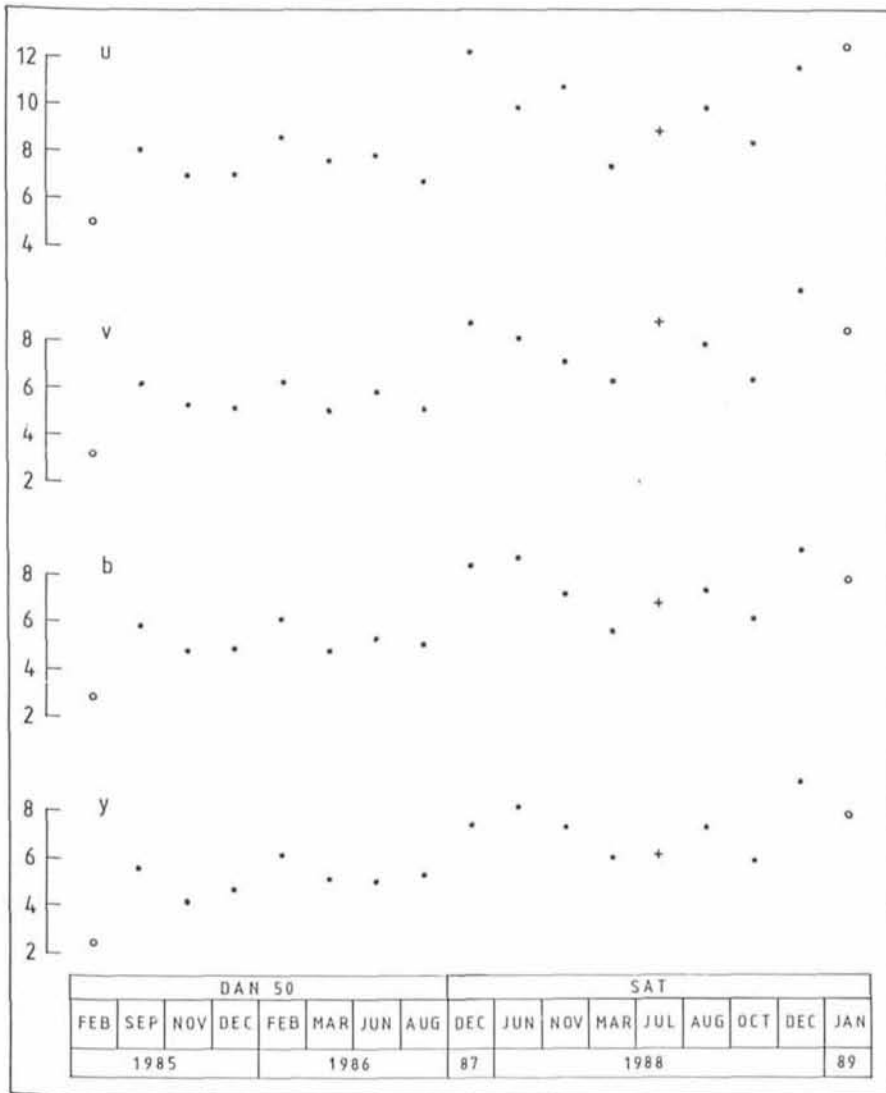


Figure 1: Systematic difference (ordinate = milli-magnitudes) between mean standard deviation of one differential measurement for the same telescope and photometer operated manually (DAN50), or automatically (SAT). Open circles denote measurements obtained by the same observer, and the + sign is a reference point obtained at the ESO 50-cm telescope.

Automatic telescopes are perfectly suited for observations which do not require decisions that only a human operator can take. This does not mean that complex decisions cannot be taken: computers can be programmed to execute evaluations well beyond the capacity of a human observer in terms of complexity and speed. This includes decision-taking according to the accomplished part of the programmed task, and interaction with data coming from on-line reduction.

Automatic telescopes are of course suited for observations beyond photometry, but photometry has been a test ground for the first telescope of this kind because classical photometric observations are easy to perform, and the field of application – even on bright stars – is gigantic and – in the classical approach – needs a large amount of manpower. In addition, complete automatization eliminates travel and lodging costs of

the observers (a very important factor, even for large telescopes where observing runs are shorter and where there is a faster turnaround of observers), and is a more economy-efficient solution than remote control observing.

Automatic telescopes, specifically built for observing without human assistance, will always have an edge over conventional telescopes, even over those which are computer controlled, since they can move more quickly from star to star. Dedicated telescopes such as the commercially available APT's (Automatic Photometric Telescopes) are optimal in this respect since they take only a few seconds for pointing and centring. Automatized telescopes on the other hand suffer from their large inertial momentum and need tens of seconds to find and centre a star. Roughly speaking, a quarter to half of the possible observing time is lost, and the interval between successive star pointings is

roughly twice as long as it could be, so that larger changes in the atmospheric conditions will intervene.

2. Our Experience with an Automated Manual Telescope

The SAT (Strömgren Automatic Telescope, Florentin Nielsen et al., 1987) is the name given to the ESO Danish 50-cm telescope after it was refurbished and provided with full computer control. The SAT has now been used for several years with considerable success. It is essentially a mission instrument where as a rule each observer gets a few weeks observing time per run. A rather flexible programming language was developed, and it is the responsibility of the user to code his observing sequences for each night, and hence each observer programmes the telescope in his own way. The result is that the SAT is functioning essentially in the same way as before automation, but that it is faster and has a larger output. However, when compared to dedicated APT's its typical setting time of 30 seconds is pretty long.

A big advantage of the SAT (over any existing APT) is its four-channel photometer which allows the measurement in the four Strömgren bands at the same time. Moreover, H β photometry can be performed by simply commanding the turning of a lever to enter the H β mode which yields simultaneous measurements in the two β bands. Hence the slowness of the telescope motion is largely compensated by the simultaneity of the measurements in the different colours, and by full-time availability of the H β mode.

Programming the SAT in an efficient way requires a thorough knowledge of the language, and an evaluation of all possible situations that can be expected during the night. Any programme will contain several loops and conditional evaluations. Since observing runs are of relatively short duration, few astronomers make the effort to thoroughly study the programming language. They either construct short programmed sequences and monitor the telescope all night, or they hastily write a poor programme, and leave the telescope unattended for many hours. This frequently leads to inferior results because standard stars are sometimes observed at too high airmasses, or because a critical phase of an eclipsing binary has been missed. Our experience shows that, for a similar observing programme, the average airmass over a full night is larger in automatic mode by systematically 0.05 to 0.15. Since the SAT telescope is a small instrument, with many stars having more than 5 mmag photon noise, the policy is to increase the number of in-

tegrations for the fainter stars. This is a rule which is easily forgotten when programming the sequences in automatic mode, especially if the telescope is used by people with limited observing experience in photometry.

In the framework of the Long Term Photometry of Variables programme at ESO (Sterken, 1983), a lot of observing time has been attributed on the SAT. Several observers have carried out the observations with varying degrees of success. Each observer had about one month of observing time, and would design the programme on the spot (eventually along the lines of a programme made by a predecessor).

The graph shown in Figure 1 gives the rms value of the differential results obtained for pairs of constant stars having more than 10 measurements. This is probably the best estimate of the overall accuracy of each run. All observations occurred according to the same instructions, except for the first and last run, which are the only runs carried out by the same observer (C.S., but with a very different observing programme). The run indicated with a cross is an observing run carried out at the ESO 50-cm telescope, and is given for reference only. "Automatic" operation started in December 1987. It is clear that rather large variations occur between the DAN50 and SAT block of runs (in spite of completely comparable observing missions).

Though we cannot rule out a hardware effect, such as an incorrect centring procedure (which in the case of a spectrophotometer of this type would introduce larger scatter), we think that a

large factor affecting the overall accuracy of the result may probably be found in the programming of the SAT. The worst cases were obtained by inexperienced astronomers who wanted to write long programmes and leave the telescope alone during a major part of the night. It is absolutely necessary to do such programming very carefully and test the code exhaustively in order to avoid unpleasant errors. This shows the importance of the software in developing APT systems. A lot of planning has to be done before efficient observations are carried out. We conclude that automatic telescopes are an improvement only when they are being programmed by observers who have extensive experience in manually conducted observations.

3. Conclusion

The SAT telescope unveils the promises of automatic telescopes. It is a substantial improvement compared to the old Danish 50-cm configuration in almost every aspect. The experience we got on the SAT is certainly positive, but we believe that most of the problems we encountered would not appear in the APT environment.

Three major lessons have been learned.

(i) Automatic telescopes are only as good as the software that runs them. The programming language has to be highly sophisticated to allow very flexible operation during the observations. This is a clear example of a situation where expert-systems or "artificial in-

telligence" is needed. The similarity with satellite operation is striking.

(ii) A good programming language is not enough. Not only the instructions given by the astronomer must make sense, also the command files written by the user or the controller should be complete and well-tested.

(iii) Refurbishing an old telescope for automatic operation is not the only solution. The costs of retrofitting may even be comparable to the cost of building or buying a very compact specifically-designed photometric telescope.

Implantation and operation costs of automatic telescopes of the one-metre class are very small compared to the scientific return. Such photometric telescopes are fundamental as support for large ground-based telescopes and – as more and more astronomers have found out during the last years – also for observations from space. In addition, they can perform tasks that are too tedious to be undertaken by astronomers, such as monitoring of objects during several months. Moreover, such telescopes can be linked in a local or global network. A cluster of small automatic telescopes at ESO may become a crucial node in such a global network, and eventually provide a unique opportunity for European astronomers for collecting photometric data.

References

- Florentin Nielsen, R., Norregaard, P., Olsen, E.H.: 1987 *The Messenger*, **50**, 45.
Sterken, C.: 1983, *The Messenger*, **33**, 10.

New Literature in the La Silla Library

Excerpt from TORUS by James Follett (Mandarin Paperbacks, London 1990), p. 205 to 217)

"... There were more celebrations at the end of 1989 when the excavation of the line of four thirty-metre-square pits was completed. Each of the huge pits was twenty metres deep. The model of the finished telescope in the planning office showed the four telescopes that made up the system aiming their lattice frameworks at the heavens like the projectors of a science fiction battle cruiser in a big budget space movie.

... It was the first telescope and not due to start observation work until 1999. The entire system of the four linked telescopes with their giant ten-metre diameter mirrors was not scheduled to be fully operational until 2002. Diem could only wonder at the determination of a people who, in their ceaseless quest for knowledge, were prepared to spend such vast amounts of money and resources. And it wasn't only the Soviets; giant

telescopes were being built all over the Pacific by different nations, such as the mighty Geck telescope on Hawaii, although none rivalled the Kuro Multiple Mirror instrument that Diem's employers were building.

... Hundreds of computer-controlled actuators hooked to the back of the giant floppy mirror to maintain its parabolic curve – providing continuous compensation for distortions caused by wind, temperature changes and gravity. It was the design breakthrough that had made the ten-metre supertelescopes possible."

Like the person in this science fiction paperback playing in the late 1990's, did you never wonder at the *real* reason why we are prepared to sink so much money into super-telescopes? Here the stunning answer is revealed, together with design details that were

till now not available in the open literature. Read all about CCDs, active optics, site selection techniques, mirror making and much more at a level *you* understand. The first two hundred pages are a bit dreary and consist of the usual staff thrillers are made of: determined men, beautiful women, violence and sex. After having plodded through this part, you'll be rewarded by insights into VLT budget fiddles and personalities of some key personnel.

Insiders will easily see through the obvious trick to replace ESO by a certain country and will have fun matching the book's characters (communists, crooks and mad scientists, sometimes all at once!) with their ESO counterparts. The ending of the novel is not to be revealed here. Let it suffice to say that it ends like all mad scientist projects.

H. DEKKER, ESO



Paranal: January 1991. An ESO video/photo team (Claus Madsen and Herbert Zodet) visited La Silla and the Paranal area to obtain footage for the coming ESO video film: "How we chose Paranal for the VLT". During a flight around the mountain, they made this low-altitude photo from the north-east. It shows the Paranal peak (left) with the so-called "NTT-peak" in the middle and Cerro La Montura to the right. On all three, the bases for the seeing telescopes are visible as white spots. The Pacific Ocean is seen in the background. It will be interesting to compare this picture with one taken 15 years from now!



Prince Phillippe Visits ESO Headquarters

On March 6, 1991, ESO was honoured by the visit of the successor to the Belgian throne, His Royal Highness Prince Phillippe, to the Headquarters in Garching. The Prince was accompanied by several high officials from Belgium and Bavaria, including the Belgian Ambassador to Germany, His Excellency, Mr. Georges Van der Espt, and the Belgian Consul General in Munich, Mr. Michael Godfrind. On the photo, Klaus Banse demonstrates the MIDAS Image Processing System during the walk through the building. The Director General, Harry van der Laan, and the other ESO astronomers were pleased to note His Royal Highness' personal interest in various astronomical themes, in particular within the field of cosmology, and they were very happy to inform about the most recent scientific discoveries at La Silla.

ESO, the European Southern Observatory, was created in 1962 to . . . establish and operate an astronomical observatory in the southern hemisphere, equipped with powerful instruments, with the aim of furthering and organizing collaboration in astronomy . . . It is supported by eight countries: Belgium, Denmark, France, Germany, Italy, the Netherlands, Sweden and Switzerland. It operates the La Silla observatory in the Atacama desert, 600 km north of Santiago de Chile, at 2,400 m altitude, where fourteen optical telescopes with diameters up to 3.6 m and a 15-m sub-millimetre radio telescope (SEST) are now in operation. The 3.5-m New Technology Telescope (NTT) became operational in 1990, and a giant telescope (VLT=Very Large Telescope), consisting of four 8-m telescopes (equivalent aperture = 16 m) is under construction. Eight hundred scientists make proposals each year for the use of the telescopes at La Silla. The ESO Headquarters are located in Garching, near Munich, Germany. It is the scientific-technical and administrative centre of ESO, where technical development programmes are carried out to provide the La Silla observatory with the most advanced instruments. There are also extensive facilities which enable the scientists to analyze their data. In Europe ESO employs about 150 international Staff members, Fellows and Associates; at La Silla about 40 and, in addition, 150 local Staff members.

The ESO MESSENGER is published four times a year: normally in March, June, September and December. ESO also publishes Conference Proceedings, Preprints, Technical Notes and other material connected to its activities. Press Releases inform the media about particular events. For further information, contact the ESO Information Service at the following address:

EUROPEAN
SOUTHERN OBSERVATORY
Karl-Schwarzschild-Str. 2
D-8046 Garching bei München
Germany
Tel. (089) 32006-0
Telex 5-28282-0 eo d
Telefax: (089) 3202362
Bitnet address: IPS@DGAESO51

The ESO Messenger:
Editor: Richard M. West
Technical editor: Kurt Kjær

Printed by Universitäts-Druckerei
Dr. C. Wolf & Sohn
Heidemannstraße 166
8000 München 45
Germany

ISSN 0722-6691

Contents

J. Chotomiewski and E.A. Valentijn: A New Southern Hemisphere Galactic Extinction Map Based on Surface Brightnesses of External Galaxies	1
M. Della Valle, B. J. Jarvis and R. M. West: The Recent Outburst of (X-Ray) Nova Muscae 1991	3
Tentative Time-table of Council Sessions and Committee meetings in 1991	5
The editor: Schott Successfully Casts an 8-m Mirror Blank	5
J. Breysacher and M. Tarenghi: Flexible Scheduling at the NTT, a New Approach to Astronomical Observations	6
G.A. Tammann et al.: Profile of a Key Programme: The Distance of the Centaurus Group – a Test for Various Distance Indicators	8
Idyllic La Silla!	9
Announcement of SEST Users' Meeting and Workshop on Millimetre-Wave Interferometry	10
Staff Movements	10
J.P. Swings: Instrumentation Beyond the Year 2000. Panel Discussion at the XII ERAM in Davos	11
R. S. Booth: Radio Astronomy – Towards the 21st Century	11
R. Genzel: Infrared/Sub-mm Astronomy after ISO (1 μ m-0.3 mm)	15
R. N. Wilson: Post-VLT Optics and Telescopes	15
"Tours du Monde, Tours du Ciel"	17
G. F. Bignami: X- and Gamma Ray Astronomy Beyond the Year 2000	18
J. Lequeux: Astronomy and Astrophysics: To Be an Editor	20
The editor: Dramatic Eruption on Comet Halley	22
Visiting Astronomers	22
Vacancies on La Silla	23
Minor Planet Named after Guido and Oscar Pizarro!	24
A. Blaauw: ESO's Early History, 1953–1975. X. The Schmidt Telescope: Design, Construction, the ESO-SRC Agreement and the Onset of Survey Projects	25
B. Nordström and J. Andersen: Open Clusters under the Microscope	34
A. Ardeberg, H. Lindgren and I. Lundström: The Oldest Stars	37
Announcement of ESO Workshop Proceedings: "Rapid Variability of OB-stars: Nature and Diagnostic Value"	41
P. Goudfrooij: Dust and Extended Ionized Gas in NGC 5044 and its Fellow Radio Elliptical Galaxies	42
E.A. Valentijn: Spiral Galaxies on the Chess Board	45
New ESO Scientific Reprints	49
L. M. Buson et al.: Supermassive Galaxies	50
M.-H. Ulrich: On the Origin of the Continuum Radiation at Optical and Ultraviolet Wavelengths in AGN/Quasars	52
B. J. Jarvis: A New Jet in M87?	54
A. F. M. Moorwood and E. Oliva: Infrared Coronal Lines in Active Galaxies	57
E. Hammer and O. Le Fèvre: New NTT Discoveries on Distant Galaxies and Gravitational Lensing	59
I. F. Mirabel: Ultraluminous Infrared Galaxies	64
E. Giraud: Blue Galaxies in the Field of the Quasar PKS 0812 + 02	67
H.-M. Adorf: Artificial Intelligence for Astronomy	69
Editorial Note	72
H. Dekker et al.: Multi Object Spectroscopy with the ESO Multi Mode Instrument at the NTT	73
G. Gehring and F. Rigaut: New Year's Eve with Adaptive Optics	76
A. Moorwood, A. Moneti and R. Gredel: New 2D Array Detector Installed in IRSPEC and IRAC	77
ESO Image Processing Group: MIDAS Memo	79
C. Sterken and J. Manfroid: Automatic Photometry at La Silla	80
H. Dekker: New Literature in the La Silla Library	82
Paranal: January 1991	83
Prince Philippe Visits ESO Headquarters	83